INVEST. BUILD. GROW.

MANITOBA

REPORT OF ACTIVITIES 2021

Manitoba Geological Survey

Manitoba

REPORT OF ACTIVITIES
2021

Manitoba Agriculture and Resource Development
Manitoba Geological Survey

When using information from this publication in other publications or presentations, due acknowledgment should be given to the Manitoba Geological Survey. The following reference format is recommended:

Manitoba Agriculture and Resource Development 2021: Report of Activities 2021; Manitoba Agriculture and Resource Development, Manitoba Geological Survey, 96 p.

Published by:
Manitoba Agriculture and Resource Development
Manitoba Geological Survey
360–1395 Ellice Avenue
Winnipeg, Manitoba
R3G 3P2 Canada
Telephone: 1-800-223-5215 (General Enquiry)
204-945-6569 (Publication Sales)
Fax: 204-945-8427
Email: minesinfo@gov.mb.ca
Website: manitoba.ca/minerals

ISBN: 978-0-7711-1629-2

This publication is available to download free of charge at manitoba.ca/minerals

Front cover photos:
Left: MGS geologist Chris Couëslan examining a rock sample at Russell Lake, Manitoba.
Right: Sand and gravel deposits from a depleted pit near Gillam (GS2021-10, this volume).

REPORT OF ACTIVITIES 2021

Minister's Message

As Minister of Agriculture and Resource Development, it is an honour to introduce the *Report of Activities 2021*, a comprehensive update on key geoscience projects and activities over the past year.

Exemplary geoscience is the bedrock of exploration and mining activity in the province, and drives important investment in the sector. I applaud the commitment and hard work of the Manitoba Geological Survey (MGS). In particular, I want to extend my appreciation to the MGS for their productivity and professional delivery of a record number of publication releases this past year, during challenging and unprecedented times.

This year's 10 reports presented in the *Report of Activities* illustrates the wide range of geoscience applications, commodities, and regions around the province addressed by the MGS. The dedication and new collaborations with a large number of university partners in Manitoba and across the country by the MGS are evident. As part of their fieldwork, geoscientists are 'on the ground' experts whose knowledge and connection with industry and exchange of local geoscience information, priorities and collaborative opportunities is of great value to ongoing sector growth and development.

In 2020-21, MGS staff actively participated in the co-development of the Pan-Canadian Geoscience Strategy (PGS) with the Geological Survey of Canada and Canadian geological survey organizations to provide positive direction for the future of the sector. I endorse this collaborative initiative and thank the MGS for their contributions to this essential federal-provincial-territorial effort. The long-term vision of the PGS to "provide geoscience information for the responsible development of Canada's geological resources, and to serve the public good" will help us explore options for advancing public geoscience collaborations in Manitoba and neighbouring jurisdictions.

Manitoba is home to rich natural resources and various critical minerals, which positions the province for minerals sector growth to support green industry development.

The Manitoba Critical Minerals team, including representation from the MGS, supports the national Critical Mineral Task Force on critical minerals and the battery supply chain. Key minerals and critical metals mined in the province include zinc, nickel, silver, copper, gold and cesium, with historical production and reserves of lithium. Most of these commodities are a direct focus of the reports in the *Report of Activities 2021*.

Manitoba's other significant mineral resources with high potential include platinum-group elements, rare-earth elements, uranium, titanium, vanadium, chromite, silica, tungsten, graphite, diamonds and potash. Many of these are part of current MGS geoscience studies, helping to guide the MGS in providing relevant geoscience information and to focus and de-risk exploration and decision-making.

I invite you to reach out to our talented MGS team and geologists to discuss their findings and talk about your needs, in an effort to move forward in making the most of our shared potential and opportunities.

Looking at our minerals sector, alongside the growing demand for critical minerals and key mineral resources, and recognizing our tremendous people, we have everything it takes to succeed and support investment in Manitoba. Let's move forward with confidence.

Original signed by

Honourable Ralph Eichler
Manitoba Agriculture and Resource Development

Rapport d'activités 2021

Message du ministre

À titre de ministre de l'Agriculture et du Développement des ressources, je suis honoré de présenter le *Rapport d'activités de 2021*, qui fait le point de façon exhaustive sur les projets et les activités clés de la dernière année en géoscience.

La géoscience exemplaire est le fondement des activités d'exploration et d'extraction exercées dans la province; elle donne lieu à d'importants investissements dans le secteur. J'applaudis la détermination et le travail acharné de la Direction des services géologiques du Manitoba (la « Direction »). Je tiens notamment à remercier la Direction pour sa productivité et sa réalisation professionnelle d'un nombre record de publications au cours de la dernière année, en cette période difficile et sans précédent.

Cette année, les 10 rapports présentés dans le *Rapport d'activités* illustrent la diversité de l'éventail d'applications, de marchandises et de régions liées à la géoscience que la Direction traite à l'échelle de la province. Le dévouement de la Direction et sa nouvelle collaboration avec un grand nombre de partenaires universitaires du Manitoba et du pays sont évidents. Dans le cadre de leur travail de terrain, les géoscientifiques agissent en experts « sur place » dont les connaissances et les relations avec l'industrie ainsi que l'échange de données locales, de priorités et d'occasions de collaboration en géoscience jouent un rôle très important dans le maintien de la croissance et du développement du secteur.

En 2020-2021, le personnel de la Direction a participé activement à l'élaboration de la stratégie pancanadienne de géoscience avec la Commission géologique du Canada et des organisations géologiques du pays afin d'offrir une orientation confirmée pour l'avenir du secteur. J'appuie cette initiative collaborative et je remercie la Direction de ses contributions à ce programme fédéral-provincial-territorial essentiel. La vision à long terme de la stratégie, qui a pour but de fournir des données de géoscience aux fins du développement responsable des ressources géologiques du Canada et de servir le bien public, nous aidera à examiner les options d'avancement des collaborations publiques en géoscience au Manitoba et chez ses voisins.

Le Manitoba, qui est riche en ressources naturelles et en divers minéraux critiques, est bien placé pour assurer la croissance de son secteur des minéraux afin d'appuyer le développement de l›industrie verte.

L'équipe manitobaine chargée des minéraux critiques, qui comprend des représentants de la Direction, appuie le Groupe de travail sur les minéraux critiques du Canada à l'égard des minéraux critiques et de la chaîne d'approvisionnement des piles. Les métaux critiques et les minéraux clés extraits dans la province comprennent le zinc, le nickel, l'argent, le cuivre, l'or et le césium, en plus de la production et des réserves historiques de lithium. Les rapports mentionnés dans le *Rapport d'activités de 2021* traitent directement la plupart de ces marchandises.

Les autres ressources minérales importantes à potentiel élevé du Manitoba comprennent les éléments du groupe platine, les éléments des terres rares, l'uranium, le titane, le vanadium, la chromite, la silice, le tungstène, le graphite, les diamants et la potasse. La plupart de ceux-ci sont présentement visés par des études de géoscience de la Direction qui l'aideront à fournir des données de géoscience pertinentes ainsi qu'à cibler et à rendre moins risquées l'exploration et la prise de décisions.

Je vous invite à communiquer avec les membres talentueux de l'équipe de la Direction, y compris ses géologues, pour discuter de leurs conclusions ou de vos besoins, et à aller de l'avant dans l'exploitation optimale de nos possibilités et de notre potentiel communs.

Compte tenu de notre secteur des minéraux, de la demande croissante en minéraux critiques et en ressources minérales clés, et de nos équipes remarquables, nous avons tout ce qu'il faut pour réussir – et pour favoriser les investissements au Manitoba. Allons de l'avant avec confiance.

Origional signé par

Ralph Eichler
Agriculture et Développement des ressources

Director's Message

The year 2021 was full of challenges for the sector, and the Manitoba Geological Survey (MGS) encountered changes to its organizational structure and restrictions imposed by external natural forces. The *Report of Activities 2021* is a testament to the dedication and passion of an exceptional team. In the short time I have been with the branch, I witnessed the incredible sense of family and extraordinary leadership within the Survey. Looking out for and caring for each other was the driving force behind the successes of each project presented here.

When you read through these reports, keep in mind that the team covers an immense jurisdiction full of incredible potential. Discoveries of geological structural significance through the mapping in the Snow Lake area along with thousands of previously unknown mineral occurrences should provide the sector a great catalyst to consider Manitoba as a favourable jurisdiction for unique prospecting and exploration opportunities.

Many thanks to the sector's contributions mentioned in the Foreword. Industry support continues to be vital for the advancement of geoscientific exploration and discovery in our province, summarized in each volume of the *Report of Activities*.

It is an honour and a privilege to be part of a team that has the true heart of geology at its core. I thank the MGS team for your dedication, resilience and professionalism to continue exploring and providing high-quality scientific and technical discoveries to the public for the benefit of all Manitobans.

Tafa Kennedy, P. Geo.
Director, Mining, Oil and Gas Branch

Message de la directrice

En 2021, notre secteur a fait face à de nombreux défis, et la Direction des services géologiques a subi à la fois des changements à sa structure organisationnelle et des restrictions imposées par des forces naturelles externes. Le *rapport d'activités de 2021* témoigne de l'engagement et de la passion d'une équipe exceptionnelle. Même si je fais partie de la Direction depuis peu de temps, j'ai déjà été témoin du grand esprit de famille et de l'extraordinaire leadership qui en émanent. Prendre soin les uns des autres a été au cœur du succès de chaque projet présenté ici.

Lorsque vous lirez les documents, rappelez-vous que l'équipe couvre un immense territoire dont le potentiel est extraordinaire. Les découvertes d'importance concernant la structure géologique faites grâce à la cartographie de la région du lac Snow et les milliers de venues minérales qui nous étaient jusqu'alors inconnues devraient servir de catalyseur au secteur pour que le Manitoba soit considéré comme un territoire favorable à la prospection et à l'exploration.

Je remercie grandement le secteur de ses contributions mentionnées dans l'avant-propos. Le soutien de l'industrie continue d'être essentiel pour l'exploration et la recherche géoscientifiques dans la province, tel que résumé dans chaque volume du *rapport d'activités*.

C'est un honneur et un privilège de faire partie d'une équipe à qui l'esprit de la géologie tient à cœur. Je vous remercie pour votre engagement, votre résilience et votre professionnalisme dans la poursuite de l'exploration et la présentation de découvertes scientifiques et techniques de haute qualité à la population manitobaine.

Tafa Kennedy, géo. professionnelle
Directrice, Direction des mines, du pétrole et du gaz

In Memoriam: Barry B. Bannatyne

by M.P.B. Nicolas

On January 13, 2021 at the age of 87, Barry Ballenden Bannatyne passed away peacefully. Born and raised in Winnipeg, he grew up in St. James, attending and graduating from St. James Collegiate in 1950. Barry put down roots in Fort Garry with Barbara, his wife of 59 years. They had two daughters, Sandra and Sharon, whom were predeceased by their infant son, Brian. Barry graduated from the University of Manitoba with a B.Sc. (Honours) Geology in 1954, followed by an M.Sc. in 1959.

Barry spent his entire 30-year career with the Manitoba Geological Survey (MGS), although the MGS went by many different names during those years. He was the first Industrial Minerals Geologist for the province, authoring many of the initial industrial mineral inventories and publications. His thorough and detailed publications have stood the test of time and are still relevant and regularly referenced today, including his reports on Manitoba potash, bentonite, dolomite, clays and shales, high-calcium limestone, gypsum and peat.

Barry worked closely with Hugh McCabe, Manitoba's first petroleum geologist and Phanerozoic stratigrapher, to help describe and establish the Manitoba lithostratigraphic framework. They initiated the Manitoba Stratigraphic Drillhole and Industrial Minerals Drilling Program in 1968. Both Barry and Hugh were mentors and coaches for the province's industrial minerals geologists and stratigraphers who followed them until and beyond their joint retirements in 1988. This caring career assistance has been gratefully acknowledged by many of their successors for over 30 years.

After having spent all his summers in the field doing geological mapping, as well as scouting drill hole locations and amassing an impressive number of publications to his name, Barry became the technical editor for all the MGS geological reports towards the end of his career. In his retirement, Barry spent winters in Arizona and summers at his cottage at Albert Beach where he enjoyed spending his time reading and doing jigsaw puzzles.

I first knew Barry from the cottage, having grown up next door to him during the summers over my whole life. During those days, his time at the cottage was shared with times in the field. It wasn't until I started my studies in geology that I learned about Barry's professional side and could put some context to it all. When I started to work for the MGS, my admiration and respect for him grew. I felt honoured to have known him personally—this tall, quiet, intelligent man—who was so important to Manitoba geology, but also feel a sense of awe and inspiration when I open one of his many reports.

Foreword

On behalf of the Manitoba Geological Survey (MGS), it is my privilege to present the *Report of Activities 2021*—the annual peer-reviewed volume of geoscience projects results by the MGS.

On April 1, 2021, the Department of Agriculture and Resource Development (ARD) was strategically restructured to focus on designing a solid framework that delivers the department's mandate and advance industry. This restructuring has created four new divisions: Corporate Services and Innovation; Industry Advancement; Ecosystem Management; and Production Stewardship. The MGS is now a section situated within the new Production Stewardship Division, within the Mining, Oil and Gas (MOG) Branch. Along with the MGS, MOG also includes the Regulatory Services and the Tenure Services sections.

The MGS currently has over 30 active geoscience projects, each one at various stages of execution, with 10 of them reported in this volume. A gradual return to "a new normal" after the pandemic last year could be seen across the mineral sector. The MGS approached its field season cautiously, but optimistic that a field season could still take place. The drought that took hold in the prairies this summer was extreme, and hundreds of forest fires raged across the province, with some of them threatening to cancel, cut short or delay our field programs. With careful planning and protocols in place, the field program was a success, despite some delays caused by the commandeering of a helicopter to fight local wildfires.

A total of seven field programs were successfully completed this year, with most field programs feeding data and information to more than one active project. Each annual volume of the *Report of Activities* along with accompanying preliminary maps and data repositories present the findings of new and advanced projects, and include important contributions to Manitoba geology and mineral potential. This summer marked the beginning of the new Geomapping for Energy and Minerals (GEM) GeoNorth program—a 7-year, federally-run geoscience program that provides collaborative and funding opportunities for geoscience in Canada's north, administered by the Geological Survey of Canada. The call for proposals for the GEM 2021/22 year was for projects with a one-year timeframe for completion. The MGS was included as collaborators in several GEM proposals, with four of those approved for funding this year. Quaternary geology investigations in the Hudson Bay Lowland in northeast Manitoba (GS2021-8 and GS2021-10, this volume) received funding from the GEM-GeoNorth program to cover indicator mineral processing and to characterize intertill nonglacial deposits. One GEM project the MGS contributed to this summer is focused on the "four corners" region, where Manitoba, Saskatchewan, Nunavut and the Northwest Territories meet. This project consisted of the preparation and submission of archival lake sediment samples for geochemical analysis, and archival bedrock samples for geochronological, isotopic and geochemical analysis.

Critical minerals continue to be an important focus for our projects, with some of those reported herein. These include studies in lithium remobilization in the Tanco area pegmatites (GS2021-2, this volume); updated geological framework with rare metals and gold potential in the Lynn Lake belt (GS2021-5, this volume); and nickel mineralization relationships in the Thompson nickel belt (GS2021-3, this volume). The MGS also continues to work on internal initiatives such as updating the Mineral Deposits Database (GS2021-1, this volume) to add thousands of new mineral occurrences including many critical metals such as rare-earth elements, graphite, platinum-group elements, antimony, bismuth, chromium, cobalt, copper, gallium, germanium, molybdenum, nickel, niobium, tantalum, tellurium, tungsten, vanadium, and zinc. Looking beyond the classic critical metals to precious metals and diamonds, the MGS continues to be active on these important commodities including new mapping in the Snow Lake area towards a continued refinement of a geological model that can inform gold exploration (GS2021-4, this volume), and kimberlite-indicator mineral results (GS2021-9, this volume).

The maintenance, refinement and expansion of the geological knowledge infrastructure in Manitoba is the foundation of the work done by the MGS. That important work can occur in focused projects on single NTS sheets, or in regional work that includes reconnaissance mapping, data collection and archival compilations. The data collected from these projects can then be assembled to inform multi-dimensional regional maps derived from multiple layers of information. The compilation process towards the modelling of a Quaternary depth to bedrock thickness map for northeastern Manitoba is described in GS2021-7 (this volume), which will increase the effectiveness of drift prospecting in areas covered with thick sediments. Compilation and analysis of data of all kinds can also serve to identify areas that need more focused attention, or that is affected by unconscious/unintentional biases. The identification of Late Cretaceous vertebrate collection biases in southwestern Manitoba is one such example (GS2021-6, this volume). Fossils, and the insight they provide in paleogeographic and paleoenvironmental reconstructions, provide context to the sediments that host them by positioning them in time and space. Without accurate representation of the fossil assemblages, the risk of inaccurate labelling of a unit may occur, which then may lead to errors in correlation. Refinement of local geological environment interpretation ensures accuracy when extrapolating to global correlations of stratigraphic units, and ultimately inform the exploration for sedimentary-hosted commodities.

A large portion of the reports this year required the collaboration of companies, organizations, individuals and neighboring jurisdictions. This near symbiotic relationship is vital to the advancement of the scientific knowledge of the province and increases the MGS coverage and discoveries that will benefit all Manitobans today and into the future. I would like to acknowledge the support, information sharing and contributions made by external institutions and industry partners, including the Geological Survey of Canada, Saskatchewan Geological Survey, University of Manitoba, Western University, University of Waterloo, University of British Columbia, University of Calgary, University of Fraser Valley, University of Toronto, Charles University (Prague, Czech Republic), Vale, Alamos Gold, Hudbay, Sinomine, and Vanadian Energy.

The recent passing of Barry Bannatyne, the first industrial mineral geologist in the MGS, serves as a reminder to us all of the lasting impact our work at the MGS can have on the geological community, and the geoscience information we contribute to through our publications and maps. Barry's legacy has stood the test of time, as his work continues to educate and inform us about Manitoba geology. My condolences go out to the Bannatyne family.

The dedicated and diligent work of many including the MGS Chief Geologist Christian Böhm, all the project geologists, Geoscience Data manager Greg Keller and his team of GIS professionals, and lab technicians went into the production of the *Report of Activities 2021*. I would like to acknowledge Bob Davie and his hard-working team from RnD Technical who carefully performed technical editing, and Craig Steffano who managed report production and publication layout. I would like to thank everyone at the MGS for their valuable contributions to Manitoba geology, and the dedication and enthusiasm they bring to their work and profession.

Michelle P.G. Nicolas, P. Geo., FGC
Provincial Geologist and Manager, Manitoba Geological Survey

Avant-propos

Au nom de la Direction des services géologiques du Manitoba (la Direction), j'ai l'honneur de présenter le *rapport d'activités de 2021*, un recueil annuel examiné par les pairs compilant les résultats de projets géoscientifiques exécutés par la Direction.

Le 1er avril 2021, on a procédé à une restructuration stratégique du ministère de l'Agriculture et du Développement des ressources (Agriculture et Développement des ressources) pour mettre l'accent sur l'élaboration d'un cadre solide qui assure l'exécution du mandat du ministère et le progrès de l'industrie. Cette restructuration a créé quatre nouvelles divisions : Services ministériels et innovation, Promotion de l'industrie, Gestion des écosystèmes et Gestion des ressources. La Direction des services géologiques est devenue une section de la Direction des mines, du pétrole et du gaz, au sein de la nouvelle Division de la gestion des ressources. En plus de la Direction des services géologiques, la Direction des mines, du pétrole et du gaz comprend aussi la Section de la gestion des droits fonciers et la Section des services de réglementation.

La Direction des services géologiques (la Direction) compte actuellement plus de 30 projets géoscientifiques actifs, chacun à divers stades d'exécution, dont dix qui sont inclus au présent rapport. Après la pandémie l'an dernier, un retour graduel à la « nouvelle normalité » s'est opéré dans l'ensemble du secteur minier. La Direction a abordé sa saison de travaux de prospection avec prudence, mais de manière optimiste quant au fait qu'elle pourrait avoir lieu. Cet été, une sécheresse extrême a sévi dans les prairies et des centaines de feux de forêt ont ravagé la province, dont certains qui menaçaient d'annuler, d'abréger ou de retarder nos programmes de prospection. Grâce à une planification et des protocoles soignés, le programme de prospection a été une réussite malgré les retards entraînés par la réquisition d'un hélicoptère pour lutter contre des feux locaux incontrôlés.

Nous avons complété avec succès sept programmes de prospection cette année, dont la plupart ont permis de recueillir des données et des renseignements pour plusieurs projets actifs. Chaque volume annuel du *rapport d'activités* et ses cartes préliminaires et référentiels présentent les conclusions de projets nouveaux et avancés et comprennent des contributions importantes au potentiel géologique et minier du Manitoba. Cet été a marqué le début du nouveau programme de géocartographie de l'énergie et des minéraux, GEM-GéoNord : un programme fédéral de géosciences de sept ans qui propose des occasions de financement et de collaboration pour des initiatives de géosciences dans le Nord canadien. Le programme GEM-GéoNord est administré par la Commission géologique du Canada. L'appel de propositions du programme GEM 2021-2022 s'appliquait à des projets d'une durée d'un an. La Direction a été nommée à titre de collaborateur dans plusieurs propositions au programme GEM dont quatre qui ont reçu un financement cette année. Les recherches en géologie du quaternaire dans les basses-terres de la baie d'Hudson au nord-est du Manitoba (GS2021-8 et GS2021-10 dans le présent rapport) ont obtenu un financement du programme GEM-GéoNord pour le traitement de minéraux indicateurs et la caractérisation de dépôts intertill non glaciaires. Un projet GEM auquel la Direction a participé cet été s'intéresse à la région des « quatre coins », soit le point de rencontre du Manitoba, de la Saskatchewan, du Nunavut et des Territoires du Nord-Ouest. Ce projet consistait en la préparation et la soumission d'échantillons de sédiments de lacs archivés aux fins d'analyse géochimique et d'échantillons de substratum rocheux aux fins d'analyses géochronologique, isotopique et géochimique.

Nos projets continuent de mettre un accent considérable sur les minéraux critiques, y compris des projets inclus dans le présent rapport. Ces projets comprennent des études sur la remise en mouvement du lithium dans les pegmatites de la région de Tanco (GS2021-2 dans le présent rapport); la mise à jour du cadre géologique pour inclure les métaux rares et le potentiel aurifère dans la zone de Lynn Lake (GS2021-5 dans le présent rapport) et les relations des minéralisations nickélifères dans la zone de nickel de Thompson (GS2021-3 dans le présent rapport). La Direction a également poursuivi le travail sur des initiatives telles que la mise à jour de la base de données des gisements (GS2021-1 dans le présent rapport) pour ajouter des milliers de venues minérales, y compris de nombreux métaux critiques comme : minéraux à éléments de terres rares, graphite, éléments du groupe du platine, antimoine, bismuth, chrome, cobalt, cuivre, gallium, germanium, molybdène, nickel, niobium, tantale, tellure, tungstène, vanadium et zinc. La Direction étend ses activités au-delà des métaux critiques classiques pour demeurer active dans les matières premières importantes des métaux précieux et des diamants, notamment la nouvelle cartographie de la région du lac Snow pour permettre le perfectionnement continu d'un modèle géologique qui servira à l'exploration aurifère (GS2021-4 dans le présent rapport) et les résultats de minéraux indicateurs de kimberlite (GS2021-9 dans le présent rapport).

Le travail de la Direction repose sur l'entretien, le perfectionnement et l'expansion de l'infrastructure du savoir géologique au Manitoba. Ce travail important peut s'effectuer dans le cadre de projets ciblés sur des feuilles uniques du SNRC ou lors de travaux régionaux qui impliquent la cartographie de reconnaissance, la collecte de données et la compilation archivistique. Les données recueillies de ces projets sont réunies pour créer des cartes régionales multidimensionnelles grâce à de multiples niveaux d'information. Le processus de compilation pour la modélisation d'une carte de la profondeur du quaternaire relative à l'épaisseur du substratum dans le nord-est du Manitoba est décrit au GS2021-7 (dans le présent rapport) et viendra accroître l'efficacité de la prospection glaciosédimentaire dans les zones couvertes d'épais sédiments. Par la compilation et l'analyse de données de toutes sortes, on peut également repérer des zones qui nécessitent une attention plus ciblée ou qui ont été affectées par une partialité inconsciente ou involontaire. La reconnaissance d'une partialité pour la collecte de vertébrés du Crétacé tardif dans le sud-ouest du Manitoba en est un bon exemple (GS2021-6 dans le présent rapport). Les fossiles et la perspective qu'ils apportent aux reconstructions paléogéographiques et paléoenvironnementales permettent de mettre en contexte les sédiments dans lesquels ils se trouvent. Il devient alors possible de déterminer leur position dans le temps et l'espace. Sans une représentation exacte des ensembles de fossiles, on risque d'étiqueter incorrectement une unité, ce qui peut entraîner des erreurs de corrélation. Le perfectionnement de l'interprétation d'environnements géologiques locaux assure une exactitude lors de l'extrapolation de corrélations globales d'unités stratigraphiques, ce qui, au final, contribue à l'exploration de matières premières encaissées dans les sédiments.

Cette année, une grande partie des rapports a nécessité la collaboration d'entreprises, d'organisations, de particuliers et de provinces et territoires avoisinants. Cette relation quasi symbiotique est essentielle au progrès du savoir scientifique dans la province, en plus d'accroître la couverture et les découvertes de la Direction, au bénéfice de la population manitobaine d'aujourd'hui et de demain. Je tiens à souligner le soutien, le partage d'information et les contributions d'établissements externes et de partenaires industriels, notamment la Commission géologique du Canada, la Saskatchewan Geological Survey, l'Université du Manitoba, l'Université Western, l'Université de Waterloo, l'Université de la Colombie-Britannique, l'Université de Calgary, l'Université de Fraser Valley, l'Université de Toronto, la Charles University (à Prague, en République tchèque), Vale, Alamos Gold, Hudbay, Sinomine et Vanadian Energy.

Le décès récent de Barry Bannatyne, premier géologue en minéral industriel de la Direction, nous sert de rappel de l'incidence durable que notre travail à la Direction peut avoir sur la communauté géologique, en plus de l'information géoscientifique que nous partageons au moyen de nos publications et de nos cartes. L'héritage de Barry a résisté à l'épreuve du temps puisque son travail continue de nous informer sur la géologie du Manitoba. J'offre mes condoléances à la famille Bannatyne.

Le travail dévoué et minutieux de nombreux collaborateurs, y compris de Christian Böhm, géologue en chef de la Direction, de tous les géologues de projets, de Greg Keller, gestionnaire des données de géosciences, et de son équipe de professionnels du SIG et enfin des techniciens de laboratoire, a permis la production du *rapport d'activités de 2021*. Je tiens à saluer Bob Davie et son équipe à RnD Technical, qui ont pris soin de la révision technique, et Craig Steffano, qui a géré la production du rapport et la mise en pages de la publication. Je remercie enfin tous les membres de la Direction de leur participation précieuse à la géologie du Manitoba et du dévouement et de l'enthousiasme qu'ils consacrent à leur travail et à leur profession.

Michelle P.G. Nicolas, géo. professionnelle, FGC
Géologue provinciale et gestionnaire, Direction des services géologiques du Manitoba

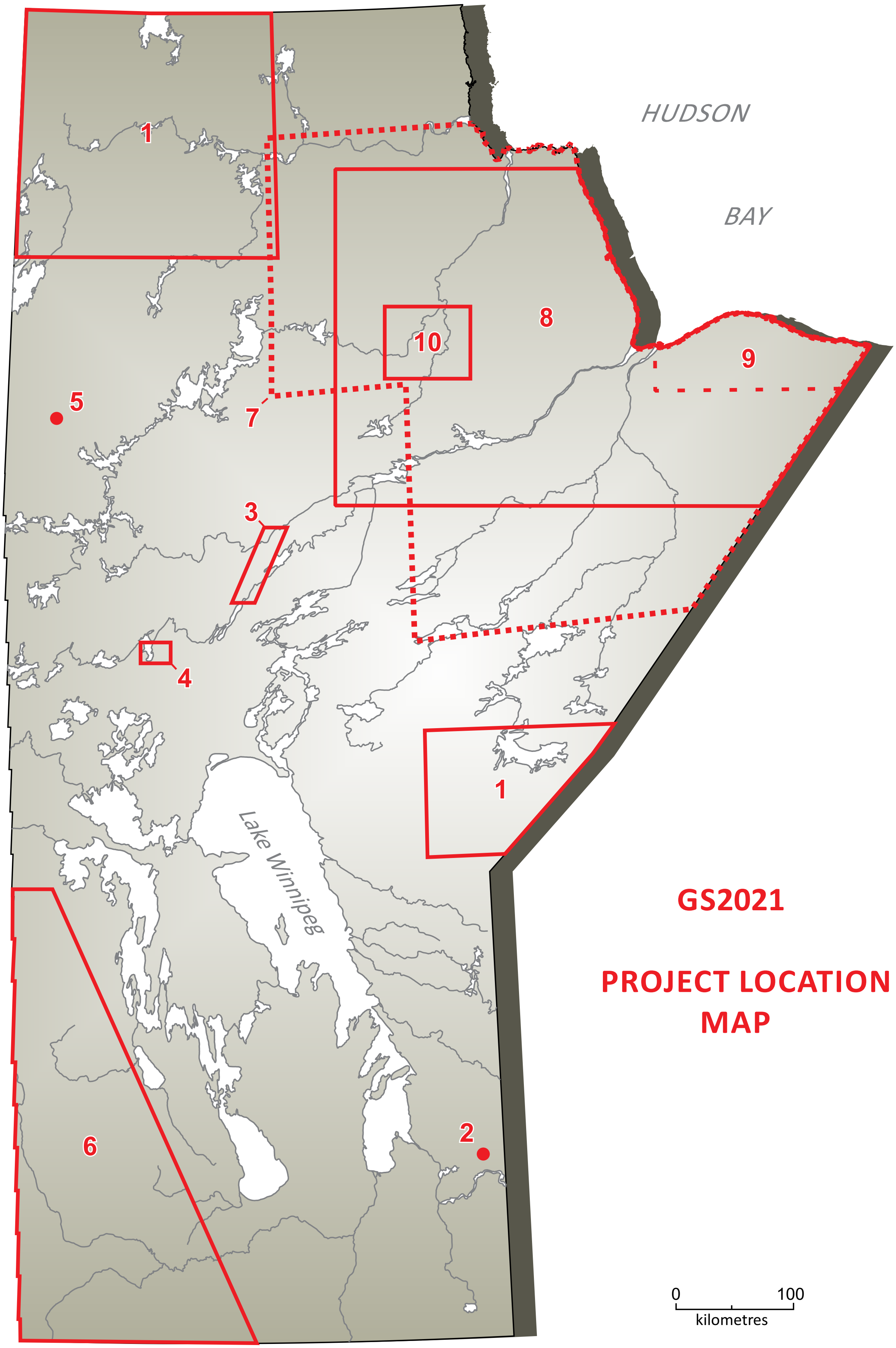

GS2021

PROJECT LOCATION MAP

Table of Contents

PUBLICATIONS

GS2021-1

Updates to the Manitoba Mineral Deposits Database, east-central and northwestern Manitoba (NTS 53E, F, 64J, K, N, O)

by M.L. Rinne

In Brief:

- Approximately 22 000 new mineral occurrences have been tentatively identified in Manitoba
- Findings include high-grade gold and graphite occurrences in the Island Lake region, and significant rare-earth element and uranium occurrences in northwestern Manitoba
- Updates are being released in batches by region; Island Lake region (NTS 53E, F) updates are completed, and northwestern Manitoba (NTS 64J, K, N, O) is in progress

Citation:

Rinne, M.L. 2021: Updates to the Manitoba Mineral Deposits Database, east-central and northwestern Manitoba (NTS 53E, F, 64J, K, N, O); *in* Report of Activities 2021, Manitoba Agriculture and Resource Development, Manitoba Geological Survey, p. 1–7.

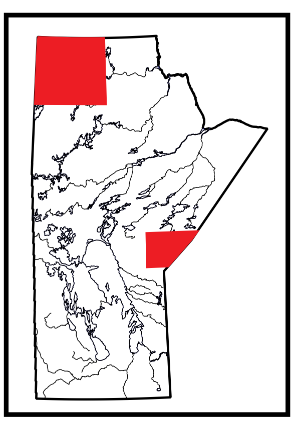

Summary

The Manitoba Geological Survey began work to update Manitoba's Mineral Deposits Database (MDD) in 2020. Continued efforts during the past year have led to the preliminary identification of 22 070 new occurrences with relevant geochemical data in Manitoba, encompassing a wide range of commodity types. In this report, recent changes to the methods and definitions used for the MDD update are outlined and a summary of occurrences added so far to NTS areas 53E, F, and 64J, K, N and O is provided.

Introduction

Accurate and comprehensive mineral occurrence data are necessary to inform land-use plans, mineral development strategies and related assessments of critical mineral potential in Manitoba. Because mineral occurrence data are also used by the minerals sector to guide their exploration decisions, the identification of new (or previously unrecognized) mineral occurrences can spur industry investment in underexplored regions. The MDD, which serves as the primary inventory of mineral occurrence data in Manitoba, was therefore identified as a priority for updates starting in 2020.

Prior to this year's updates, the latest version of the MDD was published in 2009 (Conley et al., 2009), containing a total of 2760 occurrences in Manitoba. The rationale and methods used to improve the MDD are explained in Rinne (2020). In this report, changes to the methods employed to update the MDD since last year are summarized, notably including the introduction of software to assist or partially automate the extraction of mineral occurrence information from historical reports. A brief overview of occurrences recently added to parts of the Island Lake region and northwestern Manitoba is also provided.

Definitions and methods

Mineral occurrence grade criteria

Terms used to classify entries in the MDD include 'mineral occurrence', 'mineral deposit' and 'discretionary occurrence', as defined in Rinne (2020). Most mineral occurrences are identified based on geochemical results, where values exceed a defined minimum in a rock sample. The minimum values used have been updated since 2020 and are listed in Table GS2021-1-1.

Although many of the minimum grade requirements were initially based on those defined in Ontario's equivalent database (Ontario Mineral Deposit Inventory; Ontario Geological Survey, 2020), several have since been adjusted based on the issues discussed below. Minimum grade criteria for the MDD have also been expanded to include a wider range of commodities not normally captured in equivalent databases for other jurisdictions.

The general aim in defining minimum occurrence values is to capture any results or observations that could reasonably be associated with (or form distal to) mineral deposits, without flagging too many irrelevant and/or background results. A purely statistical approach—for example, a value exceeding three standard deviations above mean crustal abundance—was found to be inappropriate for this purpose. Instead, most of the minimum values are based on the geochemistry of known ore deposits, with minimum values typically between half and one fifth of deposit grades globally. Exceptions to this guideline are generally intended to capture results that might indicate potential for other commodities. For example, 500 ppm Bi is lower than 1/20th of values typical in bismuth ore deposits, but bismuth contents of 500 ppm could mark the distal portions of some gold-mineralizing systems (e.g., Kadel-Harder et al., 2021). Similarly, 1% F is lower than 1/10th of most known fluorine deposit grades (Hayes et al., 2017), but is considered an occurrence in the

Table GS2021-1-1: Minimum grade or mineral criteria for occurrence classification in the Manitoba Mineral Deposits Database.

Commodity	Minimum grade or mineral content for occurrence classification
Ag	>35 ppm (>1 opt[1])
Au	>0.5 ppm (>0.015 opt[1]) OR visible gold
Al	Bauxite or gibbsite present
As	Evaluation[2]
B	>10 000 ppm (>1%) OR minerals present (e.g., ulexite, borax)
Ba	>30 000 ppm Ba OR >5% barite
Be	>50 ppm OR minerals present (e.g., beryl, bertrandite)
Bi	>500 ppm
Graphite	>5% OR present as coarse flakes or seams
Co	>200 ppm
Coal (metallurgical)	Evaluation[2]
Cr	>10 000 ppm (>1.5% Cr_2O_3)
Cs	>1000 ppm OR minerals present (e.g., pollucite)
Cu	>2500 ppm
Diamond	Mineral present
F	>1% F OR >2% fluorite
Fe	>12.5% (>16.1% FeO or >17.9% Fe_2O_3) AND unit >5 m thick
Ga	>100 ppm
Ge	>30 ppm
Gypsum	>40%
He	>0.3 mol % (from natural gas production)
Hf	>150 ppm
In	>5 ppm
Li	>1000 ppm Li (>0.2% Li_2O) OR minerals present (e.g., spodumene, lepidolite, petalite) OR >30 ppm Li in brines
Mg	>10% magnesite ($MgCO_3$) OR >15% brucite ($Mg(OH)_2$) OR >10% carnallite
Mn	>50 000 ppm (>6.5% MnO)
Mo	>200 ppm
Nb	>200 ppm OR minerals present (e.g., columbite, pyrochlore)
Ni	>800 ppm
Pb	>10 000 ppm
PGE[3] (Pt+Pd+Rh+Ir+Ru+Os)	>0.5 ppm total PGE
P	>10% P_2O_5
Potash	>7.5% potash
Rb	>1000 ppm
Re	>10 ppm
REE[4] (lanthanides + Sc, Y)	>0.3% total rare-earth oxides OR minerals present (e.g., monazite) OR La, Ce, Nd, Sc, or Y >500 ppm OR Pr, Sm, Gd, Dy, Er, or Yb >50 ppm OR Eu, Tb, Ho, Tm, or Lu >10 ppm
Sb	>500 ppm
Se	>100 ppm
Silicon	Quartzite >5 m thick OR high-purity silica sand
Sn	>1000 ppm
Sr	>50 000 ppm (>5%) OR minerals present (e.g., celestite)
Ta	>100 ppm OR minerals present (e.g., tantalite, pyrochlore)
Te	>100 ppm
Th	>250 ppm OR minerals present (e.g., monazite)
TiO_2	>7.5% (>45 000 ppm Ti)
Tl	>100 ppm
U	>250 ppm (>0.03% U_3O_8) OR minerals present
V	>1000 ppm
W	>500 ppm
Zn	>1000 ppm
Zr	>5000 ppm
Other (carbonatite, kimberlite and related rocks, semi-precious gemstones, high-purity limestone, etc.)	Evaluation[2]

[1] Troy ounces per short ton
[2] Requires review by a geologist to determine whether the occurrence is significant
[3] PGE, platinum-group element
[4] REE, rare-earth element

MDD because it may indicate potential for Nb or rare-earth element (REE) mineralization in some rocks.

Some commodities (e.g., Ga, Ge, In, Rb, Se, Te, Tl) are extracted mostly or exclusively as byproduct from other ores. In those cases, values are based on limited information reported for ores of the relevant deposits. Finally, some commodities have strictly metallurgical/mineral criteria. For example, there is no minimum grade specified for an aluminum occurrence; an occurrence would instead be noted where the presence of bauxite or gibbsite has been documented.

Further adjustments to the values in Table GS2021-1-1 may be necessary in the future, perhaps in response to significant changes in market prices, development of new metallurgical techniques, or other aspects that are difficult to forecast. In any case, users of the updated MDD should note that geochemical values are recorded in new occurrence entries; users can therefore filter the occurrence data to increase the minimum grade requirements if desired.

Data collection methods

The general approach to the MDD updates remains the same as described in Rinne (2020). The aim is to capture key occurrence characteristics as quickly as reasonable, including a compromise to omit several of the more detailed fields (e.g., detailed geological descriptions, exploration history) in new mineral-occurrence entries.

As MDD updates progressed through 2020 and the number of new occurrences increased beyond what was initially expected, it became clear that a fully manual compilation of occurrences from all assessment files in Manitoba would be an unreasonable task. Last year, much of the project work was therefore devoted to investigating software tools that could partially automate or assist in the identification of mineral occurrences. The results of this work are summarized below.

Optical character recognition

Nearly all PDF reports in the Manitoba Mines Branch Assessment Library comprise scanned images that lack embedded text data. Optical character recognition (OCR) is therefore necessary to process the report contents. Several OCR tools were tested using a series of representative assessment-file pages that include poor-quality scans, handwritten drill logs and large tables. Amazon Textract® and ABBYY FineReader® were found to produce the most consistently useful results.

Phrase matching

Some mineral occurrences are reported only in the main text of assessment files, in phrases such as “coarse graphite from 27 m to 53 m,” “visible gold in sample 3423,” or “carbonatite dikes.” Reading through the main body of an assessment file to identify such phrases is one of the most time-consuming parts of the MDD update. Results so far indicate that this step can be partially automated using indexing and search software (e.g., dtSearch®) to flag any matches from a list of specific terms or phrases in each report.

To account for natural language variations, search terms applied to the assessment files include a combination of fuzzy and proximity matching, wildcard characters and other expressions. For example, using dtSearch® syntax, a search for “coarse& w/3 graphit*” will flag any occurrence of ‘graphite’ or ‘graphitic’ within three words of ‘coarse’ or any of its synonyms. Likewise, having ‘fuzzy search’ enabled for the term ‘spodumene’ will flag mentions of spodumene along with typos or OCR errors such as ‘spoqumere’.

Preliminary applications of these text searches have led to rapid identification of some graphite and gold occurrences in reports from the Island Lake region. However, continued work with these search results has required several iterations/adjustments to the strings used, mostly to reduce false positives as well as the amount of time needed for a human to page through the search hits in each set of reports. Because of the large number of commodities and related search terms involved, the current list of search phrases is a work in progress.

Table data

Most of the mineral occurrences encountered in the assessment files to date were found in geochemical results or assay-data tables, typically in appendices. Identifying occurrences in these tables is a generally straightforward exercise in finding values that exceed the occurrence minima listed in Table GS2021-1-1. However, the process can be time-consuming, particularly in the case of large tables spanning multiple pages, or in cases where sample standards are not clearly indicated.

Attempts to automate the process of extracting occurrence data from tables have yielded promising results. Provided large or high-quality scans of tables in reports with an OCR text layer, an open-source tool called Tabula is used to extract tables as CSV files from PDF documents. Values exceeding a given number are then easily identified in each table. Unfortunately, many of the scanned report tables contain small or low-resolution text that hinders the accuracy of OCR results, to the extent that confirming occurrence results often takes longer than simply reading the table in the original scan.

In addition to the work described above, several of the more recent assessment files were originally submitted with geochemical results in digital format such as Excel® tables. A total of 3720 such files have been retrieved and sorted. Occurrences contained in these tables are being processed by NTS area.

Occurrence-location data

After each occurrence identified in text or table results is manually confirmed to be valid (to exclude the results of e.g., faulty OCR or elevated assay values from sample standards), further work is then required to determine the occurrence location. Because co-ordinates are rarely included in older reports, most of this work involves georeferencing of sample location maps. The lower scan quality of the assessment file PDF documents often requires retrieving the original document to then find the locations of specific sample numbers on large-format maps. This stage of the process is understandably time-consuming and represents the last step prior to the public release of new occurrence data. Although some interesting work has been published regarding automated georeferencing of maps (e.g., Arriaga-Varela and Takahashi, 2019), it is not yet clear how easily this can be incorporated into the MDD update process.

Results to date

At the time of writing, 22 070 new occurrences have been tentatively identified from assessment file tables and text. This represents a significant increase from the previous version's 2760 total occurrences (several of which are minor and are being removed during the database update). More occurrences are anticipated as text searches continue to be carried out through assessment files, and as other sources of data (e.g., Manitoba Geological Survey [MGS] geochemistry results) are incorporated into the database updates.

Some of these new occurrence data are available in MGS Data Repository Item DRI2021019[1] (Rinne, 2021), which contains results from NTS areas 53E and F. Publication of the remaining results first requires confirmation of each finding, along with the above-described process of locating each occurrence. Attempts to use the centre of each assessment-file polygon as a provisional location estimate were found to be potentially misleading, as many of the assessment areas are very large. Further update releases will therefore proceed by region, after location data have been entered.

In addition to the published mineral-occurrence data from NTS areas 53E and F (Rinne, 2021), location data entry is partially completed for NTS areas 64 J, K, N and O. The results for both these regions are described below.

NTS areas 53E and 53F

Much of the Island Lake domain of the northern Superior province is included in NTS areas 53E and 53F (Figure GS2021-1-1). Since beginning the MDD update in 2020, a total of 348 mineral occurrences were added to NTS areas 53E and 53F, and a further 27 existing occurrences were updated, mostly with the addition of relevant geochemical data (Rinne, 2021). Twenty-five occurrences in the previous version of the MDD were removed from the region, as they were deemed trivial findings (such as occurrences of sulphide-facies iron formation or pyrite veins with no significant assay results).

Among the new occurrences provided in Rinne (2021), a few notable examples are described below, numbered as shown in Figure GS2021-1-1:

1) Gold, copper, and tellurium occurrences added near Willow Lake include findings of visible gold, tetradymite, and grades of up to 374 ppm Au in quartz veins (Assessment Files 91149, 93215 and 94339, Manitoba Agriculture and Resource Development, Winnipeg).
2) Several mineral occurrences were added near the eastern shore of Bigstone Lake, including multiple zinc occurrences, drillcore samples with elevated nickel and palladium contents, intervals of 'well-mineralized to near-solid graphite', and one unconfirmed finding of wolframite. Also nearby are the Diamond Queen gold veins discovered in the 1930s (Assessment File 91148) along with a related series of veins discovered in 2017, with several surface samples containing >30 ppm Au (Rinne, 2017).
3) New gold occurrences were added along an east-southeast trend in the eastern half of the Bigstone Lake greenstone belt, along with several potentially significant intersections of graphite in drillcore (based on logs describing 'solid graphite', 'mineralized graphite', or '25–40% graphite' over intervals up to 8 m thick).
4) Occurrence data were added in the vicinity of the Bella Lake pluton. The area contains chalcopyrite, bornite and molybdenite in veins of quartz, potassium feldspar and biotite, within a zone of potassic alteration surrounded by propylitic alteration (Assessment File 90001). Although Archean porphyry deposits are rare, these sulphide- and alteration-zonation features are broadly consistent with porphyry-style mineralization (e.g., Sillitoe, 2010).
5) A series of previously undocumented occurrences were added (and several existing occurrences updated) along an east-southeast trend from the Island Lake mine into Sagawitchewan Bay. These occurrences include values of up to 145 ppm Ag, 301 ppm Au, 0.78% Cu, 760 ppm Mo, 1400 ppm Ni, 2.83% Pb, 3155 ppm Sb, 1470 ppm W and 7.06% Zn, along with occurrences of abundant graphite in drillcore.
6) Assay data reported from surface sampling near Rose Lake in 1980 include results of 0.5 ppm Au, 0.06% Co, 1.94% Cu, 0.75% Ni, 0.48 ppm Pd and 0.41 ppm Pt (Assessment File 92726). Earlier drilling in the area (1961) intersected sul-

[1] MGS Data Repository Item DRI2021019, containing the data or other information sources used to compile this report, is available online to download free of charge at https://www.gov.mb.ca/iem/info/library/downloads/index.html, or on request from minesinfo@gov.mb.ca, or by contacting the Resource Centre, Manitoba Agriculture and Resource Development, 360–1395 Ellice Avenue, Winnipeg, Manitoba R3G 3P2, Canada.

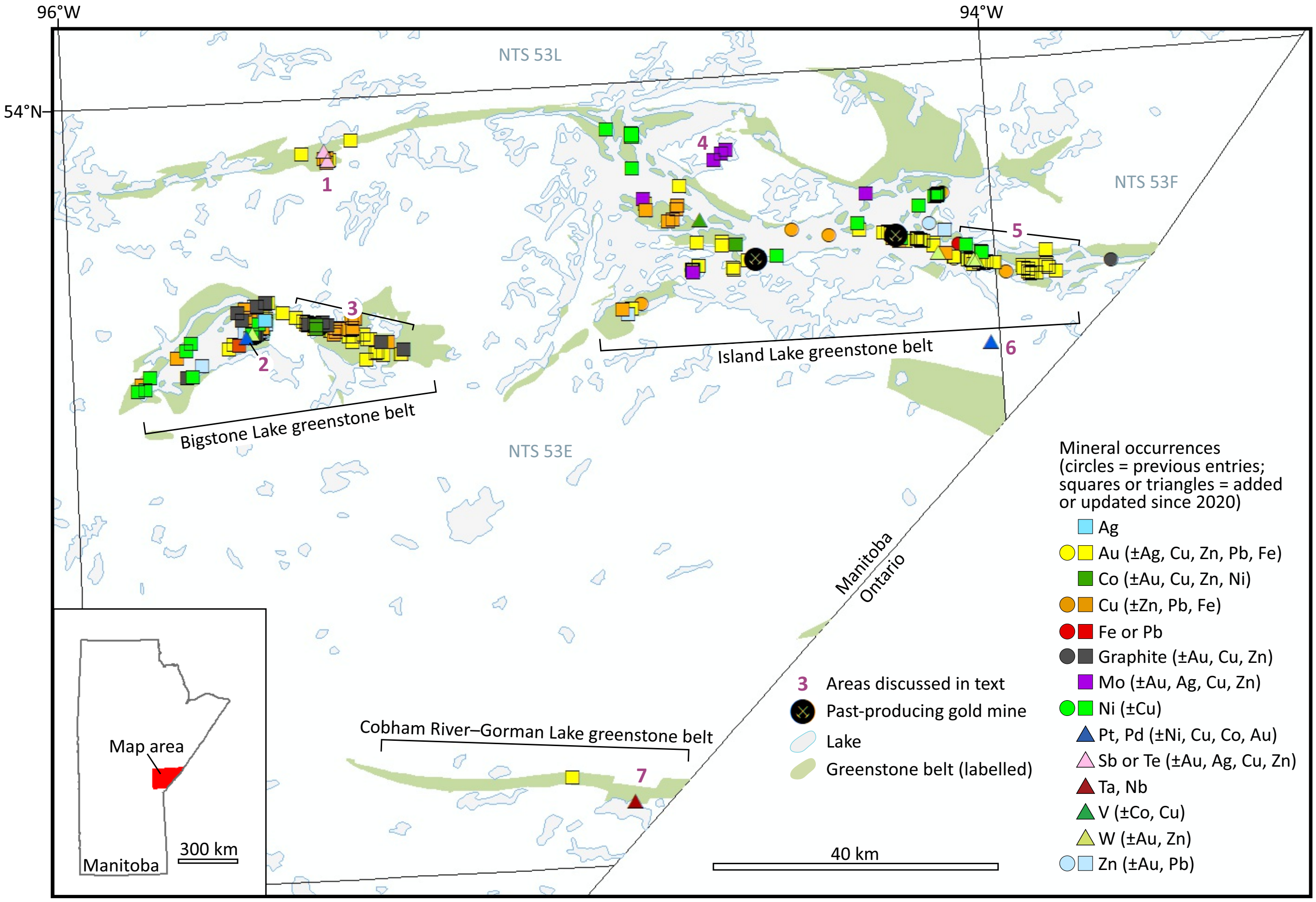

***Figure GS2021-1-1:** NTS areas 53E and 53F showing mineral occurrences, including new data added to the Manitoba Mineral Deposits Database since 2020.*

phide-mineralized pyroxenite and gabbro, but no assays were reported.

7) Tantalite, columbite and tourmaline were reported by Quinn (1960) near the northeastern shore of Gorman Lake; this showing lacks geochemical data and has been classified as a discretionary occurrence.

NTS areas 64J, K, N and O

The NTS areas 64J, K, N and O occupy the northwestern corner of Manitoba (Figure GS2021-1-2), including parts of the Wollaston basin and Seal River domain. This year, a total of 916 mineral occurrences were added to the region, including relevant geochemical data. A further 427 occurrences have been tentatively identified from assessment files but are pending confirmation and location information. Many of the new occurrences, including several of the high-grade uranium findings, correspond to boulder samples and are identified as such in the MDD entries. Most of the occurrences in the original MDD (marked with circle symbols in Figure GS2021-1-2) have not yet been evaluated in detail, and some may be removed as updates continue.

Most of the preliminary occurrence data added this year are clustered in areas discussed below (areas numbered as shown in Figure GS2021-1-2):

1) Uranium-mineralized boulders in areas southeast of Brandson Lake returned values of up to 6553 ppm U (Assessment Files 93420 and 93494).

2) Areas east of Putahow Lake contain elevated U and Th in outcrop (up to 597 ppm U and 537 ppm Th) and in drill-core (up to 0.085% ThO_2 and 0.065% U_3O_8; Assessment Files 92136 and 92212).

3) A total of 240 occurrences were added to areas west and southwest of Snyder Lake. Results from samples in this area include values of up to 4040 ppm Mo, 2.16% Th, 9.30% U and 8145 ppm total rare-earth elements (REE; Assessment File 74417). Phosphorus and beryllium contents are also locally elevated, with samples returning up to 13.6% P_2O_5 and 200 ppm Be.

4) Geochemical data and new occurrence locations were added to areas south and west of Munroe Lake, including surface and shallow-outcrop drill-sample results of up to

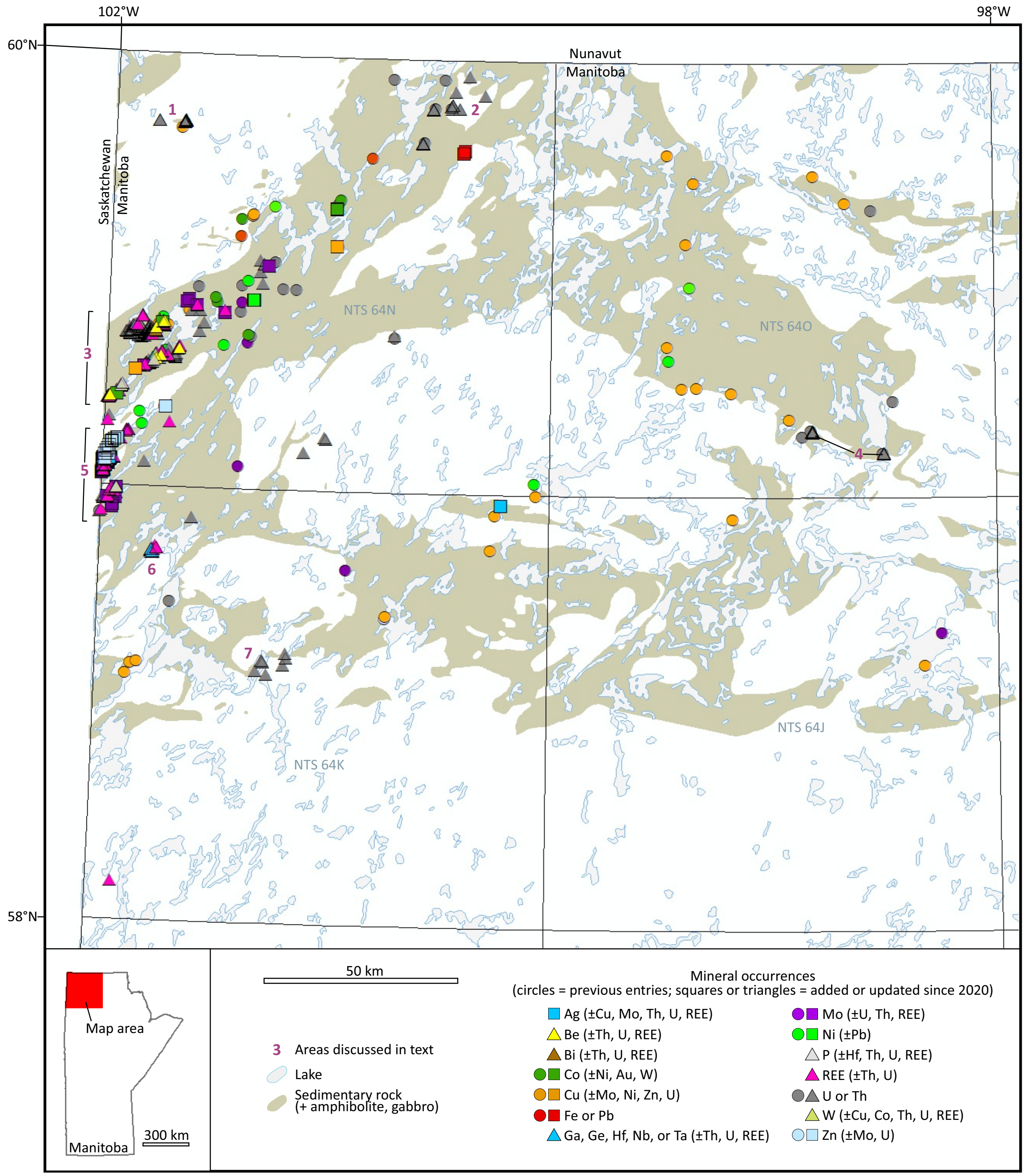

***Figure GS2021-1-2:** NTS areas 64J, K, N and O showing mineral occurrences, including new data added to the Manitoba Mineral Deposits Database in 2021.*

1.43% U and 1009 ppm Th (Assessment Files 92143 and 92137).

5) A total of 327 occurrences were added to areas north and south of Allnutt Lake. In addition to widespread anomalies of uranium and thorium (up to 3.22% U and 1.52% Th), boulder sampling in this area returned many significant REE and Mo values (up to 9.1% total REE—including 3.8% Ce and 1.8% La—and 5.5% Mo; Assessment File 74417). A series of zinc occurrences is also evident along a northnortheast trend near the Saskatchewan border (Figure GS2021-1-2), with Zn contents of up to 5900 ppm from surface, and up to 2400 ppm in drillcore (Assessment Files 74417 and 90211). South of Allnutt Lake, hafnium and phosphorus occurrences include values of up to 553 ppm Hf and 14.1% P_2O_5.

6) Several samples containing >5% total REE were added near the southwestern shore of Misty Lake, including one sample with 10.5% total REE (or approximately 12.3%

total rare-earth oxides; Assessment File 74417). Some of the samples also contain elevated Ga (up to 113 ppm) and Hf (up to 295 ppm). Although the MDD did not previously include any occurrences in this area, Kremer et al. (2010) did comment on the "significant potential for high-grade U and REE deposits" in the region.

7) A series of boulder samples collected from an area north of Peacey Lake contain elevated thorium contents (up to 0.08% ThO_2; Assessment File 93419).

Economic considerations

Current results of the MDD update project highlight the value of data hidden in historical datasets such as industry assessment reports. Among the mineral occurrences added to parts of northwestern Manitoba and the Island Lake region, several warrant emphasis in mineral-potential assessments, and may directly inform related land-use planning, future survey activities, or mineral-sector investment decisions. Examples of significant findings not featured in the previous version of the MDD include the above-described high-grade gold, Ni-Cu-Pt-Pd and graphite in the Island Lake region, and high-grade REE and uranium in northwestern Manitoba. These new results can be filtered or classified by grade, as relevant geochemical data are included in all new MDD entries.

Critical minerals, including resources required for low-carbon technologies such as batteries and solar panels, are anticipated to play an increasing role in the Canadian economy (Natural Resources Canada, 2021). In addition to the above-mentioned occurrences of REE, graphite and platinum-group elements, new critical-mineral occurrences identified in parts of Manitoba so far include findings of antimony, bismuth, chromium, cobalt, copper, gallium, germanium, molybdenum, nickel, niobium, tantalum, tellurium, tungsten, vanadium and zinc. Many of these occurrences were effectively ignored in the historical reports and it is expected that continued MDD updates will lead to improved understanding of critical-mineral potential in Manitoba.

Acknowledgments

The author thanks S. Gallagher, P. Goernert, J. Janssens and K. St. Paul for their assistance with the MDD update; C. Böhm and T. Martins for their reviews; E. Orovan and G. Fortin (British Columbia Geological Survey) for their advice and collaboration on some aspects of this work; and various staff at Orix Geoscience Inc. and Purple Rock Inc. for their helpful advice.

References

Arriaga-Varela, E.J. and Takahashi, T. 2019: Automatic georeferencing of heterogeneous historic and illustrated maps; Abstracts of the International Cartographic Association, v. 1, abstract 15, URL <https://doi.org/10.5194/ica-abs-1-15-2019>.

Conley, G.G., Heine, T.H., Prouse, D.E. and Leskiw, P.D. 2009: Mineral Deposits Database; Manitoba Science, Technology, Energy and Mines, Manitoba Geological Survey, URL <https://www.manitoba.ca/iem/geo/gis/databases.html> [January 2021].

Hayes, T.S., Miller, M.M., Orris, G.J. and Piatak, N.M. 2017: Fluorine; Chapter G *in* Critical mineral resources of the United States–Economic and environmental geology and prospects for future supply, K.J. Schulz, J.H. DeYoung, R.R. Seal and D.C. Bradley (ed.), U.S. Geological Survey Professional Paper 1802, p. G1–G80.

Kadel-Harder, I.M., Spry, P.G., McCombs, A.L. and Zhang, H. 2021: Identifying pathfinder elements for gold in bulk-rock geochemical data from the Cripple Creek Au–Te deposit: a statistical approach; Geochemistry: Exploration, Environment, Analysis, v. 21, no. 1, URL <https://doi.org/10.1144/geochem2020-048>.

Kremer, P.D., Carlson, A.R. and Couëslan, C.G. 2010: Far North Geomapping Initiative: geological mapping of the Misty Lake area, Manitoba (parts of NTS 64K12, 13, 64N4); *in* Report of Activities 2010, Manitoba Innovation, Energy and Mines, Manitoba Geological Survey, p. 50–61, URL <https://www.manitoba.ca/iem/geo/field/roa10pdfs/GS-4.pdf> [September 2021].

Natural Resources Canada 2021: Critical minerals; Natural resources Canada, URL <https://www.nrcan.gc.ca/our-natural-resources/minerals-mining/critical-minerals/23414> [September 2021].

Ontario Geological Survey 2020: Mineral Deposit Inventory; Ontario Geological Survey, Mineral Deposit Inventory (September 2020 update), online database, URL <https://www.geologyontario.mndm.gov.on.ca/MDI_Description.html> [January 2021].

Quinn, H.A. 1960: Island Lake, Manitoba-Ontario; Geological Survey of Canada, Map 26-1960, scale 1:253 440, with descriptive notes.

Rinne, M.L. 2017: Preliminary results of bedrock mapping at Bigstone Lake and Knight Lake, northwestern Superior province, Manitoba (parts of NTS 53E11, 12, 13, 14); *in* Report of Activities 2017, Manitoba Growth, Enterprise and Trade, Manitoba Geological Survey, p. 19–29, URL <https://www.manitoba.ca/iem/geo/field/roa17pdfs/GS2017-3.pdf> [October 2021].

Rinne, M.L. 2020: Progress report on updates to the Manitoba Mineral Deposits Database, east-central Manitoba (NTS 53E, F); *in* Report of Activities 2020, Manitoba Agriculture and Resource Development, Manitoba Geological Survey, p. 9–12, URL <https://www.manitoba.ca/iem/geo/field/roa20pdfs/GS2020-2.pdf> [October 2021].

Rinne, M.L. 2021: Updates to the Manitoba Mineral Deposits Database, east-central Manitoba (NTS 53E, F); Manitoba Agriculture and Resource Development, Manitoba Geological Survey, Data Repository Item DRI2021019, Microsoft® Excel® file, URL <https://www.manitoba.ca/iem/info/libmin/DRI2021019.xlsx> [November 2021].

Sillitoe, R.H. 2010: Porphyry copper systems; Economic Geology, v. 105, p. 3–41.

GS2021-2

Results of a preliminary investigation into the lithium mineralization, distribution trends and remobilization in the Tanco pegmatite, southeastern Manitoba (part of NTS 52L6)

by C.M. Breasley[1], T. Martins, L.A. Groat[1] and R.L. Linnen[2]

In Brief:

- Samples of the Tanco pegmatite were taken from drillcore showing different mineralogies, textures and zones associated with lithium mineralization
- High lithium assay values do not always correspond to lithium aluminosilicate (e.g., spodumene) rich zones
- Future analysis of samples will include petrography, electron probe analysis and geochronology of columbite and apatite minerals

Citation:
Breasley, C.M., Martins, T., Groat, L.A. and Linnen, R.L. 2021: Results of a preliminary investigation into the lithium mineralization, distribution trends and remobilization in the Tanco pegmatite, southeastern Manitoba (part of NTS 52L6); *in* Report of Activities 2021, Manitoba Agriculture and Resource Development, Manitoba Geological Survey, p. 8–17.

Summary

Drillcore and underground samples were collected at the Tanco pegmatite of southeastern Manitoba in August 2021 to investigate the timing of mineralization phases and subsequent metasomatic processes, which influenced the modern-day Li distributions. Samples taken recorded representative changes in mineralogy, textures and zonation in the southwestern Li-rich region of the pegmatite. Preliminary observations show diverse mineralogical assemblages in drillcore crosscutting zones that correlate with high Li assay values. Future work will include thin-section petrography to confirm the relations of minerals, electron microprobe–based analysis to investigate the mineral chemistry of different generations of Li mineralization, and in situ geochronology of columbite group minerals and apatite to provide ages for the mineralization.

Introduction

Pegmatites are a compelling field of study due to both the dynamic and scientifically interesting modes of genesis and the significant economic importance they can possess (London and Kontak, 2012). The Li-Cs-Ta (LCT) Tanco pegmatite, part of the Winnipeg River–Cat Lake pegmatite field in southeastern Manitoba, presents an exceptional example of pegmatite evolution, fractionation and zonation on all scales from regional to mineralogical. Underground sampling and access to the core library at Tanco provide an excellent opportunity to collect a range of samples from each pegmatite zone, including subsurface exposures. This project aims to investigate the timing of mineralization phases and subsequent metasomatic processes that influenced the modern-day Li distributions. Analysis of the distributions of primary spodumene, petalite, lepidolite and Li phosphates will elucidate crystallization relationships and relative timings of pegmatite emplacement and alteration. This will allow the analysis of mineralization trends from which larger scale conclusions can be drawn and related to other deposits. In addition, this project presents an opportunity to utilize new methods that have been developed more recently and helped improve the general understanding of pegmatite emplacement and development to provide a new perspective on the geological history of this world-class deposit.

Due to logistical and access difficulties, the field sites at Tanco have not been open to sample collection and scientific study for the last decade (e.g., Van Lichtervelde et al., 2008; Kremer, 2010; Camacho et al., 2012). Fieldwork and analysis of this area provides an excellent opportunity to develop new ideas and constrain the Li evolution and mineralization of the region.

Geological setting

The Tanco pegmatite is located within the Bernic Lake group of pegmatites in the Cat Lake–Winnipeg River pegmatite district of southeastern Manitoba (Figure GS2021-2-1). The pegmatites form part of the southern limb of the Bird River greenstone belt (2.75–2.72 Ga; Gilbert, 2006). This belt hosts multiple units divided into northern and southern assemblages, and forms part of the greater Archean Superior province. For detailed descriptions of the Bird River greenstone belt lithologies, refer to Gilbert (2006, 2007, 2008). The Bernic Lake formation (2724.6 ±1 Ma; Gilbert, 2008) forms a 2 by 45 km unit that is composed predominantly of mafic volcanic rocks. It is found in the southern region of the Bird River greenstone belt and contains the Tanco gabbro, the main host of the Tanco pegmatite. The Tanco gabbro crystallized at 2723.1 ±0.8 Ma and was subsequently subjected to amphibolite-grade metamorphic conditions, along with other lithologies in the region, that produced a classic Abukuma-style metamorphic assemblage (Černý, 2005; Gilbert,

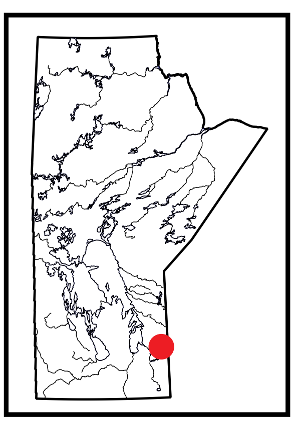

[1] Department of Earth, Ocean and Atmospheric Sciences, The University of British Columbia, Vancouver, British Columbia
[2] Department of Earth Sciences, Western University, London, Ontario

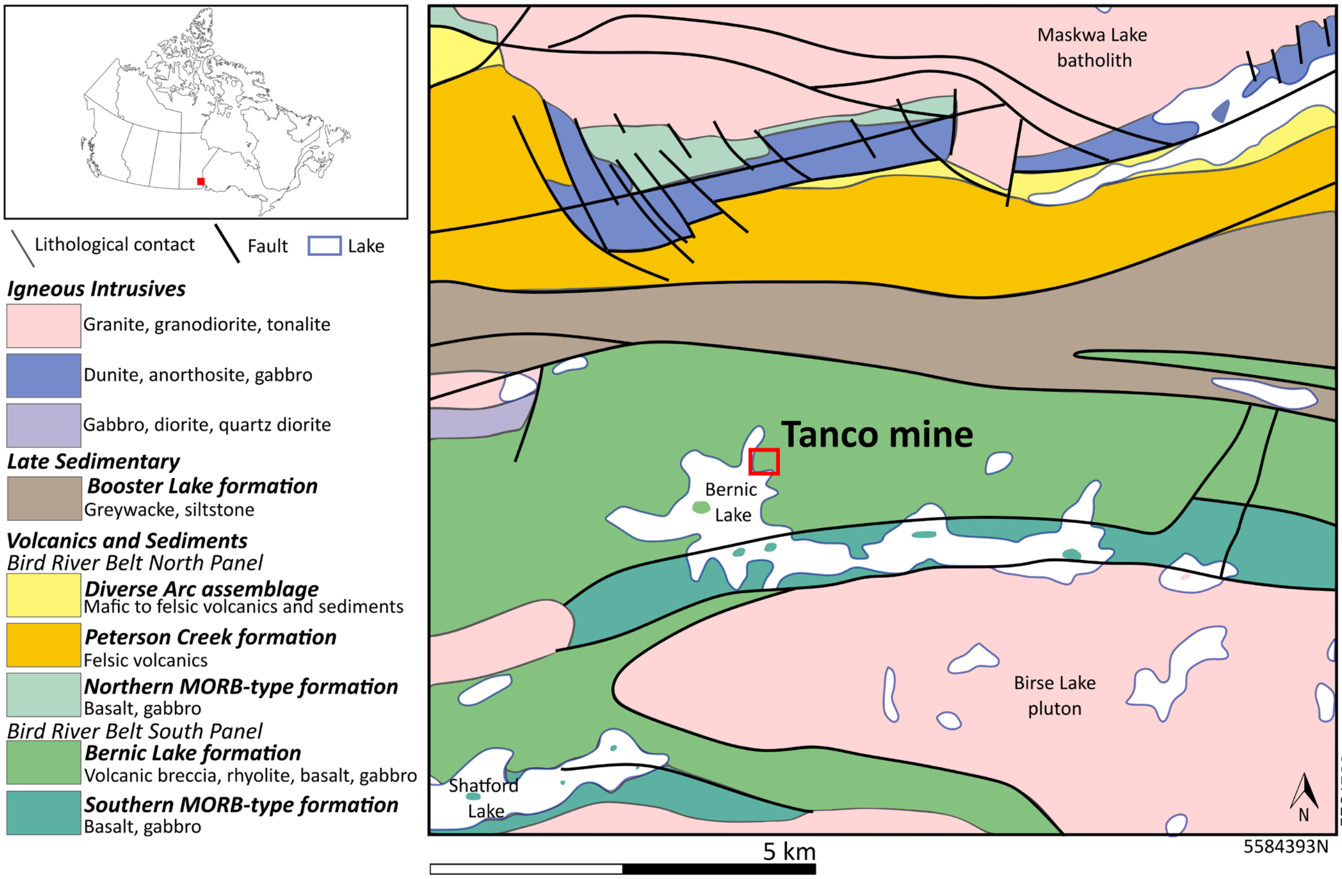

Figure GS2021-2-1: *Geographic location and local geology of the Tanco mine (red square) area, southeastern Manitoba (adapted from Gilbert, 2008). Abbreviation: MORB, mid-ocean–ridge basalt.*

2008; Kremer, 2010). Ages and spatial associations suggest that the Bernic Lake Formation and the Tanco gabbro formed as a result of a single episode (Kremer, 2010).

The Cat Lake–Winnipeg River pegmatite district is large and is subdivided into the Winnipeg River and the Cat Lake–Maskwa Lake subdistricts (Černý et al., 1981). There are multiple further groups within these divisions, including the Bernic Lake pegmatite group (part of the Winnipeg River subdistrict) that includes the Tanco pegmatite. The Bernic Lake group hosts multiple pegmatites that are enriched in Li, but no others are the size and proportions of Tanco, the largest and most Li-rich pegmatite of the group.

Tanco pegmatite

The morphology of the Tanco pegmatite is bilobate and can be traced for 1520 m in length, 1060 m in width and 100 m in thickness (Černý, 2005). It is entirely located in the subsurface and does not outcrop, but has been extensively drilled during past mining and exploration endeavours.

The Tanco pegmatite has been interpreted to have intruded at 2641 ±3 Ma (U-Pb tantalite dating; Camacho et al., 2012) and 2647.4 ±1 Ma (U-Pb zircon dating; Kremer, 2010). These dates correspond with a phase of tectonism in the region at 2650–2640 Ma that is hypothesized to have reactivated the Bernic Lake shear zone, which facilitated intrusion of the pegmatite along the west- and east-trending fault system of the region (Kremer, 2010; Martins et al., 2013). Although the parental granitic source or feeder zone for the pegmatite has not been found (Černý et al., 1996), it has been hypothesized that it should be located beneath the crystallized zone (Bradley et al., 2017). Upon emplacement, the intrusion crystallized in a unique pattern. In contrast to the typical pegmatite crystallization pattern of border zone inward solidification, Tanco is thought to have crystallized in a honeycomb-shaped pattern, leading to complex, evolutionary, geochemical enrichment patterns in the various zones (London, 2008).

Tanco is classified as a complex LCT pegmatite of petalite subtype (Černý and Ercit, 2005) that is peraluminous in composition and depleted in Fe, Mg and Ca (London, 2008). This classification was selected because the dominant primary phase of Li mineralization was petalite, even though the vast majority of this mineralogy subsequently re-equilibrated to spodumene and quartz (SQUI) intergrowths. The presence of mineral assemblages that are indicative of other LCT subclasses, such as primary spodumene, amblygonite-montebrasite and lepidolite, also occur in this pegmatite (Černý, 2005).

Zone mineralization

Tanco has been historically divided into nine major mineralized zones that are geochemically, texturally and mineralogically distinct (Stilling, 1998). These zones have been described extensively in previous works (e.g., Černý et al., 1998; Černý, 2005; Stilling et al., 2006); this report presents a brief overview of the main characteristics of each zone.

Zone 10 (border zone): This is a fine crystalline contact zone with amphibolitic country rock that represents the portions of the Tanco pegmatite that crystallized first. It is the least geochemically evolved section of the pegmatite, typically hosts a composition of mainly albite and quartz, and is less than 30 cm in thickness.

Zone 20 (wall zone): This zone is located in the footwall, has a thickness of up to 35 cm and is predominantly megacrystic microcline-perthite with major components of quartz, albite and lithian muscovite.

Zone 30 (albitic aplite zone): The main constituents of this zone, which can exceed 16 m in some areas, include albite and quartz with lesser muscovite. An interesting feature is the presence of a 'beryl fringe' found at contact zones with other units, and it is typically associated with Ta and Nb mineralization.

Zone 40 (lower intermediate zone or mixed zone): This zone is up to 25 m thick and consists mainly of microcline-perthite crystals and intimate growths of spodumene and quartz that follow the remnant crystalline structure of petalite crystals. Other components include quartz, albite, mica and amblygonite.

Zone 50 (upper intermediate zone): This unit is up to 24 m thick and generally has a gradational contact with zone 40. There is a notable lack of albite and mica, which aids in distinguishing it from zone 40. The main components are SQUI, amblygonite, petalite and pollucite.

Zone 60 (central intermediate zone): This zone is up to 45 m thick and has notably sharp contacts. It hosts prominent Ta- and Nb-oxide mineralization within major components of microcline-perthite, quartz, albite and muscovite.

Zone 70 (quartz zone): Zone 70 comprises monomineralic lenses as opposed to the classic quartz-rich core typically found in highly evolved pegmatites. It is difficult to distinguish in drillcore from quartz pods present in other zones and can contain minor amblygonite and spodumene as rare accessory phases.

Zone 80 (pollucite zone): This zone is geochemically part of zone 50 but large enough in scale to be defined as a new unit. It hosts a remarkably 75% pure pollucite unit and is commonly crosscut by later veins of lepidolite, quartz and feldspar.

Zone 90 (lepidolite zone): This zone is >18 m thick and is predominantly composed of relatively fine-grained lithian mica. It is economically important due to the high content of Rb and Cs micas, and Ta and Nb oxides.

The multiple geological cross-sections that have been constructed using these zone definitions at Tanco show the complex nature and spatial relationships of the zones (Stilling et al., 2006).

Geochemical evolution

The degree of fractional crystallization at Tanco can be revealed by whole-rock geochemical evolutionary-trend indicators: K/Rb = 4.7, K/Cs = 9.3, Rb/Cs = 2.0, Rb/Tl = 137, Fe/Mn = 0.63, Mg/Li = 0.02, Al/Ga = 917, Zr/Hf = 2.6, Zr/Sn = 0.21 and Nb/Ta = 0.19 (Stilling et al., 2006). These values suggest that the Tanco pegmatite represents a highly evolved pegmatitic melt (Černý, 2005).

From less to more evolved zones of the pegmatite, the mineralogies of different crystal groups are seen to reflect the increase in volatiles and incompatible elements over time as the body crystallized. These studies suggest that Tanco underwent a complex crystallization history and preserved an interesting end-member scenario of least to most evolved zones. An increase in rare alkalis in feldspar and beryl with evolution is evidenced by the incorporation of increasing Li, Rb and Cs into crystal structures (London, 2008). Tourmalines exhibit a transition from Fe- and Al-rich schorl-foitite-olenite to Li- and Al-rich elbaite-rossmanite (Selway et al., 2000a; London, 2008). Oxides in the deposit tend to shift from columbite and wodginite assemblages (disordered Sn, Nb and Ta minerals) to more ordered simpsonite, stibiotantalite, tantite and lithiowodginite (Grice et al., 1972; Selway et al., 2000a; Černý, 2005). A muscovite to lepidolite mica transition was also noted (Van Lichtervelde et al., 2008).

Mineralogy

Tanco is known for its diverse mineralogy, with more than 100 minerals having been identified within the pegmatite (Černý, 2005; Martins et al., 2013). This section describes the dominant mineral phases that were sampled in this study for their potential Li-bearing nature or association with Li mineralization.

Silicates

Lithium aluminosilicates: petalite ($LiAlSi_4O_{10}$), spodumene ($LiAlSi_2O_6$) and eucryptite ($LiAlSiO_4$)

Petalite is found in zones 50 and 80 as individual crystals with amblygonite-montebrasite, pollucite and feldspar (Černý and Ferguson, 1972). Petalite is not common throughout the pegmatite and is mostly replaced by SQUI.

Spodumene is milky white in colour and can range in size from micro-SQUI texture to megacrysts. Černý and Ferguson (1972) described three different types of spodumene at the Tanco pegmatite: 1) secondary breakdown product of petalite into spodumene and quartz intergrowths (known as SQUI); 2) primary spodumene; and 3) spodumene that has broken down and recrystallized into spodumene and quartz. This final spodumene type is distinct from SQUI and occurs as coarser crystals that lack the intimate intergrowth textures shown by SQUI. In zones 40 and 50, 90% of the spodumene is SQUI, which is the target for Li exploration and mining.

Eucryptite at Tanco is grey to pink with a distinct red-orange fluorescence in ultraviolet light (Černý, 1972). Crystals are up to 4 cm long and occur as individual crystals, intergrown with SQUI or in crosscutting vein structures.

The Li aluminosilicate relationships at Tanco are explained by a reaction path that shows the nature of primary Li crystallization (London, 1986; London, 1990; Černý et al., 1998). The hypothesized crystallization path shows an initial primary petalite crystallization phase from a hydrous melt. As the melt cools, it crosses the petalite-spodumene reaction boundary, where the bulk of petalite is hypothesized to have broken down into SQUI. The crystallization path then shows a period of primary spodumene growth, followed by a transition to primary eucryptite growth as the spodumene-eucryptite reaction boundary is crossed at 270°C and 1.8 kbar.

Feldspars

Feldspars found at Tanco include albite, which is commonly present as radial aggregates that show a cleavelandite texture. The albite is typically milky white and characteristically shows multiple striations. Microcline-perthite also occurs commonly and is orange to pale pink with mottled internal exsolution textures visible in hand sample. Orthoclase has also been identified but is more rare (Brown et al., 2017).

Quartz

Quartz occurs as equant primary phases in multiple zones (e.g., zones 70, 90, and 60; Černý et al., 1996). It can be found as smoky quartz (where related to Ta mineralization) and intergrown with spodumene (Černý et al., 1996), as well as equant pale white-grey crystals.

Micas

A wide variety of micas can be found in nearly all zones of the Tanco pegmatite. Magnesium-rich, dark brown to black biotite is found in zone 10, whereas late-stage green metasomatic mica, white muscovite, lithian mica and lepidolite occur elsewhere (Rinaldi, 1972). There are noticeable changes in the growth habits of micas from curvilamellar 'ballpeen' crystals to normal micaceous books. The micas at Tanco were described by Rinaldi (1972) and were investigated in relation to Ta mineralization by Van Lichtervelde et al. (2008).

Tourmalines

Tourmaline is easily distinguishable and abundant in many zones. Multiple types have been identified that have highly variable colours based on their crystal chemistry and correlate with different mineralogical zones. In zones 10, 20, 30 and 60, the tourmalines tend to be brown/black, and occasionally green, in colour. Pink and green tourmalines are found in zones 40 and 50 (Selway et al., 2000a). Tourmalines present a detailed geochemical evolution series and are also found in contact zones with the country rock (Selway et al., 2000b).

Beryls

Beryl is a common accessory phase found in almost every pegmatite zone at Tanco. It has a variable composition and colour and is typically found as hexagonal dispersed crystals (Černý and Simpson, 1977). A prominent example of this is the white, Cs-rich beryl in zone 30 (Martins et al., 2013).

Phosphates

Amblygonite-montebrasite

The amblygonite-montebrasite series occurs as large primary crystals up to 1.5 m in size but can also be present as smaller tabular aggregates (from 1 to 3 cm in size). Montebrasite can also be present as a secondary phase along grain boundaries and fractures (Černá et al., 1972).

Apatite

Apatite occurs as an accessory phase in almost all zones at Tanco, commonly in a pale blue to blue-black colour (Černý et al., 1996).

There are multiple other phosphates present, but this study details minerals that occur in large amounts. It has never been economical to mine phosphates at Tanco, but analysis of the Li distributions in the different mineral phases could provide information on future mining sources, which could become economic.

Oxides

Ta/Nb oxides

Tantalum and niobium oxides represent one of the most economically important groups of minerals found at Tanco. They typically occur as discrete dark specks accompanied by proximal red staining and can be difficult to classify in hand sample (Černý et al., 1996).

Other

Other minor phases at Tanco include sulphides, native elements, halides, carbonates, sulphates and borates. Tanco has also been the source of major new mineral discoveries, including černýte, $Cu_2(Cd,Zn,Fe)SnS_4$, a tetragonal metallic sulphide (Kissin et al., 1978); and tancoite, $HNa_2LiAl(PO_4)_2(OH)$, an orthorhombic-dipyramidal anhydrous phosphate (Ramik et al., 1980). Ercitite, $Na_2(H_2O)_4[Mn^{3+}{}_2(OH)_2(PO_4)_2]$ was also identified at Tanco (Fransolet et al., 2000). Groatite, $NaCaMn_2(PO_4)[PO_3(OH)]_2$, a translucent and vitreous phosphate typically found in acicular sprays, was also discovered (Cooper et al., 2009), along with titanowodginite, (Mn>Fe)(Ti>Sn, Ta, Fe)$(Ta{>}Nb)_2O_8$, a monoclinic-prismatic oxide (Ercit et al., 1992). For an extensive list of minerals present at Tanco the reader is referred to Martins et al. (2013).

Lithium at Tanco

Lithium exploration and extraction is becoming increasingly important as the world transitions to greener sources of energy that depend heavily on the use of rechargeable batteries. The Li mineralization at Tanco is also commercially important for use in ceramics due to its low Fe content (Černý and Ferguson, 1972).

The bulk of Li mineralization at Tanco is found in the Upper Intermediate zone (zone 50), where the megacrystic nature and low Fe content make spodumene an attractive exploration target. However, the majority of the spodumene at Tanco occurs in a recrystallized SQUI form (Černý, 2005). This breakdown, as previously mentioned, is interpreted to have replaced petalite; however, it is debated whether this process is entirely isochemical (Lima and Dias, 2019). As petalite can only take up a certain volume of Fe into its structure, it can be expected that the SQUI would inherit this low Fe content if the breakdown process is entirely isochemical. If the breakdown path is not isochemical, unfavourable chemical contamination from external fluids and reactions can make the spodumene less economically viable for extraction. Secondary hydrothermal alteration can also introduce Fe contamination from fluids, which is undesirable for extraction purposes (Černý, 1972).

The metasomatic effect of Tanco on the country rock is known to have occurred on a large scale (Morgan and London, 1987). Whether other metasomatic processes were pervasive throughout the entire crystallized body is unknown. This is an important field of study, as this knock-on effect has the potential to alter the economic viability of Li extraction at Tanco.

Analysis of whether Li was remobilized during interaction with hydrothermal fluids on a large scale is also important, as high-grade regions within the pegmatite could be the result of reprecipitation along fractures. Weathering processes have also acted on Tanco, where primary Li silicates have broken down into secondary assemblages (e.g., petalite breaking down into montmorillonite; Černý, 2005).

It is traditionally assumed that spodumene and petalite are the most important minerals for Li extraction (Kesler et al., 2012), with spodumene and SQUI being the current targets of mining at Tanco. There has been little research to assess the Li concentrations of other minerals, so potential exists to open up new avenues of future economic viability.

Understanding the nature of Li distribution between minerals and assessing its mode of transportation are key in analyzing enrichment patterns and drawing conclusions regarding deposit-scale mineralization. Two of the greatest unknowns in the current understanding of pegmatites are 1) the distinction between magmatic and metasomatic processes; and 2) the impact these processes have on the control of mineralization (Kontak, 2020). This is particularly true for Li because the relations between Li-bearing silicate and phosphate minerals in magmatic, metasomatic and hydrothermal environments remain poorly constrained.

Summary of fieldwork

Between the 9th and 20th of August 2021, underground sampling and drillcore logging and sampling were conducted at the Tanco mine. The underground zone selected for sampling was an area that is currently being mined for Li and hosts lithologies with diverse zonation and mineralogy (Figure GS2021-2-2). This region is thus promising for an investigation of how Li-mineral assemblages are dispersed and altered.

Sampling strategy

Drillcore sampling

Four transects of drillholes were selected in the Li-rich region of the pegmatite. These transects, labelled A, B, C and D, are oriented east-west and cores from six drillholes were sampled per transect (Figure GS2021-2-2).

Drillcore logs and assay values were cross-referenced with drillcore upon sampling. Rock samples were collected to be representative of the different mineralized zones described in the drillcore logs and assay values (Sinomine, unpublished data, 2021). Major textural changes within the cores were noted and sampled, and mineral assemblages from each drillhole were sampled for further analysis. These mineral assemblages included Li silicates, amblygonite, mica, quartz, albite, potassium feldspar, phosphates, apatite, Ta oxides, tourmaline and any other notable mineralized phases (Figure GS2021-2-3).

Notes were made on whether the minerals appeared to be primary or secondary in nature, based on textural evidence, crystal size and appearance. Samples of the upper and lower contact of the pegmatite with the country rock were also taken, along with a sample as far as possible from the pegmatite lower contact for potential future Ar/Ar analysis.

Underground sampling

Lithium West and Lithium South, two regions of active Li mining, were visited over two days and pegmatite zones and mineral assemblages were identified and sampled. Both areas contain large (up to 5 m) crystals of SQUI and spodumene, with other megacrysts of feldspars and quartz (Figure GS2021-

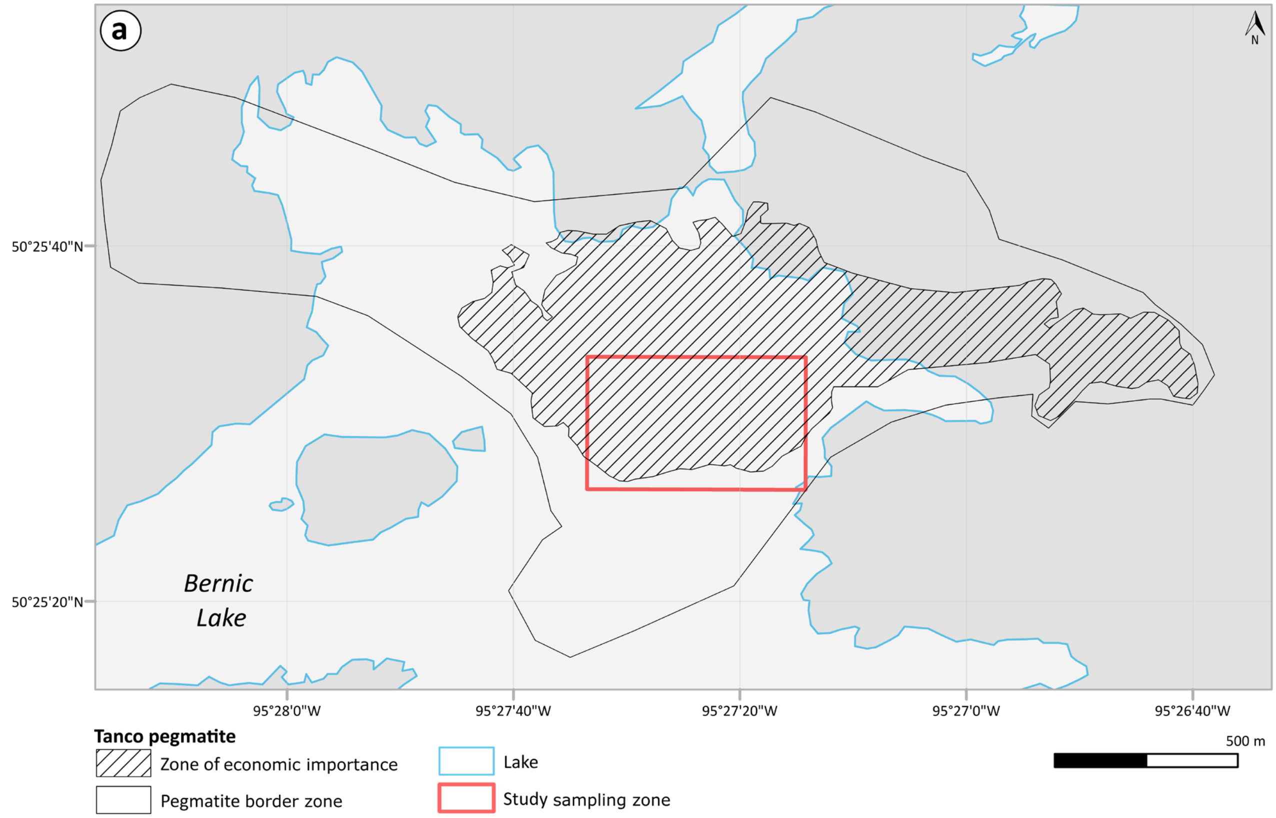

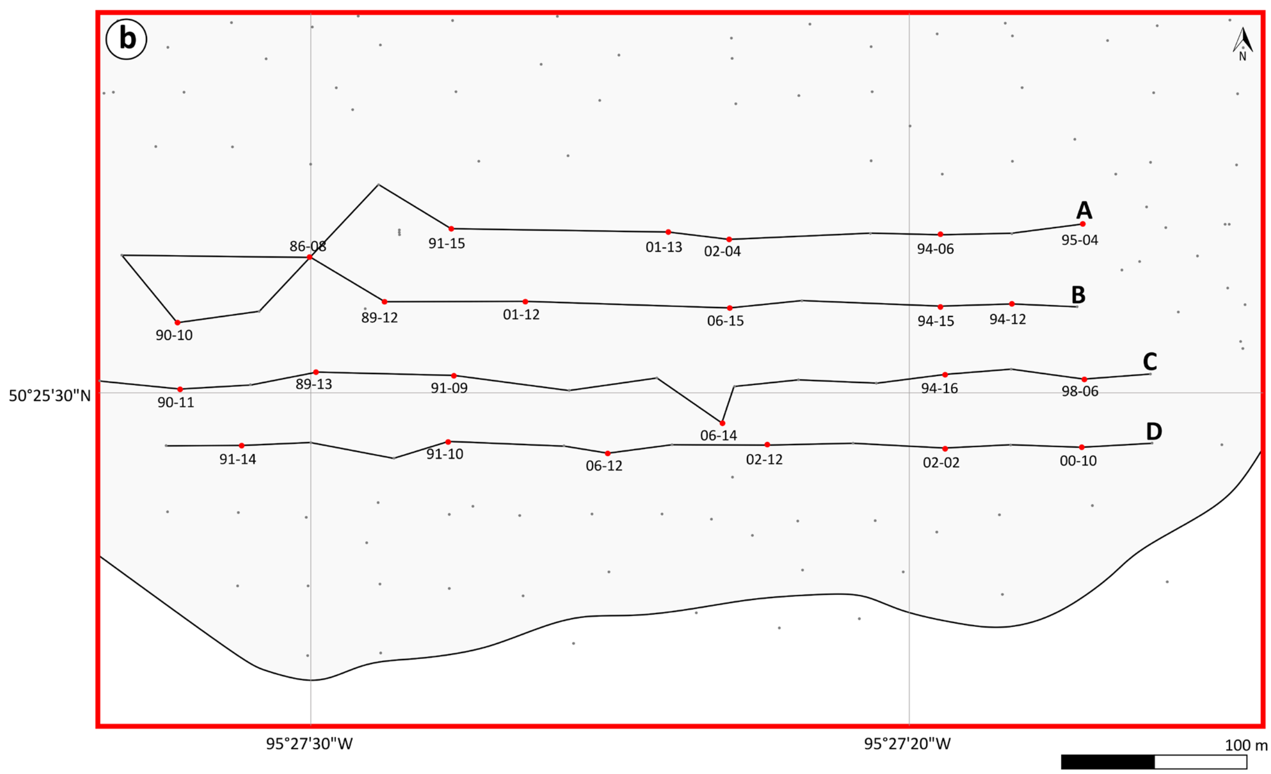

Figure GS2021-2-2: a) *Outline of the Tanco pegmatite border zone (Stilling et al., 2006) and zone of economic importance (Sinomine, unpublished data, 2021) projected to surface and shown in relation to Bernic Lake; study area is highlighted by red box;* ***b)*** *Sampled drillcore locations along four selected transects (A, B, C and D) of a Li-rich region of the Tanco pegmatite (shown by diagonal hatching on grey background). Red dots indicate location of sampled drillcore (with drillhole number). Grey dots beyond transect lines indicate drillholes not sampled.*

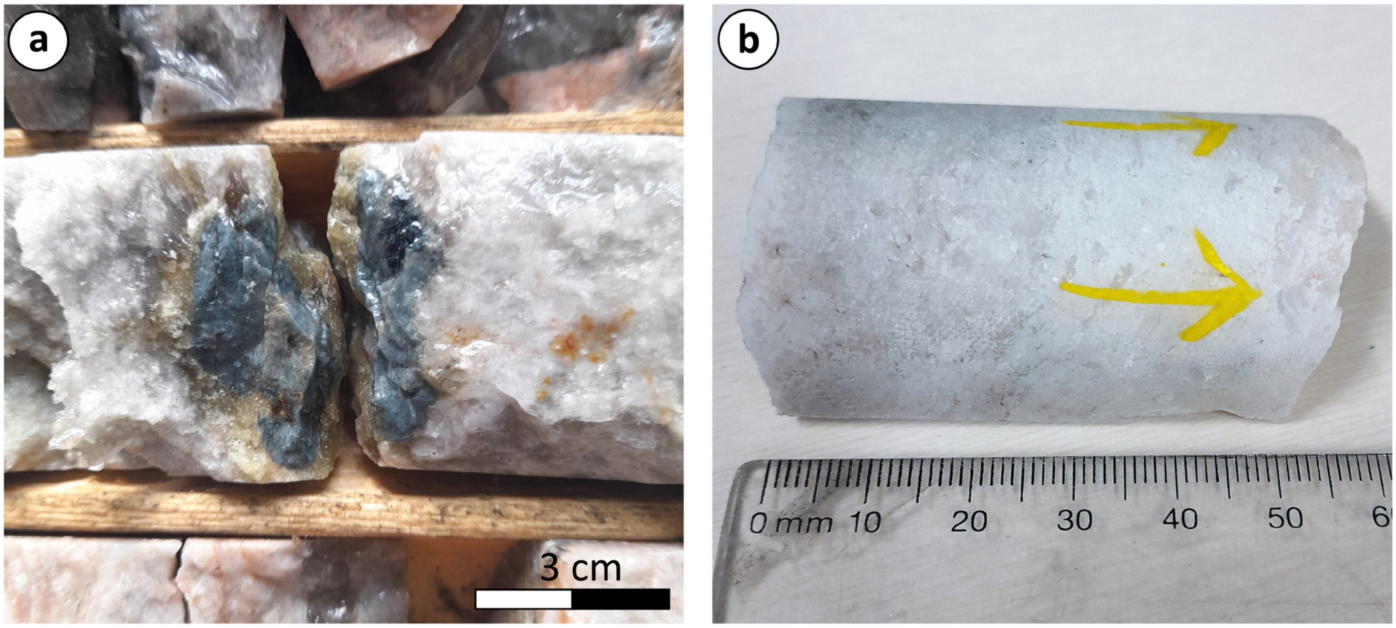

Figure GS2021-2-3: *Drillcore samples showing **a)** large central apatite crystal (blue) with secondary metasomatic microcrystalline mica halo (green) within pale grey SQUI (sample CB18.08.21, 91-10, B5C3, 173.9–174.4 ft); and **b)** classic SQUI intergrowth textures after petalite (sample CB12.08.21, 94-12, B3C2, 95–95.2 ft).*

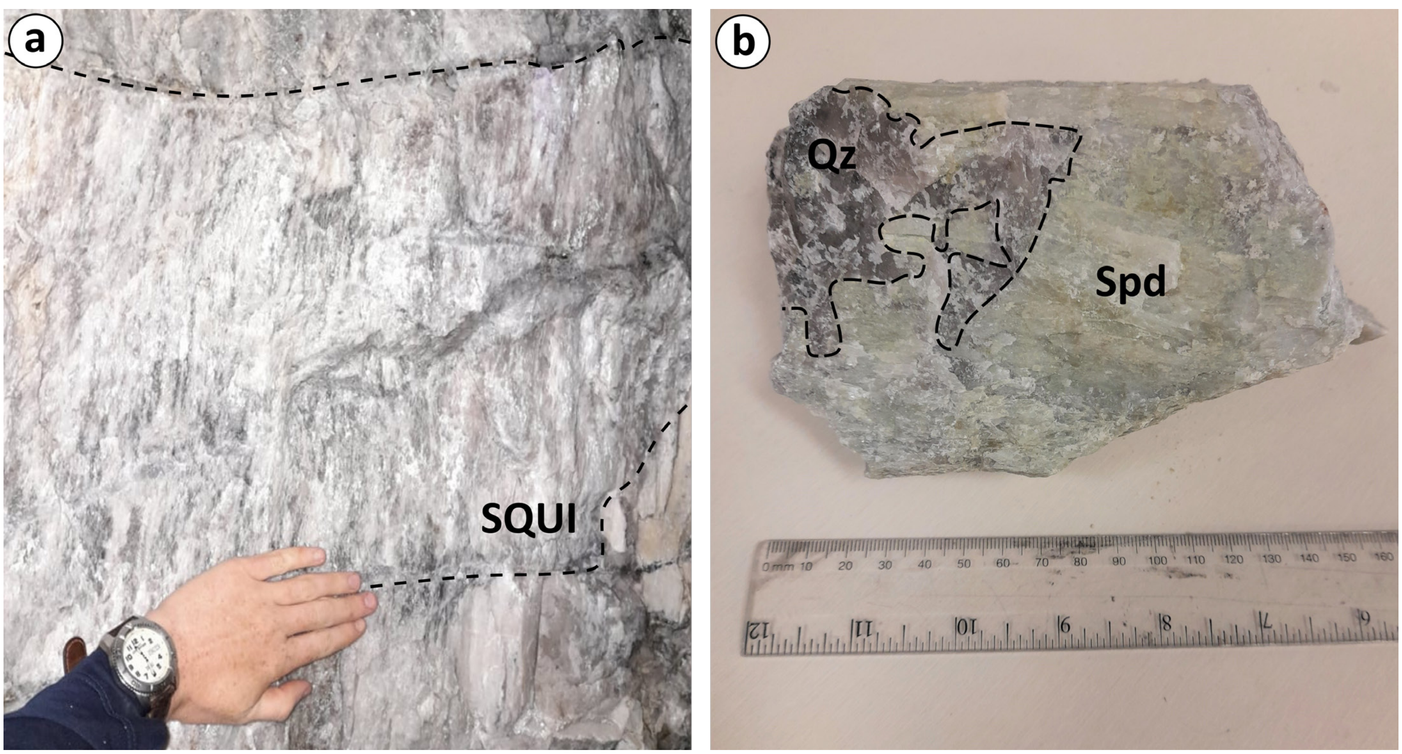

Figure GS2021-2-4: *Underground images and samples showing **a)** large in-place SQUI (spodumene and quartz intergrowth) crystal showing characteristic replacement textures (highlighted with dashed line; hand for scale); and **b)** sample of green spodumene (Spd) and smoky quartz (Qz) from the Li-rich zone.*

2-4). Interesting textures observed include regions indicative of rapid cooling, honeycomb texture and sharp contacts between zones. Multiple underground zones showed transitional boundaries between country-rock rafts and pegmatite mineralization.

Preliminary observations

Some preliminary observations could be made based on sampling of drillcore and underground features. Identification and sampling of multiple minerals, when correlated with Li assay values, suggests that Li concentrations may not be entirely from Li aluminosilicates such as spodumene. Low assay values typically correspond to quartz pods or country-rock rafts, but some regions with diverse mineralogies (in particular the highly variable zone 40) were remarkably low in Li. The multiple spodumene textures observed were interpreted to show both primary and secondary features. Large, pale white spodumene crystals with equant quartz crystals were interpreted to be primary phases (Figure GS2021-2-5a). In contrast, large amounts of SQUI were identified where spodumene occurs as elongate crystals that are intimately intergrown with quartz (Figure GS2021-2-4a). These crystals follow remnant shapes of previous petalite crystals and show finer growths of oriented crystals in comparison to the primary spodumene.

Evidence of metasomatism includes green colouring of micas, fine to coarse crystalline growth in vein structures and mineralogical differences, all of which cut through primary textures within the rock. Various mica growth habits were identified in cores, including ballpeen habit, books of primary micaceous growth and coarse secondary metasomatic growths.

The pegmatite shows varied contact boundaries ranging from gradational to sharp. Some contact zones show monomineralic growth of crystals (in particular beryl) at boundary zones, while others exhibit a submillimetre transition of microcrystalline mineralogy (Figure GS2021-2-5b).

Future work

Laboratory analyses will include thin-section petrography to analyze textural relationships and geochemical analysis to constrain the relative timing of mineralization phases. The micas in the Tanco pegmatite provide a unique opportunity to employ electron microprobe–based analysis to investigate the different generations of precipitation (Tischendorf et al., 1997). The use of electron microprobe and laser-ablation inductively coupled plasma–mass spectrometry techniques will provide new insights into the Li content of the mineral phases and information on the geochemical-partition behaviour of Li into different phases and how this is potentially altered by metasomatic processes. These techniques will also be used to investigate how Li mineralization relates to the various generations of mica precipitation.

Oxygen- and Li-isotope distributions within the rock samples will differentiate fluid-flow processes of metasomatic and hydrothermal origin (Liu et al., 2010; Deveaud et al., 2015). The timing of Li mineralization will be investigated via textural relationships and in situ geochronology of columbite-group minerals, apatite and other suitable minerals. Samples were also collected for possible future Ar/Ar dating of amphibole and mica. This would provide information on the crystallization history and speed of cooling of the pegmatite.

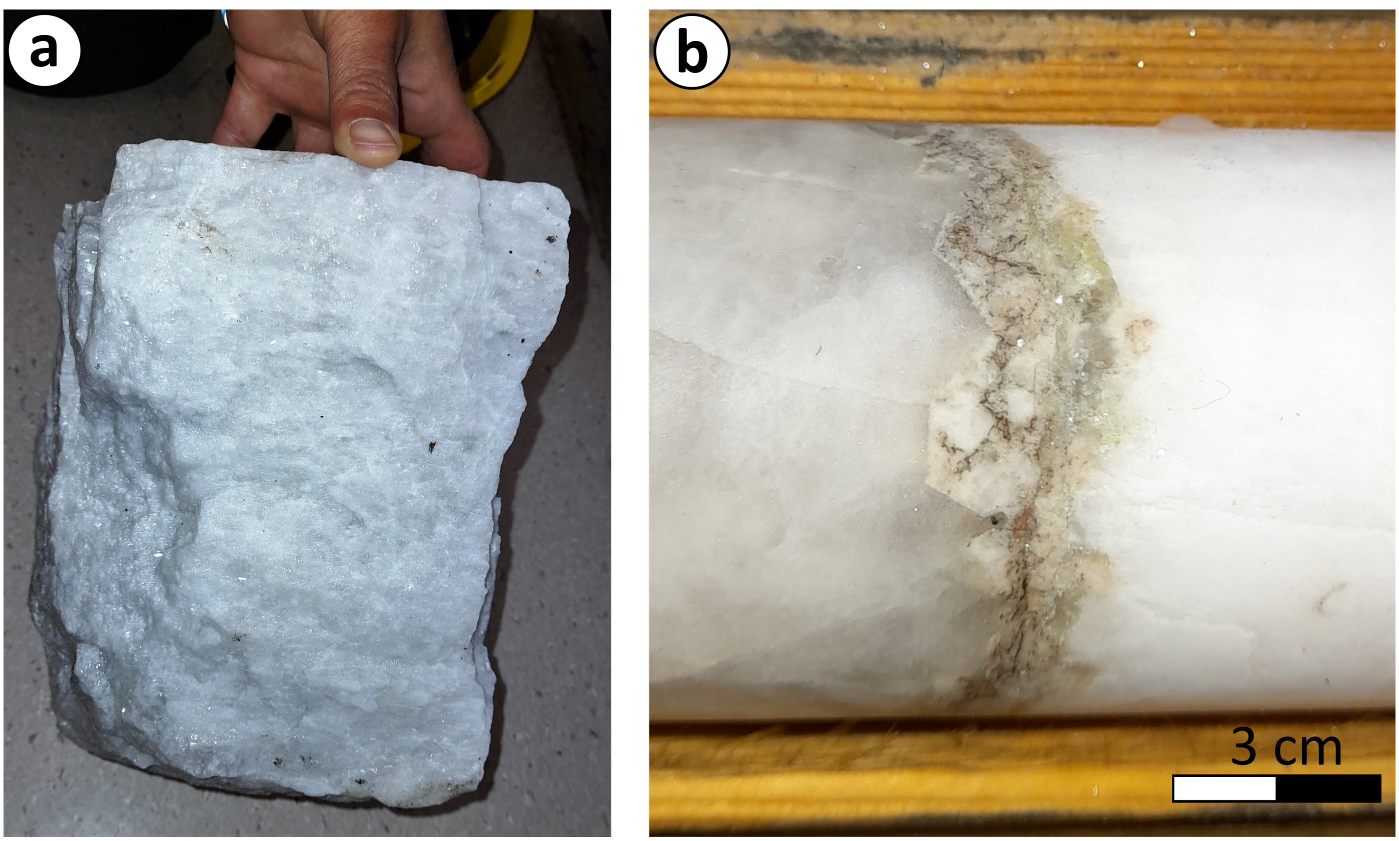

Figure GS2021-2-5: *Images illustrating preliminary observations of* ***a)*** *large monomineralic spodumene sample hypothesized to be primary in nature (hand for scale); and* ***b)*** *beryl fringe showing contact between pale grey quartz (left) and milky white albite (right), with a thin band of green metasomatic mica.*

Economic considerations

Lithium-cesium-tantalum pegmatites host a suite of economically critical elements (Linnen et al., 2012). Lithium is a prime example of a critical element, with research into this element seen to be essential as the world transitions to green technology and a decarbonized economy (Zubi et al., 2018). Furthermore, the government of Canada has recognized it as a critical mineral (Government of Canada, 2021). From use in batteries to ceramics, Li is an important commodity and is often found in association with other critical elements. Examples of these include Ta, Rb and Be. Manitoba has abundant sources of Li, the richest and most economically viable of which lies within the Tanco pegmatite detailed in this study. Knowledge of the processes that led to the accumulation and concentration of Li within this pegmatite is therefore key for targeting and exploring Li sources in this deposit and elsewhere in the region.

Understanding the nature of Li distributions between minerals and assessing its mode of transportation are important in analyzing enrichment patterns and drawing conclusions regarding deposit-scale mineralization. These relationships are vital for targeting and analyzing the economic viability of the deposit and will improve the general scientific understanding of one of the world's best-known examples of highly evolved, economically important pegmatites. The post-fieldwork analysis of these samples currently being undertaken will help elucidate these relationships.

Acknowledgments

The authors express their sincere gratitude to the Sinomine team at Tanco, with special thanks going to S. Rankmore, I. Zhou, and J. Champagne for enthusiastic discussions, enabling access to the underground mine and drillcore, and providing 3-D visualisations of the pegmatite. Thanks are also extended to C. Deveau (Sinomine), who provided continual support during the creation and completion of this project. The authors also thank the Manitoba Geological Survey for supporting this fieldwork and C. Pastula from the University of Winnipeg for valuable field assistance. Edits provided by M. Rinne and C. Böhm assisted in improving drafts of this manuscript. RnD Technical editing services are acknowledged for assistance in editorial work and C. Steffano is thanked for layout and final edits.

References

Bradley, D.C., McCauley, A.D. and Stillings, L.M. 2017: Mineral-deposit model for lithium-cesium-tantalum pegmatites; U.S. Geological Survey, Scientific Investigations Report 2010–5070–O, p. 48, URL <https://doi.org/10.3133/sir20105070O>.

Brown, J.A., Martins, T. and Černý, P. 2017: The Tanco pegmatite at Bernic Lake, Manitoba, XVII – Mineralogy and geochemistry of alkali feldspars; The Canadian Mineralogist, v. 55, p. 483–500, URL <https://doi.org/10.3749/canmin.1700008>.

Camacho, A., Baadsgaard, H., Davis, D.W. and Černý, P. 2012: Radiogenic isotope systematics of the Tanco and Silverleaf granitic pegmatites, Winnipeg River pegmatite district, Manitoba; The Canadian Mineralogist, v. 50, no. 6, p. 1775–1792.

Černá, I., Černý, P. and Ferguson, R.B. 1972: The Tanco pegmatite at Bernic Lake, Manitoba, III – Amblygonite-montebrasite; The Canadian Mineralogist, v. 11, no. 3, p. 643–659.

Černý, P. 1972: The Tanco pegmatite at Bernic Lake, Manitoba, VII – Eucryptite; The Canadian Mineralogist, v. 11, no. 3, p. 708–713.

Černý, P. 2005: The Tanco rare-element pegmatite deposit, Manitoba: regional context, internal anatomy, and global comparisons; *in* Rare-Element Geochemistry and Mineral Deposits, R.L. Linnen and I.M. Samson (ed.), Geological Association of Canada, Short Course Notes, v. 17, p. 127–158.

Černý, P. and Ercit, T.S. 2005: The classification of granitic pegmatites revisited; The Canadian Mineralogist, v. 43, no. 6, p. 2005–2026.

Černý, P. and Ferguson, R.B. 1972: The Tanco pegmatite at Bernic Lake, Manitoba, IV – Petalite and spodumene relations; The Canadian Mineralogist, v. 11, no. 3, p. 660–678.

Černý, P. and Simpson, F.M. 1977: The Tanco pegmatite at Bernic Lake, Manitoba, IX – Beryl; The Canadian Mineralogist, v. 15, p. 489–499.

Černý, P., Ercit, T.S. and Vanstone., P.T. 1996: Petrology and mineralization of the Tanco rare element pegmatite, southeastern Manitoba; Geological Association of Canada/Mineralogical Association of Canada Annual Meeting, Winnipeg, Manitoba, Field Trip Guidebook A4.

Černý, P., Ercit, T. and Vanstone, P. 1998: Mineralogy and petrology of the Tanco rare-element pegmatite deposit, southeastern Manitoba; International Mineralogical Association, 17th General Meeting, Toronto, Field Trip Guidebook B6, 74 p.

Černý, P., Trueman, D.L., Ziehlke, D.V., Goad, B.E. and Paul, B.J. 1981: The Cat Lake–Winnipeg River and the Wekusko Lake pegmatite fields, Manitoba; Manitoba Department of Energy and Mines, Mineral Resources Division, Economic Geology Report ER80-1, 215 p., URL <https://www.manitoba.ca/iem/info/libmin/ER80-1.zip> [October 2021].

Cooper, M.A., Hawthorne, F.C., Ball, N.A., Ramik, R.A. and Roberts, A.C. 2009: Groatite, $Na CaMn^{2+}2(PO_4)[PO_3(OH)]_2$, a new mineral species of the alluaudite group from the Tanco pegmatite, Bernic Lake, Manitoba, Canada: description and crystal structure; The Canadian Mineralogist, v. 47, no. 5, p 1225–1235.

Deveaud, S., Millot, R. and Villaros, A. 2015: The genesis of LCT-type granitic pegmatites, as illustrated by lithium isotopes in micas; Chemical Geology, v. 411, p. 97–111.

Ercit, T.S., Hawthorne, F.C. and Černý, P. 1992: The wodginite group, I – Structural crystallography; The Canadian Mineralogist v. 30, p. 597–611.

Fransolet, A.M., Cooper, M.A., Černý, P., Hawthorne, F.C., Chapman, R. and Grice, J.D. 2000: The Tanco pegmatite at Bernic Lake, southeastern Manitoba, XV – Ercitite, $NaMn^{3+} PO_4(OH)(H2O)_2$, a new phosphate mineral species; The Canadian Mineralogist, v. 38, no. 4, p. 893–898.

Gilbert, H.P. 2006: Geological investigations in the Bird River area, southeastern Manitoba (parts of NTS 52L5N and 6); *in* Report of Activities 2006, Manitoba Science, Technology, Energy and Mines, Manitoba Geological Survey, p. 184–205, URL <https://www.manitoba.ca/iem/geo/field/roa06pdfs/GS-17.pdf> [October 2021].

Gilbert, H.P. 2007: Stratigraphic investigations in the Bird River greenstone belt, Manitoba (part of NTS 52L5, 6); *in* Report of Activities 2007, Manitoba Science, Technology, Energy and Mines, Manitoba Geological Survey, p. 129–143, URL <https://www.manitoba.ca/iem/geo/field/roa07pdfs/GS-12.pdf> [October 2021].

Gilbert, H.P. 2008: Stratigraphic investigations in the Bird River greenstone belt, Manitoba (part of NTS 52L5, 6); *in* Report of Activities 2008, Manitoba Science, Technology, Energy and Mines, Manitoba Geological Survey, p. 121–138, URL <https://www.manitoba.ca/iem/geo/field/roa08pdfs/GS-11.pdf> [October 2021].

Government of Canada 2021: Critical minerals, URL <https://www.nrcan.gc.ca/criticalminerals> [March 2021].

Grice, J.D., Černý, P. and Ferguson, R.B. 1972: The Tanco pegmatite at Bernic Lake, Manitoba, II – Wodginite, tantalite, pseudo-ixiolite and related minerals; The Canadian Mineralogist, v. 11, no. 3, p. 609–642.

Kesler, S.E., Gruber, P.W., Medina, P.A., Keoleian, G.A., Everson, M.P. and Wallington, T.J. 2012: Global lithium resources: relative importance of pegmatite, brine and other deposits; Ore Geology Reviews, v. 48, p. 55–69.

Kissin, S.A., Owens, D.R. and Roberts, W.L. 1978: Černýite, a copper-cadmium-tin sulfide with the stannite structure; The Canadian Mineralogist, v. 16, no. 2, p. 139–146.

Kontak, D.J. 2020: Evidence supporting the role of late-stage post-magmatic chaos in the formation of rare-metal pegmatitic ore systems; Geoconvention 2020 virtual event, URL <https://geoconvention.com/wp-content/uploads/abstracts/2020/57975-evidence-supporting-the-role-of-late-stage-post-ma.pdf> [October 2021].

Kremer, P.D. 2010: Structural geology and geochronology of the Bernic Lake area in the Bird River greenstone belt, Manitoba: evidence for syn-deformational emplacement of the Bernic Lake pegmatite group; M.Sc. thesis, University of Waterloo, Waterloo, Ontario, 91 p.

Lima, A. and Dias, F. 2019: Spodumene and quartz intergrowth – textural and genesis point of view; *in* Geophysical Research Abstracts, v. 21, p. 1-1.

Linnen, R.L., Van Lichtervelde, M. and Černý, P. 2012: Granitic pegmatites as sources of strategic metals; Elements, v. 8, no. 4, p. 275–280.

Liu, X.M., Rudnick, R.L., Hier-Majumder, S. and Sirbescu, M.L.C. 2010: Processes controlling lithium isotopic distribution in contact aureoles: a case study of the Florence County pegmatites, Wisconsin; Geochemistry, Geophysics, Geosystems, v. 11, no. 8, URL <https://doi.org/10.1029/2010GC003063>.

London, D. 1986: Magmatic-hydrothermal transition in the Tanco rare-element pegmatite: evidence from fluid inclusions and phase-equilibrium experiments; American Mineralogist, v. 71, no. 3–4, p. 376–395.

London, D. 1990: Internal differentiation of rare-element pegmatites: a synthesis of recent research; Geological Society of America, Special Paper 246, p. 35–50.

London, D. 2008: Pegmatites; The Canadian Mineralogist, Special Publication 10, p. 108–114.

London, D. and Kontak, D.J. 2012: Granitic pegmatites: scientific wonders and economic bonanzas; Elements, v. 8, no. 4, p. 257–261.

London, D., Zolensky, M.E. and Roedder, E. 1987: Diomignite: natural $Li_2B_4O_7$ from the Tanco pegmatite, Bernic Lake, Manitoba; The Canadian Mineralogist, v. 25, no. 1, p. 173–180.

Martins, T., Kremer, P. and Vanstone, P. 2013: The Tanco mine: geological setting, internal zonation and mineralogy of a world-class rare element pegmatite deposit; Geological Association of Canada–Mineralogical Association of Canada Joint Annual Meeting, Field Trip Guidebook FT-C1; Manitoba Innovation, Energy and Mines, Manitoba Geological Survey, Open File OF2013-8, 17 p., URL <https://www.manitoba.ca/iem/info/libmin/gacmac/OF2013-8_FT-C1.pdf> [October 2021].

Morgan, G.B. and London, D. 1987: Alteration of amphibolitic wall-rocks around the Tanco rare-element pegmatite, Bernic Lake, Manitoba; American Mineralogist, v. 72, no. 11–12, p. 1097–1121.

Ramik, R.A., Sturman, B.D., Dunn, P.J. and Povarennykh, A.S. 1980: Tancoite, a new lithium sodium aluminum phosphate from the Tanco pegmatite, Bernic Lake, Manitoba; The Canadian Mineralogist, v. 18, no. 2, p. 185–190.

Rinaldi, R., Černý, P. and Ferguson, R.B. 1972: The Tanco pegmatite at Bernic Lake, Manitoba, VI – Lithium-rubidium-cesium micas; The Canadian Mineralogist, v. 11, p. 690–707.

Selway, J.B., Černý, P., Hawthorne, F.C. and Novák, M. 2000a: The Tanco pegmatite at Bernic Lake, Manitoba, XIV – Internal tourmaline; The Canadian Mineralogist, v. 38, no. 4, p. 877–891.

Selway, J.B., Novák, M., Černý, P. and Hawthorne, F.C. 2000b: The Tanco pegmatite at Bernic Lake, Manitoba, XIII – Exocontact tourmaline; The Canadian Mineralogist, v. 38, no. 4, p. 869–876.

Stilling, A. 1998: The bulk composition of the Tanco pegmatite at Bernic Lake, Manitoba, Canada; M.Sc. thesis, University of Manitoba, Winnipeg, Manitoba, URL <http://hdl.handle.net/1993/1518> [October 2021].

Stilling, A., Ćerný, P. and Vanstone, P.J. 2006: The Tanco pegmatite at Bernic Lake, Manitoba, XVI – Zonal and bulk compositions and their petrogenetic significance; The Canadian Mineralogist, v. 44, no. 3, p. 599–623.

Tischendorf, G., Gottesmann, B., Foerster, H.J. and Trumbull, R.B. 1997: On Li-bearing micas: estimating Li from electron microprobe analyzes and an improved diagram for graphical representation; Mineralogical Magazine, v. 61, no. 6, p. 809–834.

Van Lichtervelde, M., Grégoire, M., Linnen, R.L., Béziat, D. and Salvi, S. 2008: Trace element geochemistry by laser ablation ICP-MS of micas associated with Ta mineralization in the Tanco pegmatite, Manitoba, Canada; Contributions to Mineralogy and Petrology, v. 155, no. 6, p. 791–806.

Zubi, G., Dufo-López, R., Carvalho, M. and Pasaoglu, G. 2018: The lithium-ion battery: state of the art and future perspectives; Renewable and Sustainable Energy Reviews, v. 89, p. 292–308.

GS2021-3

Collection of samples for high-resolution detrital-zircon geochronology and lithogeochemistry in the Thompson nickel belt, central Manitoba (parts of NTS 63O8, 9, 63P12)

by C.G. Couëslan

In Brief:

- Samples of Manasan and Setting formation rocks from the Ospwagan group were collected for high-resolution U-Pb dating of detrital zircon
- Metasedimentary rocks of uncertain affinity were collected from roadcuts near Joey Lake; geochemistry suggests they might be correlative with Paint sequence rocks; further study is warranted

Citation:
Couëslan, C.G. 2021: Collection of samples for high-resolution detrital-zircon geochronology and lithogeochemistry in the Thompson nickel belt, central Manitoba (parts of NTS 63O8, 9, 63P12); *in* Report of Activities 2021, Manitoba Agriculture and Resource Development, Manitoba Geological Survey, p. 18–28.

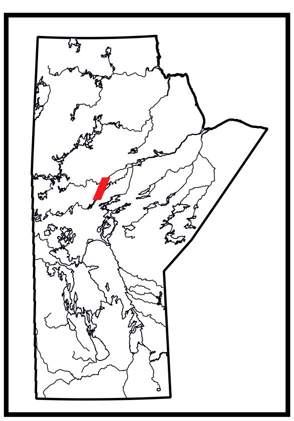

Summary

A project was initiated in 2021 to conduct sampling for high-resolution U-Pb dating of detrital zircon in the Ospwagan group. Samples were collected of Manasan formation M1 member conglomerate and sandstone, and M2 member semipelite, as well as a sample of Setting formation sandstone. All known economic Ni-Cu deposits in the Thompson nickel belt are associated with ultramafic bodies hosted in Ospwagan group stratigraphy. Having additional insight into the source region (provenance) and depositional history (age) of the Ospwagan group could help differentiate it from other metasedimentary rocks considered less prospective for Ni exploration.

Additional metasedimentary rocks of uncertain affinity were collected for lithogeochemistry from recent roadcuts in the Joey Lake area. The roadcuts are adjacent to a belt of rocks previously identified as undifferentiated Ospwagan group and Archean gneiss. Although somewhat inconclusive, the geochemistry of the metasedimentary rocks appears more similar to Paint sequence than Ospwagan group rocks. The belt of undifferentiated rocks is also reported to contain ultramafic bodies toward the northern terminus. Further study of this belt, the metasedimentary rocks and their potential relationship with ultramafic bodies is warranted.

Introduction

All known economic Ni-Cu deposits in the Thompson nickel belt (TNB) are associated with ultramafic bodies hosted by the Ospwagan group stratigraphy. Understanding these sedimentary rocks is therefore of great importance for mineral exploration in the belt. Several geochronological studies of detrital zircon in the Ospwagan group have been completed in the last 20 years (Bleeker and Hamilton, 2001; Rayner et al., 2006; Zwanzig, unpublished data, 2008; Machado et al., 2011). However, the results of some of these studies were either not published or published only in an abstract (e.g., Bleeker and Hamilton, 2001; Zwanzig, unpublished data, 2008), while the most recent study utilized laser-ablation, inductively coupled plasma–mass spectrometry techniques that determined only ^{207}Pb/^{206}Pb isotope ages with a large variation in analytical errors and no quantification of data discordance (Machado et al., 2011). The availability of published, high-resolution U-Pb detrital-zircon data for the Ospwagan group is therefore relatively limited, and confined only to the P2 member of the Pipe formation (Rayner et al., 2006).

The discovery of a new sedimentary rock package in the TNB with potential to host ultramafic bodies (Paint sequence; Couëslan, 2016, 2018) has increased the need for high-resolution detrital-zircon data for the Ospwagan group. Although the Paint sequence appears to be geochemically distinct from the Ospwagan group, there is a large overlap in crustal residence Nd-model ages between the two sedimentary rock packages (Couëslan, 2016, 2018; Manitoba Geological Survey, 2020). High-resolution U-Pb detrital-zircon data are needed for further comparative studies.

Five samples of Ospwagan group rocks were collected during the 2021 field season for prospective U-Pb detrital-zircon analysis. These include samples from the M1 and M2 members of the Manasan formation and a sample from the Setting formation. Furthermore, the detrital-zircon data for a Setting formation sample from Setting Lake (Zwanzig, unpublished data, 2008) have been released as Data Repository Item DRI2021013 (Zwanzig et al., 2021). This new DRI, combined with the samples collected in this study and the data published by Rayner et al. (2006), will provide high-quality detrital-zircon age information from the base, middle and top of the Ospwagan group stratigraphy.

In addition to the Ospwagan group samples collected for U-Pb detrital-zircon geochronology, five rock samples were collected from relatively recent roadcuts in the Joey Lake area for lithogeochemistry. These samples consist of metasedimentary rocks and spatially associated units of uncertain affinity. All rocks discussed in this report were subjected to metamorphic conditions of at least middle-amphibolite facies; however, the 'meta-' prefix has been omitted from rock names for brevity.

Regional geology

The TNB forms a segment of the Superior boundary zone, flanked to the northwest by the Kisseynew domain of the Trans-Hudson orogen and to the southeast by the Pikwitonei granulite domain (PGD) of the Superior craton (Figure GS2021-3-1). The TNB is underlain largely by reworked Archean gneiss of the Superior craton, which is typically quartzofeldspathic with enclaves of mafic to ultramafic rock; clearly recognizable paragneiss is rare. It is commonly migmatitic and characterized by complex internal structures that are the result of multiple generations of Archean and Paleoproterozoic deformation and

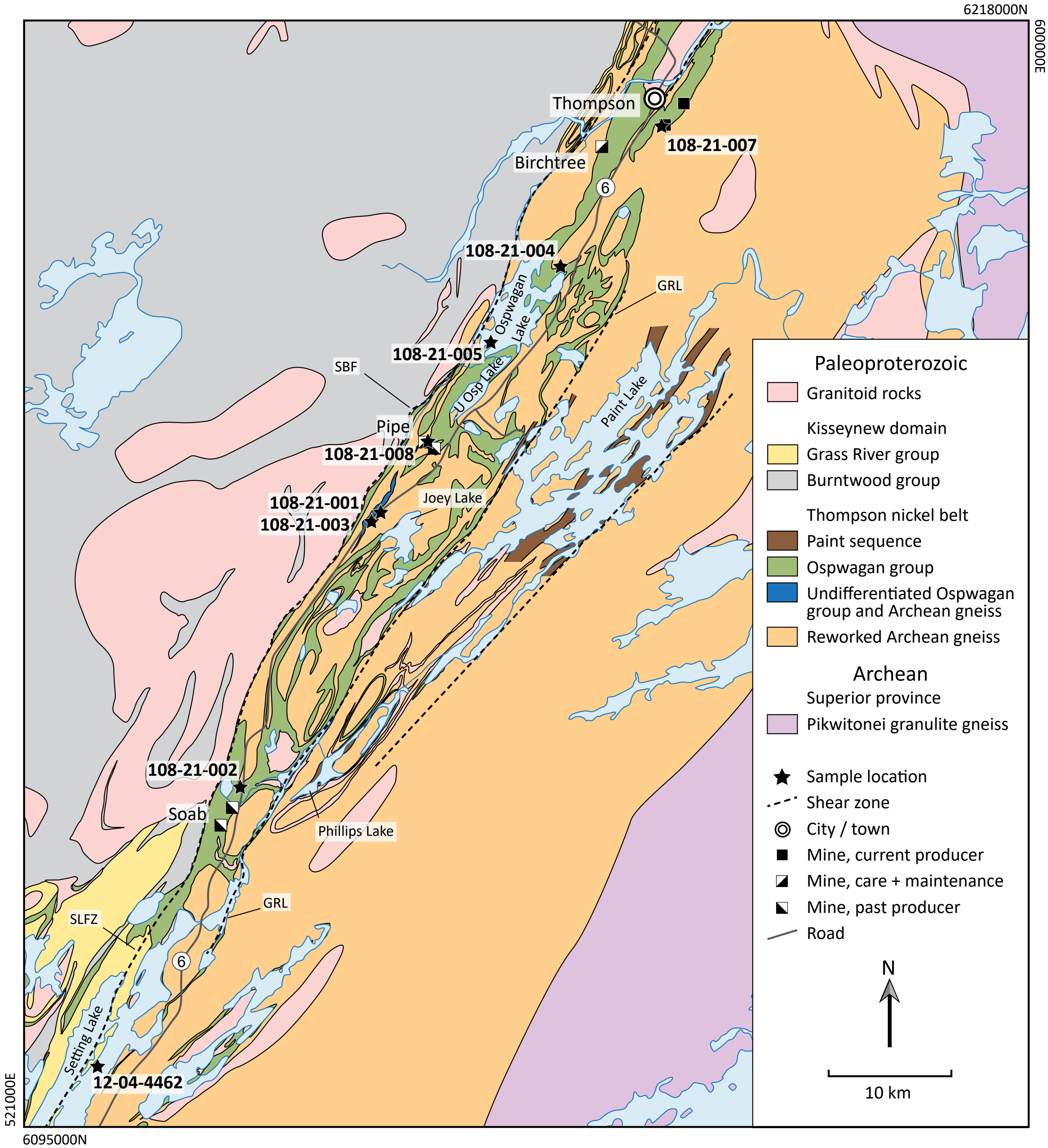

Figure GS2021-3-1: *Geology of the central Thompson nickel belt and adjacent portions of the Kisseynew domain and Superior province (modified from Macek et al., 2006; Manitoba Mineral Resources, 2013; Couëslan, 2016). Abbreviations: GRL, Grass River lineament; SBF, Superior boundary fault; SLFZ, Setting Lake fault zone; U Osp L, Upper Ospwagan Lake.*

metamorphism. The gneiss is derived from the adjacent PGD, which was subjected to granulite-facies metamorphic conditions from ca. 2720 to 2640 Ma (Hubregtse, 1980; Mezger et al., 1990; Heaman et al., 2011; Guevara et al., 2020; Couëslan, 2021a). The granulites of the PGD were exhumed and unconformably overlain by Paleoproterozoic supracrustal rocks of the Ospwagan group prior to intrusion of the Molson dike swarm and associated ultramafic intrusions ca. 1883 Ma (Bleeker, 1990; Zwanzig et al., 2007; Heaman et al., 2009; Scoates et al., 2017). The Archean basement gneiss and Paleoproterozoic supracrustal rocks were subjected to multiple generations of deformation and metamorphic conditions, ranging from middle-amphibolite facies to lower-granulite facies, during the Trans-Hudson orogeny (Bleeker, 1990; Burnham et al., 2009; Couëslan and Pattison, 2012).

The dominant phase of penetrative deformation is D_2, which affected the Ospwagan group, Paint sequence and ca. 1883 Ma magmatic rocks. This deformation phase resulted in the formation of F_2 nappe structures, which incorporated the underlying Archean gneiss. The nappe structures have been interpreted as either east verging (Bleeker, 1990; White et al., 2002) or southwest verging (Zwanzig et al., 2007; Burnham et al., 2009). The recumbent folds are associated with regionally penetrative S_2 fabrics. The D_2 phase of deformation is interpreted to be the result of convergence between the Superior craton margin and the Reindeer zone of the Trans-Hudson orogen ca. 1830–1800 Ma. This D_2 phase was accompanied by prograde metamorphism, with peak metamorphic conditions likely being attained prior to or during early D_3 (Couëslan and Pattison, 2012). The D_3 phase of deformation resulted in isoclinal folds with vertical to steeply southeast-dipping axial planes (Bleeker, 1990; Burnham et al., 2009). Mylonite zones with subvertical stretching lineations parallel many of the regional F_3 fold structures. Tightening of D_3 structures continued during D_4, marked by localized retrograde greenschist metamorphism along northeast-striking, mylonitic and cataclastic shear zones that commonly record southeast-side-up sinistral movement (Bleeker, 1990; Burnham et al., 2009). The $D_{3–4}$ structures exert a first-order control on the pattern of metamorphic-field gradients in the TNB (Couëslan and Pattison, 2012).

Ospwagan group stratigraphy

The following summary of the Ospwagan group is sourced largely from Bleeker (1990) and Zwanzig et al. (2007). The Paleoproterozoic Ospwagan group unconformably overlies Archean basement gneiss in the TNB (Figure GS2021-3-2). The lowermost unit of the Ospwagan group is the Manasan formation, which consists of two members: the lower M1 member, consisting of layered to laminated sandstone with local conglomerate layers near the base; and the overlying M2 member, consisting of semipelitic rock. The Manasan formation is interpreted as a transgressive, fining-upward sequence deposited along a passive margin. This siliciclastic system grades into the overlying calcareous sedimentary rocks of the Thompson formation.

The Thompson formation consists of three members: the T1 member comprises a variety of calcareous–siliceous rocks, including chert, calcsilicate and impure marble; the T2 member is a semipelitic calcareous gneiss that is rarely present; and the T3 member consists of impure dolomitic marble with local horizons of calcsilicate. The Thompson formation represents a transition from a siliciclastic-dominated to a carbonate-dominated system.

The Pipe formation is subdivided into three members. The P1 member consists of a graphite-rich, sulphide-facies iron formation at the base (the locus of the Pipe II and Birchtree orebodies), overlain by a silicate-facies iron formation. The top of the P1 member consists of a reddish, laminated, siliceous rock. The P1 member grades into the overlying mudstone of the P2 member, the top of which is marked by a sulphide-facies iron formation (the locus of the Thompson orebody). The overlying P3 member consists of a wide variety of rock types, including laminated, siliceous, sedimentary rocks; silicate-, carbonate- and local oxide-facies iron formations; and semipelitic rocks, calcsilicate and a local horizon of relatively pure dolomitic marble. The Pipe formation represents a mix of chemical, and fine to very fine siliciclastic sedimentary components that were deposited in either an open-marine environment (Zwanzig et al., 2007) or during the development of a foredeep basin (Bleeker, 1990).

The Setting formation is divided into two members and is defined to include all siliciclastic rocks above the uppermost iron formation of the P3 member. The S1 member consists of rhythmically interbedded quartzite and wacke–mudstone with local calcareous concretions, which are characteristic of the S1 member. The S2 member consists of thickly layered greywacke, with local horizons grading from conglomerate at the base to mudstone at the top. No contact has been observed between the S1 and S2 members. It is possible that they represent a lateral facies change as opposed to a vertical succession. The Setting formation is interpreted to have been deposited by turbidity currents in a relatively deep-marine environment, possibly a foredeep basin (Bleeker, 1990). The coarse clastic material and thick turbidite bedding of the S2 member may record the shallowing of the basin, the onset of active tectonism or a lateral sedimentary-facies change to a submarine-channel or upper-fan environment (Zwanzig et al., 2007).

At the top of the Ospwagan group is the Bah Lake assemblage, which consists of mafic to ultramafic volcanic rocks dominated by massive to pillowed basalt flows with local picrite and minor synvolcanic intrusions. The Bah Lake assemblage is dominated by a high-Mg suite, similar to normal mid-ocean–ridge basalt (N-MORB), that occurs throughout much of the main TNB; and an incompatible-element–enriched suite, similar to enriched mid-ocean–ridge basalt (E-MORB), that occurs

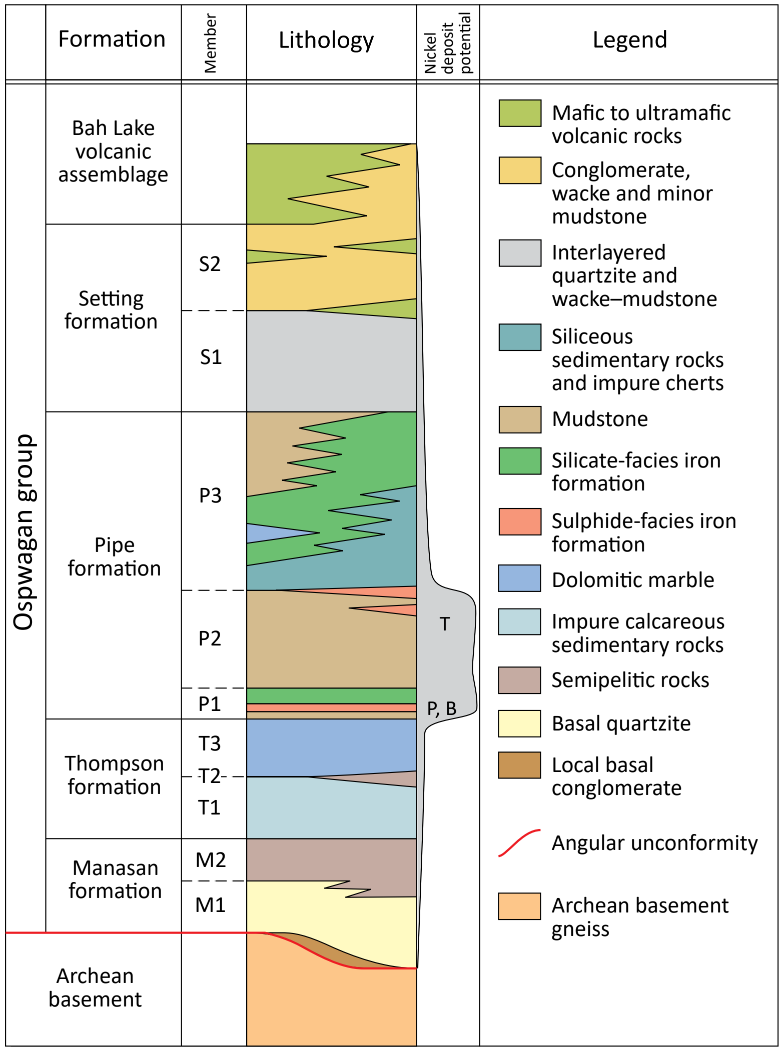

Figure GS2021-3-2: *Schematic stratigraphic column of the Ospwagan group (adapted from Bleeker, 1990). 'T', 'P' and 'B' indicate the stratigraphic positions of the mineralized ultramafic sills at the Thompson, Pipe II and Birchtree mines, respectively.*

in the northwestern Setting Lake area and along the margin of the Kisseynew domain (Zwanzig, 2005). The enriched suite is interpreted to overlie the high-Mg suite; however, it is uncertain if this represents a stratigraphic or tectonic relationship. The Bah Lake assemblage may indicate the onset of active rifting in the TNB (Zwanzig, 2005; Zwanzig et al., 2007), or that the foredeep basin was magmatically active (Bleeker, 1990).

A maximum age for the Ospwagan group is provided by a ca. 1974 Ma zircon recovered from Setting formation greywacke (Bleeker and Hamilton, 2001). A minimum age for the Ospwagan group is provided by crosscutting amphibolitized dikes interpreted to be part of the Molson dike swarm, and the possibly comagmatic Ni-ore–bearing ultramafic sills, which intruded the Ospwagan group at all stratigraphic levels ca. 1883 Ma (Bleeker, 1990; Zwanzig et al., 2007; Heaman et al., 2009; Scoates et al., 2017). Ospwagan group rocks yielded crustal-residence Nd-model ages of ca. 3.22–2.82 Ga, which are largely younger than model ages obtained from the Archean basement (ca. 3.70–3.14 Ga; Figure GS2021-3-3; Böhm et al., 2007).

Paint sequence rocks

The 'Paint sequence' refers to a suite of sedimentary rocks that occur in three northeast-striking belts in the Paint Lake area and appear to continue along strike to the Phillips Lake area (Figure GS2021-3-1; Couëslan, 2016, 2018). The stratigraphy of the Paint sequence is unconstrained but consists dominantly of wacke, with subordinate arenite and iron formation, and rare mudstone and calcsilicate. To date, the Paint sequence has only been recognized in areas of granulite-facies metamorphism where primary textures and structures are all but obliterated, except for centimetre-scale compositional layering.

Wacke is the most abundant member of the sequence. It commonly contains centimetre- to decimetre-thick layers of arenite and iron formation. Pods of in situ to in source leucosome are abundant. Outcrops of wacke are characterized by rusty weathered surfaces because of the presence of minor but ubiquitous pyrrhotite. The compositions of the wacke and arenite are gradational into each other and they can be interbedded. The arenite is typically interlayered with centime-

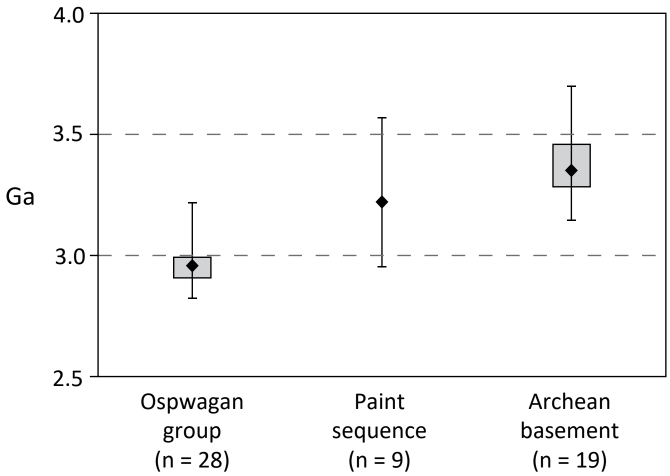

Figure GS2021-3-3: *Crustal-residence Nd-model ages of the Ospwagan group, Paint sequence and Archean basement gneiss. Black lines indicate the minimum and maximum ages for each population, grey boxes the interquartile range (middle 50% of the data from 25th to 75th percentile) and black diamonds the median age. Data sources: Ospwagan group and Archean basement from Böhm et al. (2007); Paint sequence from Couëslan (2016), Manitoba Geological Survey (2020).*

tre- to metre-thick layers of wacke. Mudstone has only been observed in east-central Paint Lake and near the marina, where it is interbedded on a centimetre scale with quartz-rich arenite. The interbedded mudstone-arenite unit contains rare garnet-rich concretions (Couëslan, 2016). The mudstone contains graphite and pyrrhotite, and is characterized by gossanous weathered surfaces. The iron formation occurs as discontinuous layers and lenses, which are up to 3 m thick but typically <1 m, within the wacke. Iron formations are typically of the silicate facies; however, significant pyrrhotite and magnetite can be present. Calcsilicate occurs only as rare centimetre-thick boudins in the wacke and arenite on Paint Lake (Couëslan, 2016); however, layers of calcsilicate and marble 2–5 m thick are observed in drillcore from Phillips Lake (Couëslan, 2018). It remains uncertain if the calcareous rocks at Phillips Lake are part of the Paint sequence stratigraphy or represent infolds or tectonic slivers of Ospwagan group rocks.

A maximum age for the Paint sequence is provided by five ca. 2435 Ma detrital-zircon grains obtained from a sample of wacke (Couëslan, 2016; Figure GS2021-3-4a). The Paint sequence rocks are intruded by relatively straight-walled mafic dikes, which are tentatively interpreted to be part of the Paleoproterozoic Molson dike swarm, suggesting a minimum age of ca. 1883 Ma for the sequence. The Paint sequence rocks differ from the Ospwagan group rocks in having unique trace-element compositions and containing early Paleoproterozoic detrital zircon (Figure GS2021-3-4); however, there is a significant overlap in crustal-residence Nd-model ages (ca. 3.57–2.95 Ga; Figure GS2021-3-3; Couëslan, 2016; Manitoba Geological Survey, 2020). The stratigraphic relationship between the Ospwagan group and Paint sequence is not known.

Geochronology samples

Five samples of Ospwagan group rocks were collected for prospective detrital-zircon U-Pb dating: three samples from the Manasan formation M1 member, one sample from the Manasan formation M2 member and one sample from the Setting formation. Whole-rock lithogeochemistry results for these samples can be found in (Couëslan, 2021d).

Manasan formation, M1 member samples

Sample 108-21-004 consists of quartz-pebble conglomerate and was collected from talus at the east end of Manasan quarry (Figure GS2021-3-1). Fifty centimetre to one metre lenses of quartz-pebble conglomerate are visible in quartzite along the north wall of the quarry, immediately above the talus pile. The conglomerate is beige, coarse grained, clast supported and strongly foliated. Pebbles are <1 cm across but commonly stretched to a length of 4 cm. Pebbles consist dominantly of quartz and are rarely quartzofeldspathic. The matrix consists of quartz with relatively abundant muscovite, chlorite and carbonate, suggesting it was likely derived from a muddy sand with some carbonate cement, or possibly a feldspathic sand where the feldspar component was altered during diagenesis or metamorphism.

Sample 108-21-002A is a quartzite that was collected from a quarry along Highway 6 near the former Soab North mine (Figures GS2021-3-1, -5a). The rock is light grey to beige, medium to coarse grained and foliated, with bedding <15 cm thick. It is quartz rich with abundant epidote, minor plagioclase and K-feldspar, and trace muscovite and Ca-amphibole. The mafic minerals appear to be pseudomorphous after feldspar, which suggests that the rock was derived from a feldspathic arenite. The abundance of epidote in the sample suggests a post–peak metamorphic alteration event. The quartzite at this location is intruded by a gabbro dike at least 50 m wide, which cuts across the south end of the quarry and is interpreted to be part of the Molson dike swarm. The quartzite sample was collected at the north end of the quarry, approximately 30 m from the dike margin, to minimize the chance of zircon U-Pb resetting caused by the intrusion of the mafic dike. A sample of fine-grained chill margin was collected from the gabbro dike for lithogeochemistry.

Sample 108-21-007 consists of well-laminated micaceous quartzite (unit M1b8 of Macek et al., 2004, 2005), which was collected from the shoulder of the South pit at the Thompson mine (Figures GS2021-3-1, -5b). The micaceous quartzite forms a 2–3 m thick layer that is underlain and overlain by cleaner, arenaceous sandstone. The micaceous quartzite is brown, medium grained and foliated, with laminations <5 mm thick. It is quartz- and K-feldspar rich, with abundant plagioclase and minor biotite and muscovite, and was likely derived from a feldspathic wacke.

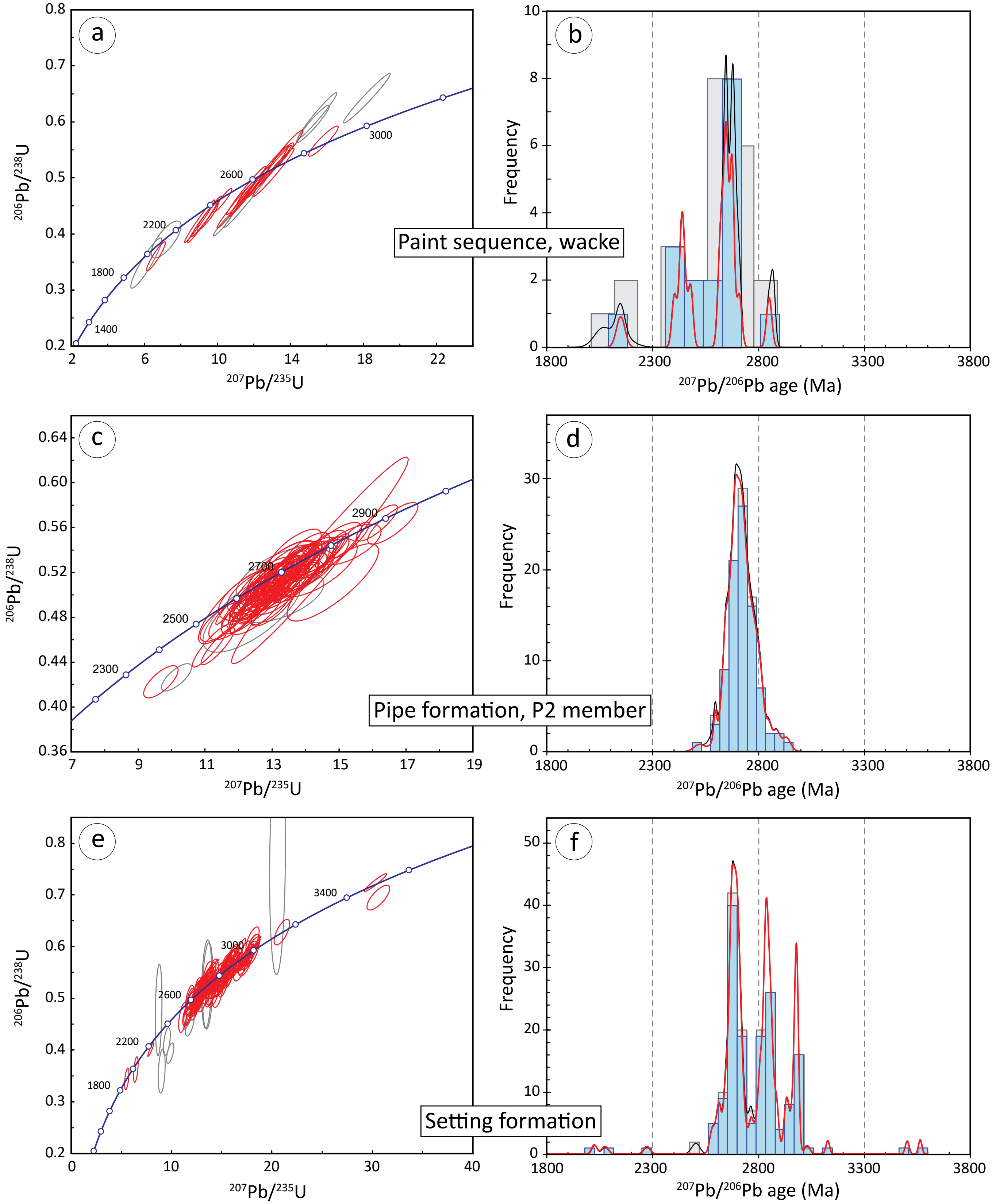

***Figure GS2021-3-4**: High-resolution detrital-zircon U-Pb results for sedimentary rocks from the Thompson nickel belt: **a)** concordia diagram and **b)** frequency histogram and probability curve for Paint sequence wacke (Couëslan, 2016); **c)** concordia diagram and **d)** frequency histogram and probability curve for Pipe formation, P2 member (Rayner et al., 2006); **e)** concordia diagram and **f)** frequency histogram and probability curve for Setting formation wacke (Zwanzig et al., 2021). In the concordia diagrams, red analyses are <10% discordant and rejected analyses are in grey; error ellipses are shown at 2σ. Coloured frequency histograms and probability curves represent analyses that are <10% discordant; grey and black represent all analyses combined.*

Figure GS2021-3-5: *Outcrop photographs of sampled units:* ***a)*** *station 108-21-002, Manasan Formation M1 member quartzite at the Soab North quarry;* ***b)*** *station 108-21-007, M1 member micaceous quartzite at the Thompson mine, south pit (tape is approximately 2.5 cm wide and arrow points upsection);* ***c)*** *station 108-21-008, M2 member semipelite at Pipe II mine open pit;* ***d)*** *station 108-21-005, Setting formation interbedded arenite and wacke at Niven Point, Ospwagan Lake;* ***e)*** *station 108-21-001, biotite gneiss of uncertain affinity at Joey Lake area roadcut;* ***f)*** *station 108-21-003, garnet-bearing wacke of uncertain affinity at Joey Lake area roadcut;* ***g)*** *station 108-21-003, garnet 'concretion' at Joey Lake area roadcut.*

The M1 member is a shallow-water marine sandstone (and minor conglomerate) package deposited along the Superior craton passive margin (Bleeker, 1990; Zwanzig et al., 2007). It represents a transgressive sequence that fines upward into the overlying M2 member (Bleeker, 1990; Zwanzig et al., 2007). The quartz-pebble conglomerate (108-21-004) was likely deposited toward the base of the M1 member (Bleeker, 1990; Zwanzig et al., 2007). The relative stratigraphic position of quartzite 108-21-002A within the M1 member is not known; however, the relatively clean sand is characteristic of deposits near the base and middle of the succession (Macek et al., 2004). The micaceous quartzite (108-21-007) occurs toward the middle of the M1 member and is characterized by an increased abundance of finer grained clastic material. It likely represents a period of transgression during a transgressive-regressive cycle.

Manasan formation, M2 member sample

Sample 108-21-008 is a fine-grained semipelitic schist collected roughly 2 m above the M1 contact at the open pit of the Pipe II mine (Figures GS2021-3-1, -5c). The schist is dark grey-brown, fine grained and foliated, with laminations <1 cm thick. Local quartz-rich segregations <2 cm across occur within the unit but were avoided during sampling. The rock consists dominantly of quartz with abundant biotite and K-feldspar, minor plagioclase, muscovite and iron oxide, and trace tourmaline. The M2 member was likely derived from offshore marine siltstone or mud-rich wacke that was deposited along the Superior craton passive margin (Bleeker, 1990; Zwanzig et al., 2007).

Setting formation sample

Sample 108-21-005 is a well-bedded quartzite collected from Niven Point on Ospwagan Lake (Figures GS2021-3-1, -5d). It occurs as part of a sequence of interbedded arenite and wacke. The quartzite is brown, fine grained and foliated, with layering <3 cm thick. It is quartz rich with abundant plagioclase, minor muscovite and biotite, and trace sulphide and garnet, and was likely derived from a feldspathic wacke. The Setting formation is interpreted as offshore marine turbidite deposits that were shed from the Superior craton (Zwanzig et al., 2007), possibly into a foredeep basin (Bleeker, 1990).

Joey Lake area samples

Five samples were collected for lithogeochemistry from relatively recent roadcuts along Highway 6 in the Joey Lake area (Figure GS2021-3-1). The samples include three sedimentary rocks of unknown affinity, a spatially associated ultramafic schist and a spatially associated biotite gneiss of uncertain affinity. The roadcuts occur within 70 m of an area indicated to be underlain by undifferentiated Ospwagan group and Archean rocks on the Thompson nickel belt geological compilation map of Macek et al. (2006). The aim is to determine if these rocks share affinity with the Ospwagan group, the Archean basement or the Paint sequence.

Sample descriptions

A roadcut approximately 1.4 km northeast of the Manitoba Hydro radio tower near Joey Lake consists largely of biotite gneiss of uncertain affinity, intruded by diabase and pegmatitic granite dikes (Figures GS2021-3-1, -5e). Sparse horizons <1 m thick within the biotite gneiss are garnet bearing. A sample of gneiss was collected from one of the garnet-bearing zones (108-21-001). The gneiss is brown-grey, coarse grained and strongly foliated, with crude layering <10 cm thick. It is quartz and plagioclase rich, with 10–20% biotite, 2–3% garnet and 1–2% hornblende. It is uncertain if the biotite gneiss represents a quartzofeldspathic sedimentary rock or is part of the Archean basement gneiss.

A roadcut approximately 0.3 km northeast of the radio tower contains a >50 m thick package of sedimentary rocks consisting dominantly of garnet-bearing wacke (108-21-003A; Figures GS2021-3-1, -5f). The wacke is brownish grey, medium grained and foliated, with bedding <5 cm thick. It is quartz and plagioclase rich, with 10–20% biotite and trace–2% garnet. The wacke contains sparse layers of ironstone <20 cm thick (108-21-003B), ferruginous mudstone <10 cm thick (108-21-003D) and boudins of ultramafic schist <50 cm thick (108-21-003C). Rare, pinkish brown ‘concretions’ <15 cm thick occur within the wacke (Figure GS2021-3-5g). The concretions are mantled by dark selvages <3 cm thick. Similar concretions are found in quartzite and wacke of the Setting formation, and in the interbedded pelite-arenite unit of the Paint sequence (Bleeker, 1990; Zwanzig et al., 2007; Couëslan, 2016).

Lithogeochemistry

Following the methodology outlined by Zwanzig et al. (2007), whole-rock geochemical data for the Joey Lake rocks was normalized by average Pipe formation, P2 member and plotted on multi-element diagrams in order to compare with wackes, mudstones and iron formations of the Ospwagan group (Figure GS2021-3-6a–d) and Paint sequence (Figure GS2021-3-6e–f). The diagrams utilize elements considered to be relatively immobile in the metamorphic environment (e.g., rare-earth elements [REE] and high-field-strength elements [HFSE]). The lithogeochemical data, and sampling and analytical methods for the Joey Lake rocks are being released in Data Repository Item DRI2021017[1] (Couëslan, 2021d).

[1] MGS Data Repository Item DRI2021017, containing the data or other information sources used to compile this report, is available online to download free of charge at https://www.gov.mb.ca/iem/info/library/downloads/index.html, or on request from minesinfo@gov.mb.ca, or by contacting the Resource Centre, Manitoba Agriculture and Resource Development, 360–1395 Ellice Avenue, Winnipeg, Manitoba R3G 3P2, Canada.

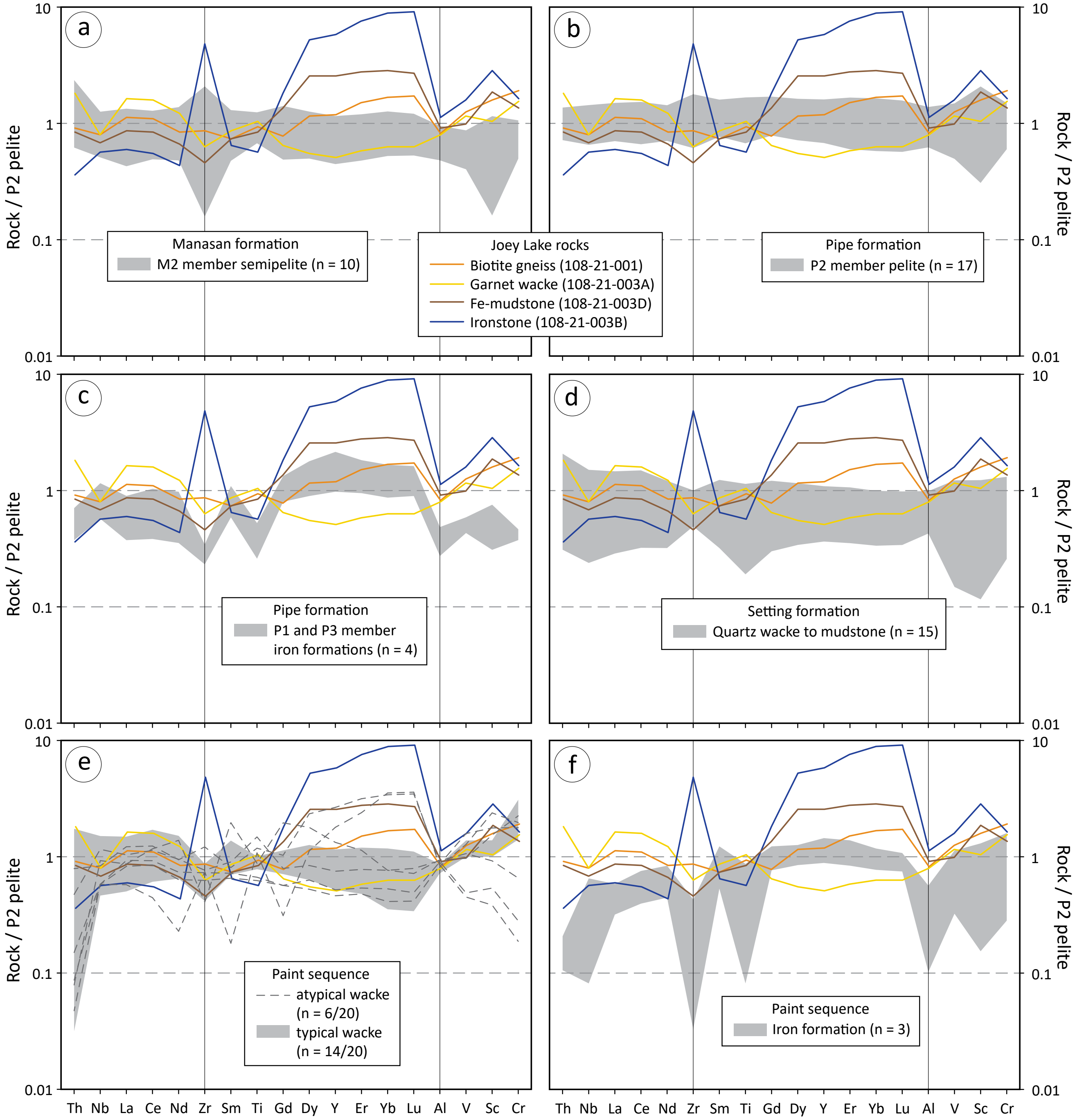

Figure GS2021-3-6: *Multi-element profiles of Joey Lake area samples normalized to average P2 mudstone of Zwanzig et al. (2007) and compared to the profile ranges of other TNB stratigraphy:* ***a)*** *Manasan formation, M2 member semipelite;* ***b)*** *Pipe formation, P2 member mudstone;* ***c)*** *Pipe formation silicate-facies iron formation;* ***d)*** *Setting formation wacke to mudstone;* ***e)*** *Paint sequence wacke;* ***f)*** *Paint sequence silicate-facies iron formation. Data sources: Ospwagan group rocks, Zwanzig et al. (2007), Couëslan (2020, 2021c); Paint sequence rocks, Couëslan (2016, 2021b).*

The shallow positive slope of the biotite gneiss profile (108-21-001) is not a close fit to any of the other profiles (Figure GS2021-3-6), although it does largely fit within the range of Pipe formation, P2 member profiles (Figure GS2021-3-6b) and bears some similarities to atypical Paint sequence wacke (Figure GS2021-3-6e). The negative slope of the Joey Lake garnet wacke profile (108-21-003A) largely fits within the range of Setting formation rocks (Figure GS2021-3-6d) and typical Paint sequence wacke (Figure GS2021-3-6e). In particular, the enrichment of Cr and overall positive slope from Al to Cr is a characteristic shared by the Paint sequence rocks. However, the concave-upward heavy rare-earth element (HREE) portion of the profile does not correlate with either the Paint sequence or the Setting formation rocks.

The positive-sloping profile of the ferruginous mudstone (108-21-003D) does not correlate well with any of the profile ranges in Figure GS2021-3-6; however, it strongly resembles some atypical profiles of the Paint sequence wacke

(Figure GS2021-3-6e). The profile of the ironstone (108-21-003B) does not correlate well with any of the profiles in Figure GS2021-3-6 and, most notably, it differs greatly from both the Ospwagan group and Paint sequence iron formations (Figure GS2021-3-6c, f). The values for Zr and HREE are anomalous, especially for a sedimentary rock believed to have a significant chemical component; however, zircon is found to be relatively abundant in thin section. The ironstone profile does resemble the overall shape of some of the atypical Paint sequence wacke profiles (Figure GS2021-3-6e).

Overall, the Joey Lake sedimentary rocks appear to correlate more closely with the Paint sequence than the Ospwagan group; however, none of the samples are a precise match with 'typical' Paint sequence wacke. All previously documented examples of Paint sequence rocks occur in the Paint Lake–Phillips Lake area and contain granulite-facies metamorphic assemblages. If these rocks do represent Paint sequence, they are the first to occur west of that area and the first to consist of amphibolite-facies metamorphic assemblages. Because the rocks occur at a lower metamorphic grade, there may be better potential for the preservation of primary sedimentary features. This suggests that additional study of the rocks contained within the belt of undifferentiated Ospwagan group and Archean gneiss of Macek et al. (2006) is warranted.

Economic considerations

All known economic Ni-Cu deposits in the TNB are associated with ultramafic bodies hosted by Ospwagan group rocks. High-resolution U-Pb detrital-zircon ages for the Ospwagan group stratigraphy could provide additional insight into the source region(s) and depositional history of the sedimentary sequence. Differences in source regions between the Ospwagan group and Paint sequence could indicate differences in tectonic setting at the time of their deposition. Variations in detrital-zircon populations could also help differentiate Ospwagan group rocks from other sedimentary units within the TNB, which are considered to be less prospective for hosting Ni deposits.

If the sedimentary rocks sampled near Joey Lake correlate with the Paint sequence, it could be that the nearby belt of undifferentiated Ospwagan group and Archean gneiss in Macek et al. (2006) actually consists largely of Paint sequence rocks. This belt, which has a strike length of approximately 7.6 km, is known to contain ultramafic bodies toward its northern terminus. Paint sequence rocks are known to contain sedimentary sulphide (a potential source of sulphur for intruding ultramafic magmas), and it has been suggested that the mineralized ultramafic body at Phillips Lake could be hosted by Paint sequence rocks (Couëslan, 2018). Further study of this belt of sedimentary rocks could provide additional information regarding the relationship between the Paint sequence and the Ni-hosting ultramafic bodies of the TNB.

Acknowledgments

The author thanks S. Kirby and staff at Vale Exploration–Thompson for providing access to Vale properties for sampling and assisting with sampling on Ospwagan Lake. Logistical support and lithogeochemical sample preparation was provided by C. Epp and P. Belanger at the Manitoba Geological Survey Midland Sample and Core Library. Reviews and suggestions for previous drafts of this report were provided by C.O. Böhm and T. Martins.

References

Bleeker, W. 1990: Evolution of the Thompson Nickel Belt and its nickel deposits, Manitoba, Canada; Ph.D. thesis, University of New Brunswick, Fredericton, New Brunswick, 400 p.

Bleeker, W. and Hamilton, M.A. 2001: New SHRIMP U-Pb ages for the Ospwagan Group: implications for the SE margin of the Trans-Hudson Orogen; Geological Association of Canada–Mineralogical Association of Canada, Joint Annual Meeting 2001, May 27–30, 2001, St. John's, Newfoundland, Abstracts, v. 26, p. 15.

Böhm, C.O., Zwanzig, H.V. and Creaser, R.A. 2007: Sm-Nd isotope technique as an exploration tool: delineating the northern extension of the Thompson Nickel Belt, Manitoba, Canada; Economic Geology, v. 102, p. 1217–1231.

Burnham, O.M., Halden, N., Layton-Matthews, D., Lesher, C.M., Liwanag, J., Heaman, L., Hulbert, L., Machado, N., Michalak, D., Pacey, M., Peck, D.C., Potrel, A., Theyer, P., Toope, K. and Zwanzig, H. 2009: CAMIRO project 97E-02, Thompson Nickel Belt: final report, March 2002, revised and updated June 2003; Manitoba Science, Technology, Energy and Mines, Manitoba Geological Survey, Open File OF2008-11, 434 p. plus appendices and GIS shape files for use with ArcInfo®, URL <https://www.manitoba.ca/iem/info/libmin/OF2008-11.zip> [October 2021].

Couëslan, C.G. 2016: Geology of the Paint and Phillips lakes area, Thompson nickel belt, central Manitoba (parts of NTS 63O1, 8, 9, 63P5, 12); Manitoba Growth, Enterprise and Trade, Manitoba Geological Survey, Geoscientific Report GR2016-1, 44 p. plus 1 map at 1:50 000 scale, URL <https://www.manitoba.ca/iem/info/libmin/GR2016-1.zip> [September 2021].

Couëslan, C.G. 2018: Re-examination of drillcore from southern Phillips Lake, and the possibility of a new nickel-mineralization–hosting sequence in the Thompson nickel belt, central Manitoba (part of NTS 63O1); *in* Report of Activities 2018, Manitoba Growth, Enterprise and Trade, Manitoba Geological Survey, p. 1–16, URL <https://www.manitoba.ca/iem/geo/field/roa18pdfs/GS2018-1.pdf> [September 2021].

Couëslan, C.G. 2021a: Bedrock geology of the central Sipiwesk Lake area, Pikwitonei granulite domain, central Manitoba (part of NTS 63P4); Manitoba Agriculture and Resource Development, Manitoba Geological Survey, Geoscientific Report GR2021-1, 47 p. plus 1 appendix and 1 map at 1:20 000 scale, URL <https://www.manitoba.ca/iem/info/libmin/GR2021-1.zip> [September 2021].

Couëslan, C.G. 2021b: Lithogeochemistry of drillcore from the Phillips Lake area, and samples from the Paint Lake area, Thompson nickel belt, central Manitoba (NTS 63P5 and 63O1, 8); Manitoba Agriculture and Resource Development, Manitoba Geological Survey, Data Repository Item DRI2021015, Microsoft® Excel® file, URL <https://www.manitoba.ca/iem/info/libmin/DRI2021015.xlsx> [September 2021].

Couëslan, C.G. 2021c: Lithogeochemistry of iron formation, calcsilicate, marble, and mafic dikes from the Thompson nickel belt, central Manitoba (NTS 63O8, 9 and 63P5, 12, 15); Manitoba Agriculture and Resource Development, Manitoba Geological Survey, Data Repository Item DRI2021016, Microsoft® Excel® file, URL <https://www.manitoba.ca/iem/info/libmin/DRI2021016.xlsx> [September 2021].

Couëslan, C.G. 2021d: Lithogeochemistry of metasedimentary rocks of uncertain affinity from the Joey Lake area, and Ospwagan group and related rocks, Thompson nickel belt, central Manitoba (NTS 63O8, 9 and 63P12); Manitoba Agriculture and Resource Development, Manitoba Geological Survey, Data Repository Item DRI2021017, Microsoft® Excel® file, URL <https://www.manitoba.ca/iem/info/libmin/DRI2021017.xlsx> [November 2021].

Couëslan, C.G. and Pattison, D.R.M. 2012: Low-pressure regional amphibolite-facies to granulite-facies metamorphism of the Paleoproterozoic Thompson Nickel Belt, Manitoba; Canadian Journal of Earth Sciences, v. 49, p. 1117–1153.

Guevara, V.E., MacLennan, S.A., Dragovic, B., Caddick, M.J., Schoene, B., Kylander-Clark, A.K.C. and Couëslan, C.G. 2020: Polyphase zircon growth during slow cooling from ultrahigh temperature: an example from the Archean Pikwitonei granulite domain; Journal of Petrology, v. 61, art. egaa021, URL <https://doi.org/10.1093/petrology/egaa021>.

Heaman, L.M., Böhm, C.O., Machado, N., Krogh, T.E., Weber, W. and Corkery, M.T. 2011: The Pikwitonei Granulite Domain, Manitoba: a giant Neoarchean high-grade terrane in the northwest Superior Province; Canadian Journal of Earth Sciences, v. 48, p. 205–245.

Heaman, L.M., Peck, D. and Toope, K. 2009: Timing and geochemistry of 1.88 Ga Molson Igneous Events, Manitoba: insights into the formation of a craton-scale magmatic and metallogenic province; Precambrian Research, v. 172, p. 143–162, URL <https://doi.org/10.1016/j.precamres.2009.03.015>.

Hubregtse, J.J.M.W. 1980: The Archean Pikwitonei granulite domain and its position at the margin of the northwestern Superior Province (central Manitoba); Manitoba Energy and Mines, Manitoba Geological Survey, Geological Paper GP80-3, 16 p., URL <https://www.manitoba.ca/iem/info/libmin/GP80-3.pdf> [September 2021].

Macek, J.J., McGregor, C.R. and Zwanzig, H.V. 2004: Thompson Nickel Belt Project, Manitoba (part of NTS 63P): geology of the South pit, Thompson mine; *in* Report of Activities 2004, Manitoba Industry, Economic Development and Mines, Manitoba Geological Survey, p. 135–148, URL <https://www.manitoba.ca/iem/geo/field/roa04pdfs/GS-12.pdf> [September 2021].

Macek, J.J., McGregor, C.R. and Zwanzig, H.V. 2005: Geology of the South pit (northwest shoulder), Thompson mine, Thompson, Manitoba (part of NTS 63P12); Manitoba Industry, Economic Development and Mines, Manitoba Geological Survey, Geoscientific Map MAP2005-1, scale 1:200, URL <https://www.manitoba.ca/iem/info/libmin/MAP2005-1.pdf> [September 2021].

Macek, J.J., Zwanzig, H.V. and Pacey, J.M. 2006: Thompson Nickel Belt geological compilation map, Manitoba (parts of NTS 63G, J, O, P and 64A and B); Manitoba Science, Technology, Energy and Mines, Manitoba Geological Survey, Open File Report OF2006-33, digital map on CD, URL <https://www.manitoba.ca/iem/info/libmin/OF2006-33.zip> [September 2021].

Machado, N., Gapais, D., Potrel, A., Gauthier, G. and Hallot, E. 2011: Chronology of transpression, magmatism, and sedimentation in the Thompson Nickel Belt (Manitoba, Canada) and the timing of Trans-Hudson Orogen–Superior Province collision; Canadian Journal of Earth Sciences, v. 48, p. 295–324.

Manitoba Geological Survey 2020: Compilation of Sm-Nd isotope results from the Manitoba Geological Survey 2018/2019 season; Manitoba Agriculture and Resource Development, Manitoba Geological Survey, Data Repository Item DRI2020012, Microsoft® Excel® file, URL <https://www.manitoba.ca/iem/info/libmin/DRI2020012.xlsx> [September 2021].

Manitoba Mineral Resources 2013: Bedrock geology, Manitoba; *in* Map Gallery – Geoscientific Maps, Manitoba Mineral Resources, Manitoba Geological Survey, URL <http://web33.gov.mb.ca/mapgallery/mgg-gmm.html> [January 2019].

Mezger, K., Bohlen, S.R. and Hanson, G.N. 1990: Metamorphic history of the Archean Pikwitonei granulite domain and the Cross Lake subprovince, Superior Province, Manitoba, Canada; Journal of Petrology, v. 31, p. 483–517.

Rayner, N., Zwanzig, H.V. and Percival, J.A. 2006: Detrital zircon provenance of the Pipe Formation, Ospwagan Group, Thompson Nickel Belt, Manitoba, NTS 63O8; *in* Report of Activities 2007, Manitoba Science, Technology, Energy and Mines, Manitoba Geological Survey, p. 116–124, URL <https://www.manitoba.ca/iem/geo/field/roa06pdfs/GS-11.pdf> [September 2021].

Scoates, J.S., Scoates, J.R.F., Wall, C.J., Friedman, R.M. and Couëslan, C.G. 2017: Direct dating of ultramafic sills and mafic intrusions associated with Ni-sulfide mineralization in the Thompson nickel belt, Manitoba, Canada; Economic Geology, v. 112, p. 675–692.

White, D.J., Lucas, S.B., Bleeker, W., Hajnal, Z., Lewry, J.F. and Zwanzig, H.V. 2002: Suture-zone geometry along an irregular Paleoproterozoic margin: the Superior boundary zone, Manitoba, Canada; Geology, v. 30, p. 735–738.

Zwanzig, H.V. 2005: Geochemistry, Sm-Nd isotope data and age constraints of the Bah Lake assemblage, Thompson Nickel Belt and Kisseynew Domain margin: relation to Thompson-type ultramafic bodies and a tectonic model (NTS 63J, O and P); *in* Report of Activities 2005, Manitoba Industry, Economic Development and Mines, Manitoba Geological Survey, p. 40–53, URL <https://www.manitoba.ca/iem/geo/field/roa05pdfs/GS-06.pdf> [September 2021].

Zwanzig, H.V., Macek, J.J. and McGregor, C.R. 2007: Lithostratigraphy and geochemistry of the high-grade metasedimentary rocks in the Thompson Nickel Belt and adjacent Kisseynew Domain, Manitoba: implications for nickel exploration; Economic Geology, v. 102, p. 1197–1216.

Zwanzig, H.V., Böhm, C.O. and Couëslan, C.G. 2021: Laser-ablation, multicollector, inductively coupled plasma–mass spectrometry U-Pb isotopic analyses of detrital zircon grains from the Ospwagan group, Setting formation metagreywacke sample 12-04-4462, Setting Lake, central Manitoba (part of NTS 63O2); Manitoba Agriculture and Resource Development, Manitoba Geological Survey, Data Repository Item DRI2021013, Microsoft® Excel® file, URL <https://www.manitoba.ca/iem/info/libmin/DRI2021013.xlsx> [September 2021].

GS2021-4

Results of bedrock geological mapping in the Stuart Bay–Chickadee Lake area (east of Wekusko Lake), north-central Manitoba (parts of NTS 63J12, 13)

by K.D. Reid

In Brief:

- A complex volcanic stratigraphy is recorded within the Herb Lake fold with facing directions that suggest it represents a major syncline
- Close association of mafic crystal-rich turbidite and conglomerate of the McCafferty Liftover fault block suggest these were deposited in a deep-water environment by concurrent turbidity currents and debris flows, possibly adjacent to a fault scarp or elevated volcanic edifice
- The Crowduck Bay fault is a deep-seated ductile structure with strong penetrative fabrics that overprint earlier structures in the hangingwall and footwall

Citation:

Reid, K.D. 2021: Results of bedrock geological mapping in the Stuart Bay–Chickadee Lake area (east of Wekusko Lake), north-central Manitoba (parts of NTS 63J12, 13); *in* Report of Activities 2021, Manitoba Agriculture and Resource Development, Manitoba Geological Survey, p. 29–39.

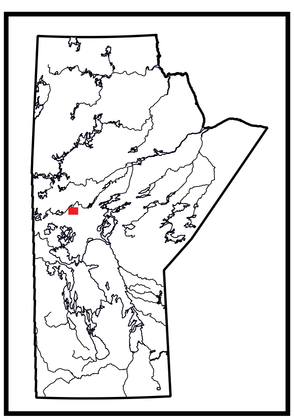

Summary

Bedrock geological mapping during the 2021 summer field season continued with 1:20 000 scale mapping east of Wekusko Lake, including the area around Stuart Bay, Chickadee Lake and the historical community of Herb Lake near the historic Rex-Laguna gold mine. The area encompasses a structurally complex confluence of at least three lithostratigraphically distinct tectonic blocks, recording the geological evolution of rocks in the eastern Paleoproterozoic Reindeer zone over a period lasting approximately 70 m.y. (ca. 1.91–1.83 Ga). In addition, these rocks have been of significant economic interest for over a century, following the discovery of gold here in 1914.

Introduction

In 1914, M.J. Hackett and R. Woosey discovered gold along the eastern shores of Wekusko Lake, near the community of Herb Lake. Subsequently, gold was intermittently produced from the Rex-Laguna deposit from 1918–1940. The Geological Survey of Canada conducted field mapping of the Herb Lake area at a scale of 1:12 000 (1 in. to 1000 ft.; Stockwell, 1937), but the stratigraphic context was not well understood at the time. In the 1940s, the Geological Survey of Canada surveyed the region at a scale of 1:63 360 (1 in. to 1 mile; e.g., Armstrong, 1941; Frarey, 1950); the resulting maps provide much of the basis for later compilations in the area, such as those by the NATMAP Shield Margin Project Working Group (1998). Geochemical studies of the Herb Lake volcanic rocks by Gordon and Lemkow (1987) were guided by the mapping of Stockwell (1937). Ansdell et al. (1999) and Connors et al. (1999) conducted detailed structural, geochemical and geochronological studies of sedimentary and volcanic rocks; however, no comprehensive geological maps were published.

The current geological mapping focuses on rocks east of Wekusko Lake; in particular, the area north and east of Stuart and Puella bays encompassing the Western Missi, Herb Lake, McCafferty Liftover and the Eastern Missi fault blocks (Figure GS2021-4-1; Ansdell et al., 1999; Connors et al., 1999). Primary objectives of the 2021 summer fieldwork include

- developing a 1:20 000 scale map detailing the stratigraphic framework of the 1.88–1.83 Ga arc volcanic and sedimentary rocks east and north of Stuart and Puella bays;
- examining complex structural relationships between southwest-directed fold-and-thrust faulting (D_2) and northwest-directed transpression (D_3);
- incorporating high-resolution geophysical data with bedrock data to better constrain geological contacts and structures in poorly exposed areas; and
- using the lithostratigraphic and structural framework to evaluate the mineral potential of rocks east of Wekusko Lake.

Regional setting and stratigraphic framework

The Flin Flon domain (FFD) is part of a series of Paleoproterozoic domains that form the internal Reindeer zone of the Trans-Hudson orogen (Lewry and Collerson, 1990) in north-central Manitoba. It has a distinct volcano-sedimentary stratigraphy that evolved from 1.91–1.83 Ga. The FFD is approximately 250 km from west to east, with an exposed north-south extent of approximately 40–50 km. The FFD is bounded to the east by the Superior province and the Superior boundary zone, is bounded to the north by turbidite greywacke and mudstone of the Kisseynew domain, and dips shallowly to the south under younger Phanerozoic platform carbonate rocks. Previous work by Stern et al. (1995) identified significant stratigraphic and geochemical differences between arc volcanic rocks west of Reed Lake (Amisk collage) versus those in the Snow Lake area (i.e., Snow

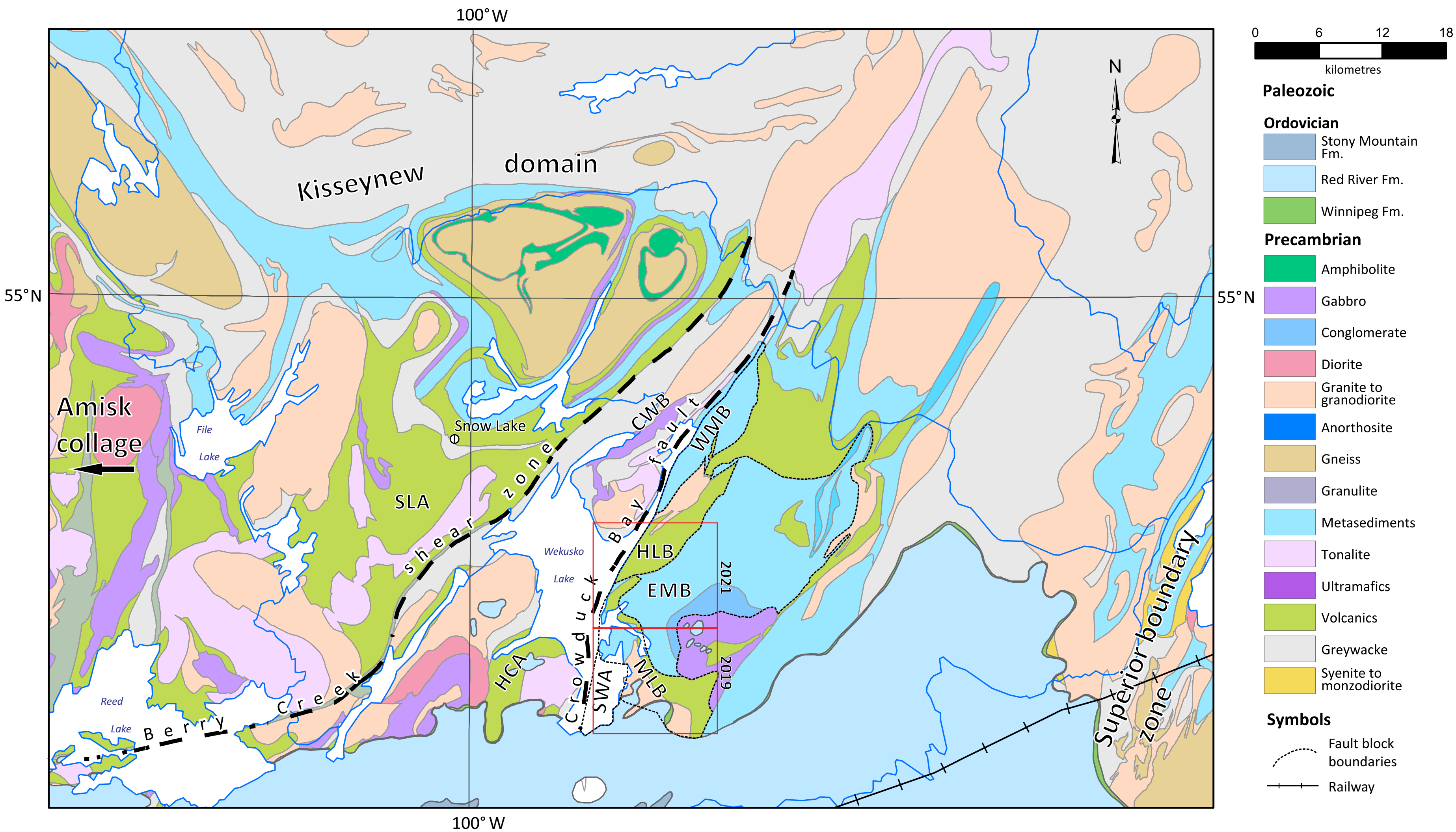

Figure GS2021-4-1: *Regional geological map showing the eastern segment of the Flin Flon domain including the areas mapped in 2019 and 2021 (see red rectangles; map is modified from an unpublished 1:250 000 scale provincial compilation), north-central Manitoba. Note the Kisseynew domain to the north, the Superior boundary zone to the east and Paleozoic cover rocks to the south. The Snow Lake arc assemblage (SLA), Hayward Creek arc assemblage (HCA), South Wekusko assemblage (SWA), McCafferty Liftover fault block (MLB), Eastern Missi fault block (EMB), Herb Lake fault block (HLB), Western Missi fault block (WMB) and Central Wekusko fault block (CWB) are shown relative to the Berry Creek shear zone and Crowduck Bay fault.*

Lake arc assemblage), indicating that these segments of the FFD may have formed in distinct tectonic settings.

Figure GS2021-4-1 shows the location of the 2021 mapping area relative to Wekusko Lake. The Snow Lake subdomain (rocks between File and Reed lakes and the Superior boundary zone) consists of fault-bounded blocks, the most well known of these being the Snow Lake arc assemblage (SLA) to the northwest of Wekusko Lake. The Berry Creek shear zone and Crowduck Bay fault constrain a 15–20 km wide package of greywacke and mudstone, which extends southwest from the Kisseynew domain into the central portion of Wekusko Lake referred to by Ansdell et al. (1999) as the Central Wekusko fault block (CWB; Figure GS2021-4-1). Southwest of Wekusko Lake within the CWB is the Hayward Creek arc assemblage (HCA). Though no age determinations are presently available for these rocks, it is thought to be a juvenile arc (e.g., ca. 1.89 Ga) in thrust contact with Burntwood group sediments. Fault-bounded lithotectonic blocks east of the Crowduck Bay fault include ocean-floor basalts of the South Wekusko assemblage (SWA), evolved arc volcanic rocks of the McCafferty Liftover fault block (MLB) and Herb Lake fault block (HLB), and fluvial-alluvial sedimentary rocks of the Western Missi fault block (WMB) and Eastern Missi fault block (EMB; e.g., Ansdell et al., 1999; Gilbert and Bailes, 2005; Figure GS2021-4-1). A detailed review of the stratigraphic and structural context of the project area is given by Reid (2019a).

Results of 2021 fieldwork

Bedrock mapping in the Stuart Bay–Chickadee Lake area documented a number of structural and stratigraphic features, which have been used to develop a preliminary map (PMAP2021-1; Reid, 2021) and simplified page figure (Figure GS2021-4-2). A brief description of each map unit (oldest to youngest) and related features is provided below.

Pillowed basalt of probable ocean-floor affinity (unit F1)

South of the HLB (~2 km north of McCafferty Lift Over [ML]; Figure GS2021-4-2), pillowed basalts of probable ocean-floor affinity (unit F1) are in structural contact and appear to have been folded by the same regional structure as the HLB. This is evidenced by a change in facing direction of the pillowed basalts moving from northwest to southeast. Northwest of the apparent fold axial trace (Herb Lake syncline; Figure GS2021-4-2) the facing direction is overturned and younging to the northwest, whereas southeast of the axial trace it is upright and younging to the southeast toward the McCafferty fault. The basalt is weakly feldspar-pyroxene porphyritic and is characterized by blue-green weathering, thin (1–2 cm) chilled margins with minor epidote-altered interpillow hyaloclastite and lack of amygdules (Figure GS2021-4-3a). These rocks are considered ocean-floor basalt (unit F1) given their similarities to the blue-green–weathered pillow basalts along the southern and southeastern shores of Wekusko Lake, which have an ocean-floor affinity (N-MORB; Gilbert and Bailes, 2005).

McCafferty Liftover fault block (units S1–4)

Ansdell et al. (1999) referred to intermediate to felsic volcanic and volcaniclastic rocks in the Puella and Stuart bays area as the MLB, whereas Gilbert and Bailes (2005) called these rocks the Puella Bay suite and NATMAP Shield Margin Project Working Group (1998) classified them as the Schist-Wekusko assemblage. In this report, they are referred to as rocks of the MLB. The McCafferty fault separates feldspar-phyric andesite conglomerate (unit S1), feldspar-crystal–rich turbidite (unit S3) and volcaniclastic dacite (units S4a, b) from pillowed basalts (unit F1) and volcanic rocks of the HLB.

Unit S1 is clast-supported, heterolithic, volcanic cobble and boulder conglomerate comprising mainly subrounded plagioclase-phyric andesite clasts but also local dacite clasts (Figure GS2021-4-2; see unit S2 in Gilbert and Bailes, 2005). Weakly plagioclase-phyric massive andesite (unit S2) was observed in an outcrop (UTM Zone 14N, NAD83, 448600E, 6062983N) south of Puella Bay, outside the mapping area, and is inferred to occur underwater in the southwestern corner of the map; it contains rare amygdules but lacks features characteristic of cohesive flows and thus is possibly intrusive. A large flat-lying outcrop 100 m northwest of McCafferty Liftover (ML; Figure GS2021-4-2) preserves a complete 1.5 m thick feldspar-crystal–rich turbidite sequence; the feldspar-crystal–rich wacke and mudstone (unit S3) are thin to thick bedded with normally graded beds that consistently young to the east-southeast (Figure GS2021-4-3b). Farther along strike to the northeast, feldspar-crystal–rich layers are interbedded with subangular to subrounded, matrix- to clast-supported, andesite cobble conglomerate. These features are consistent with deposition as concurrent debris flows into a relatively deep-water setting with a steep adjacent slope.

The transition from unit S1 to S4a is marked by a change in matrix composition from feldspar-phyric andesite to dacite and the appearance of scoriaceous clasts. Clasts are typically 2–15 cm, subangular to subrounded and matrix supported (Figure GS2021-4-3c) in a light grey feldspar-phyric matrix. Unit S4b is a dark to medium grey, massive, weakly feldspar-phyric dacite that occurs along the south shore of Puella Bay (Figure GS2021-4-2; Reid, 2021). Feldspar in this unit commonly weathers an orangey colour and can been seen in sheared and brecciated dacite near the contact with the Puella Bay–Stuart Lake fault (Figure GS2021-4-3d). Two planar structural fabrics are common in rocks of the MLB, an early spaced cleavage that occurs in dacite (unit S4b) that strikes 310–330° and dips steeply to the northeast. The spaced cleavage is overprinted by a strong penetrative foliation that strikes 10–20° and dips steeply to the southeast toward Wekusko Lake and the Crowduck Bay fault (Figure GS2021-4-2).

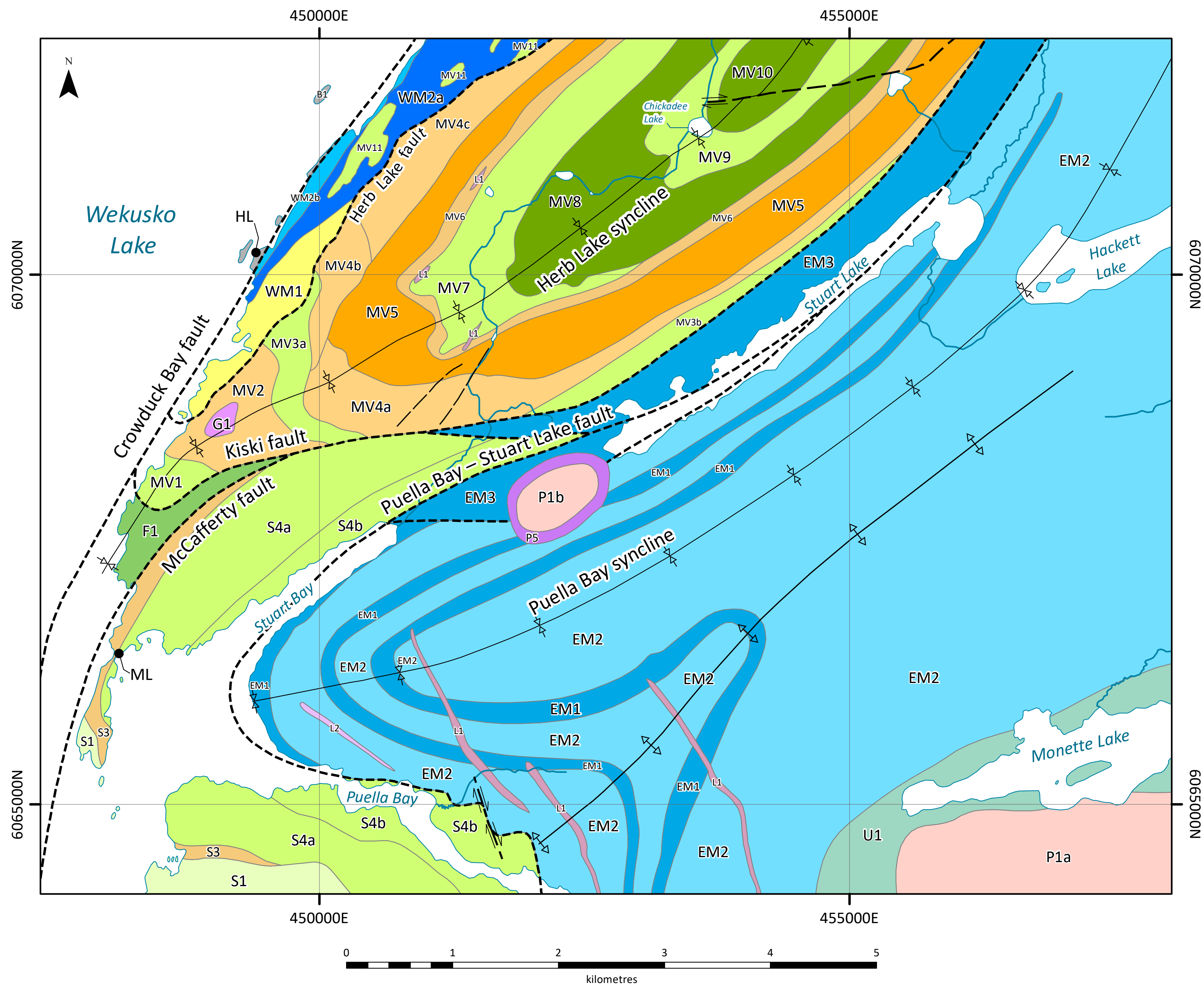

Figure GS2021-4-2: *Simplified geological map of the project area including historical points of reference (Herb Lake community [HL], McCafferty Lift Over [ML]), Chickadee Lake, Stuart Lake and Stuart Bay, eastern Wekusko Lake. For more detail including unit legend, see PMAP2021-1 (Reid, 2021). All co-ordinates are in UTM Zone 14N, NAD83.*

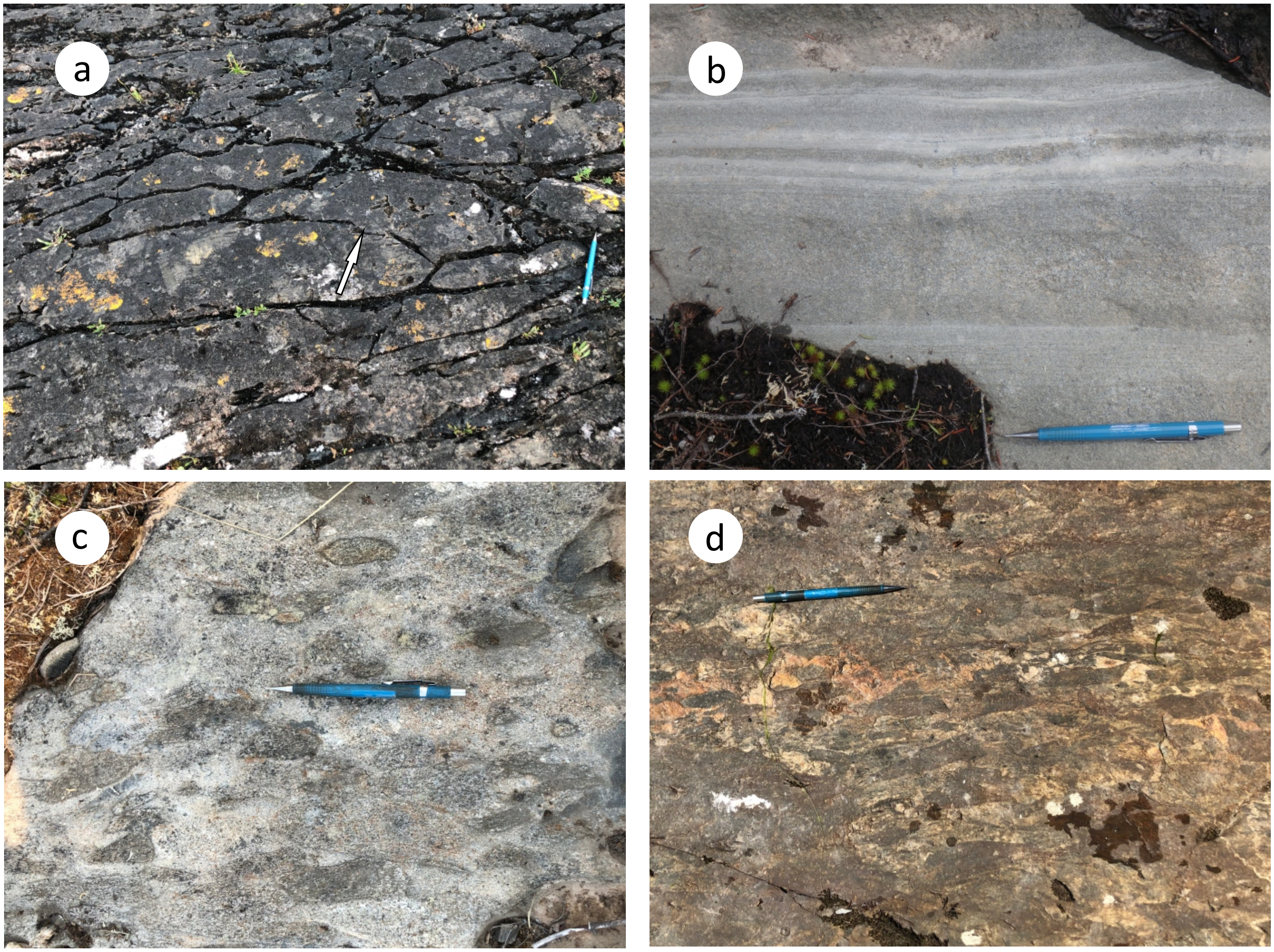

Figure GS2021-4-3: *Outcrop photographs of the South Wekusko assemblage and McCafferty Liftover fault block arc volcanic rocks:* ***a)*** *weakly feldspar-phyric pillowed basalt with classic pillow drape (arrow; unit F1; UTM Zone 14N, NAD83, 448186E, 6067872N);* ***b)*** *thin-bedded feldspar-crystal–rich wacke and mudstone (unit S3; 448684E, 6067417N);* ***c)*** *heterolithic feldspar-phyric andesite conglomerate (unit S4a; 450145E, 6068279N);* ***d)*** *brecciated orangey pink dacite (unit S4b; 451051E, 6067981N).*

Central Wekusko fault block (unit B1)

Highly strained, dark grey, thin- to thick-bedded greywacke and mudstone is observable near the Herb Lake community and along the shoreline to the northeast (Figure GS2021-4-2). These rocks display minor isoclinal folds, which are commonly rootless with their limbs sheared away. These rocks contain a strong penetrative foliation that strikes 10–20°, dips steeply to the southeast and parallels the trend of the Crowduck Bay fault (Figure GS2021-4-2).

Herb Lake fault block (units MV1–11)

Stockwell (1937) first recognized that rocks of the HLB are a complex package of volcanic strata that are tightly to isoclinally folded, and suggested the HLB represents a syncline. Recent mapping subdivides the HLB into 11 units (MV1–11) and determined that facing directions support the interpretation that it is a major syncline (Figure GS2021-4-2).

Directly north of the pillow basalts (unit F1; Figure GS2021-4-2), the rocks transition to weakly feldspar-phyric dacite (unit MV1). These rocks display two well-developed cleavages at a shallow angle to each other imparting a diamond-shaped stepped appearance to the outcrop. These fabrics are common throughout the HLB with an early spaced cleavage striking 45–60° and a later overprinting penetrative foliation that strikes 10–30°; both fabrics dip steeply to the southeast. Northeast of the MV1 dacite, the composition and mineralogy of the rocks change to become more mafic and feldspar-rich (up to 70%) with a medium grey fine-grained matrix (unit MV2). Feldspar grades from coarse to medium grained moving to the northeast; no bedding relationships were observed but occasional lithic lapilli fragments support this unit being volcaniclastic in origin (Figure GS2021-4-4a).

Moderately strained, monolithic, clast-supported, rhyolite lapillistone and minor felsic tuff (unit MV3a) occur directly northeast of unit MV2 (Figure GS2021-4-2). Thick beds of nor-

Figure GS2021-4-4: *Rocks of the Herb Lake volcanic block:* ***a)*** *feldspar-crystal–rich lapilli tuff with lithic clasts outlined by dashed lines (unit MV2; UTM Zone 14N, NAD83, 448899E, 6068340N);* ***b)*** *feldspar-phyric andesite tuff breccia to agglomerate (unit MV4b; 450312E, 6069960N), 15 cm long knife for scale;* ***c)*** *parallel-bedded feldspar volcanic sandstone with symmetric ripples draped by greywacke (unit MV6; 451520E, 6070975N);* ***d)*** *juvenile cuspate grey rhyolite fragments (arrow) in a light pink aphyric siliceous matrix (unit MV9; 453193E, 6071228N).*

mally graded felsic tuff on the northwest side of the Herb Lake syncline young to the east-southeast. Furthermore, northeast along the eastern limb of the Herb Lake syncline, a monolithic pebbly rhyolite conglomerate (unit MV3b) is considered to be the equivalent of unit MV3a (Figure GS2021-4-2); here, graded beds and minor scours indicate that this unit youngs to the northwest.

Unit MV4 is a variable intermediate volcaniclastic unit that has facies from pyroxene-plagioclase–phyric andesite conglomerate (unit MV4a) to feldspar-phyric andesite agglomerate (unit MV4b; Figure GS2021-4-4b) to heterolithic conglomerate (unit MV4c). The most distinctive of these units is the feldspar-phyric tuff breccia/agglomerate, containing irregular, subrounded, matrix- to framework-supported clasts up to 100 cm in diameter with mafic hornblende-rich rims. The change to unit MV5 is marked by a shift in extrusive character to cohesive andesite sheet flows, which are massive, containing medium-grained tabular plagioclase phenocrysts as well as amygdules and breccia near flow tops.

Thin to thick planar-bedded, volcanic, feldspar sandstone is the main constituent of unit MV6 and represents a marker unit within the volcanic pile. Along the northwest limb, it is approximately 100–150 m thick (Figure GS2021-4-2) and contains minor pebbly conglomerate and felsic ash tuff interbedded with the sandstone. An outcrop on the northwest limb preserves multiple cycles of normal gradation, minor scours and one bed with very fine sandstone draped over symmetric ripples, consistent with a younging direction to the southeast (Figure GS2021-4-4c). On the southeast limb of the fold, unit MV6 narrows slightly to 75–100 m thick and occurs as fine- to coarse-grained feldspar sandstone that lacks pebbly conglomerate and ash tuff.

Unit MV7 is mainly observed as massive feldspar-phyric dacite but minor millimetre- to centimetre-scale beds of ash tuff suggest that it is likely a series of metre-thick flows with interflow volcaniclastic rocks. This unit is approximately 400 m thick on the northwest limb of the Herb Lake syncline but is absent on the southeast limb (Figure GS2021-4-2), where unit MV6 is in direct contact with basalt of unit MV8.

Unit MV8 transitions from fine to medium grained and pyroxene porphyritic near its lower contact with unit MV7, to fine grained with sub-metre amygdule-rich domains; this is interpreted to represent a number of basalt flows several metres thick, characterized by the amygdules near the top of each flow. The top of this unit is marked by centimetre-scale bedded mafic wacke and subrounded framework-supported mafic conglomerate suggesting postdepositional epiclastic reworking.

Unit MV9 is a distinct light pinkish-grey, weakly feldspar-quartz–phyric rhyolite, which was previously termed Chickadee rhyolite (e.g., Ansdell et al., 1999). Close inspection of this unit reveals that it contains grey aphyric juvenile (cuspate) clasts in a wavy foliated pinkish and grey matrix (Figure GS2021-4-4d), interpreted as eutaxitic texture typically observed in welded pyroclastic flows (e.g., McPhie et al., 1993).

Mafic rocks of unit MV10 occur directly to the northeast of the Chickadee rhyolite. The base of this unit is a massive, dark greenish-black, fine- to medium-grained rock with approximately 60% hornblende and 40% plagioclase; whereas stratigraphically up section (to the northeast) the unit transitions to sub-metre–bedded mafic lapilli tuff with a few scattered amygdules and minor epidote alteration around lapilli clasts.

Small outcrop windows of hypabyssal quartz-feldspar–phyric rhyolite (unit MV11) are noted intruding pebble conglomerate and felsic tuff of unit MV3a as well as argillaceous sandstone of unit EM3, but only in unit WM2a of the WMB do they form mappable units (Figure GS2021-4-2).

Western Missi fault block (units WM1–2)

The WMB is a narrow wedge-shaped package of felsic volcanic, volcaniclastic and sedimentary rocks that extends approximately 2.5 km southwest of the historical Herb Lake community (HL; Figure GS2021-4-2). Connors et al. (1999) interpreted it to be structurally juxtaposed to the HLB by the Herb Lake fault (Figure GS2021-4-2). The WMB preserves the stratigraphic contact between felsic volcanic rocks (unit WM1) and heterolithic pebbly conglomerate (unit WM2a); this contact can be observed approximately 700 m south of the old Herb Lake community along the shoreline.

The stratigraphic base of the WMB contains felsic volcanic rocks, which include massive, lobate, flow-banded and volcaniclastic varieties of rhyolite and dacite. Most are porphyritic with up to 15% 1–3 mm subhedral feldspar and up to 5% 1–2 mm subhedral quartz and local spherulites (Figure GS2021-4-5a). In one location, dacite tuff breccia and lapilli tuff grade over several metres into subrounded, clast-supported, rhyolite cobble conglomerate and then into heterolithic sandy pebbly conglomerate (unit WM2a) that contains tabular crossbeds (Figure GS2021-4-5b). North of the Herb Lake community (Figure GS2021-4-2) along the lakeside, pebbly conglomerate grades into trough-crossbedded feldspathic arenite with pebbles restricted to minor centimetre-scale beds (unit WM2b).

Eastern Missi fault block (units EM1–3)

Tightly folded, laterally continuous beds of conglomerate and sandstone form a syncline–anticline pair east of Puella and Stuart bays (Figure GS2021-4-2). Subrounded to rounded, clast-supported, polymictic cobble and boulder conglomerate forms the base of the succession (unit EM1; Figure GS2021-4-5c). Conglomerate layers are separated by intervals of trough-crossbedded feldspathic arenite (unit EM2; Figure GS2021-4-5d); the arenite preserves a distinct spaced cleavage that strikes 330 to 340° and dips moderately to the northeast. Farther to the east, a weak foliation can be seen striking 50° and dips steeply to the southeast. A change in sediment character was noted in both the conglomerate and the sandstone moving upsection. The conglomerate transitions from clast to matrix supported along with a reduction in clast variety, whereas the sandstone changes from coarse to fine grained in the upper sequence with minor light grey greywacke intraclasts.

Unit EM3 is distinct from other EM units in that in has a decreased quartz-grain content corresponding with an increase in argillaceous matrix and the presence of scattered subrounded mafic cobbles. Local trough-crossbeds indicate that this unit youngs to the northwest; this has previously been interpreted to represent an anticline centred on Stuart Lake (e.g., Connors et al., 1999). However, the change in sediment character could suggest it is in fault contact with units EM1 and 2 (see Puella Bay–Stuart Lake fault; Figure GS2021-4-2) and more closely associated with the Herb Lake volcanic rocks.

Volcanic rocks of uncertain age (unit U1)

Unit U1 is the geophysical extrapolation of a matrix- to clast-supported, intermediate to felsic volcanic conglomerate (Figure GS2021-4-2) that occurs directly to the south in the 2019 mapping area (see Reid, 2019b). These rocks are separated from the EMB by a distinct topographic low that extends into the Monette Lake area to the northeast; at this time the stratigraphic context of these rocks is unknown.

Intrusive rocks (units G1, P1, P5, L1–2)

Unit G1 is a medium- to coarse-grained gabbro (Figure GS2021-4-6a) with 60% plagioclase and 40% hornblende (pseudomorphs after pyroxene), which occurs within unit MV2 of the HLB (Figure GS2021-4-2). No intrusive relationships were observed so its time of emplacement is uncertain.

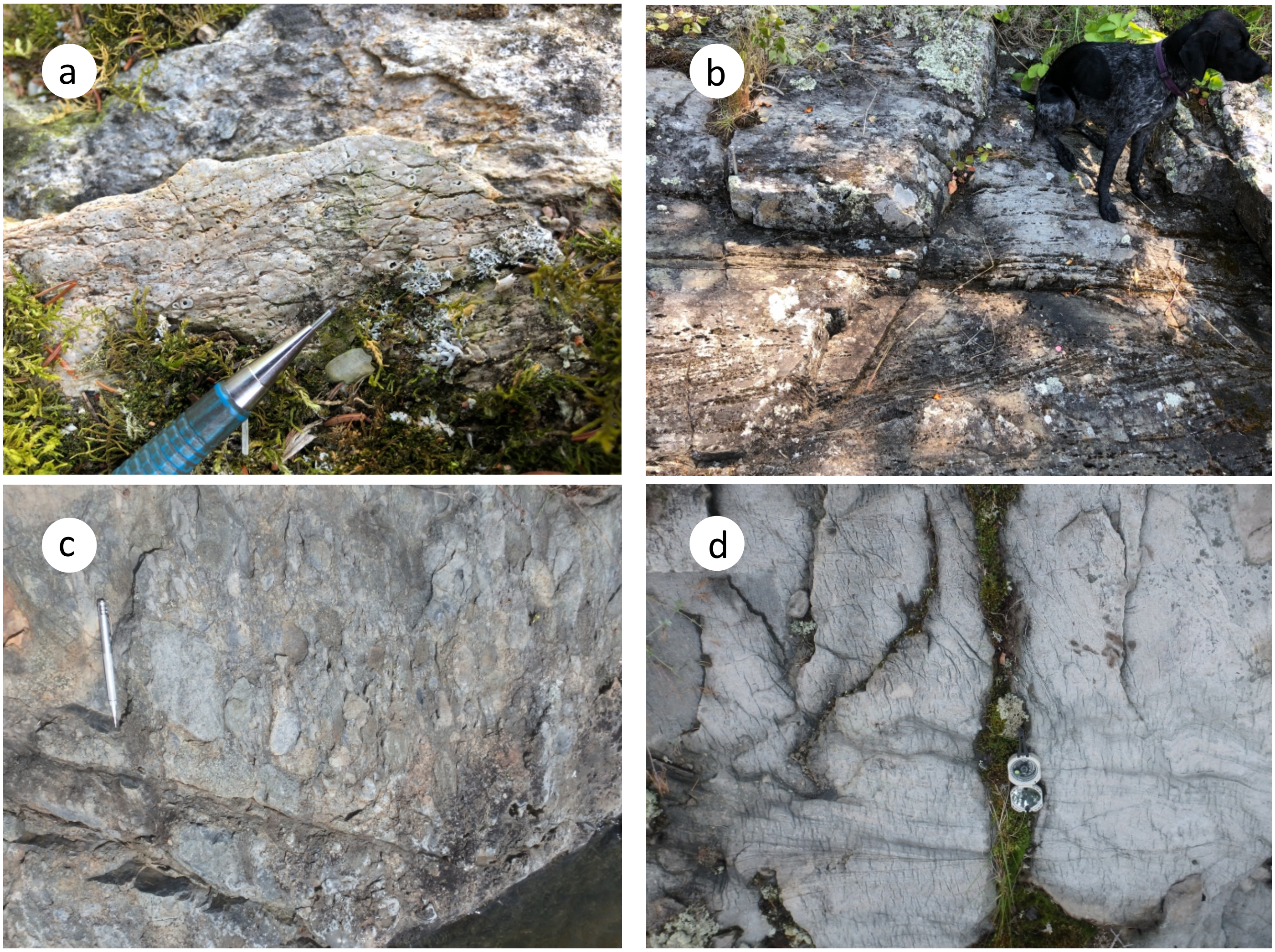

Figure GS2021-4-5: *Volcanic, volcaniclastic and sedimentary rocks of the Western Missi and Eastern Missi fault blocks:* ***a)*** *spherulitic rhyolite (unit WM1; UTM Zone 14N, NAD83, 448843E, 6068881N);* ***b)*** *planar-bedded pebbly conglomerate with tabular crossbeds (unit WM2a; 449346E, 6069829N), German short-haired pointer for scale;* ***c)*** *polymictic clast-supported heterolithic conglomerate (unit EM1; 449862E, 6065392N);* ***d)*** *trough-crossbedded sandstone with spaced cleavage (S_3; unit EM2; 450955E, 6065762N).*

Unit P1a in the southeastern corner of the map area is the geophysical extrapolation of the weakly deformed, medium-grained, Monette Lake granite observed to the south in the 2019 mapping area (see Reid, 2019b). A semicircular intrusion near the southwestern end of Stuart Lake consists of two parts: an inner granodiorite (unit P1b) and an outer quartz-bearing diorite (unit P5; Figure GS2021-4-2). Unit P1b is a pinkish-grey, medium-grained, equigranular granodiorite with 40% quartz, 35% K-feldspar, 15% plagioclase and 10% hornblende. Unit P5 has a distinct glomeroporphyritic texture, with feldspar (40%) and quartz (2–3%) forming sub-centimetre knots and the remainder being hornblende, which is pseudomorphous after pyroxene (Figure GS2021-4-6b).

A number of narrow (<75 m) gabbroic dikes cut both the EMB and the HLB (unit L1; Figure GS2021-4-2); these range from fine to medium grained with 70% hornblende and 30% plagioclase, which is typically aligned with a weak foliation (Figure GS2021-4-6c). A distinct quartz-feldspar–phyric granodiorite (unit L2) intrudes sandstone (unit EM2) of the EMB; it contains 4–15 mm subhedral quartz and feldspar in a finer-grained feldspar matrix (Figure GS2021-4-6d).

Discussion

The pillowed basalts of probable ocean-floor affinity directly north of McCafferty Lift Over (Figure GS2021-4-2; Reid, 2021) are assumed to be the oldest stratigraphic unit in the map area on the basis of their similarity to the SWA and other 1.90 Ga ocean-floor/back-arc–type rocks (e.g., Stern et al., 1995; Gilbert and Bailes, 2005). A change in pillow-facing direction corresponds to a southwestern extension of the axial trace from the Herb Lake syncline. This suggests that these units were in contact prior to the formation of the Herb Lake syncline, possibly as a result of early thrust faulting.

Rocks of the MLB form a homoclinal east-younging package bounded by the McCafferty fault to the northwest and the Puella Bay–Stuart Lake fault to the east (Figure GS2021-4-2).

Figure GS2021-4-6: *Intrusive rocks:* ***a)*** *medium- to coarse-grained gabbro (unit G1; UTM Zone 14N, NAD83, 449131E, 6068637N);* ***b)*** *glomeroporphyritic quartz diorite (unit P5; 451944E, 6067545N);* ***c)*** *medium-grained gabbro dike (unit L1) cutting Eastern Missi fault block sandstone (unit EM2; 454434E, 6065141N);* ***d)*** *quartz-feldspar–phyric granodiorite (unit L2; 449897E, 6065795N).*

The intimate association of feldspar-phyric andesite cobble/boulder conglomerate (unit S1) and feldspar-crystal–rich turbidite (unit S3) in the lower portion of the MLB record an interval of deep subaqueous deposition by concurrent turbidity currents and debris flows, likely adjacent to a fault scarp or elevated volcanic edifice. Units S4a and b mark a shift in volcanism from mafic to felsic, possibly linked to an evolving and fractionated magma chamber.

The HLB represents of a thick succession of felsic to mafic volcanic and volcaniclastic rocks. The lower portion of this volcanic pile (units MV1–4) records a period of felsic to intermediate volcaniclastic deposition followed by cohesive amygdule-bearing andesite flows (unit MV5). The feldspathic volcanic sandstone of unit MV6 is a marker bed, which can be traced from the northwest limb to the southeast limb of the Herb Lake syncline (Figure GS2021-4-2), and is interpreted to represent a hiatus in volcanic activity during which epiclastic reworking occurred prior to deposition of the overlying dacite and minor ash tuff (unit MV7). Symmetric ripples draped with finer clastic material suggest that unit MV6 may have formed in a shallow marine environment influenced by tidal variation. The upper portion of the volcanic pile is dominated by basalt (units MV8 and 10) separated by matrix-supported rhyolite lapilli tuff (unit MV9). The presence of cuspate juvenile clasts in a wispy matrix suggests that unit MV9 is at least in part pyroclastic in nature.

The WMB preserves the stratigraphic relationship between volcanism and epiclastic sedimentation. The apparent absence of a weathering profile might indicate that this transition occurred relatively quickly, reflecting a rapid shift from felsic volcanism to subaerial clastic deposition. The EMB represents a thick succession of siliciclastic material deposited in part by fluvial processes. A decrease in both clast and grain size from the base to the upper portions of this block might represent the progressive fill of a subbasin.

A summary of structural observations is as follows. Depositional features (S_0) are characterized by both volcanic and sedimentary textures. No arc accretionary structures were observed during mapping but for discussion here, S_1 has been reserved for these structures as it has for the broader Flin Flon domain (e.g., Ryan and Williams, 1999). Spaced cleavage in the HLB and weak penetrative foliation in the EMB both strike 45–60° and are considered the earliest deformation fabrics (S_2). A distinct 330–340° striking spaced cleavage (S_3), which is common in the EMB and MLB but rarely observed in the HLB, overprints the earlier formed S_2 cleavage and foliation. Within 1–2 km of the Crowduck Bay fault, a strong penetrative foliation (S_4) strikes 10–30° and overprints all other fabrics in the hanging wall and footwall.

Further investigation of the stratigraphic and tectonic setting will be constrained through geochemical and petrographic analyses of samples collected. An in-depth study and compilation of all structural data for the region will help to further the knowledge of the structural evolution of the region. The result of this work will be the focus of later geoscientific reports and maps.

Economic considerations

The Snow Lake subdomain is recognized as a world-class volcanogenic massive sulphide district, having produced both copper and zinc consistently for decades (e.g., Galley et al., 2007). Many believe this has overshadowed the region's history as a significant lode gold producer (e.g., Rex-Laguna and New Britannia gold mines). Gold mineralization discovery and production in the mapping area has a long and intermittent history from 1914 to present. For a complete history and exhaustive list of gold occurrences in the map area, the reader is referred to Richardson and Ostry (1996).

New geological mapping described here and detailed in Reid (2021) for rocks east of Wekusko Lake emphasizes the complex stratigraphic and structural evolution of several fault-bounded lithostratigraphic blocks in the hanging wall to the Crowduck Bay fault. Traditionally, exploration for gold in this area has focused on the intersection of structures with competent rheology, such as quartz-feldspar porphyry adjacent to the Crowduck Bay fault (e.g., Rex-Laguna deposit). However, provided the tightness of folding affecting Herb Lake volcanic rocks, further focus should be given to areas of potential flexural slip and fold hinge dilation along the Herb Lake syncline. In particular, the area between Puella Bay, Stuart Bay and Stuart Lake is characterized by the confluence of the Puella Bay–Stuart Lake fault with adjoining structures; this area should be further examined for both dilation jogs and/or intersecting structures that may have acted as conduits for gold mineralizing fluids.

Further work will focus on building a comprehensive geological map and refined geological model for this region, which will aid explorers in developing new gold exploration targets and ideas.

Acknowledgments

The author thanks P. Goernert and K. St. Paul for providing enthusiastic field assistance. Thank you to A. Santucci and L. Chackowsky for GIS technical support and C. Epp for logistical support and help preparing samples and thin sections. This contribution was greatly enhanced through constructive reviews by M. Rinne and C. Böhm.

References

Ansdell, K.M., Connors, K.A., Stern, R.A. and Lucas, S.B. 1999: Coeval sedimentation, magmatism, and fold-thrust domain development in the Trans-Hudson orogen: geochronological evidence from the Wekusko Lake area, Manitoba, Canada; Canadian Journal of Earth Sciences, v. 36, p. 293–312.

Armstrong, J.E. 1941: Wekusko, Manitoba; Geological Survey of Canada, Map 665A, scale 1:63 360.

Connors, K.A., Ansdell, K.M. and Lucas, S.B. 1999: Coeval sedimentation, magmatism, and fold-thrust development in the Trans-Hudson orogen: propagation of deformation into an active continental arc setting, Wekusko Lake area, Manitoba; Canadian Journal of Earth Sciences, v. 36, p. 275–291.

Frarey, M.J. 1950: Crowduck Bay, Manitoba; Geological Survey of Canada, Map 987a, scale 1:63 360.

Galley, A.G., Syme, E.C. and Bailes, A.H. 2007: Metallogeny of the Paleoproterozoic Flin Flon belt, Manitoba and Saskatchewan; *in* Mineral Deposits of Canada: a Synthesis of Major Deposit Types, District Metallogeny, the Evolution of Geological Provinces, and Exploration Methods, W.D. Goodfellow (ed.), Geological Association of Canada, Mineral Deposits Division, Special Publication 5, p. 509–531.

Gilbert, H.P. and Bailes, A.H. 2005: Geology of the southern Wekusko Lake area, Manitoba (NTS 63J12NW); Manitoba Industry, Economic Development and Mines, Manitoba Geological Survey, Geoscientific Map MAP2005-2, scale 1:20 000, URL <https://www.manitoba.ca/iem/info/libmin/MAP2005-2.pdf> [October 2021].

Gordon, T.M. and Lemkow, D. 1987: Geochemistry of Missi group volcanic rocks, Wekusko Lake, Manitoba; Geological Survey of Canada, Open File 1442, 38 p.

Lewry, J.F. and Collerson, K.D. 1990: Trans-Hudson orogen: extent, subdivisions, and problems; *in* The Proterozoic Trans-Hudson Orogen of North America, J.F. Lewry and M.R. Stauffer (ed.), Geological Association of Canada, Special Publication 37, p. 1–14.

McPhie, J., Doyle, M. and Allen, R. 1993: Volcanic textures: a guide to the interpretation of textures in volcanic rocks; University of Tasmania, Centre for Ore Deposit and Exploration Studies, Hobart, Tasmania, 197 p.

NATMAP Shield Margin Project Working Group 1998: Geology, NATMAP Shield Margin Project area, Flin Flon belt, Manitoba/Saskatchewan; Geological Survey of Canada, Map 1968A, scale 1:100 000.

Reid, K.D. 2019a: Bedrock geological mapping of the Puella Bay area (Wekusko Lake), north-central Manitoba (part of NTS 63J12); *in* Report of Activities 2019, Manitoba Agriculture and Resource Development, Manitoba Geological Survey, p. 42–51, URL <https://www.manitoba.ca/iem/geo/field/roa19pdfs/GS2019-4.pdf> [October 2021].

Reid, K.D. 2019b: Preliminary geology of the Puella Bay area, Wekusko Lake, north-central Manitoba (NTS 63J12); Manitoba Agriculture and Resource Development, Manitoba Geological Survey, Preliminary Map PMAP2019-4, scale 1:15 000, URL <https://www.manitoba.ca/iem/info/libmin/PMAP2019-4.pdf> [October 2021].

Reid, K.D. 2021: Bedrock geology of the Stuart Bay–Chickadee Lake area (east of Wekusko Lake), north-central Manitoba (parts of NTS 63J12, 13); Manitoba Agriculture and Resource Development, Manitoba Geological Survey, Preliminary Map PMAP2021-1, scale 1:15 000, URL <https://www.manitoba.ca/iem/info/libmin/PMAP2021-1.pdf> [November 2021].

Richardson, D.J. and Ostry, G. (revised by Weber, W. and Fogwill, D.) 1996: Gold deposits of Manitoba; Manitoba Energy and Mines, Economic Geology Report ER86-1 (2nd edition), 114 p., URL <https://www.manitoba.ca/iem/info/libmin/ER86-1.zip> [October 2021].

Ryan, J.J. and Williams, P.F. 1999: Structural evolution of the eastern Amisk collage, Trans-Hudson orogen, Manitoba; Canadian Journal of Earth Sciences, v. 36, p. 251–273.

Stern, R.A., Syme, E.C., Bailes, A.H. and Lucas, S.B. 1995: Paleoproterozoic (1.90–1.86 Ga) arc volcanism in the Flin Flon belt, Trans-Hudson orogen, Canada; Contributions to Mineralogy and Petrology, v. 119, p. 117–141.

Stockwell, C.H. 1937: Gold deposits of Herb Lake area, northern Manitoba; Geological Survey of Canada, Memoir 208, 46 p.

GS2021-5

Bedrock mapping at Ralph Lake, Lynn Lake greenstone belt, northwestern Manitoba (part of NTS 64C14): preliminary results and geological implications

by X.M. Yang

In Brief:

- New detailed bedrock mapping provides an updated geological framework in the Ralph Lake area, tectonic evolution reflected by the emplacement of I-type, adakite-like, and S-type granitoids
- Adakite-like granitoid intrusions of the post-Sickle intrusive suite may provide an important guide to Au mineralization
- Two-mica granite is emplaced at the boundary zone between the Lynn Lake greenstone belt and Southern Indian Lake domain and may have potential for rare metals (e.g., Li, Ta, Cs)

Citation:
Yang, X.M. 2021: Bedrock mapping at Ralph Lake, Lynn Lake greenstone belt, northwestern Manitoba (part of NTS 64C14): preliminary results and geological implications; *in* Report of Activities 2021, Manitoba Agriculture and Resource Development, Manitoba Geological Survey, p. 40–58.

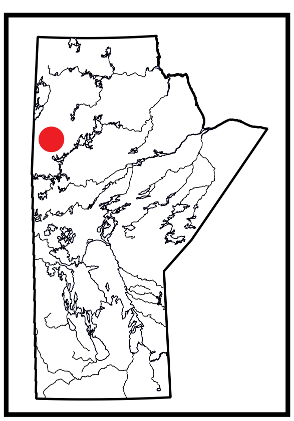

Summary

In 2021, the Manitoba Geological Survey resumed its multiyear bedrock mapping project in the Paleoproterozoic Lynn Lake greenstone belt. The mapping took advantage of outcrops exposed by bush fire east of Ralph Lake to investigate a volcano-sedimentary sequence of the Wasekwan group and overlying sedimentary rocks of the Ralph Lake and Zed Lake groups, the unconformity between them, and pre- to post-Sickle granitoid intrusions. Part of the Wasekwan group supracrustal rocks is well exposed in the burned area and, from the base to top, consists of heterolithic volcanic breccia, tuff breccia, lapillistone, lapilli tuff, tuff and plagioclase-phyric basalt to massive basalt and pillow basalt, as well as associated gabbroic intrusions. This volcanic sequence, cut by pre- and post-Sickle granitoid intrusions, is overturned and unconformably overlain by sediments of the Ralph Lake and Zed Lake groups. These sedimentary rocks are cut by a two-mica granite intrusion of the late intrusive suite. The pre- and post-Sickle intrusions are characterized by high magnetic-susceptibility (MS) values of up to 53.2×10^{-3} SI, and are typical of volcanic-arc I-type and adakite-like granitoids, respectively. The two-mica granite, displaying the lowest MS value (0.054×10^{-3} SI) in the area, is S type and was emplaced into a collisional setting. The unconformity between the Ralph Lake and Zed Lake sediments and the Wasekwan supracrustal rocks reflects a tectonic event likely linked to regional extension resulting from orogen relaxation and/or collapse triggered by slab roll-back, which may have created the synorogenic basin(s) that received sediments derived from the surrounding greenstone belt, forming the polymictic conglomerate, greywacke, psammite and siltstone. The greywacke to siltstone is characterized by porphyroblastic hornblende and muscovite (±garnet), together with hornblende-bearing matrix of the polymictic conglomerate, indicating middle amphibolite–facies metamorphism.

The pre-Sickle granitoid rocks, post-Sickle adakite-like granitoid rocks and late intrusive granite suites were emplaced into the supracrustal sequences, recording tectonic evolution from volcanic arc through extension induced by slab roll-back to terminal collision. More importantly, ore fluids related to adakite-like magmatism could be important for Au mineralization, so the adakite-like granitoids may serve as an indicator for Au exploration in the belt. Furthermore, the occurrence of late S-type granite cutting the Zed Lake greywacke suggests 1) emplacement in a collisional setting and potential association with rare-metal mineralization (e.g., Li, Cs, Ta), and 2) location of the boundary between the Lynn Lake greenstone belt and Southern Indian domain.

Introduction

The Paleoproterozoic Lynn Lake greenstone belt (LLGB; Bateman, 1945) is separated from the Kisseynew domain (basin) to the south by the Granville Lake structural zone (GLSZ; White et al., 2000; Zwanzig, 2000), which forms its southern boundary (Zwanzig, 1990; Zwanzig and Bailes, 2010). Based on modelling of seismic-reflection data and geological analysis, White et al. (2000) pointed out that the LLGB represents a volcanic-plutonic arc terrane formed by northward subduction of back-arc basin crust, and subsequent contraction and underthrusting of the Kisseynew domain beneath the LLGB during terminal collision. To the north, the LLGB is unconformably overlain by the Ralph Lake conglomerate and Zed Lake greywacke (Gilbert et al., 1980), which are likely attributed to the Southern Indian domain (SID) based on comparable rock associations. The nature of the boundary between the LLGB and SID, however, requires further investigation. The Ralph Lake area provides an excellent opportunity to decipher such relationships.

In 2021, the Manitoba Geological Survey (MGS) resumed its multiyear bedrock geological mapping program in the LLGB (Figure GS2021-5-1) of northwestern Manitoba. Detailed bedrock mapping at 1:10 000 scale was conducted in the Ralph Lake area, taking advantage of bush-fire

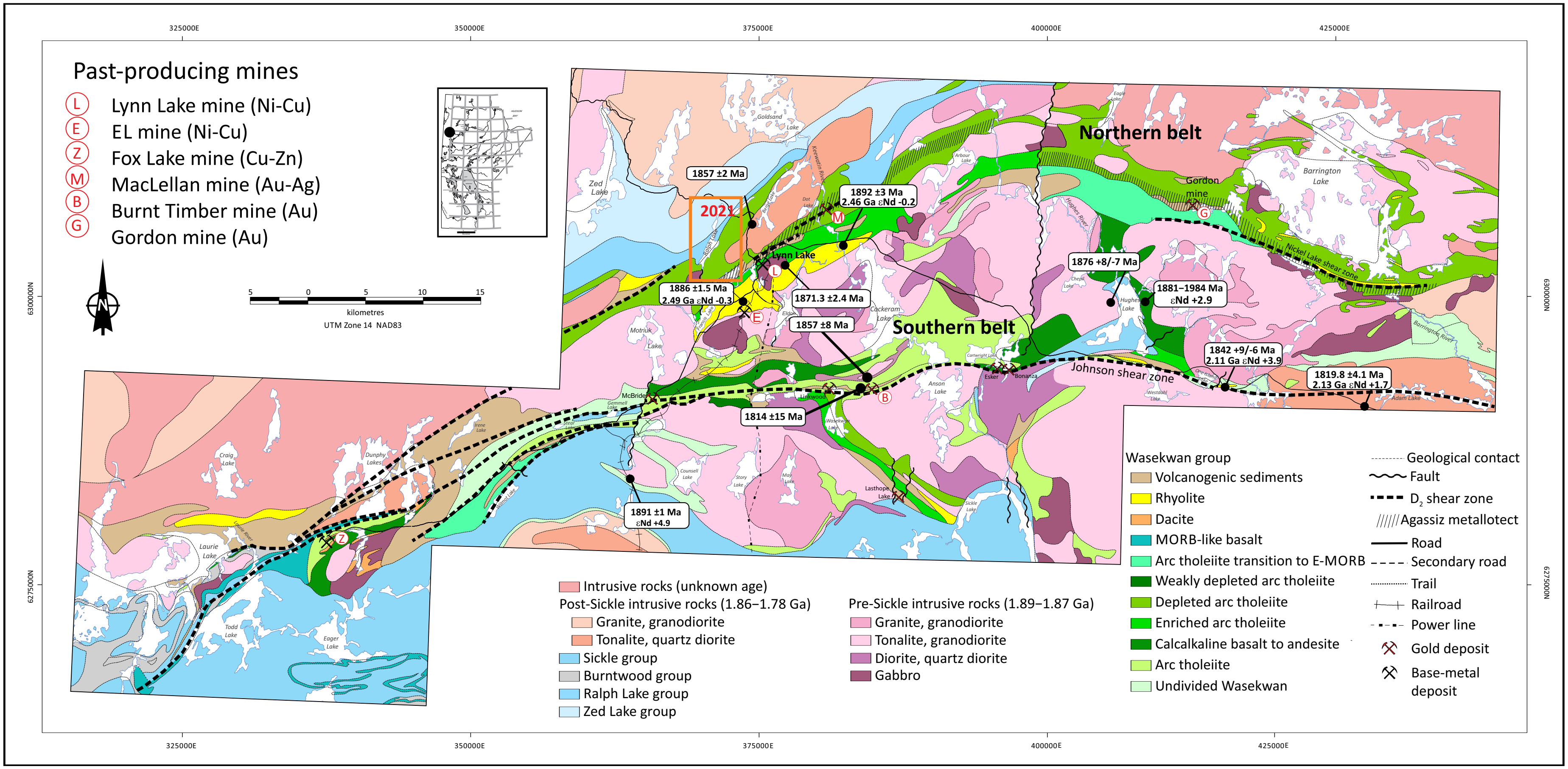

Figure GS2021-5-1: Regional geology of the Lynn Lake greenstone belt (modified and compiled from Gilbert et al., 1980; Manitoba Energy and Mines, 1986; Gilbert, 1993; Zwanzig et al., 1999; Turek et al., 2000; Beaumont-Smith and Böhm, 2002, 2003, 2004; Beaumont-Smith et al., 2006; Beaumont-Smith, 2008; Yang and Beaumont-Smith, 2015a, b, 2016, 2017). The 2021 map area is indicated by the orange box. Some of the relevant zircon U-Pb ages and Nd isotopic compositions are also shown. Abbreviations: E-MORB, enriched mid-ocean–ridge basalt; MORB, mid-ocean–ridge basalt.

exposures to investigate the contact (unconformity) between the Wasekwan group and the overlying Ralph Lake conglomerate and Zed Lake greywacke (Milligan, 1960; Gilbert et al., 1980; Zwanzig et al., 1999). The supracrustal-rock sequences are intruded by granitoid intrusions of the pre– and post–Sickle group intrusive suite, and the late intrusive suite.

This report presents new data on the geology, structure and metamorphism of the Ralph Lake area; provides an updated geological and regional structural framework for the map area; and discusses implications for Au mineralization by the post-Sickle intrusive suite and potential for rare metals (Li, Ta, Cs) in the late intrusive suite. The accompanying preliminary map (Yang, 2021) was created on the basis of 154 field stations, including 156 new structural measurements, as well as compiled historical data (48 stations from Gilbert et al., 1980), a handful of historical drill data and a regional airborne magnetic image (Manitoba Mineral Resources, 2013). During the course of the mapping, a Terraplus Inc. KT-10 magnetic susceptibility (MS) meter[1] was used with a pin to measure MS values of outcrops. Each rock type of a visited outcrop was measured at least five times, at different locations if possible, and the average of the measurements was recorded to represent the MS value of the outcrop. The MS data were used together with the field observations to constrain lithostratigraphic grouping and unit definition.

Twenty-eight whole-rock samples were collected from the map area for geochemical analysis to study geological processes (e.g., Rollinson and Pease, 2021), including eight for thin-section preparation, five for Sm-Nd isotopes and one for zircon U-Pb age determination. The results of these lab analyses are pending and will be reported in subsequent MGS publications.

General geology

The LLGB is endowed with several minerals, such as orogenic Au, magmatic Ni-Cu-Co and volcanogenic massive sulphide Zn-Cu. It is a major tectonic element of the internal Reindeer zone of the Trans-Hudson orogen (Stauffer, 1984; Lewry and Collerson, 1990), which is the largest Paleoproterozoic orogenic belt of Laurentia (Hoffman, 1988; Corrigan et al., 2007, 2009; Corrigan, 2012). To the north, the LLGB is bounded by the SID, which is composed of variably migmatitic metasedimentary rocks, various granitoids and minor metavolcanic and volcaniclastic rocks (Kremer et al., 2009; Martins et al., 2019), although the precise boundary between the LLGB and SID has been debated for years (e.g., Manitoba Energy and Mines, 1986; Manitoba Agriculture and Resource Development, 2021). Synorogenic basins, including the Kisseynew metasedimentary domain, represent the southern limit of the LLGB (Gilbert et al., 1980; Fedikow and Gale, 1982; Syme, 1985; Zwanzig et al., 1999), which is separated by the GLSZ (Zwanzig, 1990, 2000; White et al., 2000; Zwanzig and Bailes, 2010). Paleoproterozoic greenstone belts with ages and lithological assemblages similar to those of the LLGB occur to the east (Rusty Lake belt), to the west (La Ronge belt) and to the far south (Flin Flon belt; e.g., Ansdell et al., 1999; Anderson et al., 2001; Park et al., 2002; Ansdell, 2005; Corrigan et al., 2007, 2009; Corrigan, 2012; Glendenning et al., 2015; Hastie et al., 2018; Lawley et al., 2019, 2020).

The LLGB consists of two east- to northeast-trending, steeply dipping belts that contain various supracrustal rocks, known locally as the Wasekwan group/series (Bateman, 1945; Milligan, 1960; Gilbert et al., 1980), along with younger, molasse-type sedimentary rocks that constitute the Sickle group/series (Norman, 1933; Milligan, 1960; Gilbert et al., 1980). The southern and northern belts are separated by granitoid plutons of the 1.89–1.87 Ga Pool Lake intrusive suite (Gilbert et al., 1980; Baldwin et al., 1987; Beaumont-Smith and Böhm, 2003, 2004; Beaumont-Smith et al., 2006), which are divided into pre- and post-Sickle intrusions based on their temporal relationships to the Sickle group. In the central and southern parts of the LLGB, the Sickle group overlies the Wasekwan group and felsic–mafic plutonic rocks of the Pool Lake intrusive suite along an angular unconformity (Gilbert et al., 1980). The Sickle group correlates well with the 1850–1840 Ma MacLennan group in the La Ronge greenstone belt of Saskatchewan in terms of lithological composition, stratigraphic position and contact relationships (Ansdell et al., 1999; Ansdell, 2005; Corrigan et al., 2009). Volcanic and plutonic rocks in the LLGB underwent peak metamorphism at 1.81–1.80 Ga. Cutting the entire LLGB are the much younger Mackenzie dikes (ca. 1267 Ma; Baragar et al., 1996), as indicated by regional aeromagnetic data.

Significant differences in the geology and geochemistry of the northern and southern belts in the LLGB may reflect regional differences in tectonic settings that were obscured by structural transposition and imbrication during multiple stages of deformation (Gilbert et al., 1980; Syme, 1985; Zwanzig et al., 1999; Beaumont-Smith, 2008). This complexity leads to the suggestion that the term 'Wasekwan group' should be abandoned because it contains disparate volcanic assemblages that were later structurally juxtaposed during tectonic evolution of the LLGB, and thus may represent a tectonic collage (Zwanzig et al., 1999) similar to that described in the Flin Flon belt (e.g., Stern et al., 1995). Although the tectonic collage concept was used in a recent geological compilation by Manitoba Agriculture and Resource Development (2021), this report retains the term 'Wasekwan group' to maintain consistency with previous LLGB-related literature.

[1] The measurement range of magnetic susceptibility (MS) is from 0.001×10^{-3} to 1999.99×10^{-3} SI unit.

Local geology: mapping results

The Ralph Lake area is located in the northern belt of the LLGB (Figure GS2021-5-1). It consists of the Wasekwan group supracrustal rocks intruded by the Pool Lake intrusive suite, which are unconformably overlain by sedimentary rocks of the Ralph Lake and Zed Lake groups (Figure GS2021-5-2; Yang, 2021). According to previous workers (e.g., Milligan, 1960; Beaumont-Smith and Böhm, 2004), intrusions that cut only the Wasekwan group (i.e., the Pool Lake intrusive suite of Gilbert et al., 1980) and those cutting the Sickle group are called, respectively, pre-Sickle and post-Sickle (e.g., Milligan, 1960) suites. Both are cut by rocks of a late intrusive suite, comparable to those identified in the areas of the MacLellan, Gordon and Burnt Timber Au mines and at Gemmell Lake (Yang and Beaumont-Smith, 2015a, b, 2017; Yang, 2019). More recently, Lawley et al. (2020) presented new detrital zircon U-Pb age data for six samples, revealing that the Ralph Lake conglomerate and the Zed Lake greywacke were deposited at ca. 1860 Ma and are therefore likely older than the Sickle group (1836 ±15 Ma).

Nine map units, with 15 subunits, were defined in the Ralph Lake area and can be grouped into six affiliations (from oldest to youngest): Wasekwan group, pre-Sickle intrusive suite, Ralph Lake conglomerate, Zed Lake greywacke, post-Sickle intrusive suite and late intrusive suite (Table GS2021-5-1). These map units are described in the following sections and their distributions are shown in Figure GS2021-5-2 (Yang, 2021). The rocks in the LLGB were deformed and metamorphosed to greenschist and amphibolite facies (Gilbert et al., 1980; Beaumont-Smith and Böhm, 2004; Yang and Beaumont-Smith, 2015a, 2016, 2017; Yang, 2019); however, for brevity, this report omits the prefix 'meta'.

Wasekwan group (units 1 to 3)

Supracrustal rocks of the Wasekwan group in the Ralph Lake area, which are divided into three units (Table GS2021-5-1), are described below.

Volcaniclastic rocks with minor volcanic rocks and volcanic sedimentary rocks (unit 1)

Unit 1 supracrustal rocks are exposed mainly in the eastern and southern parts of the map area (Figure GS2021-5-2; Yang, 2021), where a recent bush fire exposed a major part of the volcaniclastic and volcanic sequence of the Wasekwan group. Unit 1 consists of heterolithic volcaniclastic rocks and intermediate–felsic volcanic and volcaniclastic rocks that, in places, appear to have been reworked by sedimentary processes. The volcaniclastic rocks of unit 1 include mafic to intermediate volcanic breccia, tuff breccia, lapillistone, lapilli tuff and tuff; minor mafic mudstone and intermediate to felsic lapilli tuff and tuff; and volcanic sandstone that locally contains garnet porphyroblasts (e.g., south of Sheila Lake).

Intermediate (andesitic) volcaniclastic rocks cover a spectrum of rock types in terms of fragment size, composition and proportion, including volcanic breccia, tuff breccia, lapillistone, lapilli tuff and tuff (subunits 1a and 1b). Locally, minor synvolcanic rocks (subunit 2a) are also evident in the volcaniclastic package. Andesitic breccia to tuff breccia is typically foliated and consists of varied fragments of aphanitic to plagioclase-phyric basalt to andesite to felsite bedded in lapilli tuff to tuff matrix, and thus can be termed heterolithic volcanic breccia. The volcanic fragments display a large range of size, normally from 4 to 30 cm but locally as large as a few metres. These lithic fragments are commonly stretched, elongated and aligned along the dominant (S_2) foliation planes (note that this report follows the structural terms proposed in Beaumont-Smith and Böhm, 2002, 2003, 2004). Both matrix-supported and clast-supported varieties are evidently present and poorly sorted (Figure GS2021-5-3a and -3b), although some outcrops exhibit variation in size of fragments that is indicative of involvement in sedimentary processes and younging to the south (Figure GS2021-5-3b). The matrix in some of the breccia contains up to 50% plagioclase fragments (0.1–1 cm), together with mafic minerals (e.g., amphibole) and finer materials.

Intermediate (andesitic) lapillistone, lapilli tuff and tuff (subunit 1b) typically display centimetre-scale layers thought to be beds, although they are foliated and locally folded. Lapillistone to lapilli tuff contains elongated lithic fragments of variable composition (e.g., rhyolite, porphyritic andesite, and plagioclase-phyric and aphanitic basalt) and plagioclase crystals embedded in a fine-grained matrix consisting of plagioclase, amphibole, biotite, chlorite, epidote and aphanitic material, as well as local magnetite. Lapilli tuff appears to grade laterally to fine-grained tuff that contains interbedded mafic and felsic laminae (~0.5–2 mm). It was noted that the andesitic tuff lacks larger lapilli-sized lithic fragments. Noteworthy are plagioclase crystal tuff and lapilli tuff, with thin felsic layers up to 1 cm wide containing 35–40% plagioclase fragments of varied shape (e.g., angular, irregular; Figure GS2021-5-3c) that range in size from 0.1 to 20 mm and are unevenly distributed at the outcrop scale. In places, subunit 2a diabase and/or gabbroic dikes cut andesitic lapilli tuff, tuff breccia and volcanic breccia (Figure GS2021-5-3d), and both the dikes and volcaniclastic rocks are foliated, dominantly by D_2.

Mafic volcaniclastic rocks are divided into two subunits: subunit 1c lapillistone, lapilli tuff, tuff, minor mafic mudstone and derivative garnet-biotite schist; and subunit 1d mafic tuff breccia and breccia (Table GS2021-5-1). Mafic lapillistone, lapilli tuff and tuff (subunit 1c) are characterized by the presence of mafic lithic fragments in a chloritic matrix. Minor greenish grey, very fine grained, thinly bedded mafic mudstone is also included in subunit 1c, which usually weathers light greenish brown to light grey and contains disseminated pyrrhotite and pyrite. Dark green, acicular amphibole (actinolite?) porphyroblasts (up to 5–10 mm), concentrated in foliation or

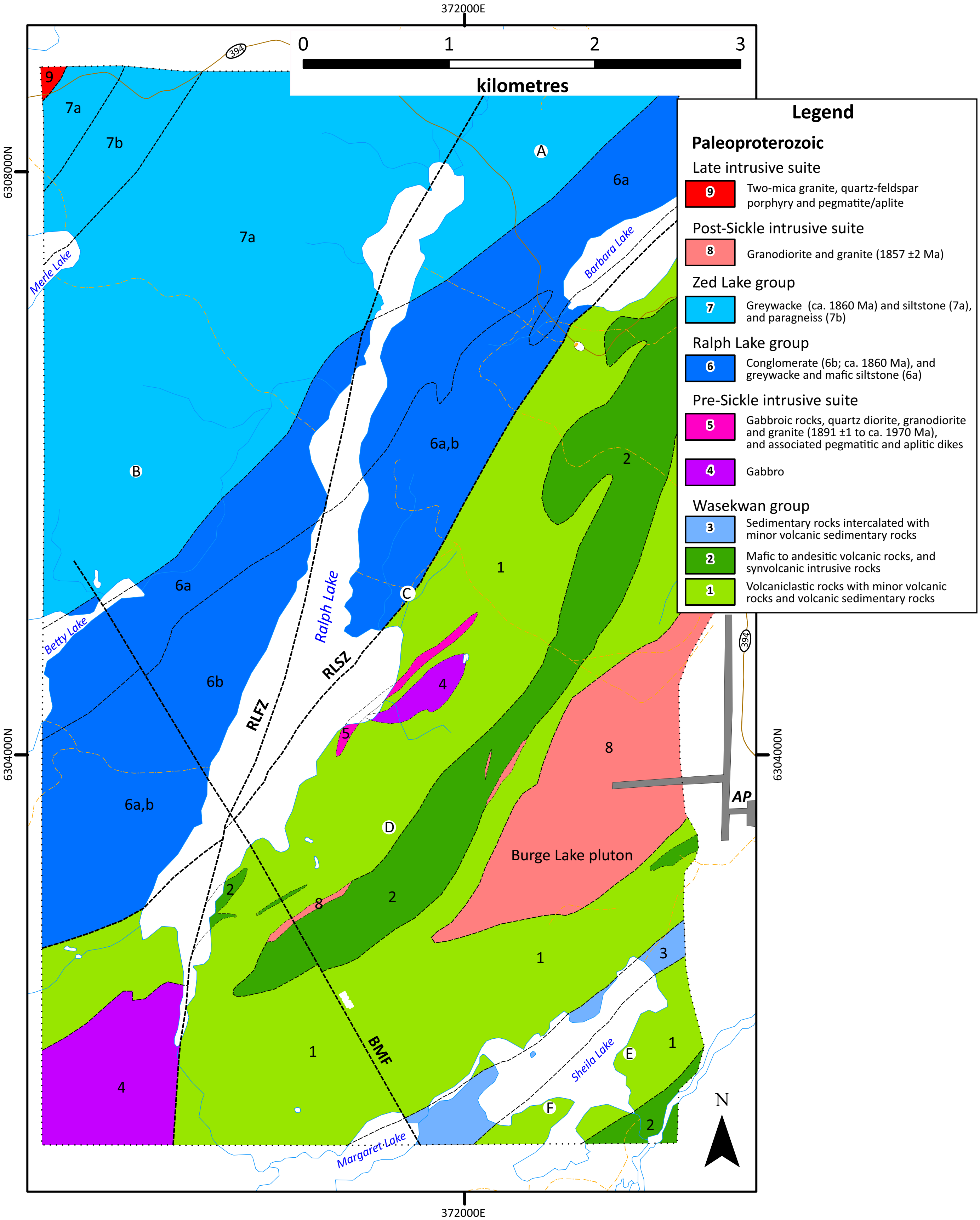

Figure GS2021-5-2: *Simplified geology of the Ralph Lake area, Lynn Lake greenstone belt, northwestern Manitoba (modified from Yang, 2021). A to E: mineral occurrences. References for zircon U-Pb ages of units are listed in Table GS2021-5-1. Abbreviations: AP, airport; BMF, Betty Lake-Margaret Lake fault; RLFZ, Ralph Lake fault zone; RLSZ, Ralph Lake shear zone.*

Table GS2021-5-1: Lithostratigraphic units of the Ralph Lake area, Lynn Lake greenstone belt, northwestern Manitoba.

Unit[1]	Rock type	Affiliation
9	Two-mica granite, quartz-feldspar porphyry, and pegmatite/aplite	Late intrusive suite
	Intrusive contact	
8	Granodiorite and granite (1857 ±2 Ma[2])	Post-Sickle intrusive suite
	Intrusive contact	
7	Metasedimentary rocks: greywacke (ca. 1860 Ma[3]), siltstone and paragneiss	Zed Lake group
7a	Greywacke and siltstone	
7b	Paragneiss	
	Conformity (?)	
6	Metasedimentary rocks: conglomerate (ca. 1860 Ma[3]) and greywacke	Ralph Lake group
6a	Greywacke and mafic siltstone	
6b	Polymictic conglomerate and minor mafic siltstone	
5	Gabbroic rocks, quartz diorite, granodiorite, granite (1891 ±1 Ma to ~1870 Ma[2, 4-5]) and associated pegmatitic and aplitic dikes	Pre-Sickle intrusive suite
4	Gabbro	
	Intrusive contact	
3	Sedimentary rocks intercalated with minor volcanic sedimentary rocks	Wasekwan group
3a	Argillite, siltstone and greywacke	
3b	Mafic to intermediate tuffaceous sandstone to tuff	
3c	Volcanic mudstone, siltstone, volcanic sandstone and minor volcanic conglomerate	
	Structural contact	
2	Mafic to andesitic volcanic rocks and synvolcanic intrusive rocks	
2a	Diabase and gabbro	
2b	Porphyritic basaltic andesite	
2c	Plagioclase-phyric basalt and aphyric basalt	
2d	Pillow basalt	
	Structural contact	
1	Volcaniclastic rocks with minor volcanic rocks and volcanic sedimentary rocks	
1a	Felsic to intermediate volcanic and volcaniclastic rocks	
1b	Intermediate lapillistone, lapilli tuff and tuff	
1c	Mafic lapillistone, mafic lapilli tuff, tuff, minor mafic mudstone and derivative garnet-biotite schist	
1d	Mafic tuff breccia and volcanic breccia	
	?	

[1] On Preliminary Map PMAP2021-2 (Yang, 2021)
[2] Beaumont-Smith et al. (2006)
[3] Lawley et al. (2020)
[4] Baldwin et al. (1987)
[5] Turek et al. (2000)

fracture planes in mafic tuff and lapilli tuff, are interpreted to have formed by retrograde metamorphism to greenschist facies. The mafic lapilli tuff and tuff (subunit 1c) are generally moderately to strongly foliated and range from texturally variable to relatively homogeneous. These rocks consist of varied amounts of aphyric lithic fragments, plagioclase (up to 40%; 0.1–5 mm) and amphibole pseudomorphs after pyroxene (up to 15%; 0.2–12 mm) in a fine-grained mafic-tuff matrix (Figure GS2021-5-3e). Mafic lapilli-sized fragments make up <25% of subunit 1c but can locally account for up to 80% of the rock, which is then termed 'mafic lapillistone'. Locally, coarse-grained to pegmatitic veins or veinlets consisting of quartz and K-feldspar crosscut subunit 3c lapilli tuff to tuff (Figure GS2021-5-3e).

Subunit 1d consists of moderately to strongly deformed and foliated heterolithic mafic tuff breccia and breccia. Volcanic fragments, ranging from 1 to 15 cm in length (typically 10–12 cm), include plagioclase-phyric basalt, aphanitic basalt, epidotic altered massive aphyric basalt, and tuff embedded in a mafic lapilli tuff and tuff matrix (Figure GS2021-5-3f). The basaltic fragments are irregular and subrounded to subangular, some exhibiting reaction rims rich in chlorite and/or epidote, and have been aligned along the generally northeast-trending foliation (S_2) planes. Again, both clast-supported and matrix-

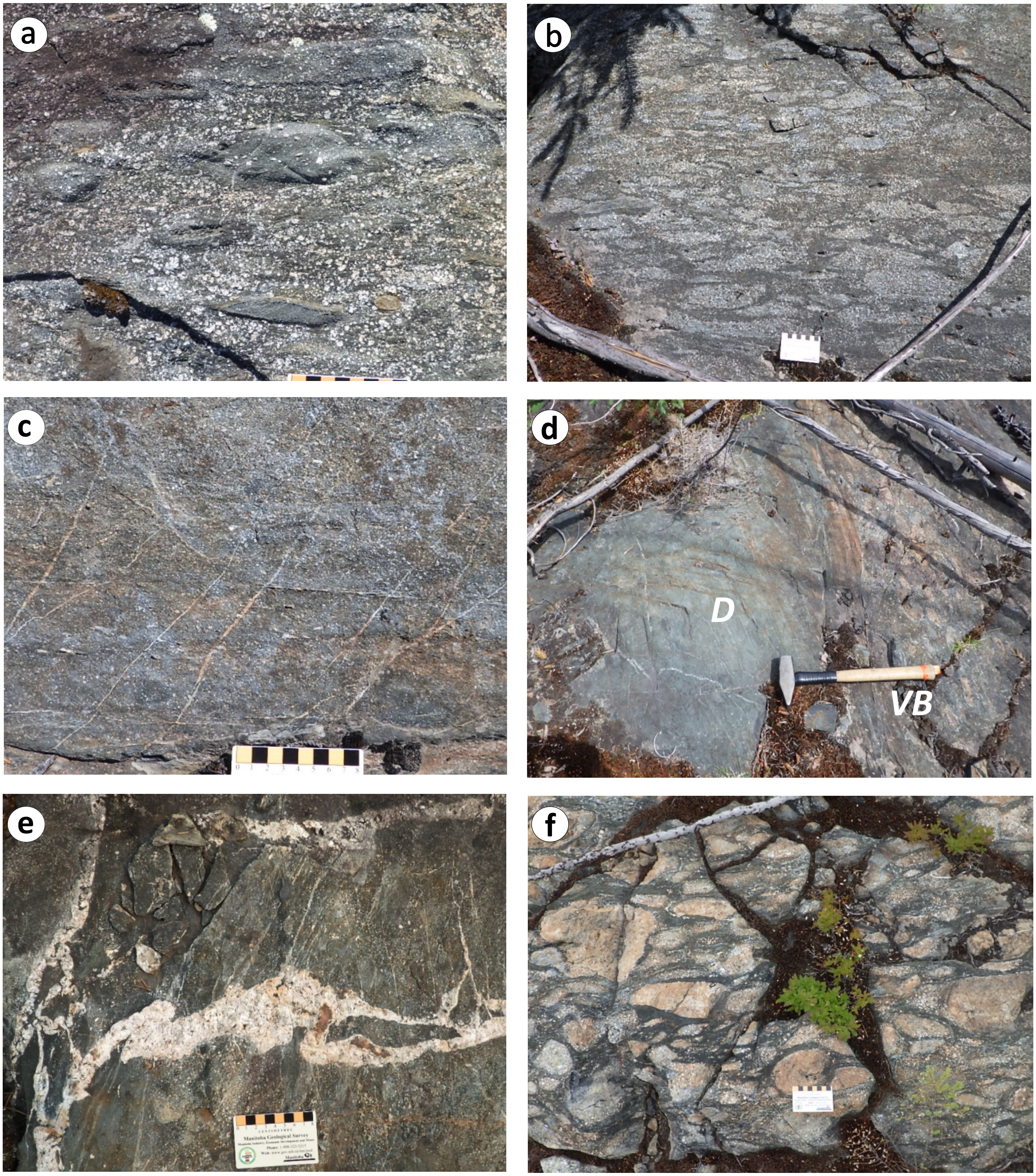

Figure GS2021-5-3: *Field photographs of unit 1 volcaniclastic rocks, with minor volcanic rocks and volcano-sedimentary rocks of the Wasekwan group in the Ralph Lake area:* ***a)*** *intermediate (andesitic) volcanic breccia, matrix supported, with varied plagioclase-phyric to aphyric volcanic fragments in plagioclase-crystal lapilli to tuff matrix (subunit 1a; UTM Zone 14N, 371349E, 6304184N, NAD 83);* ***b)*** *foliated andesitic volcanic breccia consisting mainly of varied sizes of plagioclase-rich porphyritic andesitic clasts, clast-supported, in lapilli tuff to tuff matrix (subunit 1a; UTM 3714267E, 6303962N);* ***c)*** *intermediate lapilli tuff to tuff, with up to 40% 0.1–12 mm plagioclase fragments and minor, very fine grained lithic fragments (subunit 1b; UTM 371387E, 6304007N);* ***d)*** *volcanic breccia (subunit 1b; right side of the photo) cut by 1–2 m wide diabase (gabbroic) dike (subunit 2a; UTM 371392E, 6303987N), hammer handle pointing northwest;* ***e)*** *mafic lapilli tuff to tuff (subunit 1c; UTM 371270E, 6303920N) cut by very coarse grained to pegmatitic (quartz-feldspar±muscovite) veins to veinlets (unit 9);* ***f)*** *foliated mafic volcanic breccia and breccia with varied sizes and shapes of plagioclase-phyric and aphyric basalt fragments, clast-supported, in mafic (chloritic) tuff matrix; the fragments, some of which are strongly epidote altered, are aligned along S_2 foliation (subunit 1d; UTM 371274E, 6303820N). Abbreviations: D, diabase; VB, volcanic breccia.*

supported varieties are evident in subunit 1d. In high-strain zones, lithic fragments are sheared and flattened, although the margins of some of the fragments are still discernible. Some of the aphanitic basalt fragments display epidote alteration and others show reaction rims with very fine grained assemblages of chlorite, epidote, sericite and albite. Thin- and up to 15 cm bedded layers of mafic lapilli tuff to finer tuff occur in places in the mafic tuff breccia to heterolithic breccia package(s).

Unit 1 volcaniclastic rocks with minor volcanic rocks and volcanic sedimentary rocks of the Wasekwan group have MS values mostly in the range 0.403×10^{-3} to 1.59×10^{-3} SI, although much higher values of 15.3×10^{-3} registered in three localities (station 118; UTM Zone 14N, 370690E, 6301899N, NAD 83), 21.8×10^{-3} (station 120; UTM 370349E, 6302207N) and 23.5×10^{-3} SI (station 145; UTM 373449E, 6303422N) due to the presence of fine-grained magnetite grains or a contact zone with unit 8 granodiorite (Figure GS2021-5-2).

Mafic to andesitic volcanic rocks, and synvolcanic intrusive rocks (unit 2)

Unit 2 mafic to intermediate volcanic rocks occur mainly in the northeastern (e.g., southeast of Barbara Lake), east-central (e.g., east of Ralph Lake) and southeastern (e.g., east of Sheila Lake) parts of the map area (Figure GS2021-5-2). The volcanic succession of unit 2 in the Ralph Lake area is dominated by plagioclase-phyric and aphyric basalt, with subordinate porphyritic basaltic andesite and pillow basalt, and synvolcanic diabase and gabbro dikes (Table GS2021-5-1).

Synvolcanic diabase and gabbroic rocks (subunit 2a) usually occur as dikes and small plugs intruded into unit 2 volcanic rocks and, in some cases, into unit 1 volcaniclastic rocks (Figure GS2021-5-3d). The diabase dikes weather greenish grey to grey and are greenish to dark green on fresh surfaces; they are very fine to medium grained, porphyritic and moderately to strongly foliated (Figure GS2021-5-4a). Equant to subhedral plagioclase phenocrysts (up to 10 mm) occur in a fine-grained groundmass of plagioclase, amphibole, chlorite and Fe oxides. Generally, the diabase and gabbroic rocks consist of 50–60% hornblende (after pyroxene) and 40–50% plagioclase, consistent with an amphibolite-facies metamorphic-mineral assemblage. Notably, radial aggregates of acicular amphibole (actinolite) and a few reddish euhedral garnet crystals are evidently present in some deformed subunit 2a gabbroic rocks (Figure GS2021-5-4b) that are in sheared contact with plagioclase-phyric to aphyric basalts (subunit 2c). Trace disseminated sulphide blebs (e.g., pyrrhotite; ~0.5–1 mm) are locally evident, suggesting that the magmas may have been sulphide saturated. Notably, some of the subunit 2a gabbroic intrusions contain ~1% chalcopyrite disseminations up to 3 mm (southeast side of Ralph Lake; Figure GS2021-5-4b).

Porphyritic basaltic andesite (subunit 2b) contains amphibole (±biotite) and lesser amounts of plagioclase phenocrysts in a fine-grained groundmass. Biotite and sericite alteration is a common feature of the rock. It is difficult to distinguish this from plagioclase-phyric basalt (subunit 2c) when plagioclase and amphibole phenocrysts coexist in basaltic andesite (subunit 2b), although amphibole (±biotite) phenocrysts are commonly absent in the basalt. Massive aphyric basalt (subunit 2c; GS2021-5-4c) is less common compared to plagioclase-phyric basalt in the Ralph Lake area. Vesicles and quartz±calcite amygdules are present in some outcrops (GS2021-5-4d). In most cases, the basalt is aphanitic where lacking in plagioclase phenocrysts. Chlorite and epidote alteration is common in both the plagioclase-phyric and aphyric basalts, as shown by epidote domains ranging from a few centimetres to a metre across.

Moderately to strongly foliated plagioclase-phyric to aphanitic aphyric basalt with disseminations of sulphides have a rusty appearance when weathered (subunit 2c) and locally have pyrite-bearing quartz veins along the S_2 foliation planes (GS2021-5-4e). It is common that some of the foliated, massive aphanitic basalt (subunit 2c) with disseminated pyrrhotite is invaded by late sheeted felsic veinlets (GS2021-5-4f). Pillowed basalt (subunit 2d) was reported by Gilbert et al. (1980) to occur southeast of Ralph Lake. Although preserved pillows were not encountered, hyaloclastite relicts derived from pillow selvages were observed, confirming that part of the unit 2 volcanic rocks may have formed in a subaqueous environment, as suggested by Gilbert et al. (1980).

Unit 2 mafic to intermediate rocks and synvolcanic gabbroic rocks of the Wasekwan group have MS values ranging mainly from 0.511×10^{-3} to 1.37×10^{-3} SI. An exception was a value of 24.3×10^{-3} SI for an aphanitic basalt outcrop (GPS location reading: UTM Zone 14N, 373014E, 6306963N, NAD 83), which was attributed to very fine grained magnetite in the rock.

Sedimentary rocks intercalated with minor volcanic sedimentary rocks (unit 3)

Unit 3 sedimentary rocks with minor volcanic and volcaniclastic rocks are exposed mainly on the northeastern side of Sheila Lake (Figure GS2021-5-2). This unit consists of argillite, siltstone and greywacke (subunit 3a), and mafic to intermediate tuffaceous sandstone to tuff (subunit 3b), intercalated with minor volcanic mudstone, siltstone, sandstone and conglomerate (subunit 3c; Table GS2021-5-1).

Thin- to medium-bedded quartzofeldspathic greywacke and siltstone (subunit 3a) dominate the sedimentary succession. Primary bedding (S_0) in the sedimentary rocks was transposed by the regional S_2 foliation. The medium- to coarse-grained greywacke is medium tan to yellowish grey on weathered surfaces and light grey on fresh surfaces. Quartz, feldspar,

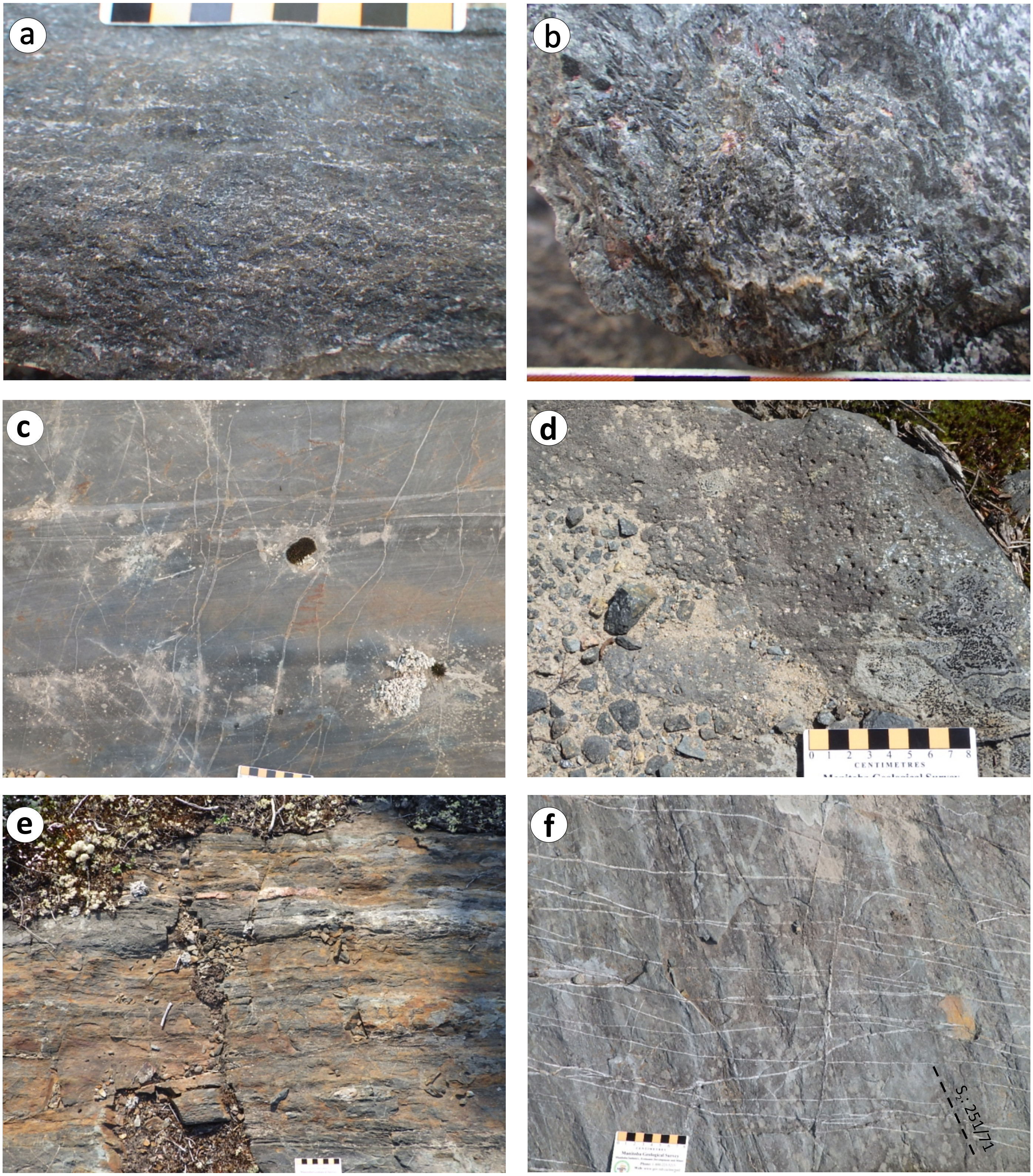

Figure GS2021-5-4: *Field photographs of mafic to intermediate volcanic rocks and synvolcanic intrusive rocks (unit 2) of the Wasekwan group in the Ralph Lake area:* ***a)*** *and* ***b)*** *synvolcanic, foliated gabbro that was recrystallized and contains acicular amphibole and reddish garnet porphyroblasts (subunit 2a; UTM Zone 14N, 370421E, 6302894N, NAD 83), interval on scale bar at bottom of photo b is 1 cm;* ***c)*** *foliated, massive, plagioclase-phyric basalt to aphanitic basalt flow (subunit 2c; UTM 372957E, 6306772N);* ***d)*** *plagioclase-phyric andesitic basalt to basaltic andesite with abundant vesicles at top of flow, indicative of younging to the southeast (subunit 2b; UTM 373296E, 6306975N);* ***e)*** *foliated, plagioclase-phyric to aphanitic basalt with disseminations of sulphides that have a rusty appearance due to weathering (subunit 2c; UTM 372735E, 6306271N); note pyrite-bearing quartz vein emplaced along the* S_2 *foliation planes;* ***f)*** *foliated, massive aphanitic basalt with disseminated pyrrhotite cut by sheeted felsic veinlets (subunit 2c; UTM 372766E, 6306223N).*

amphibole and lithic clasts are angular to subrounded and well aligned on foliation planes defined by biotite flakes and manifested by felsic- and mafic-rich layering that likely reflects transposed bedding (S_0; Figure GS2021-5-5a). Note that acicular amphibole, up to 1.5 mm, is present in finer matrix, suggestive of retrograde metamorphism of greenschist-facies.

Mafic to intermediate tuffaceous sandstone to tuff (subunit 3b) is fine to medium grained and contains up to 75% volcanic fragments (up to 2 mm in size). The bedding (S_0) of this subunit is strongly transposed by the dominant S_2 foliation. Thin to thick beds of minor volcanic sedimentary rocks (subunit 3c) consist of volcanic mudstone, siltstone and sandstone, and minor volcanic conglomerate (Table GS2021-5-1). Volcanic sandstone is dominated by laminated, fine- to medium-grained andesitic sandstone containing irregular plagioclase, biotite flakes and lithic fragments (0.5–2 mm) in a fine sandy matrix; locally, a few large lithic fragments occur along bedding transposed by regional S_2 foliation. Thick-bedded volcanic conglomerate and/or breccia (subunit 3c) consists dominantly of felsic and intermediate to mafic volcanic clasts in a coarse-grained sandy matrix (Figure GS2021-5-5b). These clasts, 2–5 cm in length, are stretched, flattened and well aligned along S_2 planes that transposed primary bedding (S_0). Although strongly deformed, the breccia appears to grade upward to volcanic sandstone, suggesting that the beds are younging to the north at this locality (Figure GS2021-5-5b).

Unit 3 sedimentary rocks of the Wasekwan group displayed consistent MS values of 0.490×10^{-3} to 0.542×10^{-3} SI.

Pre-Sickle intrusive suite (units 4 and 5)

Igneous rocks of the pre-Sickle intrusive suite occur as intrusions crosscutting the supracrustal rocks of the Wasekwan group (Gilbert et al., 1980; Baldwin et al., 1987; Beaumont-Smith and Bohm, 2004). Unit 4 gabbro and unit 5 granitoid, diorite, quartz diorite and minor gabbroic rocks are assigned to this suite (Table GS2021-5-1).

Gabbro (unit 4)

Unit 4 gabbro occurs mainly in the southwestern part of the map area and along the eastern shore of Ralph Lake (Figure GS2021-5-2). It occurs as small sill-like bodies intruding the Wasekwan group supracrustal rocks. The gabbro weathers greenish grey and is dark greenish grey to dark grey on fresh surfaces. It is medium to coarse grained, equigranular, massive and moderately to locally strongly foliated. It consists of 35–45% plagioclase laths (1–3 mm), 50–55% hornblende (pseudomorphs after pyroxene), minor magnetite and trace pyrrhotite (Figure GS2021-5-6a). In addition, foliated coarse-grained gabbro comprises euhedral to subhedral hornblende (6–8 mm) and interstitial anhedral plagioclase grains, suggestive of a cumulate phase (Figure GS2021-5-6b). The edges of both plagioclase and hornblende crystals are diffuse due to chlorite and sericite alteration. Locally, epidote veins and veinlets are evidently present along or cutting the regional foliation (S_2) planes.

Unit 4 gabbro in the southwestern Ralph Lake area yielded very high MS values of 10.5×10^{-3} to 53.2×10^{-3} SI, whereas this unit in the east-central Ralph Lake area showed much lower MS values of 0.604×10^{-3} to 0.839×10^{-3} SI, similar to the unit 1 volcaniclastic rocks.

Gabbroic rocks, quartz diorite, granodiorite, granite and associated pegmatitic and aplitic dikes (unit 5)

Unit 5 granitoid intrusions of the pre-Sickle intrusive suite are exposed mainly in the east-central Ralph Lake area (Figure GS2021-5-2), cutting the Wasekwan group supracrustal rocks.

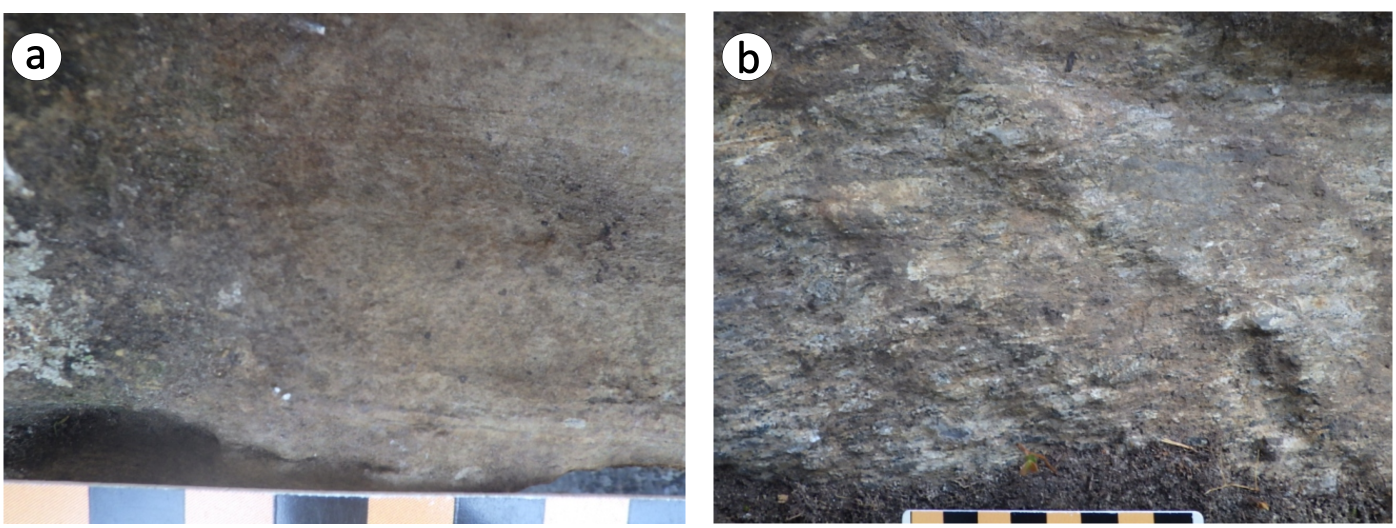

Figure GS2021-5-5: *Field photographs of sedimentary rocks intercalated with minor volcano-sedimentary rocks (unit 3) of the Wasekwan group in the Ralph Lake area:* ***a)*** *fine- to medium-grained, foliated siltstone to pebbly greywacke with recrystallized biotite along S_0/S_2 planes and acicular amphibole porphyroblasts in fine matrix (subunit 3a; UTM Zone 14N, 373361E, 6302614N, NAD 83);* ***b)*** *foliated volcanic conglomerate with felsic and mafic lithic fragments in a felsic to intermediate sandy matrix; bedding (S_0) transposed by S_2 foliation (subunit 3c; UTM 373410E, 6302547N).*

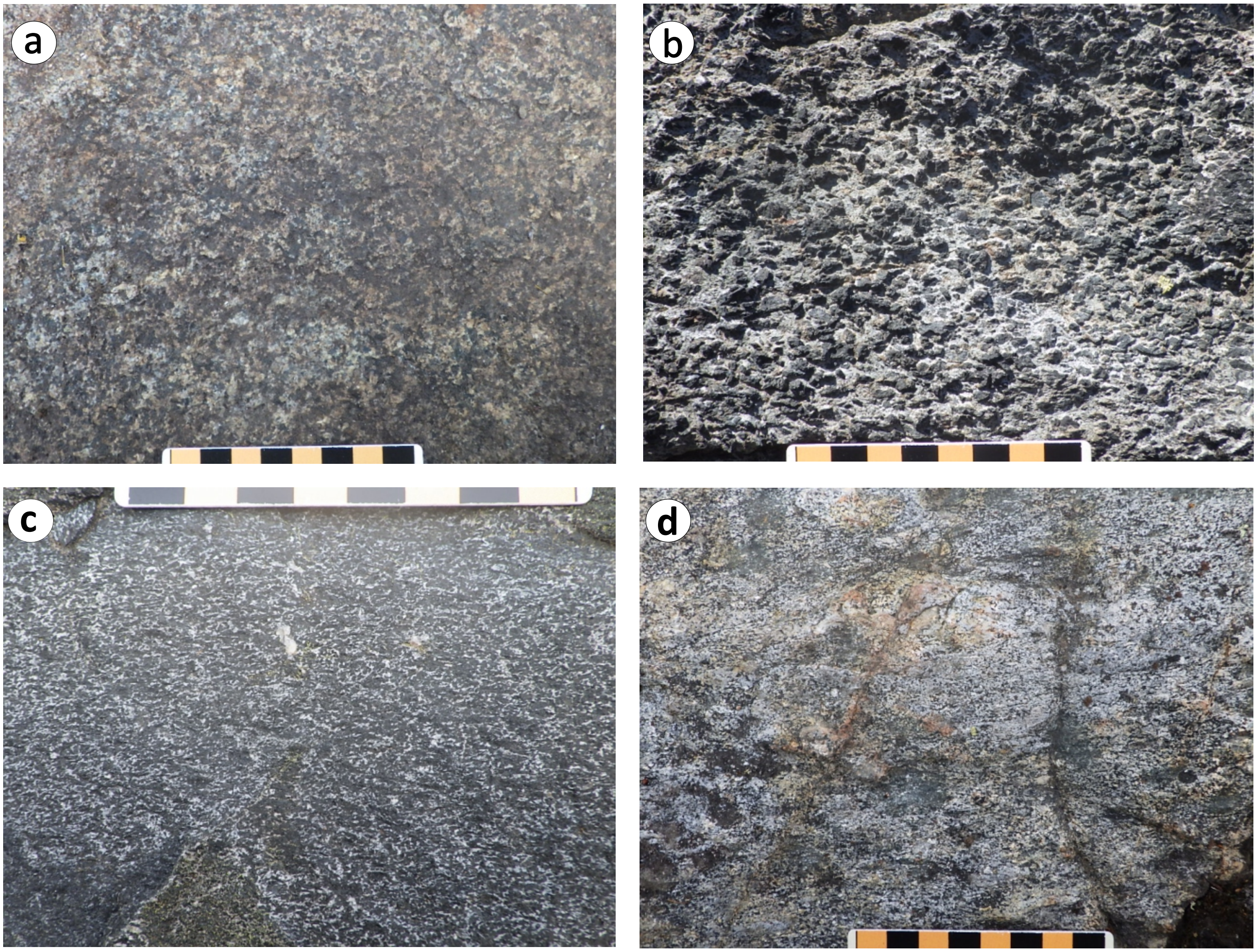

Figure GS2021-5-6: Outcrop photographs of units 4 and 5 in the Ralph Lake area: ***a)*** *massive, medium- to coarse-grained, equigranular gabbro (unit 4; UTM Zone 14N, 369600E, 6302010N, NAD 83);* ***b)*** *weakly foliated, coarse-grained gabbro comprising euhedral to subhedral hornblende (pseudomorph of pyroxene) and interstitial anhedral plagioclase grains mostly altered to finer felsic aggregates, suggestive of a cumulate phase (unit 4; UTM 371860E, 6304410N);* ***c)*** *foliated quartz gabbro (unit 5; UTM 371898E, 6304728N); and* ***d)*** *foliated, porphyritic quartz diorite (unit 5; UTM 371884E, 6304756N).*

Unit 5 consists of a range of rocks from gabbro to quartz diorite, tonalite, granodiorite, granite and associated pegmatitic and aplitic dikes. The field relationships indicate that a minor gabbroic phase occurs at the margin of a granitoid intrusion, where the quartz gabbro appears to display flow foliation even though it is largely overprinted by the regional S_2 foliation (Figure GS2021-5-6c). From the contact into the intrusion, the granitoid rocks tend to change from quartz diorite to granodiorite and granite. Locally, the quartz diorite is porphyritic and uneven in texture, and contains disseminated pyrite and pyrrhotite; both feldspar and quartz phenocrysts are present (Figure GS2021-5-6d) in association with plagioclase, hornblende ±biotite.

Granodiorite and granite of unit 5 are medium to coarse grained, massive, equigranular to locally porphyritic and weakly to moderately foliated. They weather greyish pink to light beige and consist of quartz, plagioclase, K-feldspar, hornblende (±biotite) and accessory Fe-oxide minerals. Some of the porphyritic variety contains 5% quartz phenocrysts up to 1.2 cm across, suggesting relatively shallow emplacement. Minor pegmatite and/or aplite of unit 5 occur as dikes ranging from a few centimetres to a few metres wide and consisting of quartz, feldspar and minor biotite.

Unit 5 granitoids yielded a range of MS values from 1.59×10^{-3} to 11.2×10^{-3} SI, but more evolved granite and related pegmatitic and aplitic dikes had lower MS values (as low as 0.41×10^{-3} SI). This large range in MS values is consistent with I-type granites elsewhere in the LLGB (e.g., Yang and Beaumont-Smith, 2015b; Yang and Lawley, 2018; Yang et al., 2019).

Ralph Lake group (unit 6)

The term 'Ralph Lake group' (unit 6) is used in this report instead of Ralph Lake conglomerate (Milligan, 1960; Gilbert et al., 1980; Zwanzig et al., 1999; Yang and Beaumont-Smith, 2015a) because of the presence of diverse lithologies other than just conglomerate. Unit 6 is exposed mainly between the northeastern part of Ralph Lake and the southwestern side of Barbara Lake, and occurs sparsely in the western and southwestern parts of the map area (Figure GS2021-5-2). Unit 6 sedimentary rocks seem to overlie supracrustal rocks of the Wasekwan group (Gilbert et al., 1980; Manitoba Energy and Mines, 1986; Zwanzig et al., 1999). This unit, in fact, is structurally juxtaposed with the Wasekwan rocks to the south, and separated from the Wasekwan supracrustal rocks by the northeast-trending Ralph Lake shear zone (RLSZ), which shows dextral movement, indicated by the structural fabrics, and dips subvertically to the southeast. Unit 6 consists mainly of greywacke, mafic siltstone (subunit 6a) and polymictic conglomerate (subunit 6b), which were recrystallized and metamorphosed to an assemblage of biotite, hornblende, epidote, quartz, plagioclase (±K-feldspar±muscovite±garnet) and magnetite.

Greywacke and mafic siltstone (subunit 6a)

Subunit 6a consists dominantly of thin-bedded, laminated, mafic siltstone to greywacke. In places, some of the mafic greywacke bands, characterized by porphyroblastic hornblende crystals up to 3 mm and biotite flakes, are evidently intercalated with mafic siltstone within this sedimentary package (Figure GS2021-5-7a). Such mafic-enriched wacke bands manifest the transposition of primary bedding (S_0) by the regional S_2 foliation, which strikes northeast and dips consistently to southeast. Notably, the mafic greywacke and siltstone contain very fine magnetite crystals that could be either metamorphic or detrital in origin, resulting in very high MS values of $106×10^{-3}$ to $111×10^{-3}$ SI.

Polymictic conglomerate and minor mafic siltstone (subunit 6b)

Both matrix- and clast-supported polymictic pebble to cobble conglomerates are poorly sorted (subunit 6b). Lithic clasts are variable in composition, size and shape, and are stretched and mostly well aligned along the regional foliation (S_2), which has transposed primary bedding (S_0); the S_2 foliation strikes northeast and dips to the southeast. Gradational variation in clast size appears, in places, to suggest fining upward to the northwest for the sequence and transition into unit 7 Zed Lake greywacke to the northwest. The polymictic conglomerate contains clasts of epidotic volcanic rocks, gabbro, diorite, granitoids and vein quartz; the matrix is wacke that was recrystallized to an assemblage of quartz, feldspar, hornblende, biotite, epidote and magnetite (Figure GS2021-5-7b). In many locations, thin- to thick-bedded mafic siltstone (to minor wacke) that resembles the matrix in composition occurs within the conglomerate sequence.

In moderate- to high-strain domains related to the RLSZ, subunit 6b conglomerate is moderately to intensely foliated and sheared (Figure GS2021-5-7c), and is locally protomylonitic (Figure GS2021-5-7d) to mylonitic in the high-strain domains. Based on the asymmetry of some flattened clast relicts, deformed fabrics and stretching lineations, the conglomerate experienced dextral transpressive shearing, as shown by the RLSZ.

Similar to the mafic greywacke and siltstone of subunit 6a, the polymictic conglomerate of subunit 6b yielded high MS values ranging from $10.1×10^{-3}$ to $99.2×10^{-3}$ SI, consistent with the presence of fine-grained magnetite in its recrystallized, hornblende-bearing, sandy matrix.

It is noted that maturity of the Ralph Lake conglomerate seems lower than that of its Sickle group counterpart. The presence of abundant finer grained silt to clay materials is indicative of immature sediments, although they had been metamorphosed and/or recrystallized to form biotite (±muscovite±garnet) and hornblende in the matrix and/or as porphyroblasts, suggesting that it underwent metamorphism up to middle amphibolite faces. The Ralph Lake conglomerate, together with the Zed Lake greywacke (see below), are thought in this study to be part of the Southern Indian Lake domain, based on their rock associations (Manitoba Agriculture and Resource Development, 2021) that are characterized by variably migmatitic metasedimentary rocks, various granitoids, and minor metavolcanic and volcaniclastic rocks (Kremer et al., 2009; Martins et al., 2019 and references therein).

Zed Lake group (unit 7)

The Zed Lake group (unit 7) consists dominantly of fine- to medium-grained greywacke and siltstone (subunit 7a) and derived paragneiss (subunit 7b). Rocks of this unit are exposed northwest of Ralph Lake (Figure GS2021-5-2) and its contact with the Ralph Lake sedimentary rocks (unit 6) was not observed, although the two units are distinguishable on regional airborne magnetic images and using the MS values measured as part of this study. The Zed Lake greywacke displays much lower MS values than the Ralph Lake conglomerate (see below). Detrital zircons recovered from a greywacke sample collected from an outcrop ~3 km west of Ralph Lake yielded a maximum depositional age of ca. 1860 Ma (Lawley et al., 2020), identical to that of the Ralph Lake conglomerate. Therefore, the contact between units 6 and 7 is believed to be sedimentary, which is also supported by their similar S_0/S_2 relationship (i.e., the same relationship of the fabrics), although it is unknown if a sedimentary hiatus occurred.

Greywacke and siltstone (subunit 7a)

Subunit 7a consists mainly of medium- to thick-bedded, fine- to medium-grained greywacke and siltstone. It weathers

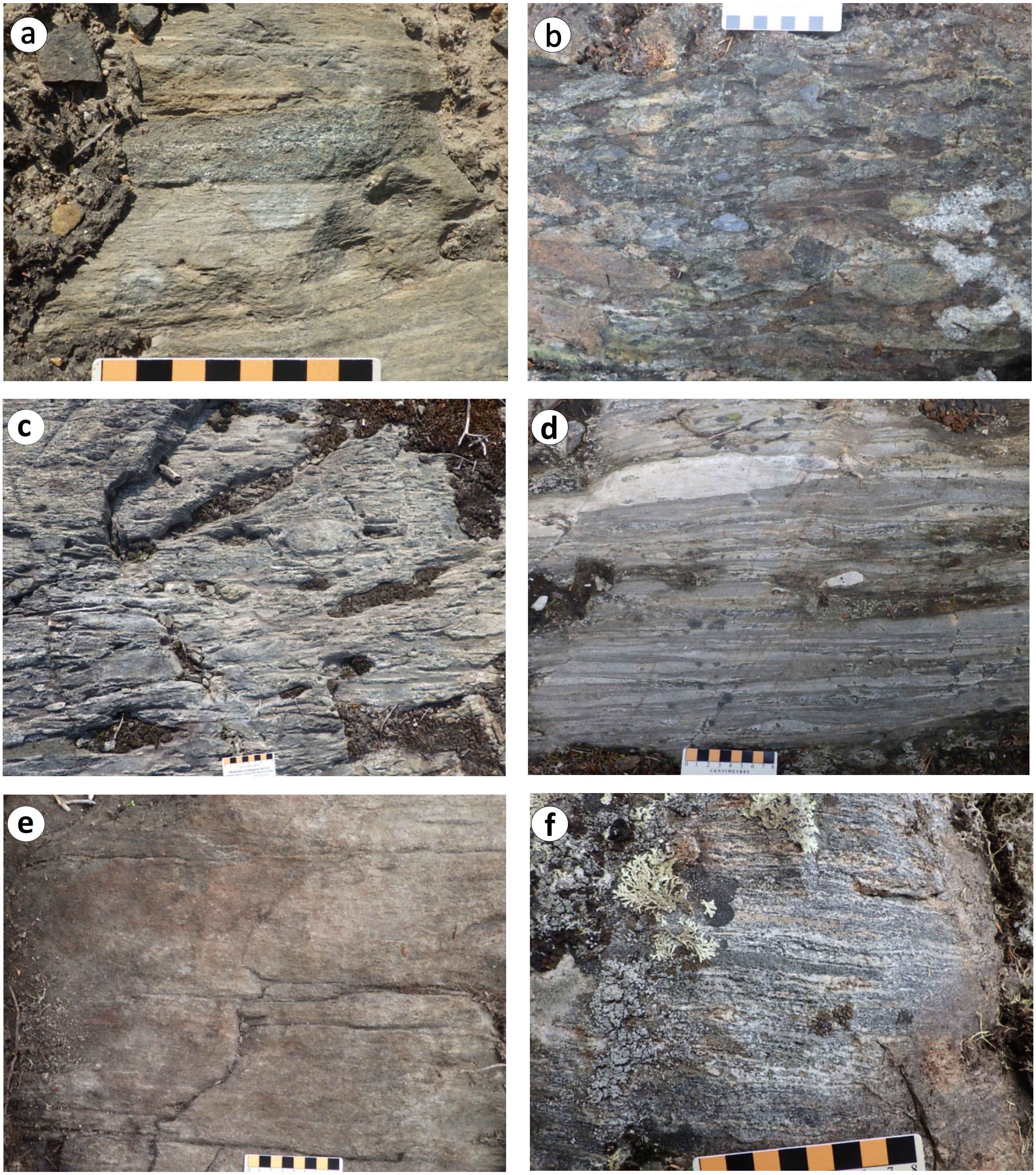

Figure GS2021-5-7: *Outcrop photographs of units 6 and 7 metasedimentary rocks in the Ralph Lake area:* ***a)*** *thin-bedded, laminated, mafic siltstone to greywacke (subunit 6a****;*** *UTM Zone 14N, 371601E, 6306735, NAD 83) with mafic wacke bands characterized by porphyroblastic hornblende crystals up to 3 mm;* ***b)*** *moderately foliated, poorly sorted, clast-supported, polymictic conglomerate with sandy matrix that was recrystallized to an assemblage of quartz, feldspar, hornblende, biotite, epidote and magnetite (subunit 6b; UTM 369994E, 6304865);* ***c)*** *strongly foliated, poorly sorted, polymictic cobble conglomerate with medium- to coarse-grained greywacke matrix (subunit 6b; UTM 364101E; 6286914N) related to the Ralph Lake shear zone (RLSZ; see Yang, 2021); the asymmetry of some deformed lithic clasts suggests a dextral sense of movement;* ***d)*** *intensively foliated to protomylonitic, poorly sorted, polymictic pebble to cobble conglomerate (subunit 6b; UTM 372417E; 6306693N); the geometry of some relict clasts reveals a dextral movement associated with the RLSZ;* ***e)*** *moderately foliated, medium-grained greywacke to siltstone containing biotite and muscovite porphyroblasts along* S_2 *planes that transposed original* S_0 *bedding (subunit 7a; UTM 3715250E; 6308525N); and* ***f)*** *medium-grained paragneiss consisting of leucosome and melanosome banding and migmatitic veins and/or veinlets containing an assemblage of quartz, plagioclase, K-feldspar, biotite, ±hornblende, ±garnet (subunit 7b; UTM 369735E; 6308374N).*

yellowish grey to grey but is light grey to grey on fresh surfaces. Texturally, the greywacke to siltstone is mostly homogeneous, consisting of quartz, feldspar, biotite flakes and finer material. Thus, it may be termed psammite (Lawley et al., 2020). Locally, coarser lithic clasts are evident in the sandy matrix; thin argillite layers up to 10 cm in thickness are present. Rocks of this subunit are moderately foliated and recrystallized, and contain biotite and muscovite porphyroblasts along S_2 planes that transposed the original S_0 bedding (Figure GS2021-5-7e).

The Zed Lake greywacke and siltstone (subunit 7a) has low MS values of 0.22×10^{-3} to 0.54×10^{-3} SI, much lower than those of the Ralph Lake greywacke (MS values >100×10^{-3} SI; see above).

Paragneiss (subunit 7b)

Subunit 7b is composed dominantly of paragneiss characterized by alternating mafic and felsic bands that show compositional layering (a few millimetres to a few centimetres in width), forming a typical gneissic texture (Figure GS2021-5-7f). Leucosome bands and/or migmatitic veinlets are common and occur along gneissosity that appears to follow the regional foliation (S_2), although late granitic pegmatite veins or veinlets crosscut the S_2 planes that are folded by F_4 folding. The paragneiss, locally varying to migmatite, is mainly medium grained and has a mineral assemblage of feldspar, quartz, biotite±hornblende±muscovite±garnet. Note that subunit 7b was mapped as conglomerate in the map area by Gilbert et al. (1980).

The subunit 7b paragneiss also has low MS values ranging from 0.317×10^{-3} to 0.378×10^{-3} SI, similar to the greywacke and siltstone of subunit 7a, and much lower than those of the Ralph Lake conglomerate (and greywacke and mafic siltstone).

Post-Sickle intrusive suite (unit 8)

Post-Sickle intrusive rocks of unit 8, represented by the Burge Lake pluton (Beaumont-Smith et al., 2006; Yang and Beaumont-Smith, 2015b), occur mainly in the east-central part of the map area (Figure GS2021-5-2). Unit 8 rocks are mainly granodiorite and granite (Table GS2021-5-1) that intruded supracrustal rocks of the Wasekwan group. Granodiorite of unit 8 is pinkish on fresh surfaces, weathers beige to tan and is medium to coarse grained, massive, moderately foliated and equigranular (Figure GS2021-5-8a) to locally porphyritic. It consists of 5–7% hornblende (partly altered to biotite), 10–15% discrete biotite flakes, 25–30% quartz, 40–50% plagioclase and 5–10% K-feldspar. Granite is minor in the Burge Lake pluton, typically containing higher K-feldspar and less plagioclase compared to the granodiorite.

Unit 8 rocks have relatively high MS values (4.79×10^{-3} to 35.7×10^{-3} SI), typical of I-type granites (Yang and Beaumont-Smith, 2015b; Yang et al., 2019) and geochemically resemble adakite-like granitoid rocks (Yang and Lawley, 2018). Interestingly, the granodiorite at the contact with the unit 1 volcaniclastic rocks (i.e., lapilli tuff to tuff) of the Wasekwan group contains disseminated pyrite, is rusty and is cut by pyrite-bearing quartz veinlets. The volcaniclastic rocks at the contact zone also display much higher MS values (up to 23.5×10^{-3} SI) than commonly seen in unit 1 rocks (<1.0×10^{-3} SI) elsewhere in the map area. Hydrothermal fluids associated with such oxidized intrusion(s) can effectively scavenge and transport Au (e.g., Boyle, 1979) and thus may have played a role in Au mineralization in the study area and the LLGB (Yang and Beaumont-Smith, 2015a; Yang and Lawley, 2018; Yang et al., 2021).

Late intrusive suite (unit 9)

Unit 9 comprises two-mica granite, quartz-feldspar porphyry and pegmatite/aplite, mainly exposed and occurring as

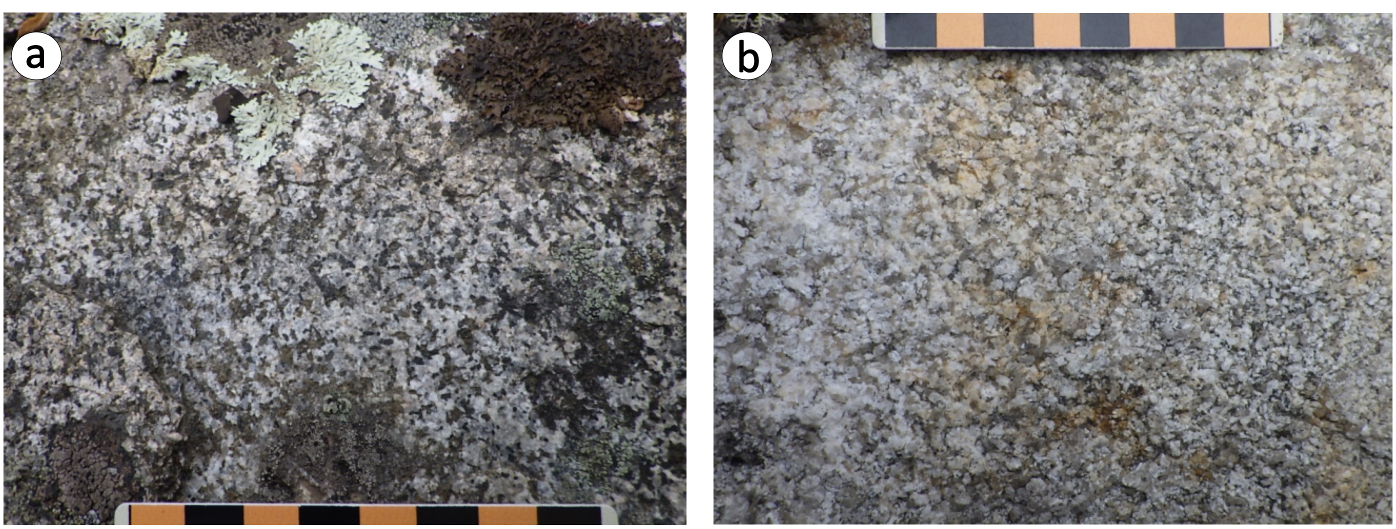

Figure GS2021-5-8: *Outcrop photographs of units 8 and 9 in the Ralph Lake area:* ***a)*** *massive, medium- to coarse-grained granodiorite with high magnetic susceptibility (MS) value of 35.7×10^{-3} SI (unit 8; UTM Zone 14N, 373715E, 6305052, NAD 83);* ***b)*** *massive, equigranular, medium- to coarse-grained two-mica granite with MS value as low as 0.054×10^{-3} SI (unit 9; UTM 369166E; 6308570N).*

small intrusions and dikes in Zed Lake greywacke (unit 7) in the northwestern corner of the map area (Figure GS2021-5-2). The two-mica granite is medium to coarse grained, undeformed, massive, equigranular and locally porphyritic, and consists of 25–35% anhedral quartz (2–4 mm), 55–60% subhedral to euhedral feldspar (2–4 mm), 4–5% biotite and about ~1% muscovite (Figure GS2021-5-8b). Thus, this two-mica granite can be termed leucogranite, and it becomes finer in grain size toward the contact with hostrocks (i.e., subunit 7a greywacke). The contact between the greywacke and two-mica granite is sharp and wavy to irregular, and concentrates biotite aggregates on the greywacke side, typical of contact metamorphism caused by the two-mica granite intrusion.

The unit 9 quartz-feldspar porphyry dikes tend to be isolated, relatively less deformed and apparently not associated with any of the larger intrusions mapped at surface. Pegmatite and aplite (unit 9) commonly have muscovite (±tourmaline) in addition to biotite, suggesting that they are not likely to be related to the pre-Sickle (subunit 5) or post-Sickle (subunit 8) intrusive suites (Yang and Beaumont-Smith, 2017).

Notably, unit 9 granitic rocks have extremely low MS values of 0.054×10^{-3} to 0.090×10^{-3} SI, consistent with typical S-type granites (Yang and Beaumont-Smith, 2015b; Yang et al., 2019).

Structural geology

The LLGB was involved in six generations of regional deformation (D_1 to D_6) according to Beaumont-Smith and Böhm (2002, 2004), although all structures formed by these events are not necessarily encountered in one area. In the Ralph Lake area, D_2 structures are dominant, are mostly penetrative and manifest as a steeply northwest-dipping S_2 foliation and tight to isoclinal folds (F_2) that have shallowly north-northeast plunging hinges and associated minor chevron folds. Foliations of this deformation (S_2) were observed in all map units except the late intrusive suite (unit 9). Typically, S_2 foliations in the Wasekwan group dip steeply to the northwest with steeply plunging mineral and stretching lineations. These L_2 lineations are well defined by a preferred orientation of minerals (e.g., amphibole, biotite, feldspar), stretched pillows and flattened pebbles and cobbles (e.g., Figure GS2021-5-7c, d).

Ductile shear zones that generally define map-unit contacts are commonly related to D_2 deformation, as the intensity of S_2 fabrics and tightness of F_2 folds increase toward contacts. The D_2 shear zones are characterized by dominantly dextral shear-sense indicators (e.g., Figure GS2021-5-7d) on horizontal surfaces and steeply plunging, generally down-dip to slightly oblique (easterly pitch) stretching lineations. The northeast-trending Ralph Lake shear zone (RLSZ) is a dextral transpressional shear zone dipping subvertically to the southeast that separates the Ralph Lake conglomerate (to the north) from the Wasekwan group (to the south; Figure GS2021-5-2); the Wasekwan rocks appear to move up along the shearing plane(s). Thus, the RLSZ is interpreted as a transpressional shear zone, separating the Wasekwan group supracrustal rocks from the Ralph Lake–Zed Lake sediments (Figure GS2021-5-2).

The regional S_2 foliation penetrating the Wasekwan volcaniclastic (unit 1), volcanic (unit 2) and volcanic-sedimentary (unit 3) rocks dips steeply to the northwest, whereas the S_2 foliation transposing the Ralph Lake–Zed Lake sediments dips to the southeast. This is interpreted to be the result of underthrusting of the Ralph–Zed lakes sedimentary package along the RLSZ beneath the Wasekwan supracrustal package. Numerous dextral shear-sense indicators (e.g., shear bands, S-C fabrics, asymmetric quartz boundins, rotated volcanic fragments) were observed on the horizontal surfaces. The development of narrow zones of shallowly plunging stretching lineations in the core of the shear zone reflects kinematics consistent with shear-zone development in response to dextral transpression. Such transpressive shear resulted in the greenstone belt appearing to ‘pop-up’ along the shear zone. Zircon U-Pb dating indicates that there was likely a pause between deposition of the unit 6 Ralph Lake sediments (ca. 1860 Ma; Lawley et al., 2020) and prior uplifting of volcanic rocks (ca. 1892–1870 Ma; Beaumont-Smith and Bohm, 2002, 2004; Beaumont-Smith et al., 2006; Manitoba Agriculture and Resource Development, 2021).

The D_3 deformation is represented by close to tight, S-asymmetric F_3 folds and northwest-trending, axial-planar S_3 crenulation cleavage. The Betty Lake–Margaret Lake fault strikes north-northwest and displays dextral movement, which is likely associated with D_3 deformation. F_4 folds are pervasive throughout the map area. These folds plunge steeply to the northeast and are associated with steeply dipping, northeast-striking, axial-planar S_4 cleavage (Figure GS2021-5-9a). Along the S_4 planes in folded paragneiss (subunit 7b) are muscovite-bearing pegmatitic veins/veinlets (Figure GS2021-5-9b), suggesting that this pegmatite phase is likely to be part of a late intrusive suite related to the D_4 event. A 40–45 cm wide dextral shear zone, striking 060° and dipping to the southeast at 72°, cuts foliated medium-grained gabbro (subunit 2a) and is likely the result of D_4 deformation. This shear zone consists of 30–35% dark reddish euhedral garnet crystals, together with amphibole, epidote and chlorite (Figure GS2021-5-9c, d), and quartz veins. Interestingly, the garnet grains are present in the hangingwall gabbro but are virtually absent in the footwall gabbro, suggesting that the garnet could have been formed by fluid associated with the D_4 shearing. The northeast-trending Ralph Lake fault zone (Figure GS2021-5-2) is thought to be related to the D_4 event that resulted in the structures having such orientations (Beaumont-Smith and Böhm (2002, 2004).

Economic considerations

The dominance in the Ralph Lake area of volcaniclastic rocks rich in plagioclase fragments, together with synvol-

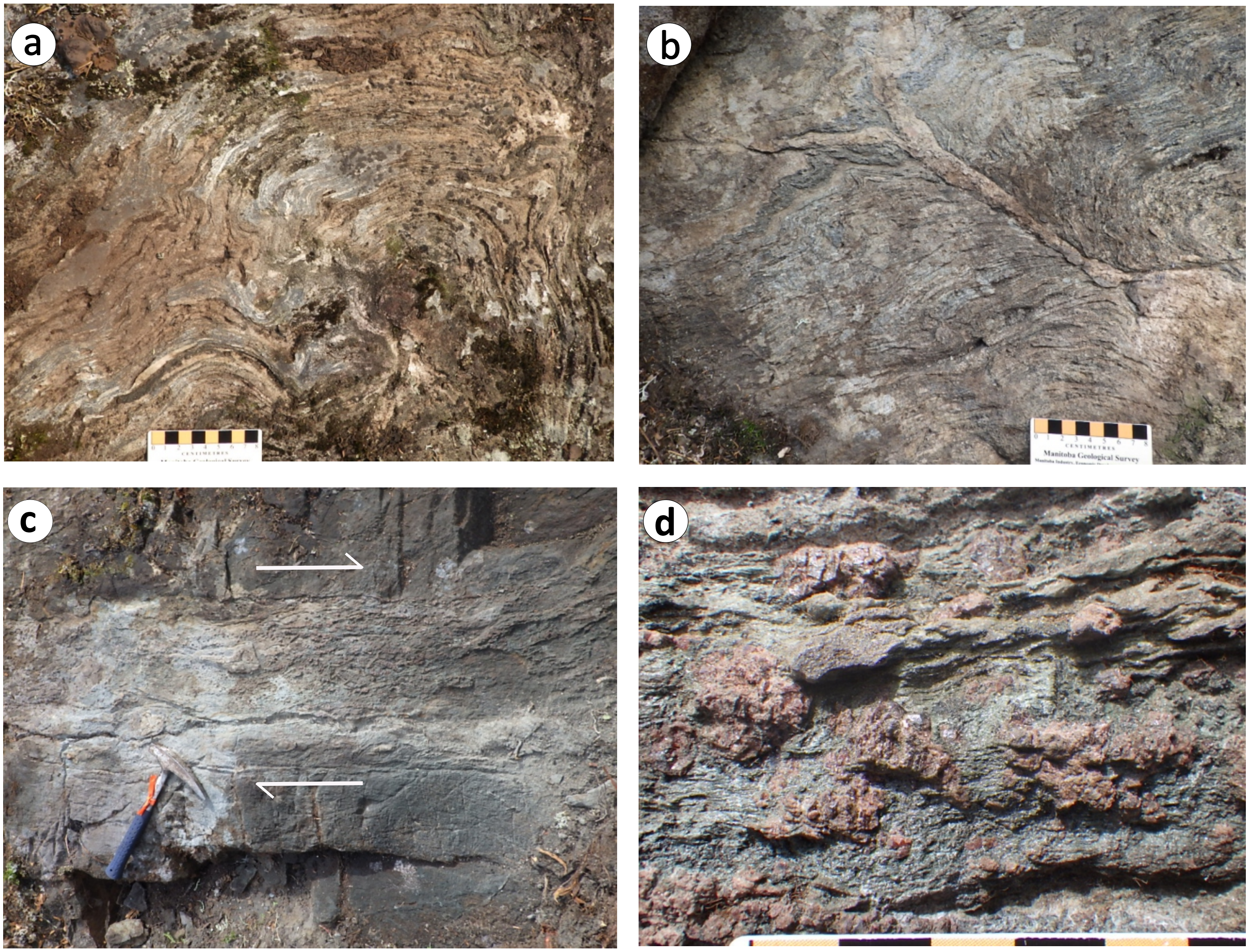

Figure GS2021-5-9: *Outcrop photographs of some mesoscopic structures and structure-related rocks evident in the Ralph Lake area:* ***a)*** *complex folding in unit 7b paragneiss (subunit 7b; UTM Zone 14N, 369735E, 6308374N, NAD 83), which is likely attributed to an F_4 fold;* ***b)*** *folded paragneiss cut by quartz-feldspar±muscovite pegmatitic veins and veinlets (unit 9; UTM 369835E; 6308478N);* ***c)*** *a 40–50 cm wide high-strain hydrothermal-alteration zone with dextral movement, striking 060° and consisting of 30–45% dark-reddish euhedral garnet porphyroblasts associated with amphibole, chlorite and quartz (UTM 363619E; 6283902N), cuts medium-grained gabbroic rock (unit 2a); hammer handle points north;* ***d)*** *closeup of part of this zone, showing the megacrystic garnets (same location as photo c).*

canic gabbroic intrusions, suggest that the Wasekwan group (units 1–3) may have been derived from hydrous, high-Al andesitic to tholeiitic magmas in a volcanic-arc to back-arc setting (e.g., Sotiriou et al., 2020). This volcanic package is intruded by the pre-Sickle intrusive suite (units 4 and 5), post-Sickle granitoid (unit 8) and, subsequently, late intrusive suite (unit 9) rocks. Unit 4 gabbroic intrusions contain disseminated pyrrhotite and locally chalcopyrite, and thus need to be further evaluated for magmatic Ni-Cu-PGE minerals. Unit 8 granitoid rocks display adakite-like signatures and may have played a role in Au mineralization (Yang and Lawley, 2018; Yang, 2019). The occurrences of I-type adakite-like to S-type granitoids in the Ralph Lake area suggest that tectonic settings may have evolved from volcanic-arc extension induced by slab roll-back to terminal collision. This interpretation, combined with the association of the supracrustal rocks in the Paleoproterozoic LLGB and much older (Mesoarchean) greenstone belts elsewhere, is a key to address the fundamental question of 'when did plate tectonics begin?' (e.g., Windley et al., 2021).

The occurrences of subunit 7b paragneiss, characterized by the assemblage quartzofeldspathic minerals, biotite±hornblende±muscovite±garnet, and unit 6 polymictic conglomerate (and mafic siltstone) with wacke matrix containing recrystallized hornblende suggest that the Zed Lake and Ralph Lake sedimentary rocks are likely part of the Southern Indian domain in terms of their similar rock associations. These sedimentary rocks are separated by the RLSZ from the volcaniclastic to volcanic rocks of the Wasekwan group of the LLGB (Figure GS2021-5-2) to the southeast, suggesting that the contact is likely a structural one or an unconformity reactivated by the RLSZ. The S-type granite (unit 9) occurs near the boundary zone, suggesting its emplacement in a collisional setting and the resulting potential for rare metal (Li, Cs, Ta) mineralization (e.g., Yang et al., 2019).

There are six mineral occurrences within the map area (Baldwin, 1989), based on the Manitoba Mineral Inventory Cards (https://mrsearch.gov.mb.ca/ltm-cat/web/minsearch.html), indicating diverse styles of mineralization (Ferreira and Baldwin, 1984). These are labeled A to F on Figure GS2021-5-2 (Yang, 2021). At location A, for example, disseminated layers and/or stringers of sulphide (pyrrhotite, pyrite) mineralization occur in quartz-biotite schist (subunit 7a). Location B contains disseminated pyrite in a 1 m thick zone of graphitic greywacke and argillite (subunit 7a). A mineralized felsic tuff (subunit 1a) at location C contains disseminated sulphide (pyrrhotite, sphalerite, chalcopyrite and pyrite) over a width of ~12 m and along a strike length of ~250 m. Amphibolite-hosted (subunit 1c mafic volcaniclastics) mineralization at location D has up to 7.8 m of disseminated to thin stringer sulphides (pyrrhotite, pyrite and minor chalcopyrite), with a 40 cm drillhole intercept containing 0.37% Cu, 2 g/t Au and 8.5 g/t Ag (Assessment File 9949, Manitoba Agriculture and Resource Development, Winnipeg). Volcaniclastic rocks (subunit 1b) at location E are host to massive-sulphide mineralization consisting of a 0.5–1 m thick zone of sulphide layers comprising mostly of pyrrhotite, lesser pyrite and minor chalcopyrite. At location F, a 40 m thick, siliceous, felsic pyritic volcanic sandstone and siltstone (subunits 1a and b) contains 2–5% disseminated pyrite and/or arsenopyrite stringers.

Acknowledgments

The author thanks W. Ezeana from the University of Manitoba for providing enthusiastic field assistance, and C. Epp and P. Belanger for logistical support, processing and cataloguing of samples. Thanks go to L. Chackowsky, A. Santucci and H.O. Adediran for assistance with GIS, setup of a hand-held electronic data collector, and drafting of the preliminary map and Figure GS2021-5-2, respectively. Technical communications and a one-day joint field excursion with personnel from Alamos Gold Inc. are highly appreciated. Constructive reviews by K.D. Reid and C.O. Böhm, technical editing by R.F. Davie and report layout by C. Steffano are gratefully acknowledged.

References

Anderson, S.D. and Beaumont-Smith, C.J. 2001: Structural analysis of the Pool Lake–Boiley Lake area, Lynn Lake greenstone belt (NTS 64C/11); *in* Report of Activities 2001, Manitoba Industry, Trade and Mines, Manitoba Geological Survey, p. 76–85, URL <https://www.manitoba.ca/iem/geo/field/roa01pdfs/01gs-12.pdf> [October 2021].

Ansdell, K.M. 2005: Tectonic evolution of the Manitoba-Saskatchewan segment of the Paleoproterozoic Trans-Hudson Orogen, Canada; Canadian Journal of Earth Sciences, v. 42, p. 741–759.

Ansdell, K.M., Corrigan, D., Stern, R. and Maxeiner, R. 1999: SHRIMP U-Pb geochronology of complex zircons from Reindeer Lake, Saskatchewan: implications for timing of sedimentation and metamorphism in the northwestern Trans-Hudson Orogen; Geological Association of Canada–Mineralogical Association of Canada, Joint Annual Meeting, Program with Abstracts, v. 24, p. 3.

Baldwin, D.A. 1989: Mineral deposits and occurrences in the Lynn Lake area, NTS 64C/14; Manitoba Energy and Mines, Geological Services, Mineral Deposit Series Report No. 6, 130 p., URL <https://www.manitoba.ca/iem/info/libmin/MDS6.zip> [October 2021].

Baldwin, D.A., Syme, E.C., Zwanzig, H.V., Gordon, T.M., Hunt, P.A. and Stevens, R.P. 1987: U-Pb zircon ages from the Lynn Lake and Rusty Lake metavolcanic belts, Manitoba: two ages of Proterozoic magmatism; Canadian Journal of Earth Sciences, v. 24, p. 1053–1063.

Baragar, W.R.A., Ernst, R.E., Hulbert, L. and Peterson, T. 1996: Longitudinal petrochemical variation in the Mackenzie dyke swarm, northwestern Canadian Shield; Journal of Petrology, v. 37, p. 317–359.

Bateman, J.D. 1945: McVeigh Lake area, Manitoba; Geological Survey of Canada, Paper 45-14, 34 p.

Beaumont-Smith, C.J. 2008: Geochemistry data for the Lynn Lake greenstone belt, Manitoba (NTS 64C11-16); Manitoba Science, Technology, Energy and Mines, Manitoba Geological Survey, Open File OF2007-1, 5 p., URL <https://www.manitoba.ca/iem/info/libmin/OF2007-1.zip> [October 2021].

Beaumont-Smith, C.J. and Böhm, C.O. 2002: Structural analysis and geochronological studies in the Lynn Lake greenstone belt and its gold-bearing shear zones (NTS 64C10, 11, 12, 14, 15 and 16), Manitoba; *in* Report of Activities 2002, Manitoba Industry, Trade and Mines, Manitoba Geological Survey, p. 159–170, URL <https://www.manitoba.ca/iem/geo/field/roa02pdfs/GS-19.pdf> [October 2021].

Beaumont-Smith, C.J. and Böhm, C.O. 2003: Tectonic evolution and gold metallogeny of the Lynn Lake greenstone belt, Manitoba (NTS 64C10, 11, 12, 14, 15 and 16), Manitoba; *in* Report of Activities 2003, Manitoba Industry, Economic Development and Mines, Manitoba Geological Survey, p. 39–49, URL <https://www.manitoba.ca/iem/geo/field/roa03pdfs/GS-06.pdf> [October 2021].

Beaumont-Smith, C.J. and Böhm, C.O. 2004: Structural analysis of the Lynn Lake greenstone belt, Manitoba (NTS 64C10, 11, 12, 14, 15 and 16); *in* Report of Activities 2004, Manitoba Industry, Economic Development and Mines, Manitoba Geological Survey, p. 55–68, URL <https://www.manitoba.ca/iem/geo/field/roa04pdfs/GS-06.pdf> [October 2021].

Beaumont-Smith, C.J., Machado, N. and Peck, D.C. 2006: New uranium-lead geochronology results from the Lynn Lake greenstone belt, Manitoba (NTS 64C11-16); Manitoba Science, Technology, Energy and Mines, Manitoba Geological Survey, Geoscientific Paper GP2006-1, 11 p., URL <https://www.manitoba.ca/iem/info/libmin/GP2006-1.pdf> [October 2021].

Boyle, R.W. 1979: The geochemistry of gold and its deposits (together with a chapter on geochemical prospecting for the element); Geological Survey of Canada Bulletin 280, 584 p.

Corrigan, D. 2012: Paleoproterozoic crustal evolution and tectonic processes: insights from the LITHOPROBE program in the Trans-Hudson orogen, Canada; Chapter 4 *in* Tectonic Styles in Canada: The LITHOPROBE Perspective, J.A. Percival, F.A. Cook and R.M. Clowes (ed.), Geological Association of Canada, Special Paper 49, p. 237–284.

Corrigan, D., Galley, A.G. and Pehrsson, S. 2007: Tectonic evolution and metallogeny of the southwestern Trans-Hudson Orogen; *in* Mineral Deposits of Canada: A Synthesis of Major Deposit-Types, District Metallogeny, the Evolution of Geological Provinces, and Exploration Methods, W.D. Goodfellow (ed.), Geological Association of Canada, Mineral Deposits Division, Special Publication 5, p. 881–902.

Corrigan, D., Pehrsson, S., Wodicka, N. and de Kemp, E. 2009: The Palaeoproterozoic Trans-Hudson Orogen: a prototype of modern accretionary processes; *in* Ancient Orogens and Modern Analogues, J.B. Murphy, J.D. Keppie and A.J. Hynes (ed.), Geological Society of London, Special Publications, v. 327, p. 457–479.

Fedikow, M.A.F. and Gale, G.H. 1982: Mineral deposit studies in the Lynn Lake area; *in* Report of Field Activities 1982, Manitoba Department of Energy and Mines, Mineral Resources Division, p. 44–54.

Ferreira, K.J. and Baldwin, D.A. 1984: Mineral deposit documentation in the Lynn Lake area; *in* Report of Field Activities 1984; Manitoba Energy and Mines; Mineral Resources, p. 12–16, URL <https://www.manitoba.ca/iem/geo/field/roa84pdfs/rofa1984.pdf> [October 2021].

Gilbert, H.P. 1993: Geology of the Barrington Lake–Melvin Lake–Fraser Lake area; Manitoba Energy and Mines, Geological Services, Geological Report GR87-3, 97 p., URL <https://www.manitoba.ca/iem/info/libmin/GR87-3.zip> [October 2021].

Gilbert, H.P., Syme, E.C. and Zwanzig, H.V. 1980: Geology of the metavolcanic and volcaniclastic metasedimentary rocks in the Lynn Lake area; Manitoba Energy and Mines, Mineral Resources Division, Geological Paper GP80-1, 118 p., URL <https://www.manitoba.ca/iem/info/libmin/GP80-1.zip> [October 2021].

Glendenning, M.W.P., Gagnon, J.E. and Polat, A. 2015: Geochemistry of the metavolcanic rocks in the vicinity of the MacLellan Au-Ag deposit and an evaluation of the tectonic setting of the Lynn Lake greenstone belt, Canada: evidence for a Paleoproterozoic-aged rifted continental margin; Lithos, v. 233, p. 46–68.

Hastie, E.C.G., Gagnon, J.E. and Samson, I.M. 2018: The Paleoproterozoic MacLellan deposit and related Au-Ag occurrences, Lynn Lake greenstone belt, Manitoba: an emerging, structurally controlled gold camp; Ore Geology Reviews, v. 94, p. 24–45.

Hoffman, P.H. 1988: United plates of America, the birth of a craton: Early Proterozoic assembly and growth of Laurentia; Annual Reviews of Earth and Planetary Sciences, v. 16, p. 543–603.

Kremer, P.D., Rayner, N. and Corkery, M.T. 2009: New results from geological mapping in the west-central and northeastern portions of Southern Indian Lake, Manitoba (parts of NTS 64G1, 2, 8, 64H4, 5); *in* Report of Activities 2009, Manitoba Science, Innovation, Energy and Mines, Manitoba Geological Survey, p. 94–107, URL <https://www.manitoba.ca/iem/geo/field/roa09pdfs/GS-9.pdf> [October 2021].

Lawley, C.J.M, Davis, W.J., Jackson, S.E., Petts, D.C., Yang, E., Zhang, S., Selby, D., O'Connor, A.R. and Schneider, D.A. 2019: Paleoproterozoic gold and its tectonic triggers and traps; *in* Targeted Geoscience Initiative: 2018 report of activities, N. Rogers (ed.), Geological Survey of Canada, Open File 8549, p. 71–75.

Lawley, C.J.M., Selby, D., Davis, W.J., Yang, E., Zhang, S., Jackson, S.E., Petts, D.C., O'Connor, A.R. and Schneider, D.A., 2020: Paleoproterozoic gold and its tectonic triggers and traps: implications from Re-Os sulphide and U-Pb detrital zircon geochronology, Lynn Lake, Manitoba; *in* Targeted Geoscience Initiative 5: Contributions to the Understanding of Canadian Gold Systems, P. Mercier-Langevin, C.J.M. Lawley and S. Castonguay (ed.), Geological Survey of Canada, Open File 8712, p. 211–222.

Lawley, C.J.M., Yang, X.M., Selby, D., Davis, W., Zhang, S., Petts, D.C. and Jackson, S.E. 2020: Sedimentary basin controls on orogenic gold deposits: new constraints from U-Pb detrital zircon and Re-Os sulphide geochronology, Lynn Lake greenstone belt, Canada; Ore Geology Reviews, v. 126, art. 103790.

Lewry, J.F. and Collerson, K.D. 1990: The Trans-Hudson Orogen: extent, subdivisions and problems; *in* The Early Proterozoic Trans-Hudson Orogen of North America, J.F. Lewry and M.R. Stauffer (ed.), Geological Association of Canada, Special Paper 37, p. 1–14.

Manitoba Agriculture and Resource Development 2021: Lynn Lake, Manitoba (NTS 64C14); Manitoba Agriculture and Resource Development, Manitoba Geological Survey, Lynn Lake Bedrock Compilation Map 64C14, scale 1:50 000, URL <https://www.manitoba.ca/iem/info/libmin/lynn_lake_compilation_2021.zip> [October 2021].

Manitoba Energy and Mines 1986: Granville Lake, NTS 64C; Manitoba Energy and Mines, Minerals Division, Bedrock Geology Compilation Map Series, Map 64C, scale 1:250 000.

Manitoba Mineral Resources 2013: Bedrock geology, Manitoba; *in* Map Gallery – Geoscientific Maps, Manitoba Mineral Resources, Manitoba Geological Survey, URL <https://www.arcgis.com/apps/webappviewer/index.html?id=8fd905c83e6349bfa126dfe035b16189> [October 2021].

Martins, T., Kremer, P.D., Corrigan, D. and Rayner, N. 2019: Geology of the Southern Indian Lake area, north-central Manitoba (parts of NTS 64G1, 2, 7–10, 64H3–6); Manitoba Growth, Enterprise and Trade, Manitoba Geological Survey, Geoscientific Report GR2019-1, 51 p. plus 4 maps at 1:50 000 scale, URL <https://www.manitoba.ca/iem/info/libmin/GR2019-1.zip> [October 2021].

Milligan, G.C. 1960: Geology of the Lynn Lake district; Manitoba Department of Mines and Natural Resources, Mines Branch, Publication 57-1, 317 p.

Norman, G.W.H. 1933: Granville Lake district, northern Manitoba; Geological Survey of Canada, Summary Report, Part C, p. 23–41.

Park, A.F., Beaumont-Smith, C.J. and Lentz, D.R. 2002: Structure and stratigraphy in the Agassiz Metallotect, Lynn Lake greenstone belt (NTS 64C/14 and /15), Manitoba; *in* Report of Activities 2002, Manitoba Industry, Trade and Mines, Manitoba Geological Survey, p. 171–186, URL <https://www.manitoba.ca/iem/geo/field/roa02pdfs/GS-20.pdf> [October 2021].

Rollinson, H. and Pease, V. 2021: Using geochemical data to understand geological processes, second edition; Cambridge University Press, Cambridge, United Kingdom, 346 p.

Sotiriou, P., Polat, A., Frei, R., Yang, X.M. and van Vessem, J. 2020: Evidence for Neoarchean hydrous arc magmatism, the anorthosite-bearing Mayville Intrusion, Western Superior Province, Canada; Lithos, v. 362–363, art. 105482.

Stauffer, M.R. 1984: Manikewan: an Early Proterozoic ocean in central Canada, its igneous history and orogenic closure; Precambrian Research, v. 25, p. 257–281.

Stern, R.A., Syme, E.C. and Lucas, S.B. 1995: Geochemistry of 1.9 Ga MORB- and OIB-like basalts from the Amisk collage, Flin Flon Belt, Canada: evidence for an intra-oceanic origin; Geochimica et Cosmochimica Acta, v. 59, p. 3131–3154.

Syme, E.C. 1985: Geochemistry of metavolcanic rocks in the Lynn Lake Belt; Manitoba Energy and Mines, Geological Services/Mines Branch, Geological Report GR84-1, 84 p.

Turek, A., Woodhead, J. and Zwanzig H.V. 2000: U-Pb age of the gabbro and other plutons at Lynn Lake (part of NTS 64C); *in* Report of Activities 2000, Manitoba Industry, Trade and Mines, Manitoba Geological Survey, p. 97–104, URL <https://www.manitoba.ca/iem/geo/field/roa00pdfs/00gs-18.pdf> [October 2021].

White, D.J., Zwanzig, H.V. and Hajnal, Z. 2000: Crustal suture preserved in the Paleoproterozoic Trans-Hudson orogeny, Canada; Geology, v. 28, p. 527–530.

Windley, B.F., Kusky, T. and Polat, A. 2021: Onset of plate tectonics by the Eoarchean; Precambrian Research, v. 352, art. 105980.

Yang, X.M. 2019: Preliminary results of bedrock mapping in the Gemmell Lake area, Lynn Lake greenstone belt, northwestern Manitoba (parts of NTS 64C11, 14); *in* Report of Activities 2019, Manitoba Agriculture and Resource Development, Manitoba Geological Survey, p. 10–29, URL <https://www.manitoba.ca/iem/geo/field/roa19pdfs/GS2019-2.pdf> [October 2021].

Yang, X.M. 2021: Bedrock geology of the Ralph Lake area, Lynn Lake greenstone belt, northwestern Manitoba (parts of NTS 64C14); Manitoba Agriculture and Resource Development, Manitoba Geological Survey, Preliminary Map PMAP2021-2, scale 1:10 000, URL <https://www.manitoba.ca/iem/info/libmin/PMAP2021-2.pdf> [November 2021].

Yang, X.M. and Beaumont-Smith, C.J. 2015a: Geological investigations of the Keewatin River area, Lynn Lake greenstone belt, northwestern Manitoba (parts of NTS 64C14, 15); *in* Report of Activities 2015, Manitoba Mineral Resources, Manitoba Geological Survey, p. 52–67, URL <https://www.manitoba.ca/iem/geo/field/roa15pdfs/GS-4.pdf> [October 2021].

Yang, X.M. and Beaumont-Smith, C.J. 2015b: Granitoid rocks in the Lynn Lake region, northwestern Manitoba: preliminary results of reconnaissance mapping and sampling; *in* Report of Activities 2015, Manitoba Mineral Resources, Manitoba Geological Survey, p. 68–78, URL <https://www.manitoba.ca/iem/geo/field/roa15pdfs/GS-5.pdf> [October 2021].

Yang, X.M. and Beaumont-Smith, C.J. 2016: Geological investigations in the Farley Lake area, Lynn Lake greenstone belt, northwestern Manitoba (part of NTS 64C16); *in* Report of Activities 2016, Manitoba Growth, Enterprise and Trade, Manitoba Geological Survey, p. 99–114, URL <https://www.manitoba.ca/iem/geo/field/roa16pdfs/GS-9.pdf> [October 2021].

Yang, X.M. and Beaumont-Smith, C.J. 2017: Geological investigations of the Wasekwan Lake area, Lynn Lake greenstone belt, northwestern Manitoba (parts of NTS 64C10, 15); *in* Report of Activities 2017, Manitoba Growth, Enterprise and Trade, Manitoba Geological Survey, p. 117–132, URL <https://www.manitoba.ca/iem/geo/field/roa17pdfs/GS2017-11.pdf> [October 2021].

Yang, X.M. and Lawley, C.J.M. 2018: Tectonic setting of the Gordon gold deposit, Lynn Lake greenstone belt, northwestern Manitoba (parts of NTS 64C16): evidence from lithogeochemistry, Nd isotopes, and U-Pb geochronology; *in* Report of Activities 2018, Manitoba Growth, Enterprise and Trade, Manitoba Geological Survey, p. 89–109, URL <https://www.manitoba.ca/iem/geo/field/roa18pdfs/GS2018-8.pdf> [October 2021].

Yang, X.M., Drayson, D. and Polat, A. 2019: S-type granites in the western Superior Province: a marker of Archean collision zones; Canadian Journal of Earth Sciences, v. 56, p. 1409–1436.

Yang, X.M., Lentz, D.R. and Chi, G. 2021: Ferric-ferrous iron oxide ratios: effect on crystallization pressure of granites estimated by Qtz-geobarometry; Lithos, v. 380–381, art. 105920.

Zwanzig, H.V. 1990: Kisseynew gneiss belt in Manitoba: stratigraphy, structure, and tectonic evolution; *in* The Early Proterozoic Trans-Hudson Orogen of North America, J.F. Lewry and M.R. Stauffer (ed.); Geological Association of Canada, Special Paper 37, p. 95–120.

Zwanzig, H.V. 2000: Geochemistry and tectonic framework of the Kisseynew Domain–Lynn Lake belt boundary (part of NTS 63P/13); *in* Report of Activities 2000, Manitoba Industry, Trade and Mines, Manitoba Geological Survey, p. 91–96, URL <https://www.manitoba.ca/iem/geo/field/roa00pdfs/00gs-17.pdf> [October 2021].

Zwanzig, H.V. and Bailes, A.H. 2010: Geology and geochemical evolution of the northern Flin Flon and southern Kisseynew domains, Kississing–File lakes area, Manitoba (parts of NTS 63K, N); Manitoba Innovation, Energy and Mines, Manitoba Geological Survey, Geoscientific Report GR2010-1, 135 p., URL <https://www.manitoba.ca/iem/info/libmin/GR2010-1.zip> [October 2021].

Zwanzig, H.V., Syme, E.C. and Gilbert, H.P. 1999: Updated trace element geochemistry of ca. 1.9 Ga metavolcanic rocks in the Paleoproterozoic Lynn Lake belt; Manitoba Industry, Trade and Mines, Geological Services, Open File Report OF99-13, 46 p., URL <https://www.manitoba.ca/iem/info/libmin/OF99-13.zip> [October 2021].

GS2021-6

Identifying Late Cretaceous vertebrate fossil collection biases, southwestern Manitoba and east-central Saskatchewan

by A.A. Kilmury[1], M.P.B. Nicolas and K.S. Brink[1]

In Brief:

- Surveys were conducted at Canadian institutions housing Manitoba escarpment vertebrate fossil collections, and several collection biases were identified
- Fossils of sharks and birds are most abundant in current collections, and fossils of reptiles and fish are least abundant
- Collection biases can be counteracted with future work that targets poorly known lithostratigraphic units and the collection of microvertebrate fossils

Citation:

Kilmury, A.A., Nicolas, M.P.B. and Brink, K.S. 2021: Identifying Late Cretaceous vertebrate fossil collection biases, southwestern Manitoba and east-central Saskatchewan; *in* Report of Activities 2021, Manitoba Agriculture and Resource Development, Manitoba Geological Survey, p. 59–65.

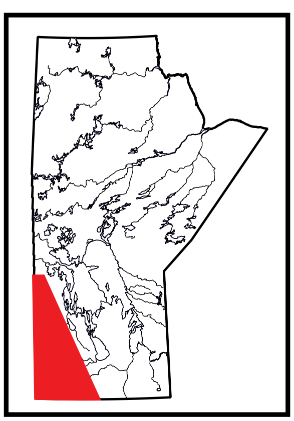

Summary

An ongoing study examining the stratigraphic distribution and composition of the Late Cretaceous vertebrate faunal associations of the Western Interior Seaway (WIS) of Manitoba has revealed several historical collection biases in current institution collections of vertebrate fossils from the Manitoba escarpment of southwestern Manitoba to east-central Saskatchewan. These biases have led to the unequal representation of some taxonomic groups in certain time periods, such as mid-Cenomanian chondrichthyans and early Campanian marine reptiles when compared to fish from all Cretaceous members. The identification and presentation of historical collection biases is necessary before analyses of faunal provinciality, habitat preferences and faunal changes through time can be undertaken, as these biases can skew interpretations of Cretaceous paleoecology of the WIS. Data-supported recommendations for future work are provided to address and reduce biases in future vertebrate fossil collection.

Introduction

Late Cretaceous (100.5–66 Ma) sedimentary strata in Manitoba were deposited in a shallow marine setting near the eastern margin of the WIS, which hosted a diverse marine vertebrate community of fish, sharks, reptiles and birds (Bardack, 1968). Exposures of Late Cretaceous deposits in Manitoba range in age from the Cenomanian to Maastrichtian and are mainly restricted to the Manitoba escarpment, a northwest-trending ridge consisting of five topographic highs and about 675 km in total length, from the Manitoba–North Dakota border near Walhalla, North Dakota, to the Manitoba–Saskatchewan border near Hudson Bay, Saskatchewan (Bamburak and Nicolas, 2013). New stratigraphic information on Cretaceous deposits of the WIS in Manitoba, including an updated lithostratigraphic framework (Bamburak and Nicolas, 2009), radiometric ages of bentonites (Bamburak et al., 2013, 2016) and defined foraminiferal zones (Nielsen et al., 2008; Schröder-Adams, 2014), made available over the last two decades has improved historically challenging regional correlations with coeval deposits in Saskatchewan and Alberta (Christopher et al., 2006; Nielsen et al., 2008) and North Dakota (McNeil and Caldwell, 1981). However, vertebrate biostratigraphy and biogeography data are currently lacking.

Institution fossil collections are essential for identifying the composition of faunal assemblages and are invaluable for examining temporal and biogeographic trends due to their large sample sizes and accessibility. For example, Nicholls and Russell (1990) described spatial differences between time-transgressive, early Campanian WIS communities on a continental scale using institution collections. However, when considering more detailed paleoecological analyses, institution collections have limitations. As the majority of Manitoba escarpment institution specimens are limited to genus-level in terms of taxonomic identification and lithostratigraphic member in terms of stratigraphic information, it can be difficult to discern small-scale changes between fossil associations through time.

Previous descriptions of vertebrate fossil collection biases in Manitoba are limited to the early Campanian Pembina Member of the Pierre Shale (Nicholls, 1989; Nicholls and Russell, 1990). Nicholls (1989) described collection biases known to affect the Pembina Member fossil collection between 1972 and 1985. These biases included time-limited access and expedited collection of specimens discovered in bentonite strip mining operations, inconsistent collecting methods and duration of collecting between localities and preferred collection of large and semi- to fully articulated specimens. Preservational biases included taphonomic factors and alteration by post-depositional crystallization of gypsum. For example, Nicholls (1989) demonstrated the number of catalogued fish specimens from the Pembina Member faunal assemblage is not indicative of their

[1] Department of Earth Sciences, University of Manitoba, 125 Dysart Road, Winnipeg, Manitoba R3T 2N2

true abundance since only articulated fish remains and no isolated fish elements were collected prior to the study, resulting in significant underrepresentation of fish in the Pembina Member collection.

In order to update the work of Nicholls and Russell (1990) and to describe the diversity of Late Cretaceous WIS vertebrate faunal associations through time, surveys of several institutions (museum and university collections; Table GS2021-6-1) housing fossil specimens collected from the Manitoba escarpment in Manitoba and Saskatchewan were conducted in 2020 and 2021. As a result of these surveys, several collection biases were identified, building on the initial biases discussed by Nicholls (1989). For the purpose of this study, collection biases are defined as fossil collecting methods or practices that have led to disproportionate representation of certain taxonomic groups within a faunal assemblage or certain lithostratigraphic units relative to others, in existing institution collections. The identification and presentation of historical collection biases is imperative for a proper understanding of the distribution of Cretaceous vertebrates in Manitoba and to test hypotheses of faunal provinciality, habitat preferences and temporal and spatial changes in faunal assemblages through time.

Results

Representative fossil specimens from either the most or second-most abundant taxon of each lithostratigraphic member collected from the Manitoba escarpment are shown in Figure GS2021-6-1. The majority of Manitoba escarpment institution specimens are fragmentary marine reptile and hesperornithiform bird (Figure GS2021-6-1g) remains from the Pembina Member, Pierre Shale, collected from bentonite mining operations in the Morden-Miami area from 1939 to 1990 (Bamburak and Nicolas, 2013). However, in terms of individual specimens, the most sampled lithostratigraphic unit of the Manitoba escarpment is the early to late Cenomanian Belle Fourche Member, Ashville Formation, particularly in the Carrot River and Bainbridge River bone beds in Saskatchewan (Cumbaa and Bryant, 2001; Schröder-Adams et al., 2001; Cumbaa et al., 2006, 2010, 2013; Underwood and Cumbaa, 2010; Figure GS2021-6-2a, b). These microvertebrate bone beds were consistently sampled over multiple years and the samples were prepared with an acid-digestion technique resulting in a relatively large and disproportionate number of recovered specimens relative to other Manitoba escarpment units and horizons.

The two Manitoba escarpment lithostratigraphic members with the least fossil representation in institution collections are the Morden Member, Carlile Formation, and the Odanah Member, Pierre Shale. The Morden Member has produced a partial actinopterygian dentary assigned to *Enchodus shumardi* and 75 chondrichthyan dermal denticles (e.g., Manitoba Museum specimen MM V-2689 and in University of Manitoba, Department of Earth Sciences [UM] Teaching Collection; Figure GS2021-6-1d), including two identified as *Cretomanta canadensis*. The Odanah Member has produced one isolated yet complete and well-preserved actinopterygian scale (Figure GS2021-6-1i).

Vertebrate specimens collected from the Manitoba escarpment are unevenly distributed in terms of both represented taxa and lithostratigraphic members. Avian specimens are mostly represented by isolated limb elements mainly consisting of tibiae, fibulae and femora (Figure GS2021-6-1g), the majority of which were collected from the Belle Fourche Member and are housed at the Royal Saskatchewan Museum (RSM), whereas those collected from the younger Pembina Member are housed at the Canadian Fossil Discovery Cen-

Table GS2021-6-1: List of institution collections surveyed for this study.

Abbreviation	Institution	Location
CFDC	Canadian Fossil Discovery Centre (previously Morden and District Museum)	Morden, Manitoba
CMN	Canadian Museum of Nature (previously National Museum of Canada)	Ottawa, Ontario
FDM	Fort Dauphin Museum	Dauphin, Manitoba
MM	Manitoba Museum (previously Manitoba Museum of Man and Nature)	Winnipeg, Manitoba
ROM	Royal Ontario Museum	Toronto, Ontario
RSM	Royal Saskatchewan Museum (previously Saskatchewan Museum of Natural History)	Regina, Saskatchewan
RTMP	Royal Tyrrell Museum of Palaeontology	Drumheller, Alberta
UA	University of Alberta, Department of Biological Sciences	Edmonton, Alberta
UM	University of Manitoba, Department of Earth Sciences (previously Department of Geological Sciences)	Winnipeg, Manitoba

***Figure GS2021-6-1**: Representative fossil specimens from each Late Cretaceous Manitoba lithostratigraphic member: **a)** Archaeolamna kopingensis tooth in labial view (Royal Saskatchewan Museum (RSM) P2466.8), Belle Fourche Member, scale bar = 1 cm; **b)** Squalicorax curvatus tooth in lingual view (University of Manitoba, Department of Earth Sciences [UM], Teaching Collection), Keld Member, scale bar = 0.25 cm; **c)** Enchodus sp. undetermined tooth (UM Teaching Collection), Marco Calcarenite, Assiniboine Member, scale bar = 0.25 cm; **d)** undetermined chondrichthyan dermal denticle (UM Teaching Collection), Morden Member, scale bar = 0.025 cm; **e)** Enchodus sp. undetermined skull in dorsal view (University of Alberta, Department of Biological Sciences, UALVP 15064), Boyne Member, scale bar = 1 cm; **f)** Archaeolamna sp. tooth in lingual view (Canadian Fossil Discovery Centre [CFDC] S.2013.03.13), Gammon Ferruginous Member, scale bar = 1 cm; **g)** Hesperornis regalis right femur in anterior view (Manitoba Museum [MM] V-137), Pembina Member, scale bar = 5 cm; **h)** Enchodus ferox(?) tooth (CFDC F.2007.06.23), Millwood Member, scale bar = 1 cm; **i)** undetermined actinopterygian scale (MM V-68), Odanah Member, scale bar = 0.5 cm.*

tre (CFDC), MM and Royal Ontario Museum (ROM). Since no avian specimens from the Assiniboine, Morden and Boyne members are represented in the collections, a significant gap in known avian specimens of approximately 11 million years exists between early Turonian and early Campanian time. Chondrichthyan specimens are almost entirely represented by teeth (Figure GS2021-6-1a, b, f) and those housed at the MM and CFDC were collected from most of the Late Cretaceous members of the Manitoba escarpment, except the Odanah Member. Chondrichthyan specimens housed at the RSM were collected from the Belle Fourche and Keld members, though the majority (over 5000 teeth) have been collected from

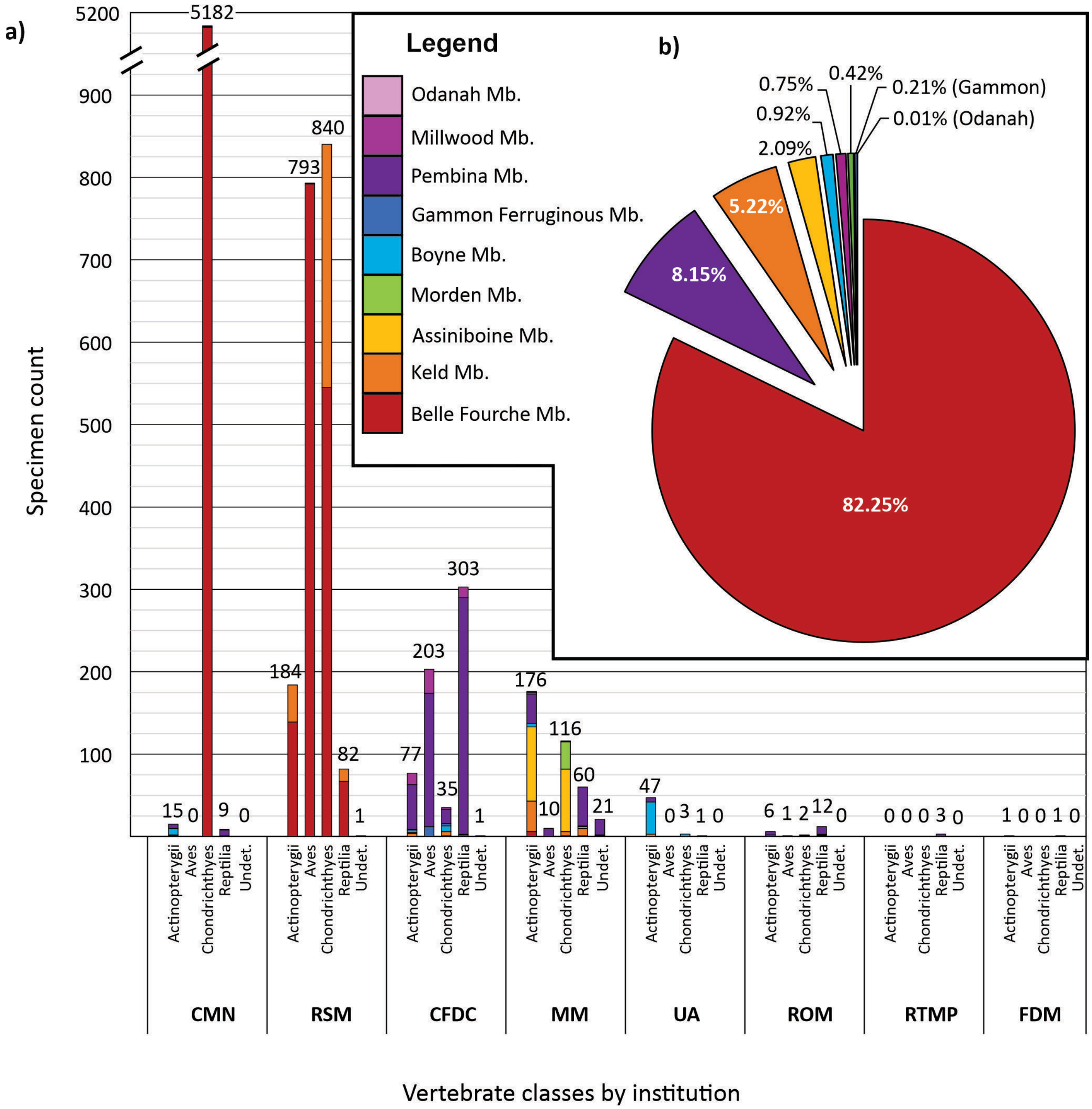

***Figure GS2021-6-2**: Distribution and abundance of Late Cretaceous vertebrate specimens collected from the Manitoba escarpment and housed in Canadian institution collections, organized by **a)** traditional vertebrate classes represented by each collection, with specimen counts by represented individuals and represented proportions of lithostratigraphic members shown as coloured stacks; and **b)** distribution of specimens by lithostratigraphic member with proportions calculated from a total of 8185 specimens. Specimen totals for the Manitoba Museum (MM) include those specimens from the University of Manitoba, Department of Earth Sciences, Teaching Collection that will be deposited at the MM in late 2021. Abbreviations: CFDC, Canadian Fossil Discovery Centre; CMN, Canadian Museum of Nature; FDM, Fort Dauphin Museum; ROM, Royal Ontario Museum; RSM, Royal Saskatchewan Museum; RTMP, Royal Tyrrell Museum of Palaeontology; UA, University of Alberta, Department of Biological Sciences; Undet., undetermined class.*

the Carrot River bone bed within the mid-Cenomanian Belle Fourche Member and are housed at the Canadian Museum of Nature (CMN). Actinopterygians are represented in nearly all institution collections and from nearly every Cretaceous member of the Manitoba escarpment (Figure GS2021-6-1c, e, h, i). The abundance of actinopterygian specimens per lithostratigraphic member has the most uneven distribution relative to other taxonomic classes, with 145 specimens from the Belle Fourche Member, 91 from the Keld Member, 91 from the Assiniboine Member, 1 from the Morden Member, 56 from the Boyne Member, 1 from the Gammon Ferruginous Member, 104 from the Pembina Member, 16 from the Millwood Member and 1 from the Odanah Member. Most Pembina Member actinopterygian specimens are housed at the MM and CFDC, whereas most Belle Fourche Member actinopterygian specimens are housed at the RSM. Keld Member actinopterygian specimens are housed at the RSM, MM, CFDC, University of Alberta, Department of Biological Sciences (UA) and the Fort Dauphin Museum (FDM).

Reptile specimens are mainly from the Pembina Member with at least 287 specimens at the CFDC, 47 at the MM, 9 at the ROM, 7 at the CMN and 3 at the Royal Tyrrell Museum of Palaeontology (RTMP). There are also 67 RSM specimens from the Belle Fourche Member; 9 MM specimens and 15 RSM specimens from the Keld Member; 13 CFDC specimens from the Millwood Member; and one to two specimens from the other members among the surveyed collections. *Terminonaris robusta* is the only known crocodile species from the Manitoba escarpment and is represented by two specimens, both collected from the Keld Member. A 30–40% complete, semi-articulated postcranial skeleton of *Terminonaris robusta* is housed at the FDM (specimen FDM MD-1055-1; Hatcher and Janzic, 2010) and a nearly complete, fully articulated skeleton is housed at the RSM (specimen RSM P2411.1; Wu et al., 2001). The known quantity of reptile specimens from strata between early Turonian and early Campanian age is relatively low, with 2 MM specimens and 1 ROM specimen from the Assiniboine Member; none from the Morden Member; and 2 CFDC specimens, 1 MM, 1 ROM, 1 UA and 1 CMN specimen from the Boyne Member. In terms of reptilian representation from other lithostratigraphic members, a total of 68 reptilian specimens, mostly partial, postcranial elements belonging to plesiosaurs, are known from the Belle Fourche Member and 14 from the Millwood Member, mainly partial teeth, jaw elements and vertebrae belonging to mosasaurs.

Discussion and recommendations for future work

The results of this survey identified several biases, including a significant size bias between Manitoba escarpment macrovertebrate fossils and microvertebrate fossils in institution collections. The two marine vertebrate bone bed faunal assemblages of the Belle Fourche Member, the Carrot River and Bainbridge River bone beds, are the most sampled horizons of the Manitoba escarpment, yielding nearly 7000 microvertebrate fossils to date. In terms of macrovertebrate specimens, the lower Pembina Member is the most sampled unit, yielding nearly 700 macrovertebrate fossils to date. This can be problematic when examining diversity between assemblages, as uneven sampling between macro- and microvertebrate can skew paleoecological interpretations. Methods for evaluating diversity coverage of sampled microvertebrate assemblages and determining the appropriate quantity of bulk sample to collect for sufficient diversity coverage are discussed in Jamniczky et al. (2003) and Close et al. (2018). Additionally, modelling and statistical methods can be used to counter uneven sampling (e.g., Brocklehurst, 2015).

In order to offset biases in microvertebrate fossil collections, surface prospecting plus bulk sampling of microvertebrate fossil horizons from lithostratigraphic units other than the Belle Fourche Member is recommended. Processing the bulk samples by screen washing in water, or acid digestion in 10–20% acetic acid, should increase yields. In Manitoba, well-preserved microvertebrate fossil specimens have been successfully recovered from the Laurier Limestone Beds of the Keld Member (specimen MM V-2733), the Marco Calcarenite of the Assiniboine Member (specimens MM V-2555, V-2556, V-2557, V-2587), Morden Member (specimen MM V-2689), Boyne Member (specimen MM V-2520), Pembina Member (specimen MM V-2519), Millwood Member (UM Teaching Collection, specimen EPD 20020729) and have been observed but not known to be collected from the Gammon Ferruginous Member. The excellent degree of fossil preservation and 10–40% microvertebrate fossil content observed within the Marco Calcarenite near the top of the Assiniboine Member indicate its faunal assemblage would be most comparable with those of the Belle Fourche Member bone beds and would warrant further bulk sampling and acid preparation.

In addition to the unequal representation of microvertebrate fossils from the Belle Fourche Member bone beds, opportunistic collection of avian, chondrichthyan and reptilian macrovertebrate fossils from the Keld and Pembina members has resulted in the disproportionate representation of these members in institution collections relative to the other Manitoba escarpment members (Figure GS2021-6-2b). Prospecting that targets currently underrepresented lithostratigraphic members and horizons will help reduce the existing biases in institution collections and gain a truer representation of the original WIS fauna. Increasing representation of the Boyne and Millwood members in institution collections in particular would prove valuable for temporal comparisons of Manitoba escarpment faunal assemblages, and also for spatial comparisons with well-sampled coeval units from other WIS localities including the Coniacian to early Campanian Smoky Hill Chalk Member of Kansas (e.g., Shimada and Fielitz, 2006) and the mid-Campanian Bearpaw Formation of Alberta (e.g., Cook et al., 2017).

In order to conduct successful surface fossil prospecting, factors determining which lithostratigraphic unit to prospect should include known fossil content abundance, degree of fossil preservation, outcrop exposure surface area and outcrop accessibility. The lithostratigraphic members and units that meet these criteria and are currently underrepresented in institution collections are recommended for future fossil prospecting in Manitoba. They include, from oldest to youngest, the Laurier Limestone Beds (Keld Member), Assiniboine Member (including the Marco Calcarenite), Boyne Member, Gammon Ferruginous Member and Millwood Member. Donation, or providing notice, of discovered fossil specimens to an institution with a publicly accessible specimen database and equipped to properly recover in situ fossils would also help in increasing representation. Publicly accessible, roadside outcrop locations of Upper Cretaceous units in southwestern Manitoba that are available for surface prospecting are provided by Bamburak and Nicolas (2013). Fossil collection should only be undertaken with possession of a heritage permit, landowner permission and appropriate training in the collection of in situ fossils.

Conclusions

Collection biases identified in institution collections of Late Cretaceous Manitoba escarpment vertebrates include 1) opportunistic sampling and acid preparation of select microvertebrate bone beds; 2) preferred collection of semi- to fully articulated macrovertebrate specimens; and 3) dependency on economic activities to facilitate fossil collection, mainly bentonite mining within the lower Pembina Member. Due to the dominant historical collection biases of opportunistic and preferred collection of chondrichthyan and avian microvertebrate specimens from the Belle Fourche Member and reptilian and avian macrovertebrate specimens from the Pembina Member, other lithostratigraphic members and taxonomic groups are significantly underrepresented in institution collections. Overall, taxonomic classes with unequal representation in existing institution collections are chondrichthyans and avians and those with underrepresentation are actinopterygians and reptilians. Lithostratigraphic members with the most representation in institution collections, in order from highest to lowest abundance, are the Belle Fourche, Pembina and Keld members. Lithostratigraphic members with the least representation, from highest to lowest abundance, are the Assiniboine, Boyne, Millwood, Gammon Ferruginous, Morden and Odanah members. Future collection should target the Laurier Limestone Beds (Keld Member), Assiniboine Member (including the Marco Calcarenite), Boyne Member, Gammon Ferruginous Member and Millwood Member to offset historical institution collection biases. This information is crucial for a better approximation of Cretaceous vertebrate diversity and understanding the paleoecology and evolutionary changes in WIS faunas over time.

Economic considerations

Fossil collections, and the information extracted from them, provide context to the lithostratigraphic units that host them. This context includes taxonomic, climatic, geographic and temporal information critical to understanding the variability and change in the geological environments through both time and space. Fossil information provides the ability to correlate stratigraphic units globally, predict and pinpoint where economic accumulations of mineral resources are most likely to occur and, just as importantly, where they do not occur. Fossil information is important for the targeting of resources, including petroleum, bentonite, brick clay and high-calcium limestone. Fully recovered, informative and excellently preserved specimens deposited in conservation-suitable institution collections in Manitoba will ultimately benefit the province's tourism sector, the global paleontology community and the general public by protecting and showcasing examples of the province's paleontological heritage and furthering the understanding of ancient life history.

Acknowledgments

The authors thank the following curators, collection managers and museum personnel for access to collections, collection lists and their assistance: G. Young, E. Dobrzanski, R. Sanchez, B. Strilisky, A. Cuetara, E. Bamforth, R. McKellar, K. Seymour, M. Currie, S. Cumbaa and J. Mallon. Special thanks to W. Buckley for collecting, preparing and donating several exceptional fossil specimens to the Manitoba Museum so that they may be available for study.

References

Bamburak, J.D. and Nicolas, M.P.B. 2009: Revisions to the Cretaceous stratigraphic nomenclature of southwest Manitoba (parts of NTS 62F, G, H, J, K, N, O, 63C, F); *in* Report of Activities 2009, Manitoba Innovation, Energy and Mines, Manitoba Geological Survey, p. 183–192, URL <https://www.manitoba.ca/iem/geo/field/roa09pdfs/GS-19.pdf> [September 2021].

Bamburak, J.D. and Nicolas, M.P.B. 2013: Upper Cretaceous-Paleocene stratigraphy and mineral resources of southwestern Manitoba (parts of NTS 62F, G); Geological Association of Canada–Mineralogical Association of Canada, Joint Annual Meeting, May 22–24, 2013, Winnipeg, Manitoba, Field Trip Guidebook FT-A4, Manitoba Innovation, Energy and Mines, Manitoba Geological Survey, Open File OF2013-9, 42 p., URL <https://www.manitoba.ca/iem/info/libmin/gacmac/OF2013-9_FT-A4.pdf> [September 2021].

Bamburak, J.D., Hamilton, M. and Heaman, L.M. 2016: Geochronology of Late Cretaceous bentonite beds in southwestern Manitoba: 2016 update; *in* Report of Activities 2016, Manitoba Growth, Enterprise and Trade, Manitoba Geological Survey, p. 168–175, URL <https://www.manitoba.ca/iem/geo/field/roa16pdfs/GS-16.pdf> [September 2021].

Bamburak, J.D., Nicolas, M.P.B. and Hatcher, J. 2013: Radiometric dating of Late Cretaceous bentonite beds in southwestern Manitoba; *in* Report of Activities 2013, Manitoba Mineral Resources, Manitoba Geological Survey, p. 129–136, URL <https://www.manitoba.ca/iem/geo/field/roa13pdfs/GS-12.pdf> [September 2021].

Bardack, D. 1968: Fossil vertebrates from the marine Cretaceous of Manitoba; Canadian Journal of Earth Sciences, v. 5, p. 145–153.

Brocklehurst, N. 2015: A simulation-based examination of residual diversity estimates as a method of correcting for sampling bias; Palaeontologia Electronica, art. 18.3.7T, p. 1–15, URL <https://doi.org/10.26879/584>.

Christopher, J.E., Yurkowski, M., Nicolas, M.P.B. and Bamburak, J. 2006: The Cenomanian–Santonian Colorado formations of eastern southern Saskatchewan and southwestern Manitoba; *in* Saskatchewan and Northern Plains Oil & Gas Symposium 2006, C.F. Gilboy and S.G. Whittaker (ed.), Saskatchewan Geological Society, Special Publication 19, p. 299–318, URL <https://archives.datapages.com/data/sgs/2006/299/299.htm> [September 2021].

Close, R.A., Evers, S.W., Alroy, J. and Butler, R.J. 2018: How should we estimate diversity in the fossil record? Testing richness estimators using sampling-standardised discovery curves; Methods in Ecology and Evolution, v. 9, no. 6, p. 1386–1400, URL <https://doi.org/10.1111/2041-210X.12987>.

Cook, T.D., Brown, E., Ralrick, P.E. and Konishi, T. 2017: A Late Campanian euselachian assemblage from the Bearpaw Formation of Alberta, Canada: some notable range extensions; Canadian Journal of Earth Sciences, v. 54, no. 9, p. 973–980, URL <https://doi.org/10.1139/cjes-2016-0233>.

Cumbaa, S.L. and Bryant, H.N. 2001: Stratigraphic position of a Late Cretaceous (Cenomanian) bonebed, east-central Saskatchewan; *in* Summary of Investigations 2001, Volume 1, Saskatchewan Geological Survey, Saskatchewan Energy and Mines, Miscellaneous Report 2001-4.1, p. 121–124, URL <https://pubsaskdev.blob.core.windows.net/pubsask-prod/88663/88663-Cumbaa-Bryant_2001_volume1_MiscRep2001-4.1.pdf> [September 2021].

Cumbaa, S.L., Schröder-Adams, C., Day, R.G. and Phillips, A.J. 2006: Cenomanian bonebed faunas from the northeastern margin, Western Interior Seaway, Canada; *in* Late Cretaceous Vertebrates from the Western Interior, S.G. Lucas and R.M. Sullivan (ed.), New Mexico Museum of Natural History and Science, Bulletin 35, p. 139–155.

Cumbaa, S.L., Shimada, K. and Cook, T.D. 2010: Mid-Cenomanian vertebrate faunas of the Western Interior Seaway of North America and their evolutionary, paleobiogeographical, and paleoecological implications; Palaeogeography, Palaeoclimatology, Palaeoecology, v. 295, p. 199–214, URL <https://doi.org/10.1016/j.palaeo.2010.05.038>.

Cumbaa, S.L., Underwood, C.J. and Schröder-Adams, C.J. 2013: Paleoenvironments and paleoecology of the vertebrate fauna from a Late Cretaceous marine bonebed, Canada; *in* Mesozoic Fishes 5 – Global Diversity and Evolution, G. Arratia, H.-P. Schultze and M.V.H. Wilson (ed.), Verlag Dr. Friedrich Pfeil, München, Germany, p. 509–524.

Hatcher, J. and Janzic, A.-M. 2010: First occurrence of the marine crocodyliform *Terminonaris* from the Upper Cretaceous (Turonian) of Manitoba; Society of Vertebrate Paleontology 70th Anniversary Meeting, October 10–13, 2010, Pittsburgh, Pennsylvania, poster presentation.

Jamniczky, H.A., Brinkman, D.B. and Russell, A.P. 2003: Vertebrate microsite sampling: how much is enough?; Journal of Vertebrate Paleontology, v. 23, no. 4, p. 725–734, URL <https://doi.org/10.1671/1>.

McNeil, D.H. and Caldwell, W.G.E. 1981: Cretaceous rocks and their foraminifera in the Manitoba escarpment; Geological Association of Canada, Special Paper no. 21, 439 p.

Nicholls, E.L. 1989: Marine vertebrates of the Pembina Member of the Pierre Shale (Campanian, Upper Cretaceous) of Manitoba and their significance to the biogeography of the Western Interior Seaway; Ph.D. thesis, University of Calgary, Calgary, Alberta, 317 p.

Nicholls, E.L. and Russell, A.P. 1990: Paleobiogeography of the Cretaceous Western Interior Seaway of North America: the vertebrate evidence; Palaeogeography, Palaeoclimatology, Palaeoecology, v. 79, p. 149–169, URL <https://doi.org/10.1016/0031-0182(90)90110-S>.

Nielsen, K.S., Schröder-Adams, C.J., Leckie, D.A., Haggart, J.W. and Elberdak, K. 2008: Turonian to Santonian paleoenvironmental changes in the Cretaceous Western Interior Sea: the Carlile and Niobrara formations in southern Alberta and southwestern Saskatchewan, Canada; Palaeogeography, Palaeoclimatology, Palaeoecology, v. 270, p. 64–91, URL <https://doi.org/10.1016/j.palaeo.2008.08.018>.

Schröder-Adams, C.J. 2014: The Cretaceous Polar and Western Interior seas: paleoenvironmental history and paleoceanographic linkages; Sedimentary Geology, v. 301, p. 26–40, URL <https://doi.org/10.1016/j.sedgeo.2013.12.003>.

Schröder-Adams, C.J., Cumbaa, S.L., Bloch, J., Leckie, D.A., Craig, J., Seif El-Dein, S.A., Simons, D.-J. and Kenig, F. 2001: Late Cretaceous (Cenomanian to Campanian) paleoenvironmental history of the eastern Canadian margin of the Western Interior Seaway: bonebeds and anoxic events; Palaeogeography, Palaeoclimatology, Palaeoecology, v. 170, p. 261–289, URL <https://doi.org/10.1016/S0031-0182(01)00259-0>.

Shimada, K. and Fielitz, C. 2006: Annotated checklist of fossil fishes from the Smoky Hill Chalk of the Niobrara Chalk (Upper Cretaceous) in Kansas; New Mexico Museum of Natural History and Science, Bulletin 35, p. 193–213.

Underwood, C.J. and Cumbaa, S.L. 2010: Chondrichthyans from a Cenomanian (Late Cretaceous) bonebed, Saskatchewan, Canada; Palaeontology, v. 53, no. 4, p. 903–944, URL <https://doi.org/10.1111/j.1475-4983.2010.00969.x>.

Wu, X.-C., Russell, A.P. and Cumbaa, S.L. 2001: *Terminonaris* (Archosauria: Crocodyliformes): new material from Saskatchewan, Canada, and comments on its phylogenetic relationships; Journal of Vertebrate Paleontology, v. 21, no. 3, p. 492–514, URL <https://doi.org/10.1671/0272-4634(2001)021[0492:TACNMF]2.0.CO;2>.

GS2021-7

Quaternary stratigraphic and depth to bedrock data compilation for northeastern Manitoba

by T.J. Hodder and M.S. Gauthier

Summary

This project involves the compilation of all available Quaternary stratigraphic and depth to bedrock data for northeastern Manitoba. Modelling of the drift thickness using point data provides the first regional-scale overview of drift thickness of the region. Increased accessibility to Quaternary stratigraphic and depth to bedrock data will increase the effectiveness of drift prospecting approaches in this remote and thick drift covered region of Manitoba.

In Brief:

- Compilation of Quaternary stratigraphic and drift thickness data in northeastern Manitoba to facilitate drift prospecting efforts

Citation:
Hodder, T.J. and Gauthier, M.S. 2021: Quaternary stratigraphic and depth to bedrock data compilation for northeastern Manitoba; *in* Report of Activities 2021, Manitoba Agriculture and Resource Development, Manitoba Geological Survey, p. 66–70.

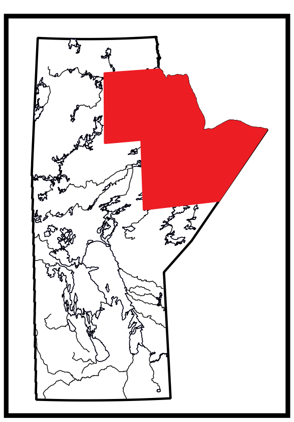

Introduction

Northeastern Manitoba contains thick Quaternary sediments, which were deposited during glacial and nonglacial periods over at least three repeated cycles (e.g., Nielsen et al., 1986; Dredge and McMartin, 2011). These sediments were first documented over 100 years ago during the pioneering work of Tyrrell (1913, 1916). Stratigraphic studies continue today, with several active Manitoba Geological Survey (MGS) projects in the region (Figure GS2021-7-1). To facilitate these investigations, a project was initiated to digitally compile all of the Quaternary stratigraphic data. The thick Quaternary sediments cover bedrock throughout most of the region, which prohibits direct observation of the bedrock geology but does offer many opportunities for drift prospecting. Effective drift prospecting approaches rely on understanding the ice-flow history and composition of glacial sediments to reconstruct dispersal patterns. The new Quaternary stratigraphic compilation helps with this. The MGS till composition studies have shown that drift thickness is a major factor to consider in drift prospecting, since thick sediments inhibit erosion of the local bedrock (e.g., Hodder et al., 2017).

To provide a regional overview of sediment thickness, this project will use the compiled stratigraphic and drillhole data to provide a working model of drift thickness in northeastern Manitoba.

Current work

Quaternary stratigraphic data compilation

The purpose of this project is to compile all existing stratigraphic data collected in the region that can be georeferenced. The majority of this data was collected from natural exposures of sediments along active rivers in the region between 1967 and 2021 (Figure GS2021-7-1). Digital compilation for each section includes

1) sediment descriptions and depth measurements;
2) ice-flow data (where available), including both till clast-fabric and lodged striated cobble and boulder measurements; and
3) sample data with depths of collection (when available), for till, geochronology and paleoenvironmental samples.

The results of this compilation will be released as part of a forthcoming MGS open file publication and will be updated as new data sources are published.

Depth to bedrock compilation

The goal of this component of the project is to produce a regional-scale depiction of the drift thickness across northeastern Manitoba. A drift thickness map has been published for the southern half of Manitoba (Keller and Matile, 2021), but is not available for the north. The remoteness of the north means that point observations of depth to bedrock are not distributed equally and are concentrated in regions of mineral exploration or where rivers have incised down to bedrock (Figure GS2021-7-2a). This data gap creates large uncertainties that are not easy to accurately model.

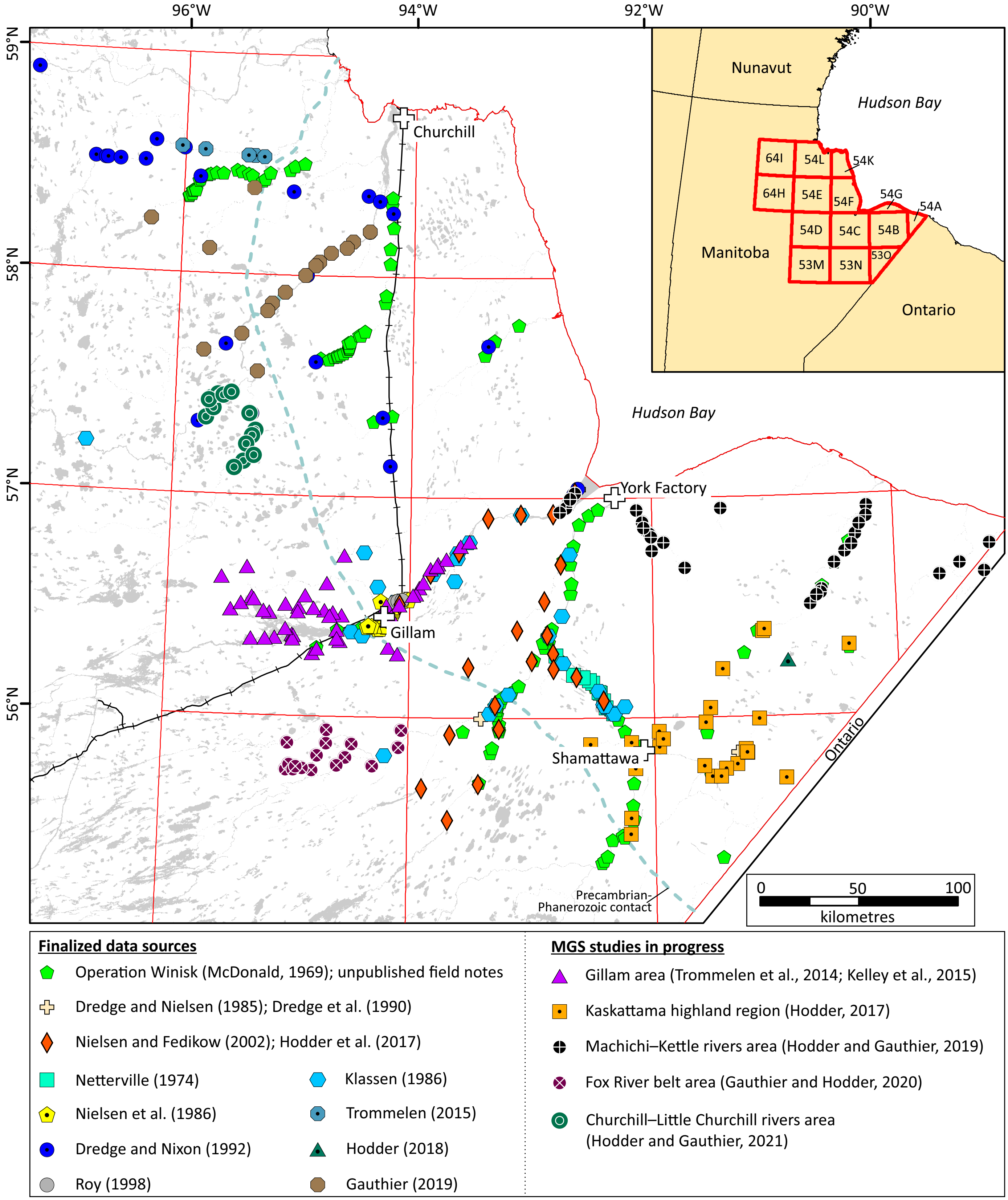

Figure GS2021-7-1: *Locations of Quaternary sections from data sources included in the compilation for northeastern Manitoba. The red lines in the upper right index figure outline the areas of the 1:250 000 scale NTS maps and correspond to the red lines on the main map. Abbreviation: MGS, Manitoba Geological Survey.*

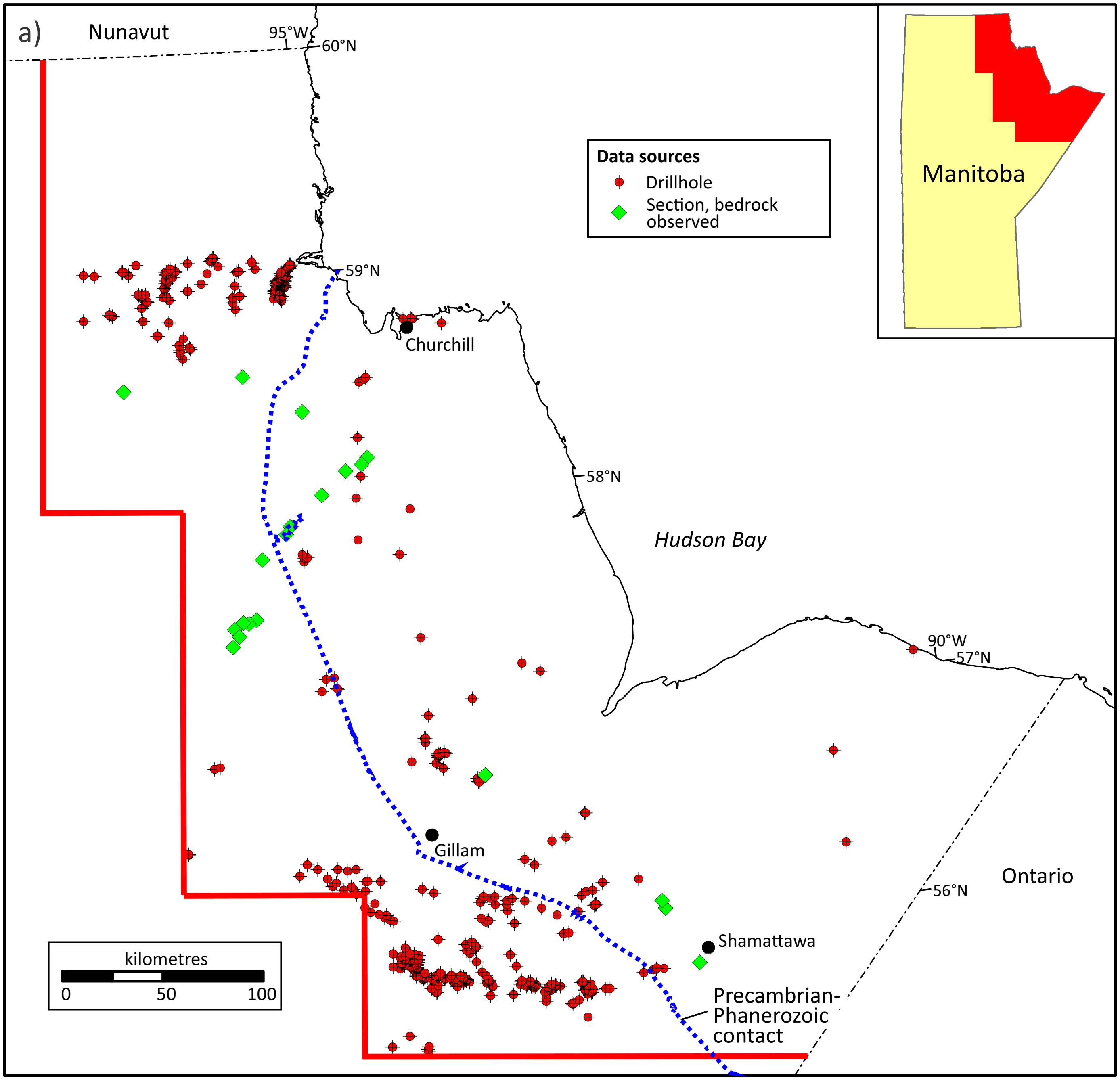

Figure GS2021-7-2: a) *Drillhole and ground-based observations are used to construct* ***b)*** *(next page) a preliminary regional model of Quaternary sediment thickness in northeastern Manitoba.*

To avoid erroneous interpolation, a raster-based approach, using a 10 by 10 km grid, was chosen (Figure GS2021-7-2b). Grid cells that do not contain drift thickness data were masked during analysis. For grid cells that contain more than one data point, the average of all the data points was calculated and assigned to the cell. All point data used to model the sediment thickness will be released as part of a forthcoming MGS open file publication.

Next step in the modelling process is to incorporate numerous sediment thickness observations, documented during fieldwork, where bedrock was not observed (Figure GS2021-7-1). These observations will provide a minimum limiting measurement of sediment thickness for the regions without drillhole coverage.

Economic considerations

The presence of thick drift across the northeastern region of Manitoba inhibits ground observation of the bedrock and increases the need for effective drift-prospecting methods. This project increases accessibility to Quaternary stratigraphic and depth to bedrock data—both critical datasets for drift exploration in the region.

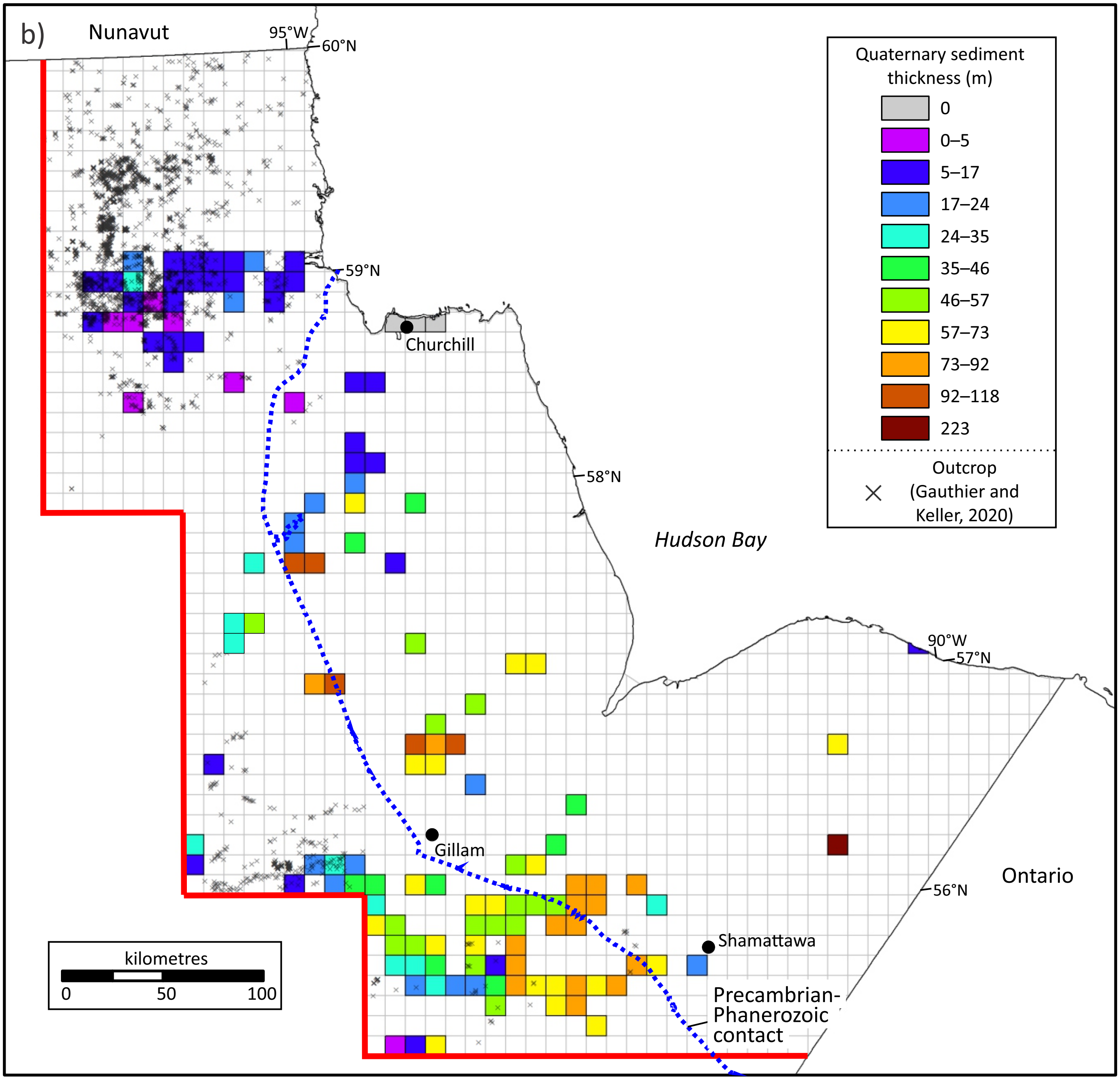

References

Dredge, L.A. and McMartin, I. 2011: Glacial stratigraphy of northern and central Manitoba; Geological Survey of Canada, Bulletin 600, 27 p.

Dredge, L.A. and Nielsen, E. 1985: Glacial and interglacial deposits in the Hudson Bay Lowlands: a summary of sites in Manitoba; *in* Current Research, Geological Survey of Canada, Paper 85-1A, p. 247–257.

Dredge, L.A. and Nixon, F.M. 1992: Glacial and environmental geology of northeastern Manitoba; Geological Survey of Canada, Memoir 432, 80 p.

Dredge, L.A., Morgan, A.V. and Nielsen, E. 1990: Sangamon and pre-Sangamon interglaciations in the Hudson Bay Lowlands of Manitoba; Geographie Physique et Quaternaire, v. 44, no. 3, p. 319–336.

Gauthier, M.S. 2019: Till composition, stratigraphy, ice-flow indicator data and glacial history of the North Knife River–Churchill River region, Manitoba (parts of NTS 54L, 64I); Manitoba Agriculture and Resource Development, Manitoba Geological Survey, Geoscientific Paper GP2019-1, 41 p., URL <https://www.manitoba.ca/iem/info/libmin/GP2019-1.zip> [October 2021].

Gauthier, M.S. and Hodder, T.J. 2020: Surficial geology mapping and till composition of the western Fox River greenstone belt area, northeastern Manitoba (NTS 53M15, 16); *in* Report of Activities 2020, Manitoba Agriculture and Resource Development, Manitoba Geological Survey, p. 47–54, URL <https://www.manitoba.ca/iem/geo/field/roa20pdfs/GS2020-7.pdf> [October 2021].

Gauthier, M.S. and Keller, G.R. 2020: Digital compilation of surficial point and line features for Manitoba: datasets; Manitoba Agriculture and Resource Development, Manitoba Geological Survey, Open File OF2020-1, 7 p., URL <https://www.manitoba.ca/iem/info/libmin/OF2020-1.zip> [October 2021].

Hodder, T.J. 2017: Quaternary stratigraphy and till sampling in the Kaskattama highland region, northeastern Manitoba (parts of NTS 53N, O, 54B, C): year two; *in* Report of Activities 2017, Manitoba Growth, Enterprise and Trade, Manitoba Geological Survey, p. 205–214, URL <https://www.manitoba.ca/iem/geo/field/roa17pdfs/GS2017-18.pdf> [October 2021].

Hodder, T.J. 2018: Till composition of the Kaskattama Kimberlite No. 1 drillcore, Kaskattama highland region, northeastern Manitoba (part of NTS 54B7); *in* Report of Activities 2018, Manitoba Growth, Enterprise and Trade, Manitoba Geological Survey, p. 166–174, URL <https://www.manitoba.ca/iem/geo/field/roa18pdfs/GS2018-14.pdf> [October 2021].

Hodder, T.J. and Gauthier, M.S. 2019: Quaternary stratigraphy and till sampling in the Machichi–Kettle rivers area, far northeastern Manitoba (parts of NTS 54A–C); *in* Report of Activities 2019, Manitoba Agriculture and Resource Development, Manitoba Geological Survey, p. 83–89, URL <https://www.manitoba.ca/iem/geo/field/roa19pdfs/GS2019-9.pdf> [October 2021].

Hodder, T.J. and Gauthier, M.S. 2021: Quaternary stratigraphy in the Churchill–Little Churchill rivers area, northeastern Manitoba (part of NTS 54E); *in* Report of Activities 2021, Manitoba Agriculture and Resource Development, Manitoba Geological Survey, p. 85–88, URL <https://www.manitoba.ca/iem/geo/field/roa21pdfs/GS2021-10.pdf> [November 2021].

Hodder, T.J., Gauthier, M.S. and Nielsen, E. 2017: Quaternary stratigraphy and till composition along the Hayes, Gods, Nelson, Fox, Stupart, Yakaw, Angling and Pennycutaway rivers, northeast Manitoba (parts of NTS 53N, 54C, 54D, 54F); Manitoba Growth, Enterprise and Trade, Manitoba Geological Survey, Open File OF2017-4, 20 p., URL <https://www.manitoba.ca/iem/info/libmin/OF2017-4.zip> [October 2021].

Keller, G.R. and Matile, G.L.D. 2021: Drift thickness of southern Manitoba; Manitoba Agriculture and Resource Development, Manitoba Geological Survey, Geoscientific Map MAP2021-2, scale 1:1 000 000, URL <https://www.manitoba.ca/iem/info/libmin/MAP2021-2.pdf> [October 2021].

Kelley, S.E., Hodder, T.J., Wang, Y., Trommelen, M.S. and Ross, M. 2015: Preliminary Quaternary geology in the Gillam area, northeastern Manitoba – year 3 (parts of NTS 54D5-9, 11, 54C12); *in* Report of Activities 2015, Manitoba Mineral Resources, Manitoba Geological Survey, p. 131–139, URL <https://www.manitoba.ca/iem/geo/field/roa15pdfs/GS-12.pdf> [October 2021].

Klassen, R.W. 1986: Surficial geology of north-central Manitoba; Geological Survey of Canada, Memoir 419, 57 p.

McDonald, B.C. 1969: Glacial and interglacial stratigraphy, Hudson Bay Lowland; *in* Earth Science Symposium on Hudson Bay, P.J. Hood (ed.), Geological Survey of Canada, Paper 68-83, p. 78–99.

Netterville, J.A. 1974: Quaternary stratigraphy of the lower Gods River region, Hudson Bay lowlands, Manitoba; M.Sc. thesis, University of Calgary, Calgary, Alberta, 79 p.

Nielsen, E. and Fedikow, M.A.F. 2002: Kimberlite indicator mineral surveys, lower Hayes River; Manitoba Industry, Trade and Mines, Manitoba Geological Survey, Geological Paper GP2002-1, 39 p., URL <https://www.manitoba.ca/iem/info/libmin/GP2002-1.zip> [October 2021].

Nielsen, E., Morgan, A.V., Morgan, A., Mott, R.J., Rutter, N.W. and Causse, C. 1986: Stratigraphy, paleoecology and glacial history of the Gillam area, Manitoba; Canadian Journal of Earth Sciences, v. 23, p. 1641–1661.

Roy, M. 1998: Pleistocene stratigraphy of the lower Nelson River area - implications for the evolution of the Hudson Bay lowland of Manitoba, Canada; M.Sc. thesis, University of Quebec, Montreal, Quebec, 220 p.

Trommelen, M.S. 2015: Surficial geology, till composition and ice-flow indicator data, Seal River–North Knife River area, Manitoba (parts of NTS 54L, M, 64I, P); Manitoba Mineral Resources, Manitoba Geological Survey, Geoscientific Paper GP2013-2, 27 p., URL <https://www.manitoba.ca/iem/info/libmin/GP2013-2.zip> [October 2021].

Trommelen, M.S., Wang, Y. and Ross, M. 2014: Preliminary Quaternary geology in the Gillam area, northeastern Manitoba (parts of NTS 54D5–11, 54C12) – year two; *in* Report of Activities 2014, Manitoba Mineral Resources, Manitoba Geological Survey, p. 187–195, URL <https://www.manitoba.ca/iem/geo/field/roa14pdfs/GS-17.pdf> [October 2021].

Tyrrell, J.B. 1913: Hudson Bay exploring expedition 1912; Ontario Bureau of Mines, Twenty-Second Annual Report, v. 22, pt. 1, p. 161–209.

Tyrrell, J.B. 1916: Notes on the geology of Nelson and Hayes rivers; Proceedings and Transactions of the Royal Society of Canada, v. 10, sec. 4, p. 1–27.

GS2021-8

Stratigraphic, paleoenvironmental and geochronological investigations of intertill nonglacial deposits in northeastern Manitoba (parts of NTS 54B–F, K, L, 64A, H, I)

by M.S. Gauthier, T.J. Hodder, O.B. Lian[1], S.A. Finkelstein[2], A.S. Dalton[3] and R.C. Paulen[4]

In Brief:

- New collaboration on the Quaternary stratigraphy in the Hudson Bay Lowland
- Field data will be enhanced by paleo-botantical data and optical dating

Citation:
Gauthier, M.S., Hodder, T.J., Lian, O.B., Finkelstein, S.A., Dalton, A.S. and Paulen, R.C. 2021: Stratigraphic, paleoenvironmental and geochronological investigations of intertill nonglacial deposits in northeastern Manitoba (parts of NTS 54B–F, K, L, 64A, H, I); *in* Report of Activities 2021, Manitoba Agriculture and Resource Development, Manitoba Geological Survey, p. 71–76.

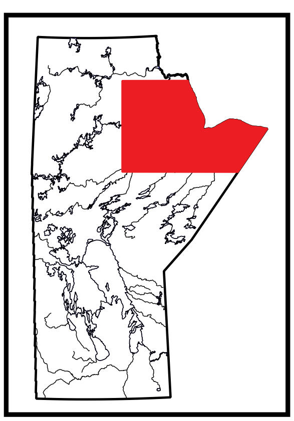

Summary

The Manitoba Geological Survey has embarked on a new collaborative study to advance the Quaternary stratigraphic framework in the Hudson Bay Lowland, an area which is critical for understanding the patterns of North American glaciation. This study uses a multiproxy approach to facilitate correlations, two of which include the age and paleoenvironment of intertill nonglacial sediments. This work endeavours to establish a better understanding of the surface and subsurface geology throughout the Hudson Bay Lowland, and advance exploration methods in the study area and other similar regions draped by thick Quaternary sediments.

Introduction

The Quaternary landscape of the Hudson Bay Lowland (HBL) in Manitoba is complex. This area has unique access to numerous sections that expose multiple till sequences interbedded with nonglacial sediments (Figure GS2021-8-1). There are thick till sections (5 to 40 m) that are not easily differentiated into stratigraphic units. Fieldwork between 2013 and 2021 demonstrates that stratigraphic sections in the Manitoba HBL expose a patchy mosaic of sediments that is variable in both space (horizontal) and time (vertical up-section; Trommelen, 2013; Trommelen et al., 2014; Kelley et al., 2015; Hodder and Kelley, 2016; Hodder, 2017; Gauthier et al., 2019; Hodder and Gauthier, 2019). The patchy stratigraphic mosaic means that the development of a regional stratigraphic framework is difficult, since observations at one section may not correlate to those at an adjacent section in a traditional and continuous 'layer cake' model (Gauthier et al., 2016; Wang, 2018). It also means that drift exploration is more complex than previously thought. The objective of this study is to develop a robust stratigraphic framework, using a multiproxy approach to facilitate correlations. Two proxies include the age and paleoenvironment of intertill nonglacial sediments. Intertill nonglacial deposits are spatially restricted, but when combined with an extensive till dataset (provenance, ice-flow direction), these stratigraphic horizons are integral to facilitating stratigraphic correlations.

Background

Intertill nonglacial sediments

Nonglacial-sorted sediments in northeastern Manitoba have been separated from glacial sediments based on the presence of organic material. Organic-rich intertill sorted sediments were then assigned a relative age of deposition pertaining to either an interglacial or interstadial period (Netterville, 1974; Dredge et al., 1990; Dredge and McMartin, 2011). Interglacial refers to a prolonged period of mild climate between two glacial periods, when the HBL was ice free and likely vegetated similar to present day (e.g., Marine Isotope Stage [MIS] 5). In contrast, interstadial refers to a minor period of less cold climate during a glacial period, when the HBL was ice free but temperatures were cooler than present day (e.g., MIS 3). Problematically, previous researchers have ascribed contrasting interpretations of subtill glacial, interglacial or interstadial to the same sediments (Netterville, 1974; Dredge et al., 1990; Dredge and McMartin, 2011). These stratigraphic issues, compounded with issues in dating these nonglacial sediments, have made it extremely

[1] University of the Fraser Valley, 33844 King Road, Abbotsford, British Columbia V2S 7M8
[2] Department of Earth Sciences, University of Toronto, 27 King's College Circle, Toronto, Ontario M5S 1A1
[3] Department of Physical Geography and Geoecology, Charles University, Opletalova 38, 110 00 Staré Město, Prague, Czech Republic
[4] Natural Resources Canada, Geological Survey of Canada, 601 Booth Street, Ottawa, Ontario K1A 0G1

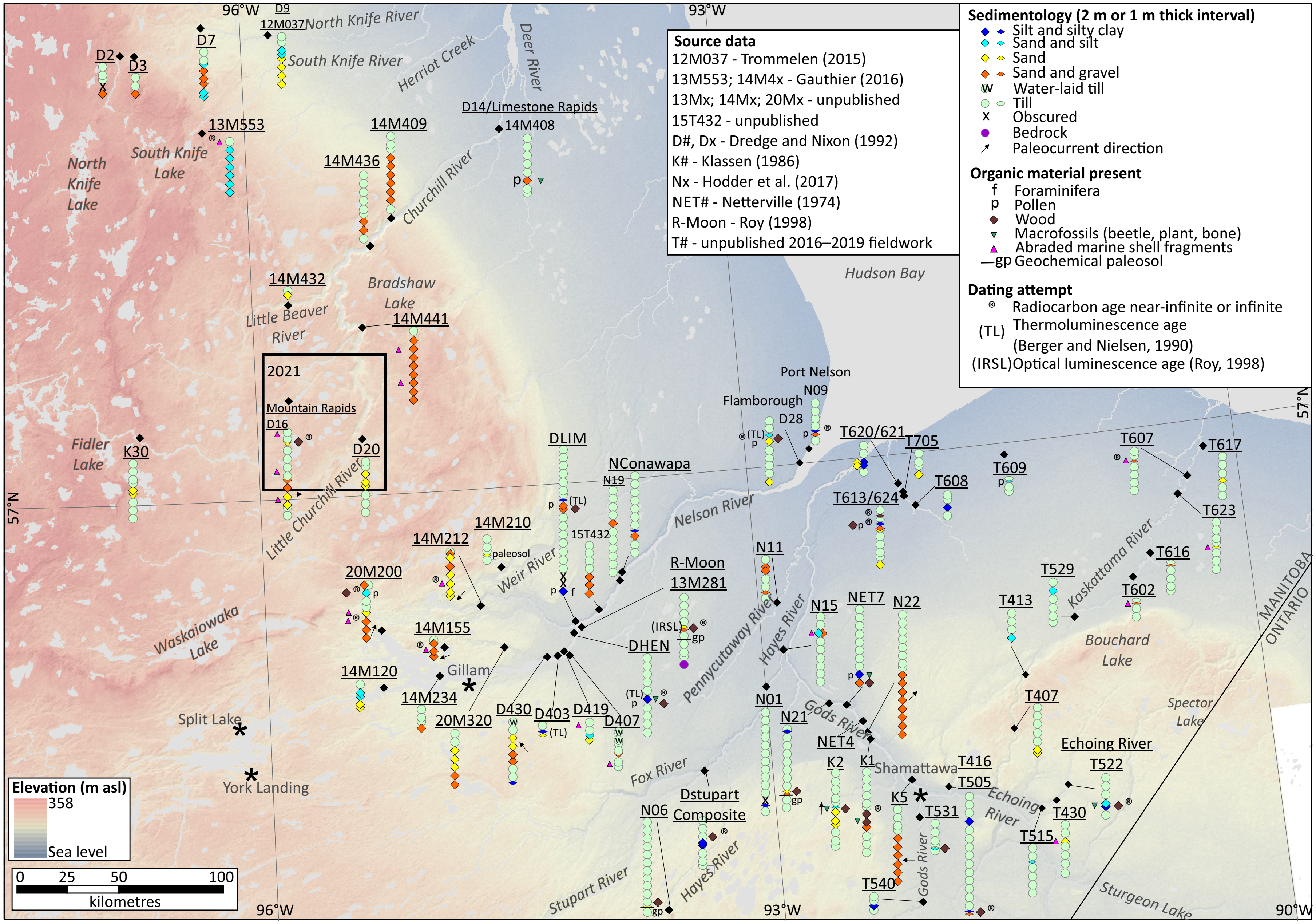

***Figure GS2021-8-1:** Map of known sites with intertill nonglacial sediments in northeastern Manitoba, together with a summary of the different data from analyses of those sediments (Netterville, 1974; Klassen, 1986; Dredge and Nixon, 1992; Roy, 1998; Trommelen, 2015; Gauthier, 2016; Hodder and Gauthier, 2017; unpublished Manitoba Geological Survey [MGS] data). Area of MGS fieldwork in 2021 indicated by black outlined box (Hodder and Gauthier, 2021). Background hillshade image was generated using Canadian Digital Surface Model (Natural Resources Canada, 2015).*

difficult to establish a regional stratigraphic framework for the HBL. Hence, a better understanding of the depositional environment(s) of these deposits is essential to determine the chronology of the nonglacial periods within the stratigraphic record.

Within the study area, there are nonglacial-sorted sediments deposited within fluvial, lacustrine, terrestrial and marine environments (McDonald, 1968; Netterville, 1974; Nielsen et al., 1986; Dredge et al., 1990). Organics within these sediments have been dated as nonfinite using radiocarbon (>50 000 ^{14}C years; compiled within Gauthier, 2021). Unfortunately, organic-bearing units are not laterally extensive and can pinch-out to organic-barren units or disappear entirely (eroded or not deposited) within a single section, which makes correlation between multiple exposures difficult (Figure GS2021-8-2). Previously mapped nonglacial sediments are situated at different elevations and contain paleoecological evidence for different depositional environments (Nielsen et al., 1986; Dredge et al., 1990; Roy, 1998). Despite these differences, all 'upper' organic-bearing nonglacial sediments have been correlated as one unit, and termed the Nelson River sediments (Nielsen et al., 1986) or the Gods River sediments (Netterville, 1974; Klassen, 1986). To the east in Ontario, most nonglacial sediments were similarly lumped into the Missinaibi Formation (Terasmae and Hughes, 1960; Skinner, 1973; Dalton et al., 2016). A second deeper nonglacial unit, interpreted as older than MIS

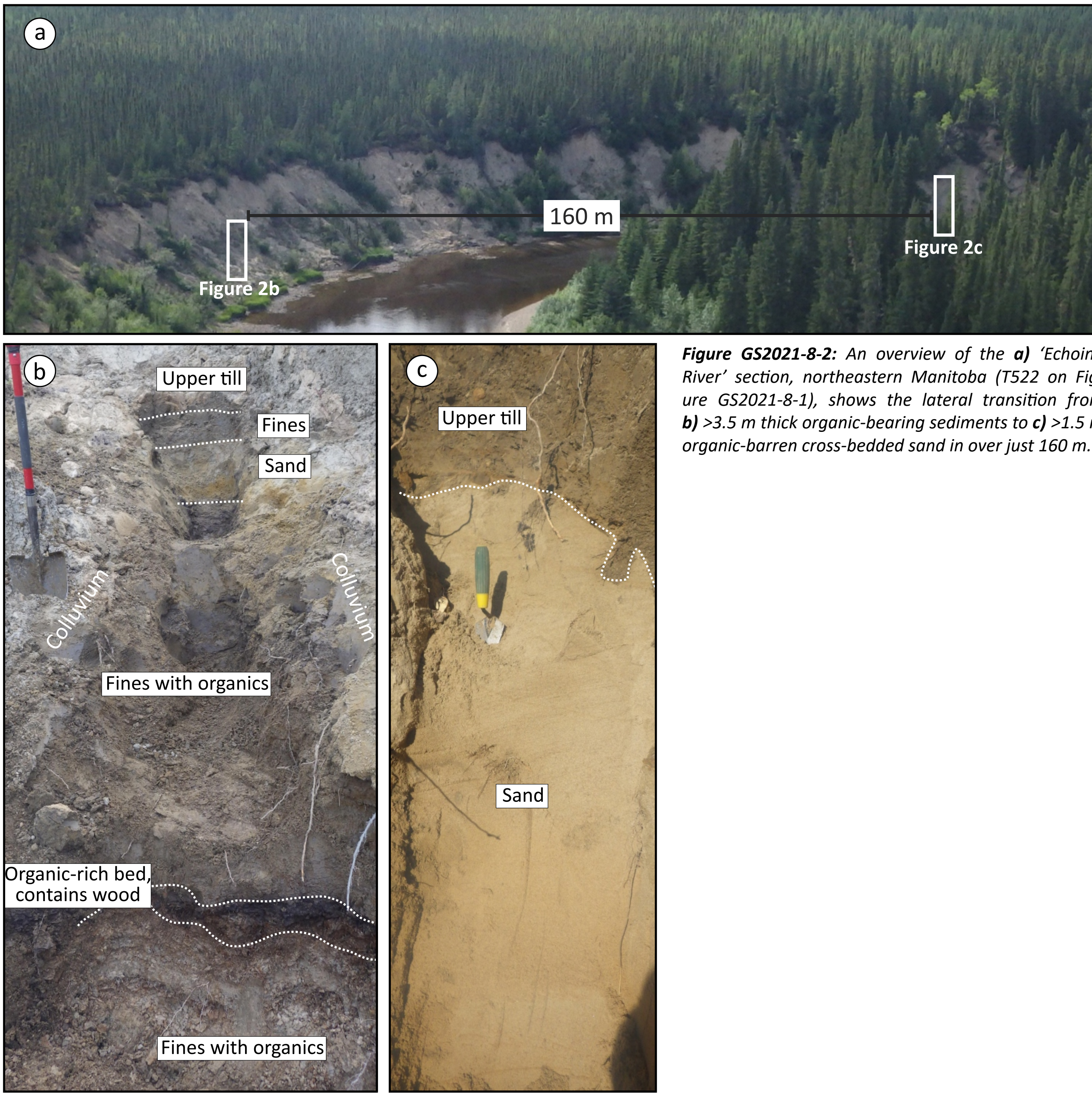

Figure GS2021-8-2: *An overview of the* ***a)*** *'Echoing River' section, northeastern Manitoba (T522 on Figure GS2021-8-1), shows the lateral transition from* ***b)*** *>3.5 m thick organic-bearing sediments to* ***c)*** *>1.5 m organic-barren cross-bedded sand in over just 160 m.*

5, was noted near Gillam along the Nelson River (section DLIM; Figure GS2021-8-1) and correlated to a paleosol developed on the lowermost till at a nearby section (Nielsen et al., 1986).

Confirming the presence of multiple different nonglacial units, Manitoba Geological Survey fieldwork in 2019 and 2021 identified additional stratigraphic sections with two subtill organic-bearing units (Figure GS2021-8-1; Hodder et al., 2020; Hodder and Gauthier, 2021). The danger of correlating nonglacial units based on stratigraphy at any one site is highlighted in eastern James Bay, Ontario, where nonglacial sediments beneath till from two different river sections were dated, using optically stimulated luminescence methods, to MIS 5e and MIS 7 (Dube-Loubert et al., 2013). Only one nonglacial unit was documented at any one section, and lumping would have erroneously assumed the units were both MIS 5e. Ongoing till-stratigraphy reconstructions support the separation of nonglacial units, as work along the Machichi and Nelson rivers has identified three or four different organic-bearing subtill units (Hodder et al., 2020).

Age determination of intertill nonglacial sediments is inherently difficult, since organic matter within these sediments is either at or beyond the ~<50 000 year limit of radiocarbon dating. Laboratory measurements near this limit need to be approached cautiously, because a small amount of contamination can have significant deleterious effects on the age determined (Reyes et al., 2020). For example, the amount of original radiocarbon used for age estimation in samples >40 ka is <1% of the initial total and is extremely sensitive to contamination during burial, sampling or laboratory processing (Pigati et al., 2007). Optical dating, in this case optically stimulated luminescence (OSL) dating, has a longer accepted age range. For quartz, ages from a few decades to about 100 ka can be achieved when the environmental dose rate is typical (approx. 1–3 grays per thousand years [Gy/ka]) and dose-response data are represented by a saturating exponential function, which is usually the case. In some cases, however, where environmental dose rates are low and/or the dose-response data are represented by an exponential plus linear function, samples as old as ~300 ka can be dated (e.g., see review by Wintle, 2008). The luminescence signal from K-feldspar (the other preferred mineral for optical dating) saturates at higher doses, which means that higher age values can be achieved. However, K-feldspar suffers from so-called anomalous fading, which results in age values that underestimate samples' true ages. For samples with linear dose responses, age values can be corrected for anomalous fading, but this usually restricts the use of K-feldspar to samples younger than ~50 ka (e.g., Lian and Roberts, 2006). It is possible to entirely, or at least partially, circumvent the malign effect of anomalous fading by using different luminescence signals from K-feldspar. Unfortunately, these signals have been found to bleach (reset) much more slowly than those traditionally used, which usually means they can only be applied to sediments that received extended exposure to direct sunlight before burial (e.g., Li et al., 2014). The two past attempts to date nonglacial Manitoban samples by luminescence have been only partly successful, as the accuracy of the Berger and Nielsen (1990) ages were questioned by Roy (1998) due to inappropriate pre-heat treatment and anomalous fading.

Methods

New data from the northeastern Manitoba intertill nonglacial beds (Figure GS2021-8-1) will help determine whether paleoenvironmental data and optical dating can be used to differentiate organic-bearing nonglacial units that were deposited during different interglacial or interstadial periods. Pollen, nonpollen palynomorphs and plant macroremains are often present, with varying degrees of preservation, in the organic-bearing sediments. These paleobotanical remains are being used to reconstruct paleoenvironments. Quantitative estimates of paleotemperature and paleoprecipitation derived from pollen assemblages can also contribute to discussions around age assignments (see Dalton et al., 2017). New optical dating of subtill sands will test the ability of this method to date these sediments.

Economic considerations

This work will help to reconcile the stratigraphy of glacial sediments, enabling better identification of exploration vectors of economic interest in the multitill, thick drift of the HBL and similar regions elsewhere.

Acknowledgments

This research is funded by the Manitoba Geological Survey and the Geological Survey of Canada's Geo-mapping for Energy and Minerals program (GEM-GeoNorth). O.B. Lian acknowledges funding support from Discovery grants and Research Tools and Instruments grants from the Natural Science and Engineering Research Council of Canada (NSERC). This report has benefited from internal reviews by C. Bohm, M. Nicholas and A. Plouffe.

Natural Resources Canada, Lands and Minerals Sector contribution 20210307

References

Berger, G.W. and Nielsen, E. 1990: Evidence from thermoluminescence dating for Middle Wisconsinan deglaciation in the Hudson Bay Lowland of Manitoba; Canadian Journal of Earth Sciences, v. 28, p. 240–249.

Dalton, A.S., Finkelstein, S.A., Barnett, P.J. and Forman, S.L. 2016: Constraining the Late Pleistocene history of the Laurentide Ice Sheet by dating the Missinaibi Formation, Hudson Bay Lowlands, Canada; Quaternary Science Reviews, v. 146, p. 288–299, URL <https://doi.org/10.1016/j.quascirev.2016.06.015>.

Dalton, A.S., Valiranta, M., Barnett, P.J. and Finkelstein, S.A. 2017: Pollen and macrofossil-inferred palaeoclimate at the Ridge Site, Hudson Bay Lowlands, Canada: evidence for a dry climate and significant recession of the Laurentide Ice Sheet during Marine Isotope Stage 3; Boreas, v. 46, p. 388–401, URL <https://doi.org/10.1111/bor.12218>.

Dredge, L.A. and McMartin, I. 2011: Glacial stratigraphy of northern and central Manitoba; Geological Survey of Canada, Bulletin 600, 27 p.

Dredge, L.A. and Nixon, F.M. 1992: Glacial and environmental geology of northeastern Manitoba; Geological Survey of Canada, Memoir 432, 80 p.

Dredge, L.A., Morgan, A.V. and Nielsen, E. 1990: Sangamon and pre-Sangamon interglaciations in the Hudson Bay Lowlands of Manitoba; Geographie Physique et Quaternaire, v. 44, no. 3, p. 319–336.

Dube-Loubert, H., Roy, M., Allard, G. and Veillette, J.J. 2013: Glacial and nonglacial events in the eastern James Bay lowlands, Canada; Canadian Journal of Earth Sciences, v. 50, p. 379–396.

Gauthier, M.S. 2016: Postglacial lacustrine and marine deposits, far northeastern Manitoba (parts of NTS 54E, L, M, 64I, P); Manitoba Mineral Resources, Manitoba Geological Survey, Geological Paper GP2015-1, 37 p. plus 4 appendices, URL <https://www.manitoba.ca/iem/info/libmin/GP2015-1.zip> [October 2021].

Gauthier, M.S. 2021: Manitoba radiocarbon ages: update; Manitoba Agriculture and Resource Development, Manitoba Geological Survey, Open File OF2021-1, 7 p. plus 2 appendices, URL <https://www.manitoba.ca/iem/info/libmin/OF2021-1.zip> [October 2021].

Gauthier, M.S., Hodder, T.J., Kelley, S.E., Wang, Y. and Ross, M. 2016: Drift exploration techniques in the Gillam area - year 4 (NTS 54D, 54C); Manitoba Growth, Enterprise and Trade, Manitoba Geological Survey, Manitoba Mining and Minerals Convention, November 15–17, 2012, Winnipeg, Manitoba, poster presentation.

Gauthier, M.S., Hodder, T.J., Ross, M., Kelley, S.E., Rochester, A. and McCausland, P. 2019: The subglacial mosaic of the Laurentide Ice Sheet; a study of the interior region of southwestern Hudson Bay; Quaternary Science Reviews, v. 214, p. 1–27, URL <https://doi.org/10.1016/j.quascirev.2019.04.015>.

Hodder, T.J. 2017: Quaternary stratigraphy and till sampling in the Kaskattama highland region, northeastern Manitoba (parts of NTS 53N, O, 54B, C) – year 2; *in* Report of Activities 2017, Manitoba Growth, Enterprise and Trade, Manitoba Geological Survey, p. 205–214, URL <https://www.manitoba.ca/iem/geo/field/roa17pdfs/GS2017-18.pdf> [September 2021].

Hodder, T.J. and Gauthier, M.S. 2017: Till composition in the Hayes River area, Hudson Bay Lowland, northeast Manitoba; Manitoba Growth, Enterprise and Trade, Manitoba Geological Survey, Manitoba Mining and Minerals Convention 2017, November 15–17, 2017, Winnipeg, Manitoba, poster presentation.

Hodder, T.J. and Gauthier, M.S. 2019: Quaternary stratigraphy and till sampling in the Machichi–Kettle rivers area, far northeastern Manitoba (parts of NTS 54A–C); *in* Report of Activities 2019, Manitoba Agriculture and Resource Development, Manitoba Geological Survey, URL <https://www.manitoba.ca/iem/geo/field/roa19pdfs/GS2019-9.pdf> [September 2021].

Hodder, T.J. and Gauthier, M.S. 2021: Quaternary stratigraphy in the Churchill–Little Churchill rivers area, northeastern Manitoba (part of NTS 54E); *in* Report of Activities 2021, Manitoba Agriculture and Resource Development, Manitoba Geological Survey, p. 85–88, URL <https://www.manitoba.ca/iem/geo/field/roa21pdfs/GS2021-10.pdf> [November 2021].

Hodder, T.J. and Kelley, S.E. 2016: Quaternary stratigraphy and till sampling in the Kaskattama highland region, northeastern Manitoba (parts of NTS 53N, O, 54B, C); *in* Report of Activities 2016, Manitoba Growth, Enterprise and Trade, Manitoba Geological Survey, p. 187–195, URL <https://www.manitoba.ca/iem/geo/field/roa16pdfs/GS-19.pdf> [September 2021].

Hodder, T.J., Gauthier, M.S. and Nielsen, E. 2017: Quaternary stratigraphy and till composition along the Hayes, Gods, Nelson, Fox, Stupart, Yakaw, Angling and Pennycutaway rivers, northeast Manitoba (parts of NTS 53N, 54C, 54D, 54F); Manitoba Growth, Enterprise and Trade, Manitoba Geological Survey, Open File OF2017-4, 20 p., URL <https://www.manitoba.ca/iem/info/libmin/OF2017-4.zip> [October 2021].

Hodder, T.J., Gauthier, M.S. and Ross, M. 2020: Deciphering the exceptional Quaternary stratigraphic record of southwest Hudson Bay, Canada; Geological Society of America, GSA 2020 Connects Online, October 29, 2020, Abstracts with Programs, v. 52, URL <https://doi.org/10.1130/abs/2020AM-352972>.

Kelley, S.E., Hodder, T.J., Wang, Y., Trommelen, M.S. and Ross, M. 2015: Preliminary Quaternary geology in the Gillam area, northeastern Manitoba – year 3 (parts of NTS 54D5–9, 11, 54C12); *in* Report of Activities 2015, Manitoba Mineral Resources, Manitoba Geological Survey, p. 131–139, URL <https://www.manitoba.ca/iem/geo/field/roa15pdfs/GS-12.pdf> [September 2020].

Klassen, R.W. 1986: Surficial geology of north-central Manitoba; Geological Survey of Canada, Memoir 419, 57 p.

Li, B., Jacobs, Z., Roberts, R.G. and Li, S.-H. 2014: Review and assessment of the potential of post-IR IRSL dating methods to circumvent the problem of anomalous fading in feldspar luminescence; Geochronometria, v. 41, p. 178–201, URL <https://doi.org/10.2478/s13386-013-0160-3>.

Lian, O.B. and Roberts, R.G. 2006: Dating the Quaternary; progress in luminescence dating of sediments; Quaternary Science Reviews, v. 35, p. 2449–2468, URL <https://doi.org/10.1016/j.quascirev.2005.11.013>.

McDonald, B.C. 1968: Glacial and interglacial stratigraphy, Hudson Bay Lowland; *in* Earth Science Symposium on Hudson Bay, P.J. Hood (ed.), Geological Survey of Canada, Paper 68-53, p. 78–99.

Netterville, J.A. 1974: Quaternary stratigraphy of the lower Gods River region, Hudson Bay lowlands, Manitoba; M.Sc. thesis, University of Calgary, Calgary, Alberta, 79 p.

Nielsen, E., Morgan, A.V., Morgan, A., Mott, R.J., Rutter, N.W. and Causse, C. 1986: Stratigraphy, paleoecology and glacial history of the Gillam area, Manitoba; Canadian Journal of Earth Sciences, v. 23, p. 1641–1661.

Pigati, J., Quade, J., Wilson, J., Jull, A.J.T. and Lifton, N.A. 2007: Development of low background vacuum extraction and graphitization systems for ^{14}C dating of old (40–60 ka) samples; Quaternary International, v. 166, p. 4–14.

Reyes, A.V., Dillman, T., Kennedy, K., Froese, D., Beaudoin, A.B. and Paulen, R.C. 2020: Legacy radiocarbon ages and the MIS 3 dating game: a cautionary tale from re-dating of pre-LGM sites in western Canada; Geological Society of America, GSA 2020 Connects Online, October 27, 2020, Abstracts with Programs, v. 52, URL <https://doi.org/10.1130/abs/2020AM-360064>.

Roy, M. 1998: Pleistocene stratigraphy of the lower Nelson River area-implications for the evolution of the Hudson Bay Lowland of Manitoba, Canada; M.Sc. thesis, University of Quebec, Montreal, Quebec, 220 p.

Skinner, R.G. 1973: Quaternary stratigraphy of the Moose River Basin, Ontario; Geological Survey of Canada, Bulletin 225, 77 p.

Terasmae, J. and Hughes, O.L. 1960: A palynological and geological study of Pleistocene deposits in the James Bay Lowlands, Ontario; Geological Survey of Canada, Bulletin 62, 15 p.

Trommelen, M.S. 2013: Preliminary Quaternary geology in the Gillam area, northeastern Manitoba (parts of NTS 54D5–9, 11, 54C12); *in* Report of Activities 2013, Manitoba Mineral Resources, Manitoba Geological Survey, p. 169–182, URL <https://www.manitoba.ca/iem/geo/field/roa13pdfs/GS-16.pdf> [September 2020].

Trommelen, M.S. 2015: Surficial geology, till composition, stratigraphy and ice-flow indicator data, Seal River–North Knife River area, Manitoba (parts of NTS 54L, M, 64I, P); Manitoba Mineral Resources, Manitoba Geological Survey, Geoscientific Paper GP2013-2, 27 p. plus 11 appendices, URL <https://www.manitoba.ca/iem/info/libmin/GP2013-2.zip> [October 2021].

Trommelen, M.S., Wang, Y. and Ross, M. 2014: Preliminary Quaternary geology in the Gillam area, northeastern Manitoba (parts of NTS 54D5–11, 54C12) – year two; *in* Report of Activities 2014, Manitoba Mineral Resources, Manitoba Geological Survey, p. 187–195, URL <https://www.manitoba.ca/iem/geo/field/roa14pdfs/GS-17.pdf> [September 2020].

Wang, Y. 2018: Statistical analysis of till geochemistry in the Nelson River area, northeastern Manitoba: implications for Quaternary glacial stratigraphy; M.Sc. thesis, University of Waterloo, Waterloo, Ontario, 175 p.

Wintle, A.G. 2008: Luminescence dating: where it has been and where it is going; Boreas, v. 37, no. 4, p. 471–482, URL <https://doi.org/10.1111/j.1502-3885.2008.00059.x>.

GS2021-9

Kimberlite-indicator-mineral results from till sampled in the Machichi–Kettle rivers area, far northeastern Manitoba (parts of NTS 54A–C)

by T.J. Hodder and M.S. Gauthier

In Brief:

- Results of a kimberlite-indicator-mineral survey in far northeastern Manitoba
- Highest KIM yields deposited by till interpreted to be deposited by NW-trending ice-flow

Citation:
Hodder, T.J. and Gauthier, M.S. 2021: Kimberlite-indicator-mineral results from till sampled in the Machichi–Kettle rivers area, far northeastern Manitoba (parts of NTS 54A–C); *in* Report of Activities 2021, Manitoba Agriculture and Resource Development, Manitoba Geological Survey, p. 77–83.

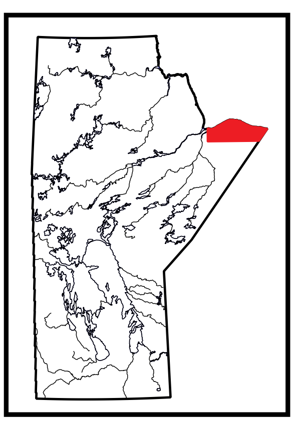

Summary

This report presents the results of a kimberlite-indicator-mineral (KIM) survey in a remote region of northeastern Manitoba. Natural exposures along waterways in the region were used to describe the stratigraphy of Quaternary sediments and sample till for KIM analysis. Stratigraphic observations, including paleo–ice-flow data, allowed for an interpretation of the provenance of KIM minerals recovered from the till. The highest KIM recovery was from the southern extent of the survey on the Kaskattama River. At sites investigated in this region, the upper till had the highest proportion of KIMs and is interpreted to have been deposited by northwest-trending ice flow, indicating a possible source to the southeast. This interpretation is being tested using additional till-provenance parameters.

Introduction

The Manitoba Geological Survey (MGS) conducted Quaternary geology fieldwork in the Machichi–Kettle rivers area of far northeastern Manitoba during the summer of 2019 (Hodder and Gauthier, 2019; Figure GS2021-9-1). This remote region of northeastern Manitoba is covered by thick Quaternary sediments with numerous till units. Kimberlite-indicator-mineral (KIM) counts from till samples by Hodder and Gauthier (2021a[1]) provide the first public assessment of the region's diamond potential. These results are being released before the comprehensive data report, to provide the mineral exploration industry timely updates on new geological knowledge.

These results build on an aeromagnetic survey in the Kaskattama–Kettle rivers region of this study area (Assessment File 93361, Manitoba Agriculture and Resource Development, Winnipeg) and a 2002 alluvial and beach KIM sampling program along the Kaskattama River (Assessment File 74009). Regionally, KIM sampling has taken place along the Nelson, Pennycutaway, Hayes and Gods rivers to the west and south of this study area (Nielsen and Fedikow, 2002; Hodder et al., 2017) and the Kaskattama highland area to the south of this study area (Hodder and Kelley, 2018).

Methods

Field collection

The MGS collected a total of 63 subsurface samples from sections exposed along the Kettle, Mistikokan, Machichi and Kaskattama rivers. Each sample was 11.4 L and weighed between 13.9 and 19.6 kg. Till geochemistry samples were also taken and analytical results were released within Hodder and Gauthier (2021b).

Kimberlite-indicator-mineral processing and classification

The KIM till samples were submitted to the De Beers Group of Companies (De Beers; Sudbury, Ontario) to be analyzed through in-kind support. The KIM sample locations were withheld from De Beers to allow equal opportunity for follow-up by all interested parties. Heavy mineral concentrate from the <0.5 mm size fraction of the till sample was passed over a 0.3 mm aperture sieve and the <0.3 mm size fraction was discarded, leaving the 0.3–0.5 mm size fraction. Sus-

[1] MGS Data Repository Item DRI2021018, containing the data or other information sources used to compile this report, is available online to download free of charge at https://www.gov.mb.ca/iem/info/library/downloads/index.html, or on request from minesinfo@gov.mb.ca, or by contacting the Resource Centre, Manitoba Agriculture and Resource Development, 360–1395 Ellice Avenue, Winnipeg, Manitoba R3G 3P2, Canada.

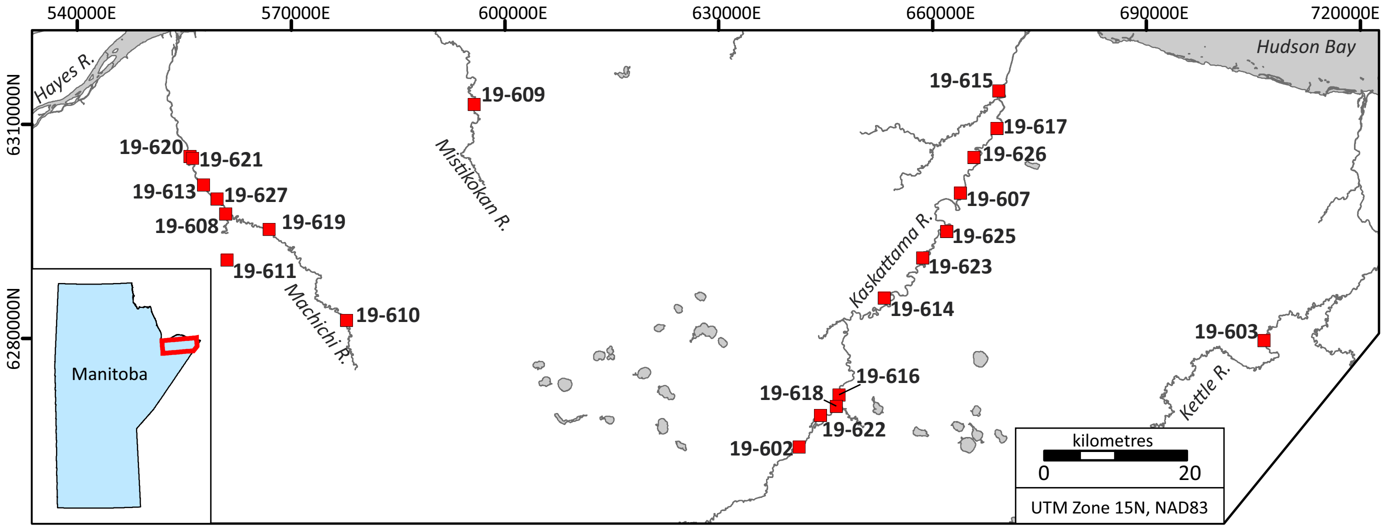

Figure GS2021-9-1: *Location of sections sampled in 2019 for kimberlite-indicator-mineral counts in Machichi–Kettle rivers study area, far north-eastern Manitoba. Section labels have been abbreviated (e.g., 112-19-602 to 19-602) relative to those found in the accompanying data repository item (DRI2021018; Hodder and Gauthier, 2021a).*

pected KIM grains were then visually selected, and analyzed by electron microprobe. The resultant KIM grains were initially classified using electron microprobe results, following the methodology outlined by Thorleifson et al. (1994). The visually identified Mg-ilmenite grains were confirmed using the compositional field defined by Wyatt et al. (2004; Figure GS2021-9-2a). Garnet grains were classified according to the method outlined by Grütter et al. (2004; Figure GS2021-9-2b). The Cr-spinel grains identified were plotted on modified discriminate diagrams to verify whether any grains were within the diamond inclusion and intergrowth fields (Figure GS2021-9-2c, d). The Cr-diopside grains were confirmed using the Cr_2O_3 versus Al_2O_3 plot defined by Nimis (2002; Figure GS2021-9-2e).

Results

Kimberlite-indicator-mineral recovery

A total of 107 KIM grains were recovered, averaging 1.1 KIM recovered per 10 kg of till processed. The visual identification, chemistry and total grain counts are presented in Hodder and Gauthier (2021a).

The majority of the KIMs recovered are chromite and Cr-spinel grains (77%; n=82). Of these grains 57% (n=47 of 82) are Cr-spinel (>45 wt. % Cr_2O_3; >10 wt. % MgO) and 43% (n=35 of 82) are chromite (>25 wt. % Cr_2O_3). Chromite and Cr-spinel were collectively grouped as Cr-spinel herein and in Hodder and Gauthier (2021a), in accordance with the terminology established in the MGS KIM database (Keller, 2019). None of these Cr-spinel grains fall within the diamond inclusion and intergrowth compositional fields (Figure GS2021-9-2c, d).

Other recovered KIMs include seventeen kimberlitic Mg-ilmenite grains, seven garnet grains and one Cr-diopside grain. The Cr-diopside composition is near the border of the diamond inclusion and intergrowth field defined by Nimis (2002; Figure GS2021-9-2e). Of the garnet KIMs, four are G9 garnets, two are G11 garnets and one is a G12 garnet.

Kimberlite-indicator-mineral trends

The KIM distribution is plotted spatially as pie charts scaled to the proportion of KIMs recovered per 10 kg of till processed (Figure GS2021-9-3). Overall, there is a higher concentration of KIMs within the eastern half of the study area (Table GS2021-9-1). The highest KIM recovery occurred along the southern extent of the survey on the Kaskattama River (Figure GS2021-9-3).

Link to till units

Figure GS2021-9-4a depicts the Quaternary stratigraphy exposed at the southern extent of the Kaskattama River (sections 19-602, 19-622 and 19-618; Figure GS2021-9-3). In this region, there are two tills documented in the subsurface, referred to as till-1 (lower) and till-2 (upper), herein. Till-2 either sharply overlies till-1 or is separated by intertill sand containing shell fragments. Till-1 is a dark greyish-brown (Munsell colour 10YR 4/2; Munsell Color–X-Rite, Incorporated, 2015) to brown (10YR 4/3) diamicton that has a silty sand to clayey sandy silt matrix. The till is compact with a blocky appearance and a massive structure (e.g., Figure GS2021-9-4b, c). Till-1 was deposited by ice flow ranging from south- to southwest-trending (183–243°). In contrast, till-2 is a brown (7.5YR 4/2; 7.5YR 4/3; 10YR 4/3) diamicton that has a sandy silt to sandy clayey silt matrix. Till-2 is less compact than the underlying till-1 at each section investigated. The till has a minor blocky appearance

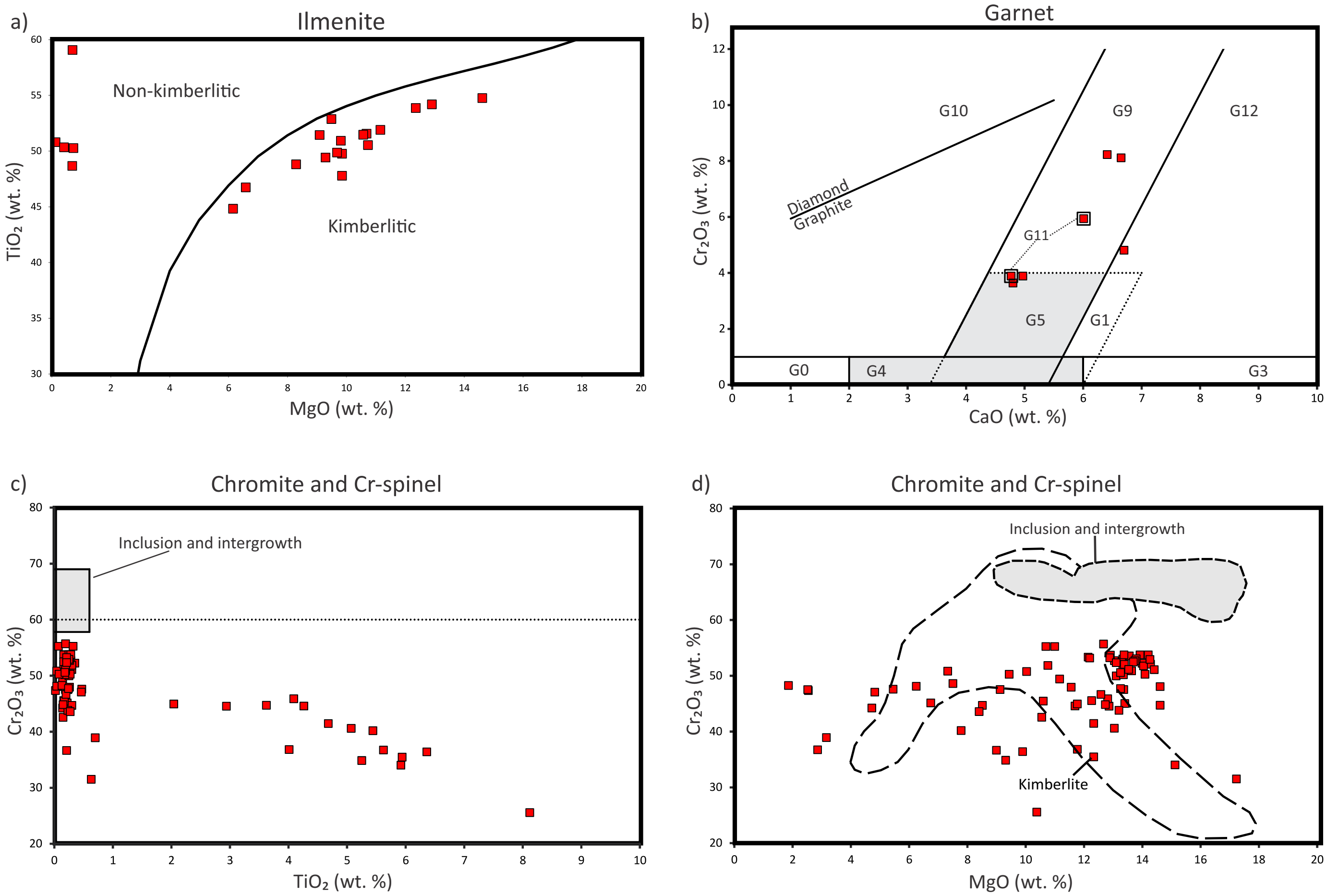

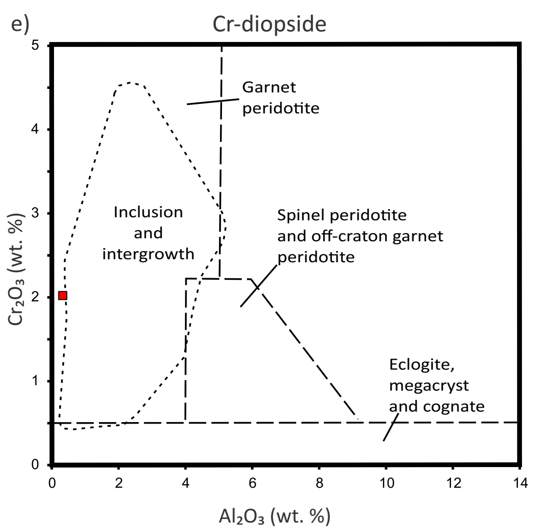

Figure GS2021-9-2: *Bivariate plots of compositional data for kimberlite-indicator minerals, Machichi–Kettle rivers study area:* ***a)*** *TiO_2 versus MgO discriminate for ilmenite grains; compositional field for kimberlite after Wyatt et al. (2004);* ***b)*** *Cr_2O_3 versus CaO for garnet grains; garnet classification fields after Grütter et al. (2004); the G5 and G4 classifications indicated by the light grey fill pattern are distinguished by Mg-number; the stippled outline of the G1 group does not overlap G4, G5, G9 or G12 categories as G1 garnet grains are distinguished by a higher TiO_2 content; G11 garnets are also classified based on a higher TiO_2 content and are differentiated from G1 garnets by a higher Cr_2O_3 content; two G11 garnets classified from this study are highlighted;* ***c)*** *Cr_2O_3 versus TiO_2 for chromite and Cr-spinel grains; diamond inclusion and intergrowth field modified after Fipke et al. (1995); a dashed line representing 60 wt. % Cr_2O_3 is shown for visual reference;* ***d)*** *Cr_2O_3 versus MgO for chromite and Cr-spinel grains; compositional field for diamond inclusion and intergrowth after Fipke et al. (1995); compositional field for kimberlite from Nowicki et al. (2007);* ***e)*** *Cr_2O_3 versus Al_2O_3 for Cr-diopside grains; compositional field for diamond inclusion and intergrowth is from Nimis (2002); other compositional fields are from Ramsay and Tompkins (1994).*

and a massive or stratified structure (e.g., Figure GS2021-9-4c, d). Ice-flow data from all three sections indicate bidirectional northwest-southeast–oriented ice flow within till-2. At section 19-622, two clast fabrics were completed within till-2. The lower clast fabric has a strong northwest-southeast orientation (130–310°) whereas the upper fabric is bimodal but interpreted to have been deposited by a dominantly 170° ice-flow orientation. The change in till-fabric orientation up-unit could indicate that till-2 was later affected by a south-trending (170°) or southwest-trending (225°) ice flow.

Till-2 provided the two highest KIM recoveries in this survey (sections 19-602 and 19-622; Figures GS2021-9-3, -4a). Strong bidirectional northwest-southeast–oriented clast fabrics were measured at both of these sample locations (Figure GS2021-9-4a). Because a unidirectional up-ice source area is needed for drift exploration, the clast lithology of till-2 was first examined. The resultant unpublished data shows elevated undifferentiated greenstone and greywacke (UGG) concentrations relative to the entire dataset (Figure GS2021-9-5a). The largest source for UGG rocks in

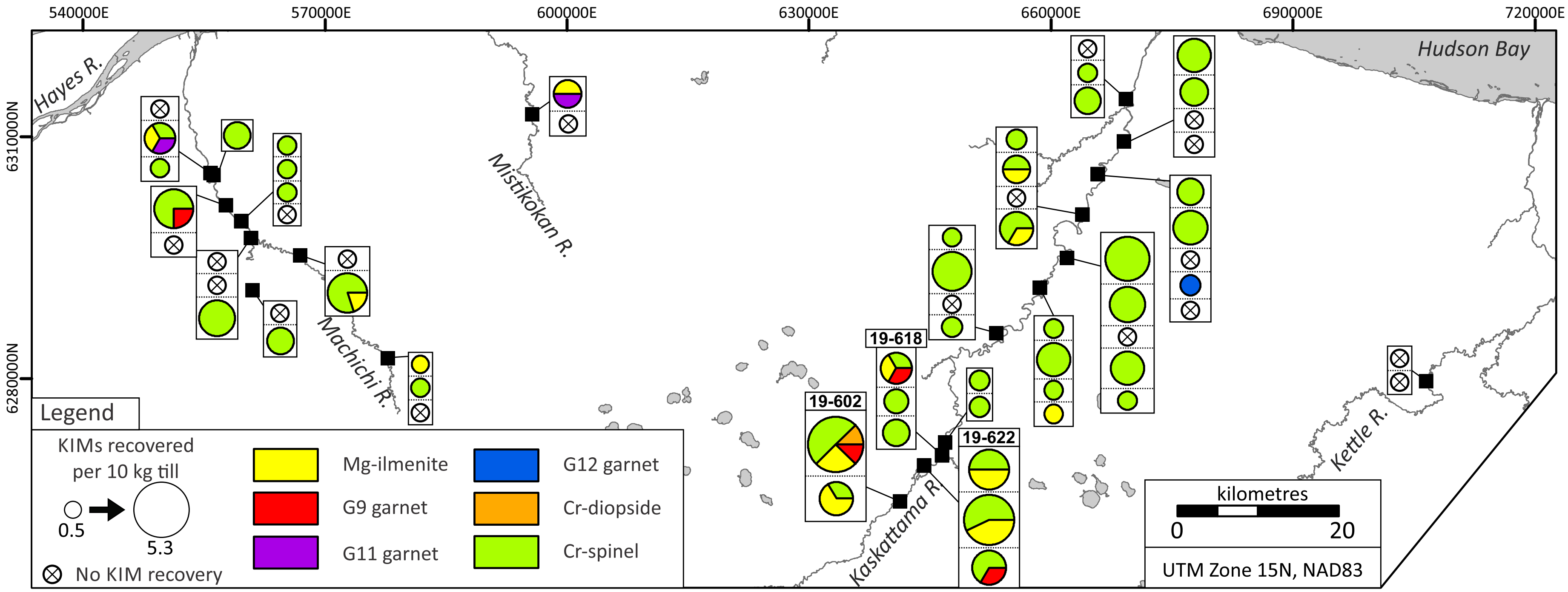

Figure GS2021-9-3: *Kimberlite-indicator-mineral (KIM) results displayed spatially as proportional-sized compositional pie charts, Machichi–Kettle rivers study area. Black squares refer to the site location and stacked boxes are multiple till samples at that site, arranged from top to bottom by increasing sample depth. Section labels have been abbreviated (e.g., 112-19-602 to 19-602) relative to those found in the accompanying data repository item (DRI2021018; Hodder and Gauthier, 2021a).*

Table GS2021-9-1: Kimberlite-indicator-mineral (KIM) data from sections in the western half (Machichi–Mistikokan rivers) and the eastern half (Kaskattama–Kettle rivers) of this study area. Abbreviations: Cr-diop, chrome diopside; Cr-sp, chrome spinel; G9, G9 garnet; G11, G11 garnet; G12, G12 garnet; KIM, kimberlite-indicator mineral; Mg-ilm, Mg-ilmenite.

Region	n	KIMs recovered	Recovery / 10 kg till	Cr-sp	Cr-diop	Mg-ilm	G9	G11	G12
Machichi–Mistikokan rivers	22	28	0.8	21	0	4	1	2	0
Kaskattama–Kettle rivers	41	79	1.2	61	1	13	3	0	1
Total	**63**	**107**	**1.1**	**82**	**1**	**17**	**4**	**2**	**1**

the region is the Circum-Superior belt (Figure GS2021-9-5b), which includes the Belcher Group and Sutton inlier to the east and southeast, and the Fox River belt to the south and southwest. There are also UGG rocks within the supracrustal greenstone belts in the surrounding Precambrian shield (Wheeler et al., 1996). Given the elevated UGG concentrations in till-2 and large source regions to the east and southeast, it is suspected that till-2 was deposited by northwest-trending ice flow.

This preliminary interpretation is being tested by determining the age of detrital hornblende within till using $^{40}Ar/^{39}Ar$ dating methods, and comparing these results with the unique metamorphic ages of geological provinces of the Precambrian shield (Figure GS2021-9-5b). The application of detrital hornblende $^{40}Ar/^{39}Ar$ age determination to assist with differentiating sediment provenance has proven to be a valuable tool in glacial sediment studies (Hemming and Hajdas, 2003; Roy et al., 2007, 2009).

Future work

The stratigraphic and till compositional data (clast-lithology and till-matrix geochemistry) from the Machichi–Kettle rivers area are currently being analyzed to assess till provenance, till stratigraphy and the ice-flow history for the region. Pending detrital hornblende $^{40}Ar/^{39}Ar$ age results from till samples will help resolve the northwest versus southeast provenance for till. Till provenance data will be synthesized with stratigraphic observations to provide a stratigraphic framework for the Kaskattama and Machichi rivers area. This data and subsequent interpretations will be combined with similar studies in the Kaskattama highland region (Hodder and Kelley, 2018) to provide an updated drift prospecting framework for northeastern Manitoba.

Economic considerations

The Machichi–Kettle rivers area of far northeastern Manitoba is a remote, thick drift covered and largely unexplored frontier area of northern Manitoba. Till sampled in this region yielded KIMs and has elucidated the diamond potential of the region. On-going till composition and stratigraphic studies will help to constrain till provenance and provide a framework for drift prospecting in the region.

References

Dalton, A.S., Margold, M., Stokes, C.R., Tarasov, L., Dyke, A.S., Adams, R.S., Allard, S., Arends, H.E., Atkinson, N., Attig, J.W., Barnett, P.J., Barnett, R.L., Batterson, M., Bernatchez, P., Borns, H.W., Jr., Breckenridge, A., Briner, J.P., Brouard, E., Campbell, J.E., Carlson, A.E. et al. 2020: An updated radiocarbon-based ice margin chronology for the last deglaciation of the North American Ice Sheet Complex; Quaternary Science Reviews, v. 234, p. 106223.

Fipke, C.E., Gurney, J.J. and Moore, R.O. 1995: Diamond exploration techniques emphasising indicator mineral geochemistry and Canadian examples; Geological Survey of Canada, Bulletin 423, 96 p.

Grütter, H.S., Gurney, J.J., Menzies, A.H. and Winter, F. 2004: An updated classification scheme for mantle-derived garnet, for use by diamond explorers; Lithos, v. 77, p. 841–857.

Hemming, S.R. and Hajdas, I. 2003: Ice-rafted detritus evidence from $^{40}Ar/^{39}Ar$ ages of individual hornblende grains for evolution of the eastern margin of the Laurentide ice sheet since 43 ^{14}C ka; Quaternary International, v. 99–100, p. 29–43.

Hodder, T.J. and Gauthier, M.S. 2019: Quaternary stratigraphy and till sampling in the Machichi–Kettle rivers area, far northeastern Manitoba (parts of NTS 54A–C); *in* Report of Activites 2019, Manitoba Agriculture and Resource Development, Manitoba Geological Survey, p. 83–89, URL <https://www.manitoba.ca/iem/geo/field/roa19pdfs/GS2019-9.pdf> [October 2021].

Hodder, T.J. and Gauthier, M.S. 2021a: Kimberlite-indicator-mineral data derived from glacial sediments (till) in the Machichi–Kettle rivers area, far northeastern Manitoba (parts of NTS 54A–C); Manitoba Agriculture and Resource Development, Manitoba Geological Survey, Data Repository Item DRI2021018, Microsoft® Excel® file, URL <https://www.manitoba.ca/iem/info/libmin/DRI2021018.xlsx> [November 2021].

Hodder, T.J. and Gauthier, M.S. 2021b: Till-matrix geochemistry data, Machichi–Kettle rivers area, far northeastern Manitoba (parts of NTS 54A–C); Manitoba Agriculture and Resource Development, Manitoba Geological Survey, Data Repository Item DRI2021007, Microsoft® Excel® file, URL <https://www.manitoba.ca/iem/info/libmin/DRI2021007.xlsx> [October 2021].

Hodder, T.J. and Kelley, S.E. 2018: Kimberlite-indicator minerals and clast-lithology composition of till, Kaskattama highland region, northeastern Manitoba (parts of NTS 53N, O, 54B, C); *in* Report of Activities 2018, Manitoba Growth, Enterprise and Trade, Manitoba Geological Survey, p. 150–156, URL <https://www.manitoba.ca/iem/geo/field/roa18pdfs/GS2018-13.pdf>[October 2021].

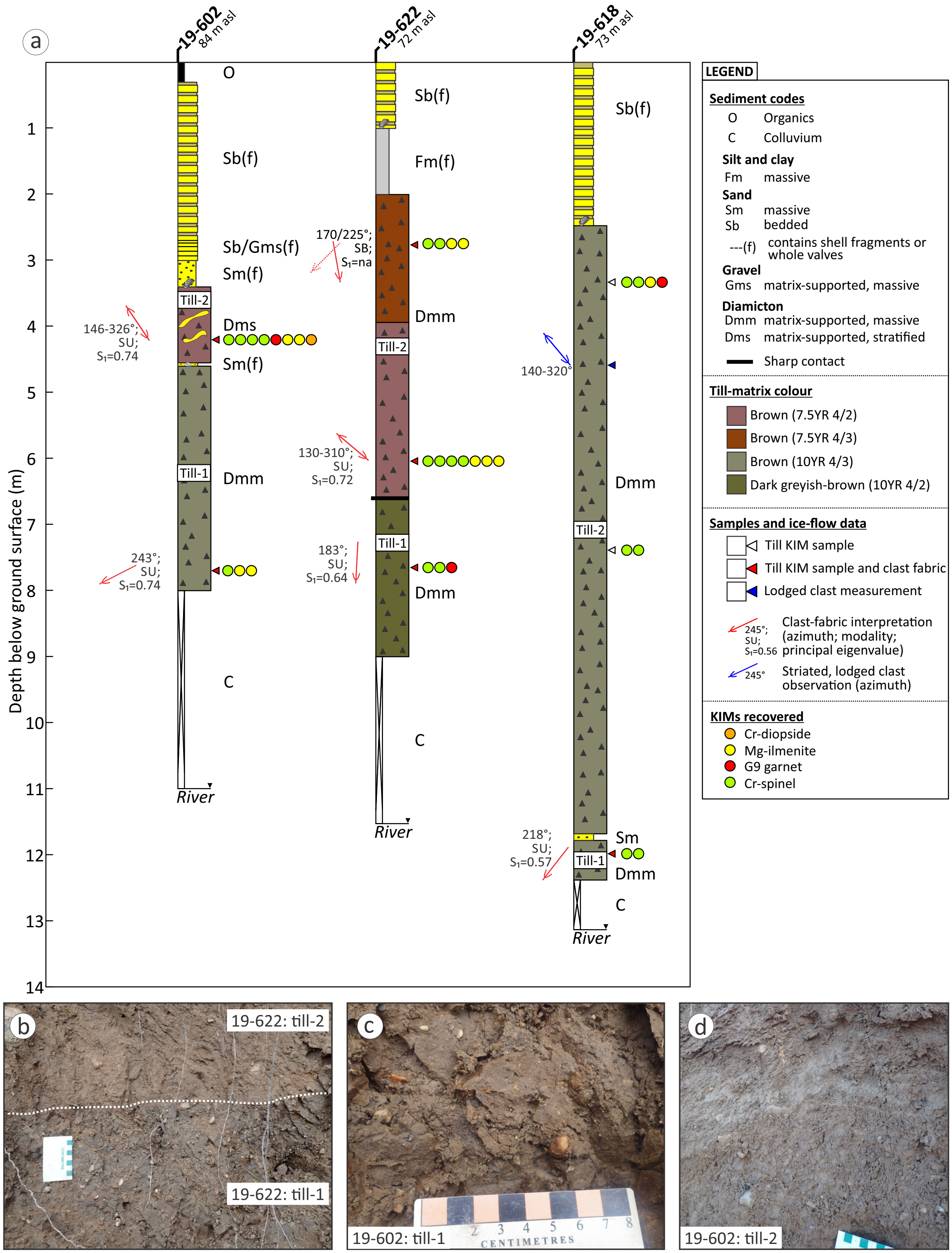

Figure GS2021-9-4: ***a)*** *Simplified Quaternary stratigraphy and kimberlite-indicator-mineral (KIM) sample results at sections 19-602, 19-618 and 19-622 on the Kaskattama River;* ***b)*** *contact between till-1 and till-2 at section 19-622;* ***c)*** *till-1 at section 19-602;* ***d)*** *till-2 at section 19-602. Section labels have been abbreviated (e.g., 112-19-602 to 19-602) relative to those found in the accompanying data repository item (DRI2021018; Hodder and Gauthier, 2021a). Till-matrix colour from Munsell Color–X-Rite, Incorporated (2015). Abbreviations: SB, spread bimodal modality; SU, spread unimodal modality.*

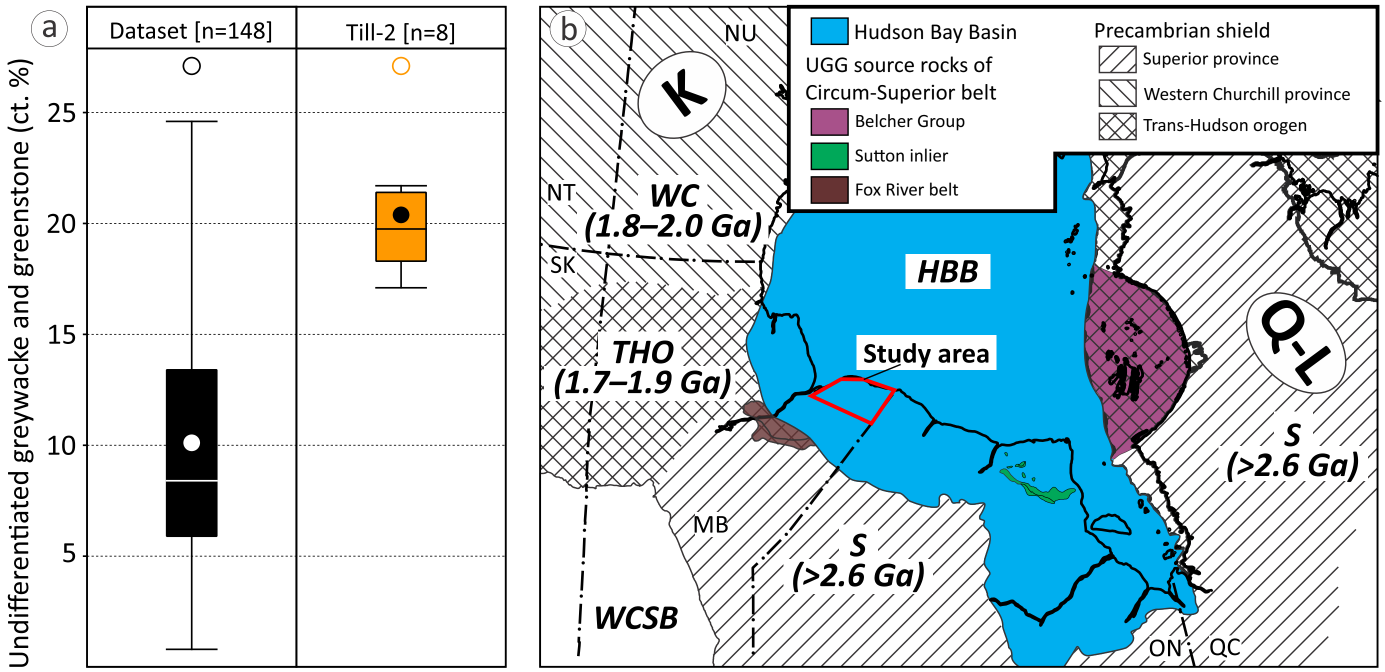

***Figure GS2021-9-5:** Concentrations and source regions of undifferentiated greenstone and greywacke (UGG) rocks: **a)** Tukey box plots showing the distribution of UGG rocks in till-2 compared to the entire dataset (Machichi–Kettle rivers study area); **b)** regional bedrock geology of central Canada (modified from Wheeler et al., 1996) and the tectonic age of geological provinces (derived from Roy et al., 2007). The location of Keewatin (K) and Quebec-Labrador (Q-L) domes of the Laurentide Ice Sheet during deglaciation are from Dalton et al. (2020). Abbreviations: HBB, Hudson Bay Basin; S, Superior province; THO, Trans-Hudson orogen; WC, western Churchill province; WCSB, Western Canada Sedimentary Basin.*

Hodder, T.J., Gauthier, M.S. and Nielsen, E. 2017: Quaternary stratigraphy and till composition along the Hayes, Gods, Nelson, Fox, Stupart, Yakaw, Angling and Pennycutaway rivers, northeast Manitoba (parts of NTS 53N, 54C, 54D, 54F); Manitoba Growth, Enterprise and Trade, Manitoba Geological Survey, Open File OF2017-4, 20 p., URL <https://www.manitoba.ca/iem/info/libmin/OF2017-4.zip> [October 2021].

Keller, G.R. 2019: Manitoba Kimberlite Indicator Mineral Database (version 3.2); Manitoba Growth, Enterprise and Trade, Manitoba Geological Survey, zipped Microsoft® Access® 2016 database, URL <https://www.manitoba.ca/iem/geo/diamonds/MBKIMDB_32.zip> [October 2021].

Munsell Color–X-Rite, Incorporated 2015: Munsell Soil Color Book; Pantone LLC, Carlstadt, New Jersey, 42 p.

Nielsen, E. and Fedikow, M.A.F. 2002: Kimberlite indicator-mineral surveys, lower Hayes River; Manitoba Industry, Trade and Mines, Manitoba Geological Survey, Geological Paper GP2002-1, 39 p., URL <https://www.manitoba.ca/iem/info/libmin/GP2002-1.zip> [October 2021].

Nimis, P. 2002: The pressures and temperatures of formation of diamond based on thermobarometry of chromian diopside inclusions; The Canadian Mineralogist, v. 40, p. 871–884.

Nowicki, T.E., Moore, R.O., Gurney, J.J. and Baumgartner, M.C. 2007: Diamonds and associated heavy minerals in kimberlite: a review of key concepts and applications; Developments in Sedimentology, v. 58, p. 1235–1267.

Ramsay, R.R. and Tompkins, L.A. 1994: The geology, heavy mineral concentrate mineralogy, and diamond prospectivity of the Boa Esperança and Cana Verde pipes, Corrego D'anta, Minas Gerais, Brazil; *in* Kimberlites, Related Rocks and Mantle Xenoliths, H.O.A. Meyer and O.H. Leonardos (ed.), Proceedings of the 5th International Kimberlite Conference, Araxá, Brazil, Companhia de Pesquisa de Recursos Minerais (CRPM), Special Publication, v. 2, p. 329–345.

Roy, M., Hemmings, S. and Parent, M. 2009: Sediment sources of northern Quebec and Labrador glacial deposits and the northeastern sector of the Laurentide Ice Sheet during ice-rafting events of the last glacial cycle; Quaternary Science Reviews, v. 28, p. 3236–3245.

Roy, M., Clark, P.U., Duncan, R.A. and Hemming, S.R. 2007: Insights into the late Cenozoic configuration of the Laurentide Ice Sheet from $^{40}Ar/^{39}Ar$ dating of glacially transported minerals in midcontinent tills; Geochemistry, Geophysics, Geosystems, v. 8, no. 9, p. 12.

Thorleifson, L.H., Garrett, R.G. and Matile, G. 1994: Prairie kimberlite study - indicator mineral geochemistry; Geological Survey of Canada, Open File 2875, 15 p.

Wheeler, J.O., Hoffman, P.F., Card, K.D., Davidson, A., Sanford, B.V., Okulitch, A.V. and Roest, W.R. 1996: Geological map of Canada; Geological Survey of Canada, Map 1860A, scale 1:5 000 000.

Wyatt, B.A., Baumgartner, M., Anckar, E. and Grütter, H.S. 2004: Compositional classification of 'kimberlitic' and 'non-kimberlitic' ilmenite; Lithos, v. 77, p. 841–857.

GS2021-10

Quaternary stratigraphy in the Churchill–Little Churchill rivers area, northeastern Manitoba (part of NTS 54E)

by T.J. Hodder and M.S. Gauthier

In Brief:

- Description of the Quaternary stratigraphy along Churchill and Little Churchill rivers
- Till samples collected for indicator mineral, geochemistry, clast-lithology and texture analysis to explore the economic potential of the region
- Intertill nonglacial sediments sampled for chronology and paleobotanical characterization

Citation:
Hodder, T.J. and Gauthier, M.S. 2021: Quaternary stratigraphy in the Churchill–Little Churchill rivers area, northeastern Manitoba (part of NTS 54E); *in* Report of Activities 2021, Manitoba Agriculture and Resource Development, Manitoba Geological Survey, p. 84–87.

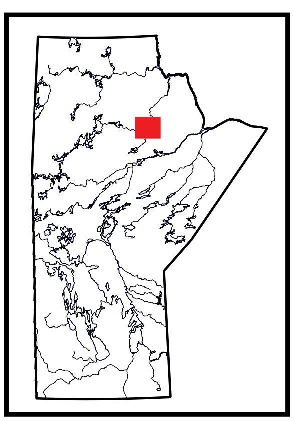

Summary

Quaternary geology fieldwork was conducted in August–September of 2021 in the Churchill–Little Churchill rivers area of northeastern Manitoba. The objectives of this study were to provide a reconnaissance of the Quaternary stratigraphy exposed along river sections, and provide background information for drift prospecting. A total of 117 till samples were collected to determine till provenance and will be submitted for geochemistry and clast-lithology analyses. At 65 sample sites, an additional indicator-mineral sample was collected to assess the regional economic potential. Clast fabrics in till were measured at 65 samples sites to determine the ice-flow direction during till deposition and contribute to understanding the regional ice-flow history. Intertill sorted sediments were examined in detail and 14 samples were collected (where an appropriate sample medium was observed) for geochronological analysis by radiocarbon and optical dating methods. Intertill sorted sediments with organics were also collected for paleobotanical analyses (total of 18 samples).

Introduction

The Manitoba Geological Survey (MGS) conducted 17 days of helicopter-supported fieldwork in August–September of 2021 in the Churchill–Little Churchill rivers area of northeastern Manitoba (part of NTS 54E). The objectives of the 2021 field season were to

- document the sediments observed at Quaternary sections found along the main rivers;
- sample till and conduct clast-fabric measurements to determine the ice-flow direction during till deposition;
- conduct indicator-mineral sampling to assess the economic potential of the region; and
- collect geochronology and paleobotanical samples to help establish stratigraphic correlations in the Hudson Bay Lowland (HBL).

Previous work

The Churchill–Little Churchill rivers area has undergone little geological study. In 1967, the Geological Survey of Canada initiated Operation Winisk to better understand the geology of the HBL region of Quebec, Ontario and Manitoba (Craig, 1969; McDonald, 1969). Within the study area, Operation Winisk fieldwork provided helicopter-supported observations at one section on the Churchill River, where 56–58 m of grey till was exposed (Figure GS2021-10-1; B.G. Craig, H. Gwyn and B.C. McDonald, unpublished notes, 1967). Dredge and Nixon (1992) investigated one section on the Churchill River and three sections on the Little Churchill River (Figure GS2021-10-1). The Churchill River section, named Mountain Rapids, contains at least one and possibly two intertill nonglacial organic-bearing units, and four till units (Dredge and Nielsen, 1985; Dredge et al., 1990; Dredge and McMartin, 2011). The surficial geology of the region has been mapped at a 1:250 000 scale (Dredge and Nixon, 1982).

2021 fieldwork

The study area is underlain by Precambrian intrusive rocks of the Churchill province and is situated between 7 and 57 km west of the contact with the Hudson Bay Basin (Figure GS2021-10-1). Bedrock was exposed at the base of each section investigated along the Churchill River or visible in the river nearby. Bedrock was not exposed at any of the sites investigated along the Little Churchill River. The banks of the Churchill River and Little Churchill River expose 20–65 and 5–17 m of sediment, respectively. The Quaternary stratigraphy was documented at seven locations on the Churchill River and seven locations on the Little Churchill River (Figure GS2021-10-1). Sediment exposures were cleared of slumped detritus, exposing a continuous section with no gap, and then

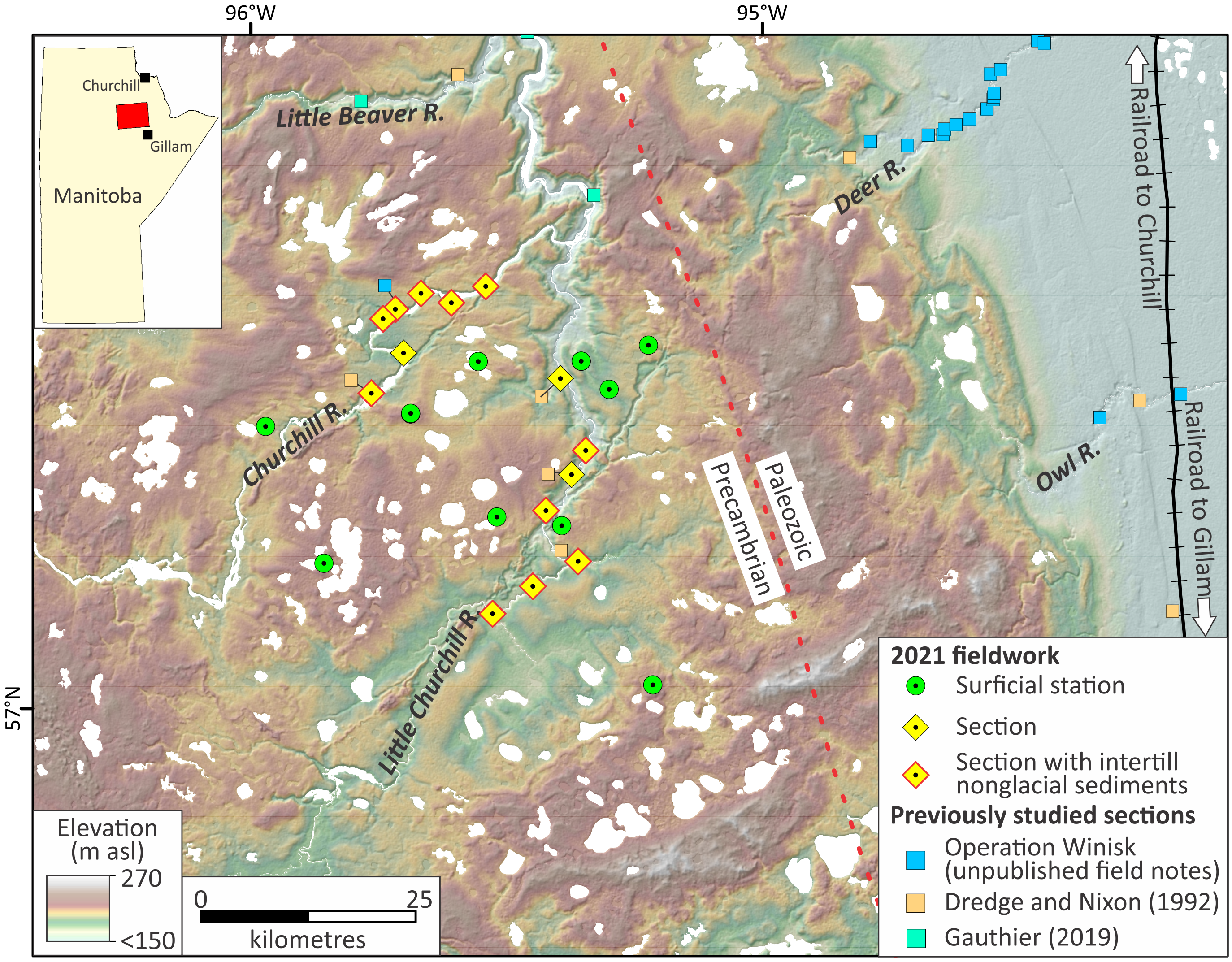

Figure GS2021-10-1: *Location of 2021 field sites and previously described sections in the Churchill–Little Churchill rivers study area. The red stippled line shows the boundary between Precambrian rocks to the west and Paleozoic Hudson Bay Basin rocks to the east. Background hillshade image was generated using Canadian Digital Surface Model (Natural Resources Canada, 2015).*

described in detail. Where encountered, till was sampled at 2 to 4 m intervals. The sediments at 10 surface stations were also described and till samples were collected using a Dutch auger or from hand-dug holes. A total of 117 till samples were collected, each weighing 2–3 kg.

The new till samples will be split for archival purposes at the MGS Midland Sample and Core Library (Winnipeg, Manitoba) and then analyzed for grain size, matrix geochemistry (<63 µm size fraction) and clast lithology. An additional 11.4 L till sample was collected for indicator-mineral analysis at 65 till samples sites. Indicator-mineral samples were submitted for analyses in collaboration with the Geological Survey of Canada.

Ice-flow data was obtained from studied sections by measuring the long-axes orientation, or fabric, of clasts within till. Elongate clasts, defined by a minimum 1.5:1.0 ratio of the a-axis (longest) to the b-axis (middle), will rotate within the till matrix and orient parallel to the direction of stress that the overriding glacier exerts on the till (Holmes, 1941). A minimum of 30 elongated clasts were measured at each of the 65 clast-fabric sites, to ensure a statistically valid result. Lodged clasts with parallel striae on their upper surface—considered to be a good indicator of ice flow—were observed at nine locations. This ice-flow data will be combined with the forthcoming till composition data and stratigraphic observations to detail the till provenance and glacial history of the study area.

Sorted sediments, underlying or between till units, were also of interest for this study as outlined in Gauthier et al. (2021). Intertill sediments interpreted to be deposited in a nonglacial environment were encountered at 11 out of the 14 sections examined (Figure GS2021-10-1). Organic-bearing units (e.g., Figure GS2021-10-2a, b) were sampled for pollen and macrofossil analysis at six sections, totalling eighteen samples. Organic matter was collected for radiocarbon dating wherever

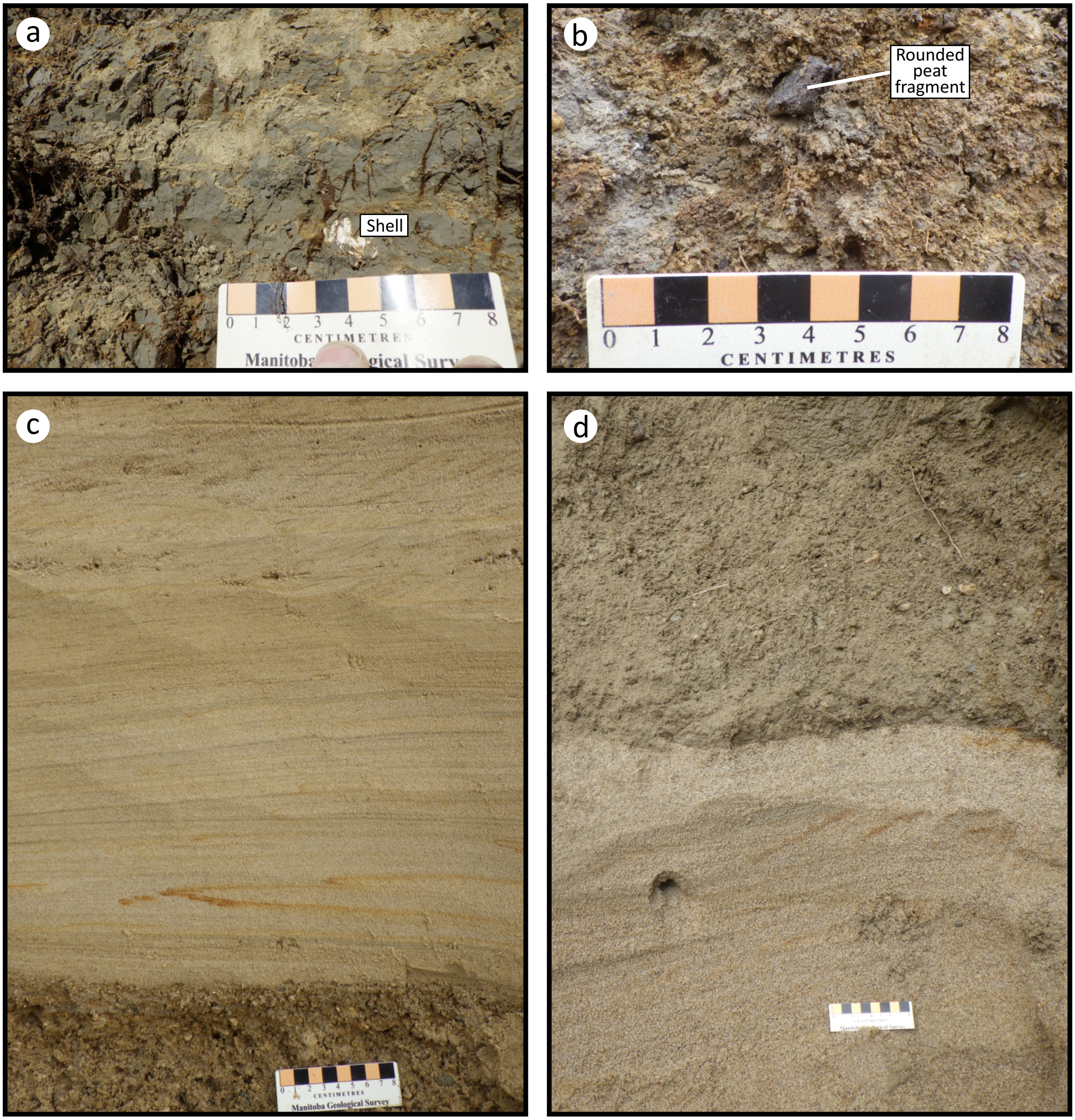

Figure GS2021-10-2: *Examples of* ***a, b)*** *organic-bearing intertill sorted sediments sampled for radiocarbon dating and* ***c, d)*** *intertill bedded sands sampled for optical dating, Churchill–Little Churchill rivers study area.*

encountered, resulting in a total of five shell or wood samples. In addition, because most organic-bearing units may be older than the limits of radiocarbon dating (~50 000 years), bedded sand units were also sampled at seven sections for optical dating (e.g., Figure GS2021-10-2c, d). As these too may be older than the limits of optical dating (~400 000 years), the youngest intertill nonglacial sediments in the stratigraphic record were targeted to determine the timing of the last deglaciation in the region.

Economic considerations

Manitoba's far northeast is a remote and largely unexplored frontier area. Results from this study will provide the first documentation of the Quaternary stratigraphy and glacial history of the study area. This will support drift prospecting efforts in this region of thick drift, which contains a depositional record spanning multiple glaciations. Results from the indicator-mineral analysis will provide the first reconnaissance-scale insight into the economic potential of the region.

Acknowledgments

M. Rinne is thanked for agreeing to join the team on short notice and providing enthusiastic field participation. This project would not have been successful without his participation. Pilot K. Dunthorne and Prairie Helicopters Inc. are thanked for providing excellent air support during this project. This research is funded by the Manitoba Geological Survey and the Geological Survey of Canada's Geo-mapping for Energy and Minerals program (GEM-GeoNorth).

References

Craig, B.G. 1969: Late glacial and post-glacial history of the Hudson Bay region; *in* Earth Science Symposium on Hudson Bay, P.J. Hood (ed.), Geological Survey of Canada, Paper 68-83, p. 63–77.

Dredge, L.A. and McMartin, I. 2011: Glacial stratigraphy of northern and central Manitoba; Geological Survey of Canada, Bulletin 600, 27 p.

Dredge, L.A. and Nielsen, E. 1985: Glacial and interglacial deposits in the Hudson Bay Lowlands: a summary of sites in Manitoba; *in* Current Research, Geological Survey of Canada, Paper 85-1A, p. 247–257.

Dredge, L.A. and Nixon, F.M. 1982: Surficial geology, Herchmer, Manitoba; Geological Survey of Canada, Preliminary Map 1-1980, scale 1:250 000.

Dredge, L.A. and Nixon, F.M. 1992: Glacial and environmental geology of northeastern Manitoba; Geological Survey of Canada, Memoir 432, 80 p.

Dredge, L.A., Morgan, A.V. and Nielsen, E. 1990: Sangamon and pre-Sangamon interglaciations in the Hudson Bay Lowlands of Manitoba; Geographie Physique et Quaternaire, v. 44, no. 3, p. 319–336.

Gauthier, M.S. 2019: Till composition, stratigraphy, ice-flow indicator data and glacial history of the North Knife River–Churchill River region, Manitoba (parts of NTS 54L, 64I); Manitoba Agriculture and Resource Development, Manitoba Geological Survey, Geoscientific Paper GP2019-1, 41 p., URL <https://www.manitoba.ca/iem/info/libmin/GP2019-1.zip> [October 2021].

Gauthier, M.S., Hodder, T.J., Lian, O.B., Finkelstein, S.A., Dalton, A.S. and Paulen, R.C. 2021: Stratigraphic, paleoenvironmental and geochronological investigations of intertill nonglacial deposits in northeastern Manitoba (parts of NTS 54B–F, K, L, 64A, H, I); *in* Report of Activities 2021, Manitoba Agriculture and Resource Development, Manitoba Geological Survey, p. 71–76, URL <https://www.manitoba.ca/iem/geo/field/roa21pdfs/GS2021-8.pdf> [November 2021].

Holmes, C.D. 1941: Till fabric; Geological Society of America, Bulletin 52, p. 1299–1354.

McDonald, B.C. 1969: Glacial and interglacial stratigraphy, Hudson Bay Lowland; *in* Earth Science Symposium on Hudson Bay, P.J. Hood (ed.), Geological Survey of Canada, Paper 68-83, p. 78–99.

Natural Resources Canada 2015: Canadian Digital Surface Model; Natural Resources Canada, URL <https://open.canada.ca/data/en/dataset/768570f8-5761-498a-bd6a-315eb6cc023d> [September 2015].

PUBLICATIONS

Data Repository Items

DRI2012001 (re-release)

Whole-rock geochemistry of the Burntwood Lake alkali-feldspar syenite, west-central Manitoba (part of NTS 63N8)

by T. Martins

Microsoft® Excel® file supplements:

Martins, T., Couëslan, C.G. and Böhm, C.O. 2011: The Burntwood Lake alkali-feldspar syenite revisited, west-central Manitoba (part of NTS 63N8); *in* Report of Activities 2011, Manitoba Innovation, Energy and Mines, Manitoba Geological Survey, p. 79–85.

DRI2017004 (re-release)

Whole-rock and mineral geochemistry as exploration tools for rare-element pegmatite in Manitoba: examples from the Cat Lake–Winnipeg River and Wekusko Lake pegmatite fields (parts of NTS 52L6, 63J13)

by T. Martins and R.L. Linnen

Microsoft® Excel® file supplements:

Martins, T., Linnen, R.L., Fedikow, M.A.F. and Singh, J. 2017: Whole-rock and mineral geochemistry as exploration tools for rare-element pegmatite in Manitoba: examples from the Cat Lake–Winnipeg River and Wekusko Lake pegmatite fields (parts of NTS 52L6, 63J13); *in* Report of Activities 2017, Manitoba Growth, Enterprise and Trade, Manitoba Geological Survey, p. 42–51.

DRI2018001 (re-release)

Kimberlite-indicator–mineral data derived from glacial sediments (till) in the Kaskattama highland area of northeastern Manitoba (parts of NTS 53N, O, 54B, C)

by T.J. Hodder

Microsoft® Excel® file supplements:

Hodder, T.J. and Kelley, S.E. 2018: Kimberlite-indicator minerals and clast-lithology composition of till, Kaskattama highland region, northeastern Manitoba (parts of NTS 53N, O, 54B, C); *in* Report of Activities 2018, Manitoba Growth, Enterprise and Trade, Manitoba Geological Survey, p. 150–165.

DRI2019007 (re-release)

Whole rock geochemistry compilation of the Oxford Lake–Knee Lake greenstone belt, northwestern Superior Province, Manitoba (parts of NTS 53L6, 12–15, 53M2, 63I9, 16)

by S. Anderson and T. Martins

Microsoft® Excel® file supplements:

Anderson, S.D., Kremer, P.D. and Martins, T. 2012: Preliminary results of bedrock mapping at Oxford Lake, northwestern Superior Province, Manitoba (parts of NTS 53L12, 13, 63I9, 16); *in* Report of Activities 2012, Manitoba Innovation, Energy and Mines, Manitoba Geological Survey, p. 6–22.

Anderson, S.D., Kremer, P.D. and Martins, T. 2013: Preliminary results of bedrock mapping at Oxford Lake, northwestern Superior province, Manitoba (parts of NTS 53L13, 14); *in* Report of Activities 2013, Manitoba Mineral Resources, Manitoba Geological Survey, p. 7–22.

Anderson, S.D., Syme, E.C., Corkery, M.T., Bailes, A.H. and Lin, S. 2015: Preliminary results of bedrock mapping at southern Knee Lake, northwestern Superior province, Manitoba (parts of NTS 53L14, 15); *in* Report of Activities 2015, Manitoba Mineral Resources, Manitoba Geological Survey, p. 9–23.

Anderson, S.D. 2016: Preliminary results of bedrock mapping at central Knee Lake, northwestern Superior province, Manitoba (parts of NTS 53L15, 53M2); *in* Report of Activities 2016, Manitoba Growth, Enterprise and Trade, Manitoba Geological Survey, p. 1–15.

Anderson, S.D. 2016: Alkaline rocks at Oxford Lake and Knee Lake, northwestern Superior province, Manitoba (NTS 53L13, 14, 15): preliminary results of new bedrock mapping and lithogeochemistry; *in* Report of Activities 2016, Manitoba Growth, Enterprise and Trade, Manitoba Geological Survey, p. 16–27.

Anderson, S.D. 2017: Preliminary geology of the diamond occurrence at southern Knee Lake, Oxford Lake–Knee Lake greenstone belt, Manitoba (NTS 53L15); Manitoba Growth, Enterprise and Trade, Manitoba Geological Survey, Open File OF2017-3, 27 p.

DRI2020028 (re-release)

Lithogeochemistry of drillcore from the Huzyk Creek property, central Manitoba (NTS 63J6)

by C.G. Couëslan

DRI2020029

Compilation of Sm-Nd isotopic results from the Seal River–Great Island area, southeast Hearne craton margin, northern Manitoba (parts of NTS 54L, M, 64I, P)

by C.O. Böhm, S.D. Anderson and E.C. Syme

Microsoft® Excel® file supplements:

Anderson, S.D. and Böhm, C.O. 2008: Far North Mapping Initiative: reconnaissance bedrock mapping and sampling of the Great Island Domain, Manitoba (parts of NTS 54L, M, 64I, P); *in* Report of Activities 2008, Manitoba Science, Technology, Energy and Mines, Manitoba Geological Survey, p. 144–153.

Anderson, S.D., Böhm, C.O. and Syme, E.C. 2010: Far North Geomapping Initiative: bedrock geological investigations in the Seal River region, northeastern Manitoba (parts of NTS 54L, M, 64I, P); *in* Report of Activities 2010, Manitoba Innovation, Energy and Mines, Manitoba Geological Survey, p. 6–22.

Anderson, S.D., Böhm, C.O. and Syme, E.C. 2010: Precambrian geology of the Seal River region, Manitoba (parts of NTS 54L, M, 64I, P); Manitoba Innovation, Energy and Mines, Manitoba Geological Survey, Preliminary Map PMAP2010-1, scale 1:175 000.

Anderson, S.D., Böhm, C.O., Syme, E.C., Carlson, A.R. and Murphy, L.A. 2009: Bedrock geology of the Great Island area, Manitoba (parts of NTS 54L13, 54M4, 64I15, 16, 64P1, 2); Manitoba Innovation, Energy and Mines, Manitoba Geological Survey, Preliminary Map PMAP2009-4, scale 1:75 000.

Anderson, S.D., Böhm, C.O., Syme, E.C., Carlson, A.R. and Murphy, L.A. 2009: Far North Geomapping Initiative: geological investigations in the Great Island area, Manitoba (parts of NTS 54L13, 54M4, 64I15, 16, 64P1, 2); *in* Report of Activities 2009, Manitoba Innovation, Energy and Mines, Manitoba Geological Survey, p. 132–147.

Rayner, N. 2010: Far North Geomapping Initiative: new U-Pb geochronological results from the Seal River region, northeastern Manitoba (parts of NTS 54L, M, 64I, P); *in* Report of Activities 2010, Manitoba Innovation, Energy and Mines, Manitoba Geological Survey, p. 23–35.

DRI2020030

Whole-rock geochemistry compilation of the Seal River–Great Island area, southeast Hearne craton margin, northern Manitoba (parts of NTS 54L, M, 64I, P)

by C.O. Böhm, S.D. Anderson, E.C. Syme, A.R. Carlson and L.A. Murphy

Microsoft® Excel® file supplements:

Anderson, S.D. and Böhm, C.O. 2008: Far North Mapping Initiative: reconnaissance bedrock mapping and sampling of the Great Island Domain, Manitoba (parts of NTS 54L, M, 64I, P); *in* Report of Activities 2008, Manitoba Science, Technology, Energy and Mines, Manitoba Geological Survey, p. 144–153.

Anderson, S.D., Böhm, C.O. and Syme, E.C. 2010: Far North Geomapping Initiative: bedrock geological investigations in the Seal River region, northeastern Manitoba (parts of NTS 54L, M, 64I, P); *in* Report of Activities 2010, Manitoba Innovation, Energy and Mines, Manitoba Geological Survey, p. 6–22.

Anderson, S.D., Böhm, C.O. and Syme, E.C. 2010: Precambrian geology of the Seal River region, Manitoba (parts of NTS 54L, M, 64I, P); Manitoba Innovation, Energy and Mines, Manitoba Geological Survey, Preliminary Map PMAP2010-1, scale 1:175 000.

Anderson, S.D., Böhm, C.O., Syme, E.C., Carlson, A.R. and Murphy, L.A. 2009: Bedrock geology of the Great Island area, Manitoba (parts of NTS 54L13, 54M4, 64I15, 16, 64P1, 2); Manitoba Innovation, Energy and Mines, Manitoba Geological Survey, Preliminary Map PMAP2009-4, scale 1:75 000.

Anderson, S.D., Böhm, C.O., Syme, E.C., Carlson, A.R. and Murphy, L.A. 2009: Far North Geomapping Initiative: geological investigations in the Great Island area, Manitoba (parts of NTS 54L13, 54M4, 64I15, 16, 64P1, 2); *in* Report of Activities 2009, Manitoba Innovation, Energy and Mines, Manitoba Geological Survey, p. 132–147.

Rayner, N. 2010: Far North Geomapping Initiative: new U-Pb geochronological results from the Seal River region, northeastern Manitoba (parts of NTS 54L, M, 64I, P); *in* Report of Activities 2010, Manitoba Innovation, Energy and Mines, Manitoba Geological Survey, p. 23–35.

DRI2021001

Whole-rock geochemistry results of Bear Lake, Superior province, east-central Manitoba (parts of NTS 53M4, 63P1)

by C.O. Böhm, R.P. Hartlaub and T. Martins

Microsoft® Excel® file supplements:

Böhm, C.O. and Hartlaub, R.P. 2006: Bedrock geology of the Bear Lake area, Manitoba (parts of NTS 53M4 and 63P1); Manitoba Science, Technology, Energy and Mines, Manitoba Geological Survey, Preliminary Map PMAP2006-2, scale 1:50 000.

Hartlaub, R.P. and Böhm, C.O. 2006: Preliminary results from geological mapping of the Bear Lake greenstone belt, Manitoba (parts of NTS 53M4 and 63P1); *in* Report of Activities 2006, Manitoba Science, Technology, Energy and Mines, Manitoba Geological Survey, p. 65–73.

DRI2021002

Whole-rock geochemistry results for Utik Lake, Superior province, east-central Manitoba (parts of NTS 53M4, 5, 63P1, 8)

by C.O. Böhm, P.D. Kremer, E.C. Syme and T. Martins

Microsoft® Excel® file supplements:

Böhm, C.O. and Kremer, P.D. 2007: Bedrock geology of the Utik Lake greenstone belt, Manitoba (parts of NTS 53M4, 5 and 63P1, 8); Manitoba Science, Technology, Energy and Mines, Manitoba Geological Survey, Preliminary Map PMAP2007-4, scale 1:25 000.

Böhm, C.O., Kremer, P.D. and Syme, E.C. 2007: Nature, evolution and gold potential of the Utik Lake greenstone belt, Manitoba (parts of NTS 53M4, 5, 63P1, 8): preliminary field results; *in* Report of Activities 2007, Manitoba Science, Technology, Energy and Mines, Manitoba Geological Survey, p. 98–113.

DRI2021003

Compilation of Sm-Nd isotope results from Utik Lake, Superior province, east-central Manitoba (parts of NTS 53M4, 5, 63P1, 8)

by C.O. Böhm, P.D. Kremer, E.C. Syme and T. Martins

Microsoft® Excel® file supplements:

Böhm, C.O. and Kremer, P.D. 2007: Bedrock geology of the Utik Lake greenstone belt, Manitoba (parts of NTS 53M4, 5 and 63P1, 8); Manitoba Science, Technology, Energy and Mines, Manitoba Geological Survey, Preliminary Map PMAP2007-4, scale 1:25 000.

Böhm, C.O., Kremer, P.D. and Syme, E.C. 2007: Nature, evolution and gold potential of the Utik Lake greenstone belt, Manitoba (parts of NTS 53M4, 5, 63P1, 8): preliminary field results; *in* Report of Activities 2007, Manitoba Science, Technology, Energy and Mines, Manitoba Geological Survey, p. 98–113.

DRI2021004

Whole-rock geochemistry of bedrock samples along East Side Road, southeastern Manitoba (parts of NTS 62P1, 7, 8, 10, 15, 63A2, 7)

by M.L. Rinne

Microsoft® Excel® file supplements:

Rinne, M.L. 2020: Results of reconnaissance bedrock mapping along East Side Road, southeastern Manitoba (parts of NTS 62P1, 7, 8, 10, 15, 63A2, 7); *in* Report of Activities 2020, Manitoba Agriculture and Resource Development, Manitoba Geological Survey, p. 1–8.

DRI2021005

Compilation of Sm-Nd isotope results from the Manitoba Geological Survey 2020/2021 season

by Manitoba Geological Survey

DRI2021006

Till geochemistry from Manigotagan to Berens River, southeastern Manitoba (parts of NTS 62P1, 7, 8, 10, 15, 63A2, 7)

by M.S. Gauthier and T.J. Hodder

DRI2021007

Till-matrix geochemistry data, Machichi–Kettle rivers area, far northeastern Manitoba (parts of NTS 54A–C)

by T.J. Hodder and M.S. Gauthier

DRI2021008

Compilation of Sm-Nd isotope results and accompanying whole-rock geochemistry (to 2017) for the Trans-Hudson orogen, Manitoba (parts of NTS 63F, J, K, 63N–P, 64A–C, 64F–H)

by Manitoba Geological Survey

DRI2021009

Whole-rock geochemistry results for Sharpe Lake, Superior province, east-central Manitoba (parts of NTS 53K5, 6)

by Manitoba Geological Survey

Microsoft® Excel® file supplements:

Beaumont-Smith, C.J., Anderson, S.D., Bailes, A.H. and Corkery, M.T. 2003: Preliminary results and economic significance of geological mapping and structural analysis at Sharpe Lake, northern Superior Province, Manitoba (parts of NTS 53K5 and 6); *in* Report of Activities 2003, Manitoba Industry, Economic Development and Mines, Manitoba Geological Survey, p. 140–158.

Corkery, M.T., Beaumont-Smith, C.J., Anderson, S.D. and Bailes, A.H. 2003: Geology of the eastern Sharpe Lake area, Manitoba (NTS 53K6); Manitoba Industry, Economic Development and Mines, Manitoba Geological Survey, Preliminary Map PMAP2003-5, scale 1:50 000.

Corkery, M.T., Beaumont-Smith, C.J., Anderson, S.D. and Bailes, A.H. 2003: Geology of the western Sharpe Lake area, Manitoba (NTS 53K5); Manitoba Industry, Economic Development and Mines, Manitoba Geological Survey, Preliminary Map PMAP2003-4, scale 1:50 000.

DRI2021010

Till geochemistry and heavy mineral analyses of the western Fox River greenstone belt area, northeastern Manitoba (NTS 53M15, 16), plus 4 samples from the Gillam area (parts of 54D7, 11)

by M.S. Gauthier and T.J. Hodder

DRI2021011

Whole-rock geochemistry of bedrock samples from the Snyder Lake area, northwestern Manitoba (part of NTS 64N5)

by P.D. Kremer, C.O. Böhm and T. Martins

Microsoft® Excel® file supplements:

Kremer, P.D., Böhm, C.O. and Rayner, N. 2011: Far North Geomapping Initiative: bedrock geology of the Snyder Lake area, northwestern Manitoba (part of NTS 64N5); *in* Report of Activities 2011, Manitoba Innovation, Energy and Mines, Manitoba Geological Survey, p. 6–17.

DRI2021012

Whole-rock geochemistry results of bedrock samples from the Misty Lake area, Manitoba (parts of NTS 64K12, 13, 64N4)

by P.D. Kremer, A.R. Carlson, C.G. Couëslan and T. Martins

Microsoft® Excel® file supplements:

Kremer, P.D., Carlson, A.R. and Couëslan, C. 2010: Far North Geomapping Initiative: geological mapping in the Misty Lake area, Manitoba (parts of NTS 64K12, 13, 64N4); *in* Report of Activities 2010, Manitoba Innovation, Energy and Mines, Manitoba Geological Survey, p. 50–61.

DRI2021013

Laser-ablation, multicollector, inductively coupled plasma–mass spectrometry U-Pb isotopic analyses of detrital zircon grains from the Ospwagan group, Setting formation metagreywacke sample 12-04-4462, Setting Lake, central Manitoba (part of NTS 63O2)

by H.V. Zwanzig, C.O. Böhm and C.G. Couëslan

DRI2021015

Lithogeochemistry of drillcore from the Phillips Lake area, and samples from the Paint Lake area, Thompson nickel belt, central Manitoba (NTS 63O1, 8, 63P5)

by C.G. Couëslan

DRI2021016

Lithogeochemistry of iron formation, calcsilicate, marble, and mafic dikes from the Thompson nickel belt, central Manitoba (NTS 63O8, 9, 63P5, 12, 15)

by C.G. Couëslan

DRI2021017

Lithogeochemistry of metasedimentary rocks of uncertain affinity from the Joey Lake area, and Ospwagan group and related rocks, Thompson nickel belt, central Manitoba (NTS 63O8, 9, 63P12)

by C.G. Couëslan

Microsoft® Excel® file supplements:

Couëslan, C.G. 2021: Collection of samples for high-resolution detrital-zircon geochronology and lithogeochemistry in the Thompson nickel belt, central Manitoba (parts of NTS 63O8, 9, 63P12); *in* Report of Activities 2021, Manitoba Agriculture and Resource Development, Manitoba Geological Survey, p. 18–28.

DRI2021018

Kimberlite-indicator-mineral data derived from glacial sediments (till) in the Machichi–Kettle rivers area, far northeastern Manitoba (parts of NTS 54A–C)

by T.J. Hodder and M.S. Gauthier

Microsoft® Excel® file supplements:

Hodder, T.J. and Gauthier, M.S. 2021: Kimberlite-indicator-mineral results from till sampled in the Machichi–Kettle rivers area, far northeastern Manitoba (parts of NTS 54A–C); *in* Report of Activities 2021, Manitoba Agriculture and Resource Development, Manitoba Geological Survey, p. 77–83.

DRI2021019

Updates to the Manitoba Mineral Deposits Database, east-central Manitoba (NTS 53E, F)

by M.L. Rinne

Microsoft® Excel® file supplements:

Rinne, M.L. 2021: Updates to the Manitoba Mineral Deposits Database, east-central and northwestern Manitoba (NTS 53E, F, 64J, K, N, O); *in* Report of Activities 2021, Manitoba Agriculture and Resource Development, Manitoba Geological Survey, p. 1–7.

DRI2021020

Kimberlite-indicator-mineral data derived from glacial sediments (till) in the Russell–McCallum lakes area of northwestern Manitoba (parts of NTS 64C3–6)

by T.J. Hodder

Microsoft® Excel® file supplements:

Hodder, T.J. 2019: Till sampling and ice-flow mapping in the Russell–McCallum lakes area, northwestern Manitoba (parts of NTS 64C3–6); *in* Report of Activities 2019, Manitoba Agriculture and Resource Development, Manitoba Geological Survey, p. 90–96.

Database

Lynn Lake Bedrock Compilation Map Database

by Manitoba Agriculture and Resource Development

Includes maps in PDF of the following areas:

- Barrington Lake, Manitoba (NTS 64C16)
- Cockeram Lake, Manitoba (NTS 64C15)
- Fraser Lake, Manitoba (NTS 64B13)
- Laurie Lake, Manitoba (NTS 64C12)

- Lynn Lake, Manitoba (NTS 64C14)
- McGavock Lake, Manitoba (NTS 64C11)
- McMillan Lake, Manitoba (NTS 64C13)
- Sickle Lake, Manitoba (NTS 64C10)

Geoscientific Maps

MAP2021-1
Bedrock topography of southern Manitoba
by G.R. Keller and G.L.D. Matile (scale 1:1 000 000)

MAP2021-2
Drift thickness of southern Manitoba
by G.R. Keller and G.L.D. Matile (scale 1:1 000 000)

Geoscientific Reports

GR2020-1
Geology of the Cat Creek–Euclid Lake area, Bird River greenstone belt, southeastern Manitoba (parts of NTS 52L11, 12)
by X.M. Yang and M.G. Houlé

GR2021-1
Bedrock geology of the central Sipiwesk Lake area, Pikwitonei granulite domain, central Manitoba (part of NTS 63P4)
by C.G. Couëslan

Open File

OF2021-1
Manitoba radiocarbon ages: update
by M.S. Gauthier

Preliminary Maps

PMAP2021-1
Bedrock geology of the Stuart Bay–Chickadee Lake area (east of Wekusko Lake), north-central Manitoba (parts of NTS 63J12, 13)
by K.D. Reid (scale 1:15 000)

PMAP2021-2
Bedrock geology of the Ralph Lake area, Lynn Lake greenstone belt, northwestern Manitoba (parts of NTS 64C14)
by X.M. Yang (scale 1:10 000)

EXTERNAL PUBLICATIONS

Benn, D., Linnen, R. and Martins, T. in press: Evaluating white mica as an indicator mineral for Lithium bearing pegmatites, Wekusko Lake pegmatite field, Manitoba Canada; *in* Targeted Geoscience Initiative 5: grant program final reports (2018-2020), Geological Survey of Canada, Open File 8755.

Bute, S.I., Yang, X., Yang, X., Girei, M.B., Kayode, A.A. and Lu, Y. 2021: Geochemistry, zircon U-Pb ages and Hf isotopes of granites and pegmatites from Gubrunde region in the eastern Nigeria Terrane: insight into magmatism and tectonic evolution of the late Pan-African orogeny; Geochemistry, v. 81, art. 125809, URL <https://doi.org/10.1016/j.chemer.2021.125809>.

Chen, F., Cui, X., Lin, S., Wang, J., Yang, X., Ren, G. and Pang, W. 2021: The 1.14 Ga mafic intrusions in the SW Yangtze block, south China: records of late Mesoproterozoic intraplate magmatism; Journal of Asian Earth Sciences, v. 205, art. 104603, URL <https://doi.org/10.1016/j.jseaes.2020.104603>.

Fabre, C., Ourti, N.E., Mercadier, J., Cardoso-Fernandes, J., Dias, F., Perrotta, M., Koerting, F., Lima, A., Kaestner, F., Koellner, N., Linnen, R., Benn, D., Martins, T. and Cauzid, J. 2021: Analyses of Li-rich minerals using handheld LIBS Tool; Data, v. 6, no. 6, p. 68, URL <https://doi.org/10.3390/data6060068>.

Hodder, T.J., Gauthier, M.S., Ross, M. and Lian, O.B. 2021: New stratigraphic and chronological constraints in western Hudson Bay Lowland, Canada, and their implications for the Laurentide Ice Sheet evolution; Geological Society of America, Annual Meeting, October 10–13, 2021, Portland, Oregon, Abstracts with Programs.

Kilmury, A.A., Brink, K.S. and Nicolas, M.P.B. 2021: Chrono-, chemo-, litho-, cyclo-, and biostratigraphy of the Late Cretaceous Manitoba escarpment in Saskatchewan and Manitoba, Canada; Geological Society of America Connects 2021, October 10–13, 2021, Oregon, Portland, poster presentation.

Kilmury, A.A., Brink, K.S. and Nicolas, M.P.B. 2021: Chrono-, chemo-, litho-, cyclo-, and biostratigraphy of the Late Cretaceous Manitoba escarpment in Saskatchewan and Manitoba, Canada; Geological Society of America, Joint 55th annual North-Central/South-Central Section Meeting, April 18–20, 2021, virtual event, poster presentation, URL <http://dx.doi.org/10.1130/abs/2021NC-362757>.

Mohammadi, N., Lentz, D.R., McFarlane, C.R.M. and Yang, X.-M. 2021: Biotite composition as a tool for exploration: an example from Sn-W-Mo-bearing Mount Douglas granite, New Brunswick, Canada; Lithos, v. 382-383, art. 105926, URL <https://doi.org/10.1016/j.lithos.2020.105926>.

Nicolas, M.P.B. 2021: A sedimentary geologist's journey from petroleum to critical minerals; Women in Mining, Winnipeg Chapter lunch series, October 19, 2021, oral presentation.

Nicolas, M.P.B. 2021: Helium and lithium brine potential of Manitoba, Canada; IMAGE '21: International Meeting for Applied Geoscience & Energy, September 26–October 1, 2021, Denver, Colorado, Technical Program, poster presentation.

Nicolas, M.P.B, Yurkowski, M. and Branscombe, P. 2021: Critical minerals: endowment and future growth in three provinces; Reservoir Magazine, Canadian Society of Petroleum Geologists, September/October 2021, issue 5, p. 34–35.

Yang, X.M. 2021: Estimating crystallization pressure(s) of granites: analysis of equilibrium, consideration of redox, textural aspects, emplacement processes with implications for metallogenesis; General Annual Meeting of the Volcanology and Igneous Petrology Division, Geological Association of Canada, May 27, 2021, URL <https://www.youtube.com/watch?v=fOq8DPbNFz8&t=2259s&ab_channel=GACVIP> [June 2021].

Yang, X.M., Lentz, D.R. and Chi, G. 2021: Ferric-ferrous iron oxide ratios: effect on crystallization pressure of granites estimated by Qtz-geobarometry; Lithos, v. 380–381, art. 105920, URL <https://doi.org/10.1016/j.lithos.2020.105920>.

Zhao, Y., Lin, S., Zhang, P., Yang, X., Gu, Y., Bi, Z. and Kou, L. 2021: Geochronology and geochemical characteristics of Paleoproterozoic syn-orogenic granitoids and constraints on the geological evolution of the Jiao-Liao-Ji orogenic Belt, North China Craton; Precambrian Research, v. 365, art. 106386, URL <https://doi.org/10.1016/j.precamres.2021.106386>.